Terms and Conditions of Use of Digitised Theses from Trinity College Library Dublin

Copyright statement

All material supplied by Trinity College Library is protected by copyright (under the Copyright and Related Rights Act, 2000 as amended) and other relevant Intellectual Property Rights. By accessing and using a Digitised Thesis from Trinity College Library you acknowledge that all Intellectual Property Rights in any Works supplied are the sole and exclusive property of the copyright and/or other IPR holder. Specific copyright holders may not be explicitly identified. Use of materials from other sources within a thesis should not be construed as a claim over them.

A non-exclusive, non-transferable licence is hereby granted to those using or reproducing, in whole or in part, the material for valid purposes, providing the copyright owners are acknowledged using the normal conventions. Where specific permission to use material is required, this is identified and such permission must be sought from the copyright holder or agency cited.

Liability statement

By using a Digitised Thesis, I accept that Trinity College Dublin bears no legal responsibility for the accuracy, legality or comprehensiveness of materials contained within the thesis, and that Trinity College Dublin accepts no liability for indirect, consequential, or incidental, damages or losses arising from use of the thesis for whatever reason. Information located in a thesis may be subject to specific use constraints, details of which may not be explicitly described. It is the responsibility of potential and actual users to be aware of such constraints and to abide by them. By making use of material from a digitised thesis, you accept these copyright and disclaimer provisions. Where it is brought to the attention of Trinity College Library that there may be a breach of copyright or other restraint, it is the policy to withdraw or take down access to a thesis while the issue is being resolved.

Access Agreement

By using a Digitised Thesis from Trinity College Library you are bound by the following Terms & Conditions. Please read them carefully.

I have read and I understand the following statement: All material supplied via a Digitised Thesis from Trinity College Library is protected by copyright and other intellectual property rights, and duplication or sale of all or part of any of a thesis is not permitted, except that material may be duplicated by you for your research use or for educational purposes in electronic or print form providing the copyright owners are acknowledged using the normal conventions. You must obtain permission for any other use. Electronic or print copies may not be offered, whether for sale or otherwise to anyone. This copy has been supplied on the understanding that it is copyright material and that no quotation from the thesis may be published without proper acknowledgement.

Carbon Nanotube-Polymer Composites

Ian O'Connor

A thesis submitted for the degree of Doctor of Philosophy to the

University of Dublin, Trinity College

Declaration

Except as otherwise indicated, the author carried out the work described herein alone. This work has not been previously submitted for a degree to this or any other university. I give my permission to the library to lend or copy this thesis.

Acknowledgements

I would like to take this opportunity to thank all the people who helped me throughout my time in Trinity College and through my PhD studies. Most important in this respect were my supervisors, Prof. Yurii Gun'ko and Prof Jonathan Coleman, thank you for all your help and encouragement.

I would like to sincerely thank all members of the academic, technical and secretarial staff in the School of Chemistry. A special thanks to Dr. John O'Brien and Dr. Manuel Ruether for obtaining NMR studies and also helping with TGA, DSC and FTIR studies. Thank you also to all the staff in the School of Physics and the CMA department. In particular Neal Leddy for all his very generous help with SEM and TEM studies, coating my samples and answering the phone sometimes.

I must thank all members of Physics group Bu and members of Johnny's group for providing assistance in areas of Physics which were previously unfamiliar to me, especially Umar and Yenny for checking over my thesis and helping with mechanical and electrical studies when I needed. I must express my heartfelt thanks to the entire Gun'ko group, who I learned much from and who have helped me in many aspects of my work and also for the many interesting conversations, and a thoroughly enjoyable work environment, Amro, Anna, Gemma, Hugh, Joe, Joe 2, Maciej, Malgozata, Mícheál, Michele, Renata, Roger, Rowan, Serena, Shane, Sivakumar, Steve and Tim and to the students who assisted me along the way Stephen and Manman.

I would like to thank Stewart and Bennetta for being so supportive while I was writing my thesis. Thank you also to my brothers Padraig and Anton and all my friends a lot of whom I haven't seen for months.

Melanie you are a wonderful person, thank you for all your support, we did it! Without you I don't think I could have written this thesis at all. I thank you with all my heart.

Finally I would like to thank my father and mother, John and Margaret, without their support and direction I would not have gotten to where I am today.

Summary

Since their discovery in 1991, carbon nanotubes have generated a lot of activity in many areas of science and engineering due to their unprecedented superlative mechanical, thermal and electronic properties. This combination of properties makes them ideal candidates as additives for polymer composites with a multitude of applications ranging from ultra-strong materials for bullet proof vests to flexible displays and electronic paper. The main aim of our work is to develop new carbon nanotube-polymer composites with enhanced mechanical and/or electrical properties.

Chapter 1 gives a background to the area of carbon nanotubes and the technological importance of polymer-carbon nanotube composites. A review of the fabrication of polymer composites and different properties of polymers is also given. We discuss a variety of techniques which are involved in polymer composite fabrication and characterisation. Some aspects of nanotube functionalisation, polymer properties and ultrasonic processing are also discussed.

In **Chapter 2**, our work is focused on the development of new functionalised nanotubes, which could be used as additives for polymer reinforcement. In this part we developed new Kevlar coated carbon nanotubes via a one step process by refluxing in a highly oxidising environment with Kevlar *in situ*, enabling a polymer coating on the surface of the nanotubes. These Kevlar coated nanotubes have been used as additives to various polymers. That resulted in composites with improved mechanical properties demonstrating up to 50% and 70% increase in tensile strength and Young's modulus respectively at very low nanotube loading levels. We have also found that the mechanical properties of Kevlar coated carbon nanotube-polymer composites strongly depend on the nature of polymer and mass percentage of nanotubes.

Chapter 3 deals with the development new ultra-strong polymer composite materials using carbon nanotube as additives to Kevlar fibres and employing our new swelling-under-ultrasound technique. We have introduced a new approach for the preparation of polymer-nanotube composite fibres. This method is based on the ultrasonic assisted swelling of the polymeric fibre in a nanotube suspension with the use of an appropriate organic solvent. The swelling of Kevlar in a carbon nanotube suspension in N-methyl-2-pyrrolidone (NMP) resulted in new Kevlar-nanotube composites. These materials

demonstrated significantly improved mechanical properties at very low content of nanotubes.

In **Chapter 4** we expand the swelling technique to develop polymer composites which have a greater significance to electrical applications. We have selected polymers which display good transparency and flexibility, demonstrating potential for applications in the field of transparent, conductive electrodes. Different solvents have been chosen using swelling theory to find the optimal solvent-polymer compatibility. We have achieved good and often homogenous penetration of nanotubes into a polymer matrix further demonstrating the potential for this technique. We have also demonstrated that post formation composite treatment with acid or metal can increase conductivity further. The best polymer composites demonstrated a significant increase in electrical conductivity (up to 10^7) while retaining 80 % transparency.

The mechanical properties of these prepared polymer composites were also explored in **Chapter 5**. The main area of research focused on the samples with the highest conductivity and deepest penetration of nanotubes. We found that the composites, which displayed enhanced electrical properties and good penetration of nanotubes into the polymer matrix, have also demonstrated enhanced mechanical properties. In general, the electrical enhancement of the polymers corresponded quite well with their mechanical enhancement. The potential utilisation of supercritical fluids to enhance polymer swelling was also explored in this chapter. We found that carbon nanotubes can be intercalated into a polymer by swelling with supercritical CO_2 in the presence of nanotubes. The resulting polymer composites displayed deep penetration of nanotubes and considerable mechanical enhancement when compared to both the original polymer and polymer subjected to the same treatment in the absence of nanotubes.

In **Chapter 6** we presented a full description of the experimental details for the procedures and techniques described in this work. Finally **Chapter 7** details the conclusions of this work and also gives a future outlook for the research performed.

Overall in this project we have developed several new polymer-nanotube composite materials and a new technique of polymer swelling under ultrasound, which has a number of advantages. We believe that this approach can also be extended for other nanomaterials. This research should open new opportunities in the fabrication of novel polymer composite materials with multitude applications.

Table of Contents

List of Figures

Chapter 1

Chapter 2

Chapter 3

Chapter 4

Chapter 5

Chapter 7

List of Tables

Chapter 1

Chapter 2

Chapter 3

Chapter 4

Chapter 5

Chapter 7

List of Abbreviations

CO_2	Carbon Dioxide
CVD	Chemical Vapour Deposition
DMF	*N,N*-Dimethylformamide
DSC	Differential Scanning Calorimetry
FNT	Kevlar Functionalised Carbon Nanotube
FTIR	Fourier Transfer Infrared
H-bond	Hydrogen Bond
HR-TEM	High Resolution Transmission Electron Microscopy
ITO	Indium-Tin Oxide
MWNT	Multi-Walled Carbon Nanotube
NMP	*N*-Methyl-2-pyrollidone
NMR	Nuclear Magnetic Resonance
NT	Nanotube
PE	Polyethylene
PET	Polyethylene Terephthalate
PMMA	Polymethylmethacralate
PNT	Pristine Carbon Nanotube
PP	Polypropylene
PPTA	Poly(*p*-phenylene terephthalamide)
PS	Polystyrene
PVA	Polyvinyl Alcohol
PVAc	Polyvinyl Acetate
PVC	Polyvinyl Chloride
QD	Quantum Dot
SC-CO_2	Super-Critical Carbon Dioxide
SEM	Scanning Electron Microscopy
SWNT	Single-Walled Carbon Nanotube
TCD	Trinity College Dublin
TEM	Transmission Electron Microscopy
TGA	Thermo-gravimetric Analysis
THF	Tetrahydrofuran

Chapter 1

Introduction

1.1 Composite Materials

The basic concept of creating composite materials for mechanical reinforcement has been around since prehistoric farmers put straw in their mud bricks to increase their longevity and strength. It was mentioned in the Biblical book of Exodus and can be seen in paintings from ancient Egypt. Evidence of unwittingly produced carbon nanotube composites has also been uncovered recently in the finding of carbon nanotubes in the swords of Muslim soldiers from the crusader era.[1] With some tailoring these composite methods and ideas are still used today in the construction industry when steel rods are placed in concrete for support. There is a plethora of other examples of composite materials throughout history and now they are ubiquitous in human society. Fundamentally we are trying to combine the properties of two or more constituent materials; these are generally of the type, *matrix* and *reinforcement*. The focus of this thesis is on the preparation and investigation of polymer - carbon nanotube composites.

1.2 Carbon Nanotubes

1.2.1 The discovery of fullerenes

Until recently only two allotropes of carbon were known; these were diamond and graphite. Diamond is a sp^3-hybridised matrix of carbon atoms arranged in a tetrahedral structure. Graphite is composed of planar sheets of tetragonal sp^2 carbons arranged in a hexagonal array. These sheets are connected by van der Waals forces. Being allotropes they are understandably very different. Diamond is a clear crystalline material which displays excellent thermal conductivity and hardness, graphite is a black soft material with interesting electrical properties. The structure of both forms is shown in **Figure 1.1**.

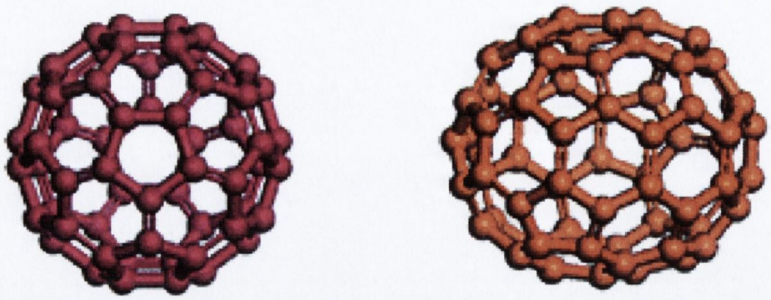

C_{60} C_{70}

Figure 1.2 Schematic diagram showing the structures of C_{60} and C_{70}, represented by combinations of pentagonally and hexagonally arranged sp^2 hybridised carbon atoms[3]

These molecules attracted immediate interest from many areas of research to find any possible applications for the fascinating new allotropes of an element that was so familiar.

1.2.2 Nanotube structure

The scientific world barely had time to take in the amazing discovery of fullerenes when Sumio Iijima first discovered carbon nanotubes in 1991.[4] He reported that they were formed by inducing an electrical arc discharge across a graphite source. The nanotubes could be represented as a sheet of graphene rolled into a tube (**Figure 1.3**) and capped on each end with half a fullerene molecule. An ideal single-walled nanotube (SWNT) consists of a seamless cylinder composed completely of hexagons and capped by hemispherical C_{60} analogues containing both pentagons and hexagons. Analysis techniques included the use of High Resolution Transmission Electron Microscopy (HR-TEM) and Raman spectroscopy to help understand the physical and chemical characteristics of the nanotubes. The structure of the nanotubes can be zigzag, armchair or chiral. These names refer to the arrangement of hexagons around the circumference of the nanotube and are sometimes referred to as the "flavour" of a nanotube. The nanotubes themselves have a high aspect ratio with diameters often found to be less than 1 nm and lengths in the millimetre scale.

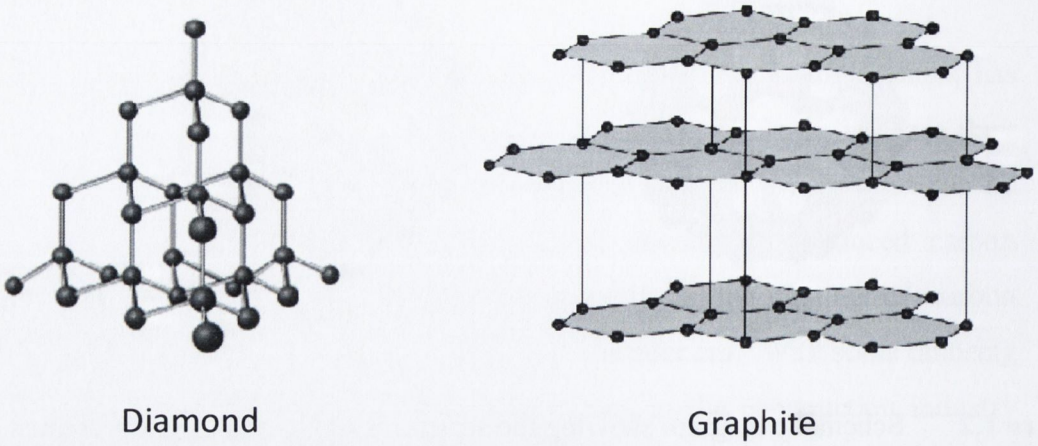

Figure 1.1 Image showing the crystal structure of the two most common allotropes of carbon, diamond, represented by sp^3 hybridised carbon atoms and graphite, represented by sp^2 hybridised carbon atoms

In 1985, however, upon analysis of soot prepared by laser ablation of graphite, another allotropic form of carbon was discovered by Smalley *et al*[2]. They found the presence of C_{60} and C_{70} species in the graphitic material. It was named Buckminsterfullerene and it along with other compounds of similar structure, e.g. C_{70}, were collectively called fullerenes. The researchers characterised the C_{60} using a variety of techniques including mass spectroscopy. For their work they were awarded the Nobel Prize for Chemistry in 1996.

In graphite the carbon atoms are arranged in 6-membered hexagonal rings. If we were to replace some of these with 5-membered pentagonal rings the resulting strain in the conformation would cause a curving of the sheets of graphite. This is still chemically permitted as the carbon atoms can still retain their four-coordinated valency. If we are dealing with very small sheets of graphite and a high ratio of 5-membered rings we can create a stabilised closed cage molecule which has unique chemical and physical properties. For example the C_{60} molecule is made up of 12 pentagonal and 20 hexagonal rings, while C_{70} has 12 pentagonal and 25 hexagonal rings (**Figure 1.2**).

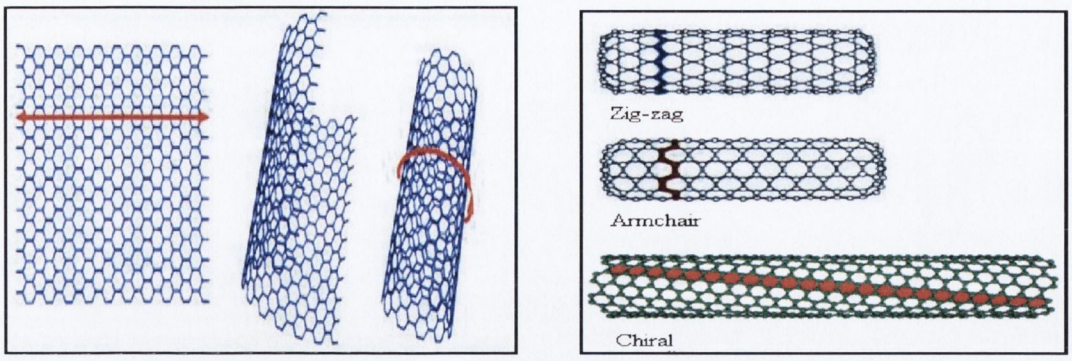

Figure 1.3 Analogous simulation of nanotube conformation and different types of nanotubes.[5] Nanotubes can be thought of as a graphene sheet rolled up into a tube (left image). Depending on the orientation of the hexagons they can be referred to as zig-zag, armchair or chiral (right image)

Several tubes can be also encapsulated concentrically inside one another to give a Multi-Walled Nanotube (MWNT) where each layer is held together by van der Waals forces.[6] These are much larger than single walled nanotubes and can have diameters of up to 50 nm.

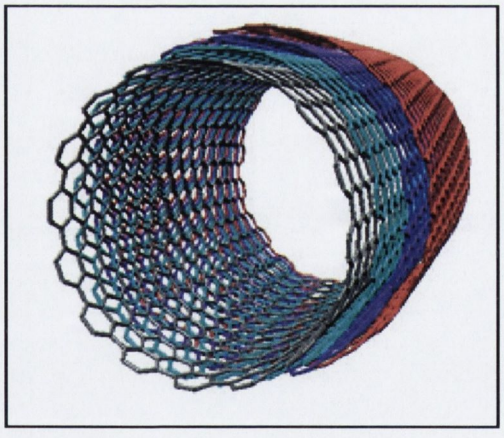

Figure 1.4 The structure of a multi-walled nanotube[7] can be explained as a number of tubes encapsulated concentrically inside one another.

Other methods of making nanotubes have since been discovered including laser ablation,[8] gas phase catalytic growth,[9] and chemical vapour deposition (CVD).[10,11] Each of these techniques allows to prepare nanotubes that have their own unique properties, defects and impurities.

Immediately, interest was focused on carbon nanotubes in anticipation of some interesting electrical and mechanical properties. The scientific world reacted quickly to their discovery and there are currently thousands of papers published on them every year.

1.2.3 Electrical properties of carbon nanotubes

Carbon nanotubes are found to have a very high thermal conductivity, even higher than diamond. Zettle *et al*[12] found the thermal conductivity for a single rope of nanotubes at room temperature could vary between 1800 - 6000 W/mK. However, it is their mechanical and electrical properties, which have attracted the most interest so far.

Depending on their shape and the orientation of the hexagonal matrix, electrical properties of carbon nanotubes can range from semi-conductive to metallic.[13,14] In fact some are potentially more conductive than copper. The differences in conductivity can be defined by the graphene sheet properties.[15] This relates to how a theoretical graphene sheet would be rolled up to form a tube (**Figure 1.5**). The aforementioned armchair nanotubes are all of metallic conductivity and for the zigzag and chiral the conductivity is defined by their vector (n,m). The remaining nanotubes' conductivities are all defined by the formula n – m = x. If the value of x is a multiple of 3 then the nanotube has metallic conductivity, if not, it should be semi-conducting. To produce a nanotube with the indices (8,8) the sheet is rolled up so that the atom at the point (0,0) is superimposed on the atom at (8,8). It should be noted from looking at the figure that m = 0 for all zigzag tubes, while n = m for all armchair tubes.

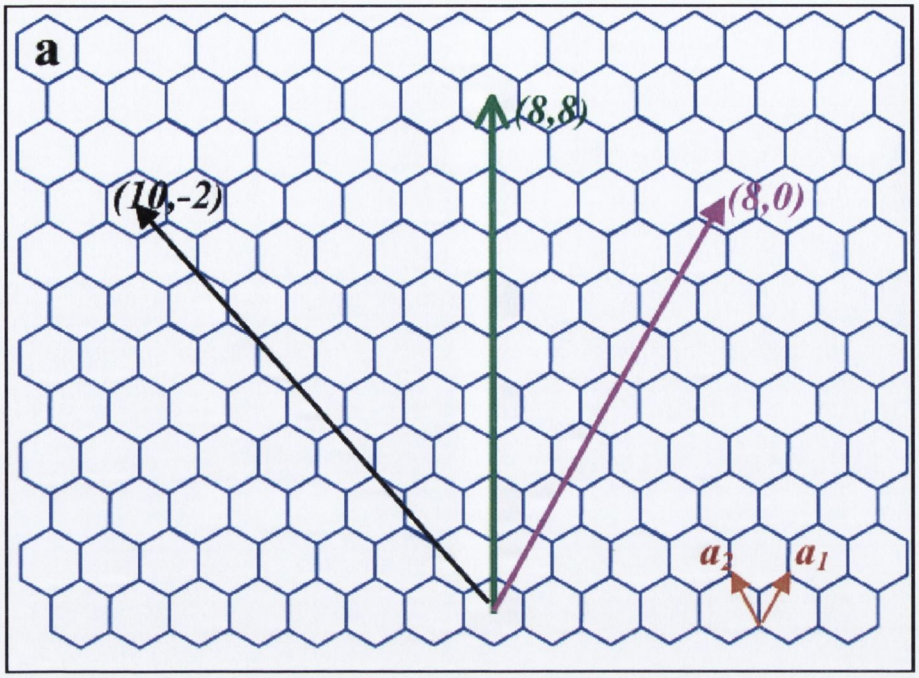

Figure 1.5 Diagrammatic representation for the calculation of the chiral vector for different forms of nanotubes.[16] When the sheet is folded, the chirality and thus the conductivity of the nanotube can be determined.

Initially conductivity measurements were made by Frank *et al*[17] who discovered that MWNT displayed ballistic conductivity and extremely high current densities of up to 10 MA/cm^{-2}. This was further supported by Sanvito *et al*[18] who showed from theoretical calculations a similar conductance.

A great obstacle to the use of nanotubes electronically, however, is the fact that it is extremely difficult, at present, to separate the conductive nanotubes from the non-conductive ones. In fact it is difficult even to separate SWNTs from each other, regardless of their electronic orientation. However, with the progressive miniaturization of computer components and the quest for ever smaller circuits it seems only a matter of time before nanotubes will be breaking into the technological mainstream. In fact, extrapolating Moore's Law, which predicts a doubling of the number of transistors on a square inch of a computer chip every 12-18 months, the era of the silicon chip will last for only another decade or so. At this point, the fundamental limits of transistor size will be reached. This will leave a void in the electronic world that may only be filled by carbon nanotubes. Some research has been done into separating nanotubes into their

different electronic flavours with Krupke *et al*[19] at the forefront of this work but serious advances in this field have not yet come through to enhance mainstream research.

1.2.4 Mechanical properties of carbon nanotubes

Carbon nanotubes have remarkable mechanical properties which are a result of high-strength sp^2 bonding hybridisation of the carbon atoms in their side walls.[20] With this inherent strength it is no surprise that they have been shown to be in the region of 100 GPa for the ultimate tensile strength[21,22] and an elastic modulus of over 1 TPa. [23,24,25] These values demonstrate that they may be up to hundreds of times stronger than steel while only being one sixth of the weight (**Table 1.1**).

Table 1.1 Comparison of mechanical properties and density of carbon nanotubes to other common materials[26]

Material	Young's Modulus (GPa)	Tensile Strength (GPa)	Density (g/cm^3)
SWNT	1054	150	1.3
MWNT	1200	150	1.8
Steel	208	0.4	7.8
Epoxy	3.5	0.005	1.25
Wood	16	0.008	0.6
Kevlar	83	3.6	1.47

If it would be possible to incorporate the nanotubes into a macroscopic material, it could result in a great enhancement of the mechanical properties of the composite material. To attain a good composite it is paramount that we achieve considerable stress transfer between the nanotube and the matrix material. A lot of current research is focused on the formation of polymer composites with nanotubes.

1.2.5 Solubility and dispersibility of carbon nanotubes

Carbon nanotubes are generally not soluble in most common solvents. Many approaches to this problem have been attempted with relatively little success. The nanotubes tend to aggregate into bundles. If these nanotubes can be separated, so they do not aggregate, they can be used a lot more efficiently. In order to make them more soluble and create a stable solution/dispersion, they were often chemically functionalised or treated with a surfactant.[27] However, this led to problems with further chemical modification of the nanotubes as they were surrounded by the surfactant and, following dispersion, the surfactant would need to be removed. Other research has uncovered some solvents which are able to enhance dispersion capabilities of pristine nanotubes and appear to keep them in a stable dispersion for relatively long periods of time. Two of the best suggested solvents are *N,N*-dimethylformamide (DMF) and *N*-methyl-2-pyrrolidone (NMP).[28] The reasons for their capabilities at dispersing nanotubes are, however, still poorly understood.

1.2.6 Functionalisation of carbon nanotubes

The surface chemistry of nanotubes and covalent functionalisation are very important for the application of nanotubes especially with regard to composite fabrication. These treatments can also decrease bundling and enhance their dispersive and chemically interactive qualities. The reactivity of a nanotube fundamentally arises from pyramidalisation at the carbon atom and also the misalignment of π-orbitals on adjacent carbon atoms due to curvature induced strain. The former tends to be more common on the more unstable fullerene-like caps on the ends of the nanotubes[29,30] and the latter in the side-walls at areas such as sp^3 hybridised defects, pentagon-heptagon pairs (Stone-Wales defects) and in vacant sites in the nanotube structure.[31] The increase in strain associated with a smaller circumference results in a corresponding increase in reactivity.

Acid treatment is often used to purify nanotubes[32,33] producing hydroxyl and carbonyl groups and ultimately Niyogi *et al*[34] found that refluxing in nitric acid increased nanotube degradation and dissolution of the metal catalyst. Chen *et al* initially solubilised nanotubes in organic solvents like dichloromethane and aromatic solvents like benzene by activating acid-purified nanotubes with thionyl chloride to produce acyl

chloride functionalities.[35] These could then be reacted with amine groups. In other work Hamon *et al* showed that ester functionalisation of defect sites can also produce nanotubes with a much greater solubility in chloroform, tetrahydrofuran (THF) and other solvents.[36] Aqueous solubility was also achieved *via* functionalisation of the nanotubes with glucosamine and 2-aminoethansulphonic acid[37,38]

Many different approaches have been taken when trying to introduce functionalities onto a nanotube, including covalently attaching simple molecules like fluorine[39] or alkanes,[40] and heating in air.[41] These often lead to further modification by reaction of the side-wall functionalisation with another functional group. This was achieved by Boul *et al* who reacted the fluorine functionality with an alky magnesium bromide Grignard reagent to produce side-wall alkylated nanotubes. The reaction occurred *via* a concerted, allylic displacement mechanism.

Nanotubes can also be functionalised to one another *via* a linker group. Koos *et al*[42] linked nanotubes using a diaminopropane linker group. They bonded the linker to the nanotube, exploiting the fact that nanotubes oxidised by acid have carboxylic acid functional groups. They found upon analysis from TEM they had achieved connections between nanotubes. Similar work was carried out by Zhao *et al*[43] who also found that the nanotubes had much increased stability in solution.

Cycloaddition reactions were performed by Holzinger *et al*[44] who observed the formation of aziridine rings via functionalisation with nitrenes. The three-membered rings are composed two carbon atoms from the the side-wall of the nanotubes and a nitrogen. This opened the opportunity again for further functionalisation through these rings.

As we will discuss in the following section, polymer grafting is another form of functionalisation and there is a variety of other approaches to nanotube functionalisation including attaching organometallic species or fullerenes.[45] Previously Blake *et al*[46,47] have shown carbon nanotubes can be lithiated using *n*-BuLi (*n*-butyllithium). These nanotubes could then be covalently bonded to chlorinated polypropylene (CPP). The addition of these CPP-grafted nanotubes to the various polymers resulted in significant improvement of their mechanical properties. Recently Hirsch *et al*[48] reported an interesting development involving a reaction sequence with *t*-BuLi, which has been used to obtain SWNTs with a high degree of *t*-butyl-

functionalisation. This year the same group published their new research on a covalent sidewall addition to SWNTs of a series of organolithium and organomagnesium compounds followed by re-oxidation.[49] A good review of the different techniques was published by Banajeree *et al* and the scheme showing many of the nanotube functionalisation approaches is presented in **Figure 1.6**.

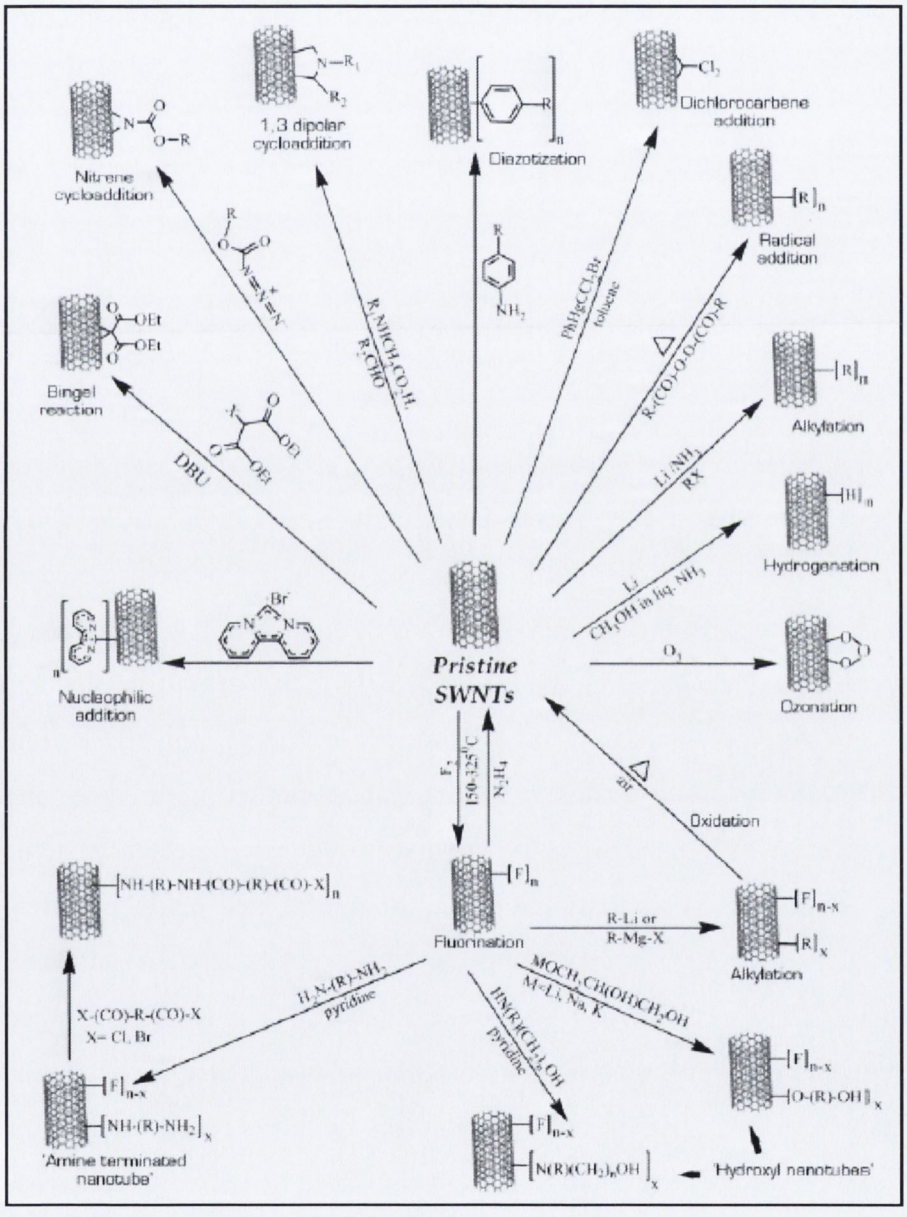

Figure 1.6 Schematic displaying many of the different chemical functionalisation capabilities of carbon nanotubes[50]

1.2.7 Carbon nanotube-polymer composites

The idea to create synthetic polymer composites based on carbon was formulated in the 1980s and the first successful attempts utilised carbon fibres to create reinforced thermoplastics and thermosets.[51,52,53] There was immediate interest in this field and other possible additives for reinforcement were explored before the discovery of carbon nanotubes. However, carbon nanotubes were considered structurally much more promising and once their structure was fully appreciated there were high expectations for their reinforcement capability. This was due to the combined effect of their quasi-one-dimensional structure and the comparatively low amount of structural defects and surface impurities when compared to related carbon fibres and other composite materials.

Fundamentally, looking at the different approaches to fabricating polymer composites, we find that nanotubes can introduce a number of both positive and negative effects into polymers' mechanical properties. There are four main system requirements for effective reinforcement, namely a large nanotube aspect ratio, good dispersion capability, alignment and a good interfacial stress transfer between the nanotube and the matrix. A large aspect ratio will maximise the load transfer to the nanotube.[54] Good dispersion will maximise polymer nanotube interface and result in greater load transfer again and a more uniform stress distribution. When a good interfacial stress transfer between the polymer and nanotubes is achieved, some of the stress that the polymer will undergo is transferred from the polymer chains to the nanotubes, improving polymers mechanical properties. If the stress transfer from the polymer to the nanotube can be achieved to a good degree we expect to see large increases in strength and modulus, often, but not necessarily always, with corresponding decreases in toughness and strain. The nanotubes may also disrupt the structure of the polymer matrix and cause imperfections, having a negative impact on the polymers mechanical properties. Previous research has also shown that the use of higher concentrations of nanotubes results in the formation of aggregates which do not infer any mechanical strength increases as they are not interacting efficiently with the polymer matrix.[55,56] This usually results in a decrease in the strength and modulus of a polymer.[57] Alignment will result in better mechanical properties by up to a factor of five, but only in the direction of the alignment.[58]

Early attempts at creating nanotube-polymer proved quite successful with many papers published displaying increases in mechanical properties.[59,60,61,62] They proved that the extraordinary mechanical properties of the carbon nanotube could be transferred to the polymer, although they were still far away from the theoretical levels of reinforcement. To achieve these kinds of reinforcement, many hurdles would have to be overcome. The biggest of these included nanotube impurity, aggregation and non-homogenous dispersion within the polymer matrix.

Impurities in nanotubes can be anything from amorphous carbon, metal catalyst, non-tubular fullerenes or graphite and soot and are formed in their syntheses as mentioned above. These tend to have a negative impact on the mechanical properties of a polymer as they have nowhere near the mechanical properties of the individual nanotubes. Impurity was initially side-stepped by a move towards using CVD nanotubes instead of arc-discharge as they had inherently much higher purity (up to 95% compared to around 10%) than their linear high-production-energy counterparts. They were also much cheaper and although were not as strong, they could still, theoretically at least, provide enormous enhancement. Many different purification methods have since been developed however, purifying CVD nanotubes even further and also enabling the use of arc-discharge variety.[63,64,65]

Primary preparation methods of polymer composites utilised the solution casting method which achieved good dispersions and reduced aggregation *via* functionalisation of the nanotubes. Solution casting is generally based on a process of dispersing nanotubes in either a solvent or polymer solution by energetic agitation. This is followed by mixing of nanotubes and polymer in solution with further energetic agitation. Finally the solvent is evaporated off in a controlled fashion resulting in a composite film. Agitation can be achieved by a number of methods including, shear mixing, stirring, reflux or ultrasonication.

Early work in this field by Jin *et al*[66] created nanotube-composite films by dispersing arc discharge MWNTs in chloroform using ultrasonication. This was followed with the dissolution of polyhydroxyaminoether in the dispersion. The mixture was placed on a Teflon mould and the solvent was allowed to evaporate overnight. Much further work has been carried out in this area by chemists like Schaffer *et al*[67,68] who demonstrated that carboxyl functionalised nanotubes were more stable in water and could be used to

create composites by evaporating the water from a solution of water-soluble polymer with nanotubes dispersed throughout. Qian *et al*[69] tried another approach without functionalisation by using high energy sonication with a sonic tip to disperse the MWNTs in toluene and subsequent mixing of this solution with another solution of polystyrene in toluene before solvent evaporation.

Solution casting is a very effective technique for producing composites; however it is wholly ineffective for the vast variety of polymers which are relatively insoluble in common solvents. For this reason another approach was taken; simply mixing of nanotubes with a thermoplastic by melt processing.[70] This is a rather straightforward method as all that is ultimately required is sufficient heating of the polymer to create a viscous liquid. The additive, in this case carbon nanotubes, can just be added directly to melted polymer by shear mixing. Extrusion or moulding of the mixture results in nanotube alignment in the matrix of the polymer composite. Jin *et al*[71]are noteworthy for developing early techniques in this work. Their work involved the mixing of a high percentage (26 %) of MWNTs with polymethylmethacralate (PMMA) at 200°C followed by compression moulding to produce slabs of composite.

A combination of both solution casting and melt processing can also be used to produce aligned nanotube composites where shear mixing is found to be difficult. This method was introduced by Thostenson and Chou[72] who dispersed MWNTs in a solution of polystyrene in THF. The solution was drop cast and after solvent evaporation the composite was cut up and extruded. This was extended to produce composite fibres by Haggenmueler *et al*[73] who first dipersed nanotubes in a solution of PMMA in DMF and following drop casting, repeatedly hot pressed the composite film to achieve a high alignment.

Approaches of fabricating composites using epoxy resins and other thermosetting polymers have also been tried with work by Ajayan *et al*[74] who simply dispersed nanotubes in the liquid epoxy and added the hardener.

Covalently attaching or grafting of polymers is also an important area. This is generally achieved by one of two methods. The first is based on the immobilisation of initiators on the surface of the nanotube and subsequent *in situ* polymerisation of the corresponding monomer. An example of this technique was developed by Ajayan *et al*[75] who generated carbanions on a nanotube surface by treatment with *sec*-butyllithium.

These served as initiators for styrene to produce polystyrene grafted nanotubes. The second approach involves reacting a ready formed polymer with functionalities on the nanotube surface. Fu *et al*[76] used this approach to convert carboxylic functionalities to acid chlorides by refluxing in thionyl chloride. The acid chloride functionalities were then reacted with the hydroxyl groups of polyethylene glycol to produced polymer grafted nanotubes.

There are a number of other methods for developing polymer composites which have also been explored including, polymer intercalation into preformed nanotube networks[77] and coagulation spinning[78,79] among many others which demonstrate the many different approaches to preparing nanotube-polymer composites. Ultimately we are moving towards even stronger materials and with new methods for creating composites emerging levels of reinforcement are advancing nearer to those predicted by theory.

The fabrication of nanotube polymer composites with an emphasis on their resultant electrical properties has also become an important focus for composite researchers. Somewhat surprisingly, the current largest commercial use of nanotubes is in the field of anti-static polymer composites,[80] a much more electrically orientated field. When nanotubes are compared to a similar common conductive filler material, carbon black, it is found that they can be more effective by achieving higher conductivities with a much lower loading.[81] It is anticipated that they could be used to produce conductive polymers with exceedingly low percolation thresholds.[82] The percolation threshold is where long-range connectivity of the nanotubes is achieved, thereby creating a good possibility for current to flow. If good percolation thresholds can be reached at lower loadings it could open up some very interesting possibilities for advancements of the electronic industry, including transparent conductive electrodes for solar cells and flexible displays.

1.3 Polymers

Polymer is a general term for a variety of highly important materials which are fundamentally made up of multiple repeating units. They can be natural, like cellulose and DNA, semi-synthetic, like vulcanised rubber or completely synthetic, like Kevlar. Man-made polymers are generally called plastics although it is not a specifically assigned term. Most plastics are employed in their respective applications because they

have desirable mechanical properties at an economical cost. The polymers used in this work are presented in the subsequent sections.

1.3.1 Kevlar

Aramid fibre is the commonly used phrase to replace the more descriptive term "aromatic polyamide fibre". They were first introduced in the 1960s. Before this time most organic fibres were of a relatively poor standard with regards to their mechanical performance. Since then, however, many different types of high performance organic fibres have been produced. Many of which are equal to or better than most classically interpreted high strength materials. There are many current applications for these fibres in use today, including ballistics, bullet-proof vests, ropes and cables, sports equipment and composite materials. Initially scientists recognised that if they could prepare certain intractable polymers with extended chains, they could achieve high strengths and moduli with stability at much higher temperatures than were currently available. The resolution of their research came with formation of polymers *via* liquid crystalline spinning of solutions. This was the beginning of the formation of aramid fibres.

In an aramid, the amide groups are found between two aromatic rings, with nothing else intervening. They tend to have considerably different properties to conventional polyamides, like nylon. This is because they contain many more aromatic groups which tend to have a large influence on the structure of the polymer chains and also provide a high thermal resistance. The aromatic ring structure gives Kevlar its high thermal stability.[83]

DuPont developed it through the research of two scientists Kwolek and Blades.[84] The chemical composition of Kevlar fibre is based on poly(*p*-phenylene terephthalamide) (PPTA), which is synthesized by terephthaloylchloride and *p*-phenylene diamine in a low temperature polycondensation reaction. The polymer they developed was an aromatic polyamide that displayed some amazing mechanical properties.[85]

There are three fundamental reasons why Kevlar has amazing mechanical properties. Firstly its molecular structure is in the *trans*- conformation, as can be seen in **Figure 1.7**, which was described by Zhang *et al*[86] If it forms the *cis*- conformation we see there is steric hindrance of two of the hydrogen atoms on adjacent phenyl rings. This is due to the aromatic groups separating the amides being very large and causing them to arrange

themselves so that they are on opposite sides of the rigid amide bond. Kevlar, therefore nearly always forms the *trans-* conformation. This characteristic, often referred to as the "rigid-rod," is a function of the substitution of the benzene ring being located in the *para-* position and gives covalent bond strength in the linear direction. Extrapolated outward we achieve a highly linear macromolecular chain which distributes axial stress evenly throughout.

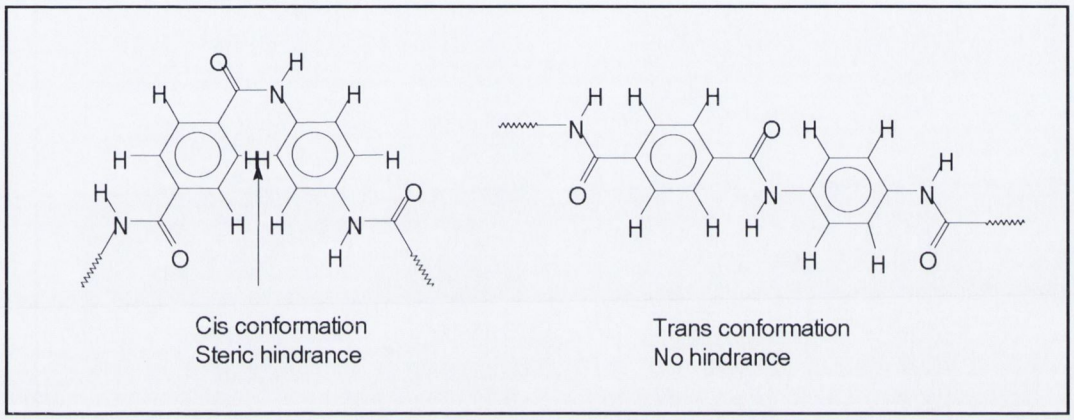

Figure 1.7 Theoretically possible conformations of Kevlar with the *trans-* conformation displaying the usual primary mechanical structure. Note how the *cis-* conformation is rarely formed due to steric hindrance from the overlapping hydrogen atoms.

Secondly because of the regularity of the structure and position of the functional groups within the matrix of the polymer strands, Kevlar fibre has a highly ordered polymeric structure with high crystallinity. Additionally there is further structural strength due to the hydrogen bonding that occurs between the amide and carbonyl end groups which lie close to each other[87], in long ordered rows (**Figure 1.8**). Although these bonds are individually nowhere near as strong as the covalent bonds that form the parallel chains, when we consider the combined effect of the thousands of them that form between the rigid aramid molecules we can understand the enormous tension that would be required to separate them all at once. This gives them their considerable strength in axial tension (tensile strength).

Thirdly, Kevlar forms pleated layers of sheets which give additional strength to its structure.[88] The hydrogen bonds that form between the polar amide groups on adjacent

chains hold the individual Kevlar polymer chains together. This leads to a high degree of alignment of long, straight polymer chains. When the X-ray diffraction data is observed it is found that the characteristic distance of adjacent polymer chains is 3Å, confirming the strong hydrogen bonding between lattice planes.

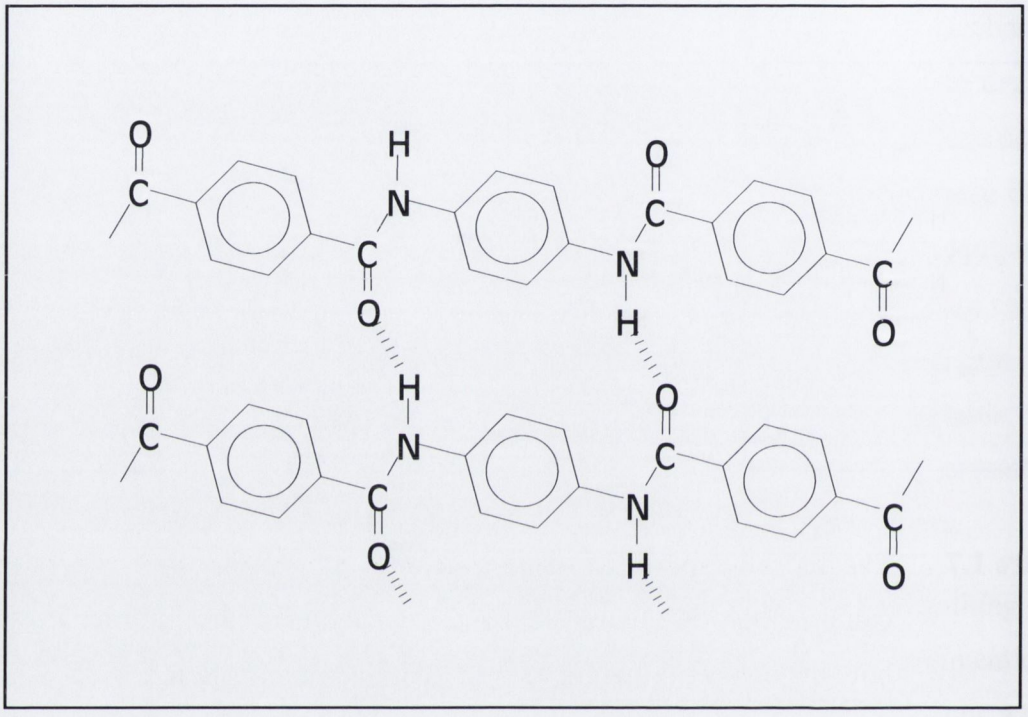

Figure 1.8 Molecular structure of an individual sheet of Kevlar displaying the hydrogen bonding ability between adjacent chains from the oxygen of the carbonyl group to the hydrogen of the amido group

In addition, in Kevlar, along with other *para*-polyamides, the orientation of the bonds as the polymer is formed produces an extremely rigid extended-chain. The liquid crystalline spinning method produces extended-chain crystallites within the fibre which are generally aligned parallel to the direction from which they are drawn and also to each other. The resulting polymer chains have a very high aspect ratio and an unbroken extremely long filament can be formed. In general, the interior of the fibre displays the highest crystallinity, along with the highest elastic modulus and both decrease as we extend outwards towards the fibre surface.[89]

Since it was launched on the market in 1972, Kevlar has been adapted to a variety of applications. It is used for many applications where strength and low weight is a priority, such as in protective clothing.

1.3.2 Polyvinyl acetate

Polyvinyl acetate (PVAc) is a colourless, water-insoluble thermoplastic and can be prepared by treating its monomer, vinyl acetate with a peroxide catalyst. It is very soluble in many other polar and aromatic solvents. One of its most important uses is as a common synthetic precursor to many polymers. Other important applications are in adhesives and latex paints. These applications require considerable mechanical properties.

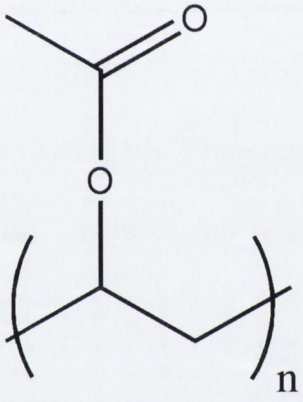

Figure 1.9 Molecular structure of polyvinyl acetate

1.3.3 Polyvinyl alcohol

Polyvinyl alcohol (PVA) is a water soluble polymer which has good mechanical properties provided it is kept dry.[90] It is however chemically resistant to many solvents, oil, and grease. It is generally produced from polyvinyl acetate by hydrolysis to remove the acetate groups[91] although there are other methods of production depending on the type required.[92,93] This is an easier approach than polymerisation of its monomer, vinyl alcohol, as that exists in its tautomeric form, acetaldehyde. It has very good adhesive properties, similar to PVAc, which is where its main use lies. It is also found in emulsifiers and colloid stabilizers.

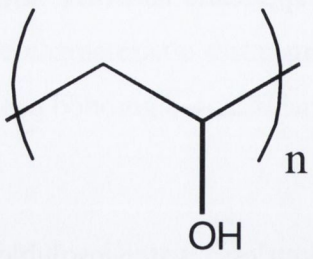

Figure 1.10 Molecular structure of polyvinyl alcohol

1.3.4 Polystyrene

Polystyrene (PS) is an aromatic thermoplastic with high thermal insulating properties and good thermal stability.[94] It also has a good solubility in a variety of solvents.[95] It can be generally formed from free radical polymerisation of its monomer styrene *via* a number of different methods including heat or ultraviolet radiation. It is one of the most widely used plastics, having applications in many different industries but is probably most recognisable routinely in both regular and expanded form in plastic drinks holders and in strong but light packaging. Another large part of its use is in the electronic and construction industry and as casing for appliances. For this reason, its strength is very important and also its rigidity.[96,97]

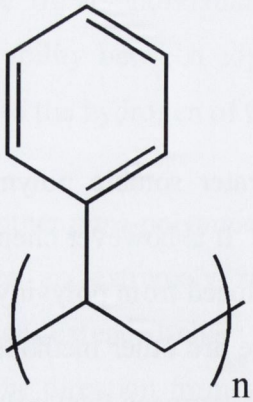

Figure 1.11 Molecular structure of polystyrene

1.3.5 Polyvinyl chloride

Polyvinyl chloride (PVC) is used in many different building applications, water and sewage pipes and gutters and strength is an inherent requirement in its applications. It is also used in the production of gramophone records, hence the name "vinyl records". It generally has to be coloured black to prevent decomposition due to sunlight.[98] It can also be produced in film form and is used in consumer packaging.

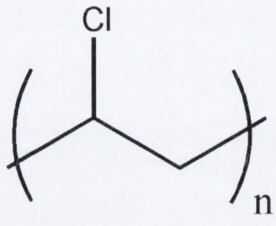

Figure 1.12 Molecular structure of polyvinyl chloride

1.3.6 Polypropylene

Polypropylene (PP) is a very common polymer, generally synthesised using a Ziegler-Natta catalyst with typical co-monomers of ethylene and 1-butene. It has an excellent resistance to chemicals and is often used in applications where this property can be exploited, like laboratory apparatus. It is cheap and generally colourless and can be produced in a transparent form. Its mechanical properties are reasonable with a moderate strength and stiffness optically it is moderately clear.

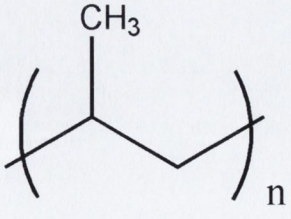

Figure 1.13 Molecular structure of polypropylene

1.3.7 Polyethylene terephthalate

Polyethylene terephthalate (PET) is an easily processible thermoplastic and displays very good optical and mechanical properties. A rigid, very high strength polymer[99] that is also very light, highly transparent and colourless. It is synthesized in a semi-crystalline form by a condensation/step-growth polymerisation of ethylene glycol and terephthalic acid with an aromatic sulphonate as a catalyst.[100] It is more commonly found in its amorphous form, however, which is achieved by fast quenching of the melted polymer. It is regularly found in plastic drink bottles due to its considerable impermeability to liquids and gases. Its high strength is also able to withstand the higher pressures of carbonated drinks.

Due to its high transparency, a more recent use for it is found in transparent electrodes where it is used as a transparent support polymer for indium-tin oxide (ITO) conducting films.[101,102] Its flexibility is reasonable, however it is relatively stiff when concerned with transparent electrodes and this may be a hinderance in some of its applications.

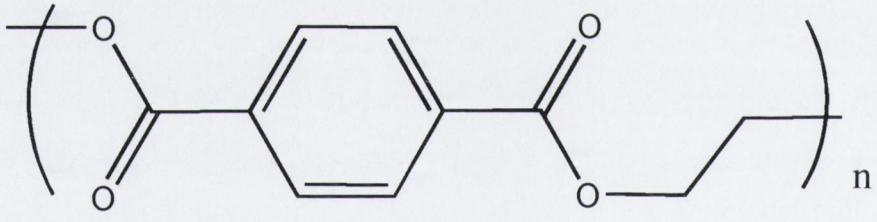

Figure 1.14 Molecular structure of polyethylene terephthalate

1.3.8 Polyethylene

Low density polyethylene has a good mix of optical and mechanical properties and is easily processed and relatively cheap to produce. Depending on its proposed usage it can be fabricated by a number of different methods.[103,104,105] Mainly it is produced under high pressure and temperature by a free radical initiator which would usually be oxygen or peroxide. The resulting polymer contains a large amount of branching with both short chain and very long chain branches, often as long as the polymer chains themselves.[106,107] It has a good chemical resistance and insolubility to most organic solvents[108] but can undergo swelling in many aromatic and some polar solvents.[109]

The electrical properties of polyethylene are relatively good for a polymer and mechanically it has a good flexibility and toughness, at the expense of stiffness and strength.[110,111] It is generally colourless when formed and its optical clarity[112] is of interest in the field of transparent conductive electrodes. It is similar to PET in this respect and if it can be shown to be a substitute for it the higher flexibility of polyethylene may make it a more attractive polymer for flexible displays. Its current major applications, however, include bags and packaging materials, coatings for paper, metals and glass and it is also easily moulded for application in toys, squeezable bottles and many other everyday items.

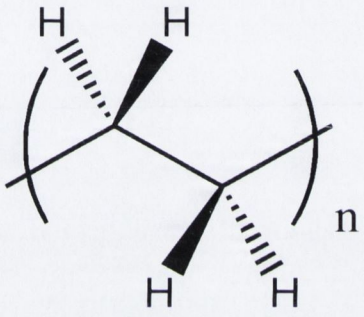

Figure 1.15 Molecular structure of polyethylene

1.4 Polymer Swelling

In polymers, and liquids or solids in general, the ability of molecules to separate from each other fully is restricted and the molecules in the polymer are generally held together quite well by intermolecular forces. These forces can be simply van der Vaals forces, hydrogen bonding, ionic bonding or covalent bonding depending on the molecules involved. To make a solution of a polymer these intermolecular forces must be overcome and the solvent must find its way between the adjacent molecules, disrupting the forces that hold them together, and then completely surrounding the solute molecules. The solvent molecules themselves also must remain separate from each other.

Normally when we add two molecular components together we can class them as soluble or insoluble. A good solution is generally achieved when the attractions between the molecules in the solvent and the solute are similar. If the polymer is

completely insoluble it can still undergo polymer swelling. This is when the interatomic distances between adjacent molecules of the polymer are increased but the polymer bonds are not fully broken. The selection of a good solvent for a particular polymer requires a method of quantifying the type and magnitude of the molecular interactions. If the strength and type of the interactions between the solvent and polymer can be matched then thermodynamically the conditions should provide attractive forces between them thereby initiating polymer swelling or solvation.

The ability of a solvent to increase the inter-atomic distances between molecules and cause swelling, or separate molecules completely from each other to make a solution, can be estimated by the Hildebrand cohesion parameter, δ (also called the Hildebrand solubility parameter). This is the square root of the cohesive energy density, c, given,

$$c = \frac{\Delta H - RT}{V_m}$$

where, ΔH is the heat of vaporization, R is the gas constant, T is the temperature and V_m is the molar volume, therefore,

$$\delta = \sqrt{c} = \left[\frac{\Delta H - RT}{V_m}\right]^{1/2}$$

Hildebrand parameters were first formulated in 1950[113] and give an extensive and qualitative indication of the behaviour of most solvent polymer systems. If the solvent and the polymer have cohesion energy densities that are close to each other they tend to be very soluble with one another or have very good swelling properties; however there can be some noticeable exceptions. If the polymer or solvent in the system is very polar or hydrogen bonded then the total cohesive energy may be made up by more than one component. This gives rise to incompatibilities in the Hildebrand parameters and so a further set of parameters is required for these systems, the most popular of these are called the Hansen parameters which were first formulated in 1967.[114] Generally the basis of Hansen Solubility Parameters is the assumption that the total cohesive energy parameter, δ_T, is made up of the different components parameters which are, additive contributions from non-polar (dispersion) interactions, δ_d, polar interactions, δ_p, and hydrogen bonding or other specific association interactions, δ_h.[115] The most general

cohesive energy interaction in all molecules is the non-polar interaction. These derive from the atomic forces in a molecule and as all molecules are made up of atoms, this attractive force is universal. The permanent dipole-dipole interactions result in the second polar cohesive energy interaction. There is some polar component to most molecules and the dipole moment is the main parameter used to calculate the interactions. Thirdly there is the hydrogen bonding cohesive energy interaction. Fundamentally this interaction occurs due to the presence of hydrogen bonds in a molecule. In general though, it is used to encompass the energies from all the other interactions not included in the first two components. Further, expanded studies resulting in increasing numbers of cohesion parameters have been carried out by Barton[116] among others. When we divide these by the molar volume as before, we end up with the square of each parameter, resulting in the formula,

$$\delta_T^2 = \delta_d^2 + \delta_p^2 + \delta_h^2$$

There are different methods[117] of calculating the individual Hansen parameters but ultimately the total cohesive energy, δ_T, by the Hansen parameter should be approximately equal to the Hildebrand parameter, δ. Both should give us a good understanding of how to swell a particular polymer with the equivalent solvent. In any system, if the Hildebrand parameters of both solvent and polymer are similar it indicates a much better swelling possibility. In systems where the two parameters are considerably different but we still see good solubility/swelling, an explanation may be found when the Hansen parameters are examined.

Table 1.2 Hildebrand and Hansen parameters for a range of solvents and polymers used in this work

Substance	Hildebrand Parameter	Hansen Parameters			
	δ(SI)	δ_d	δ_p	δ_h	δ_T
THF	18.6	16.8	5.7	8.0	19.4
Toluene	18.2	18.0	1.4	2.0	18.2
NMP	23.1	18.0	12.3	7.2	23.0
PE	18.1	18.0	0.0	2.0	18.1
PP	18.0	18.0	0.0	1.0	18.0
PET	20.0	18.0	6.2	6.2	20.0

1.5 Ultrasonic Treatment

Ultrasound is sound pitched above the level of human hearing and is currently used in a large industrial and academic scale for a large variety of applications which are far too numerous to mention here. Traditionally its use can be split into two fields. Firstly it may be used for non-destructive analytical techniques with high frequency (generally greater than 5 MHz) and low power. Secondly, it may be used to induce physical or chemical effects in a medium. This involves using lower frequencies (20 KHz to 2 MHz) but much higher powers.

As we discussed above nanotubes have an inherent property whereby they tend to bundle together in most solvents. Ultrasonication has been shown to be capable of de-aggregating and homogenising particles in a solvent[118] having little degradation effects. This has inevitable led to its being utilised to create stable dispersions of carbon nanotubes whether by surfactant[119,120] or solvent alone.[121] These capabilities are very important for the development of better stabilised nanotube dispersions and it has been shown that by employing the right solvent, long-term stable dispersions of nanotubes can be sustained in common solvents like NMP.[122] This is important for the development of nanotubes and the creation of homogenous nanotube-polymer composites. The ability of ultrasonication to greatly enhance swelling or dissolution of

polymers to create nanocomposites has also been explored.[123,124] Ultimately it is a highly adaptable technique which can be used to disperse nanotubes and swell or dissolve polymers quickly and easily. For higher and more focused, but less homogenous, energy dissipation an ultrasonic tip with a processor can be used. This is generally good for dispersing or dissolving materials but machine recommendations generally state it as being much less efficient at volumes of 10 cm^3 or more. For less focused and more homogeneous energy dissipation an ultrasonic bath is generally used.

1.6 Mechanical Analyses

Different materials will have different mechanical properties depending on their structure. There are a variety of mechanical properties that can be measured and a common systematic way of measuring the mechanical properties of a material is by measuring a stress-strain curve using tensile testing machinery. The stress (σ) on a material can be described as the average amount of force (F) per unit area (A),

$$\sigma = \frac{F}{A}$$

and is usually described as the strength of a material measured in Pascals. One Pascal is equivalent to one Newton per square metre. The strain is the geometrical measure of deformation representing the relative displacement of material and is dimensionless, usually measured in percentage increase (%) or fractional increase. If we measure the stress on a material as we vary the strain this results in a stress-strain curve (**Figure 1.16**). This can be used for comparison of mechanical properties of many different materials and some of the more important features of the curve are marked. The elastic modulus describes the tendency of a substance to deform elastically (non-permanently) when force is applied to it. It can be defined as the slope of the stress-strain curve in the elastic deformation region. This region is defined as the part of the curve below point **A** in **Figure 1.16**. The Young's modulus is this ratio when the force is applied in the axial direction and the shear modulus is the elastic modulus when acted on by opposing forces and can be referred to as rigidity.

The tensile strength is the maximum amount of stress that is required to permanently deform or break a material. This can be referred to as the yield strength, which is the stress at which a material strain changes from plastic deformation to elastic deformation

and indicates the material will not return to its original form when stress is released after this point. The upper and lower yield strengths can be found at points **B** and **C** respectively. The ultimate tensile strength is the maximum stress a material can withstand under tension and can be seen as point **D** on the curve. It is the highest stress coordinate reached on the stress-strain curve. The breaking strength is represented by the stress achieved at point **E**, the breaking point of the material. Point **E** also represents the maximum strain achieved on the strain axis.

Finally we can find the toughness of a material by taking the area under the stress-strain curve from the origin (**O**) to the breaking point (**E**). Toughness is a materials resistance to fracture when it is stressed. It is the amount of energy per unit volume that a material can absorb before fracturing and is usually measured in Joules per millimetre cubed (J/mm^3).

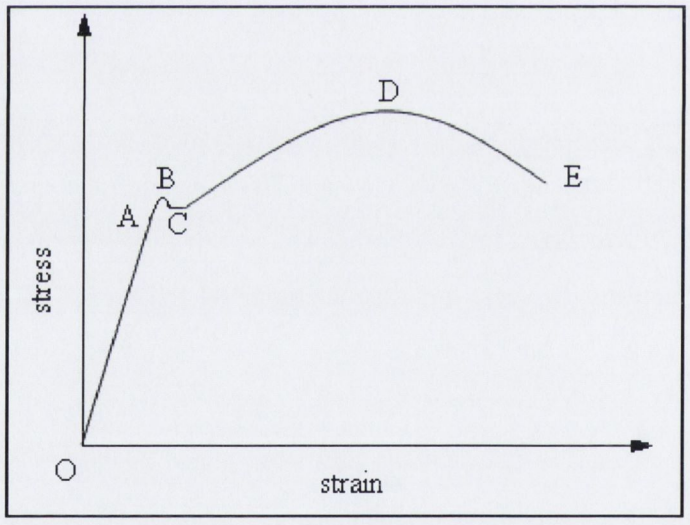

Figure 1.16 A typical stress-strain curve theoretically obtained from a ductile material stretched under tension. The curve extends from the origin (**O**) to the breaking point (**E**) also including the limit of elasticity (**A**), upper and lower yield stresses (**B** and **C**) and finally the maximum stress point (**D**)

1.7 Aims of Research

The main objective of our research is to develop new carbon nanotube-polymer composites with enhanced mechanical and/or electrical properties. Firstly we are going to explore some new approaches in the functionalisation of nanotubes, to create a more chemically and physically compatible nanotube for composite fabrication. This part of the work will be focused on the development of new Kevlar coated carbon nanotubes. The functionalised nanotubes will be examined and compared to pristine nanotubes using a number of instrumental techniques including TEM, Raman spectroscopy and sedimentation analysis. We then aim to prepare nanotube-polymer composites by the drop cast method and analyse them further, ultimately following-on with mechanical testing. Reinforcement will be attempted on a range of everyday polymers for which mechanical properties are important: polystyrene, polyvinyl acetate, polyvinyl alcohol and polyvinyl chloride. Fundamentally using the drop cast technique we are going to incorporate functionalised nanotubes into polymers expecting to produce composite materials with improved mechanical properties. Mechanical properties of the polymer composite films will then be investigated using a tensile tester.

Furthermore, we plan to use a novel technique for the preparation of nanotube composites by swelling of polymer films or fibers under ultrasound in dispersions of carbon nanotubes. Currently all existing approaches to the fabrication of nanotube-polymer composites involve complicated, expensive, time-demanding processing techniques such as solution casting, melting, moulding, extrusion, and in situ polymerisation. In addition all these technologies need large amounts of expensive carbon nanotubes to be used. In all of these techniques nanotubes must either be incorporated into a polymer solution, molten polymer or mixed with the initial monomer before the formation of the final product (e.g. yarn, ribbon, film, etc.). Our new technology is expected to allow the incorporation of nanotubes into already formed polymer products by swelling them in carbon nanotube suspensions. Using this approach we expect to obtain new polymer composites with enhanced mechanical and electrical properties by these methods and investigate these properties via comprehensive, systematic analysis of the products. Initially we plan to focus our research on a mechanically very important polymer Kevlar. After that we are going to develop this approach for modification of other commercially important polymers such as polyethylene, polypropylene and polyethylene terephthalate. Ultimately we aim to

develop a novel post processing method for incorporation of nanotubes into preformed polymer materials to fabricate new polymer composites with a multitude of potential applications.

We hope that successful outcome of this research will contribute to the further development of nanoscale physics and chemistry and augment the expansion of nanotechnological applications.

References

[1]M. Reibold, P. Paufler, A.A. Levin, W. Kochmann, N. Pätzke, D.C. Meyer, *Nature*, **444**, 286 (2006)

[2]H.W. Kroto, J. R. Heath, S. C. O'Brien, R. F. Curl and R. E. Smalley, *Nature,* **318**, 162 (1985)

[3] www.nims.go.jp/eng/news/nimsnow/Vol3/No3/p5.html

[4]S. Ijima, *Nature,* **56**, 354 (1991)

[5] www.ncnr.nist.gov

[6]J. C. Kearns, R. L. Shambaugh, *J. Appl. Polym. Sci.*, **86**, 2079 (2002).

[7]www.n-tec.no

[8]A.G. Rinzler, J. Liu, H. Dai, P. Nikolaev, C.B. Huffman, F.J. Rodriguez-Macias, *Appl. Phys. A,* **67**, 29 (1998)

[9]P. Nikolaev, M.J. Bronikowski, R.K. Bradley, F. Fohmund, D.T. Colbert, K.A. Smith, *Chem. Phys. Lett.* **313**, 91 (1999)

[10]Z.F. Ren, Z.P. Huang, J.W. Xu, J.H. Wang, P. Bush, M.P.etal. Siegal, *Science* **282**, 1105 (1998)

[11]Z.P. Huang, J.W. Xu, Z.F. Ren, J.H. Wang, M.P. Siegal and P.N. Provencio , *Appl. Phys. Lett.* **73**, 26 (1998)

[12]J. Hone, M. Whitney, A. Zettle, *Synth. Metals,* **103**, 2498 (1999)

[13]M. D. Coburn, D.G. Ott, *JACS,* **27**, 1941 (1990)

[14]P. M. Ajayan, O. Z. Zhou, *Carbon Nanotubes,* **80**, 391 (2001)

[15]P. Avouris, *Chemical Physics,* **281**, 429 (2002)

[16] D. Hongjie, *Acc Chem Res* **35**, 1035 (2002)

[17]S. Frank, P. Poncharal, Z.L. Wang, W.A. de Heer *Science,* **280,** 1744 (1998)

[18]S. Sanvito, Y.K. Kwon, D. Tomanek, C.J. Lambert, *Phys. Rev. Lett.,* **84,** 1974 (2000)

[19]R. Krupke, F. Hennrich, H. Löhneysen and M.M. Kappes, *Science* **301**, 344 (2003)

[20]E. Dujardin, T.W. Ebbesen, A. Krishnan, P.N. Yianilos, M.M.J. Treacy, *Phys. Rev. B,* **58**, 14013 (1998)

[21]M. Yu, O. Lourie, M.J. Dyer, T.F. Kelly, R.S. Ruoff, *Science* **287**, 637 (2000)

[22]S. Xie, W. Li, Z. Pan, B. Chang, L. Sun, *J Phys Chem Solids* **61**, 7 (2000)

[23]M.F. Yu, B.S. Files, S. Arepalli, R.S. Ruoff, *Phys. Rev. Lett.,* **84**, 5552 (2000)

[24]M.J. Beircuk, M.C. Llaguno, M. Radosavjevic, J.K. Hyun, J.E. Fischer, A.T. Johnson, *Appl. Phys. Lett.,* **80**, 2767 (2002)

[25]C. Wei, D. Srivastava, K. Cho, *Nano. Lett.*, **2**, 647 (2002)

[26]www.nanopedia.case.edu

[27]J. Liu, A.G. Rinzler, H.J. Dai, J.H. Hafner, R.K. Bradley, P.J. Boul, A. Lu, T. Iverson, K. Shelimov, C.B. Huffman, F. Rodriguez-Macias, Y.S. Shon, T.R. Lee, D.T. Colbert, R.E.Smalley, *Science,* **280,** 1253 (1998)

[28]J. Liu, M.J. Casavant, M. Cox, D.A. Walters, P. Boul, W. Lu, A.J. Rimberg, K.A. Smith, D.T. Colbert, R.E. Smalley, *Chem. Phys. Lett.*, **303**, 125 (1999)

[29]C.A. Dyke, J.M. Tour, *Chem. Eur. J.*, **10**, 81 (2004)

[30]D.J. Hornbaker, S-J. Kahn, S. Misra, B.W. Smith, A.T. Johnson, E.J. Mele, D.E. Luzzi, A. Yazdani, Science, **295**, 828 (2002)

[31]A. Hersch, Angew. Chem. Int. Ed., **41**, 1853 (2002)

[32]A.C. Dillon, T. Gennett, K.M. Jones; J.L. Alleman, P.A. Parilla, M.J. Heben, *Adv. Mater.* **11**, 1354 (1999)

[33]L. Vaccarini, C.Goze, R. Aznar, V. Micholet, C. Journet, P. Bernier, *Synth. Met.* **103**, 2492 (1999)

[34]S. Niyogi, M.A. Hamon, H. Hu, B. Zhao, P. Bhowmik, R. Sen, M.E. Itkis, R.C. Haddon, *Acc. Chem. Res.* **35**, 1105 (2002)

[35]J. Chen, M.A. Hamon, H. Hu, Y. Chen, A.M. Rao, P.C. Eklund, R.C. Haddon, *Science*, **285**, 95 (1998)

[36]M.A. Hamon, H. Hui, P. Bhowmik, H.M.E Itkis, R.C. Haddon, *App. Phys. A: Mat. Sci. Process*, **74**, 333 (2002)

[37] B. Li, Z. Shi, Y. Lian, Z. Gu, *Chem. Phys. Lett.*, 598 (2001)

[38] F. Pompeo, D.E. Rescasco, *Nano. Lett.*, **2**, 369 (2002)

[39]P.J. Boul, J. Liu, E.T. Mickelson, C.B. Huffman, L.M. Ericson, I.W. Chiang, K.A. Smith, D.T. Colbert, R.H. Hauge, J.L. Margave, R.E. Smalley, *Chem. Phys. Lett.* **310**, 367 (1999)

[40]G. van Lier, C.P Ewels, F. Zuliani, A. De Vita, J-C Charlier, *J. Phys. Chem. B* **109**, 6153 (2005)

[41]S. Niyogi, M.A. Hamon, H. Hu, B. Zhao, P. Bhowmik, R. Sen, M.E. Itkis, R.C. Haddon, *Acc. Chem. Res.* **35**, 1105 (2002)

[42]A.A. Koos, Z.E. Horvath, Z. Osvath, L. Tapaszto, K. Niesz, Z. Konya, I. Kiricsi, N. Grobert, M. Ruhle, L.P. Biro, *Mat. Sci. and Eng.*, **23,** 1007 (2003)

[43]C. Zhao, L. Ji, H. Liu, G. Hu, S. Zhang, M. Yang, Z. Yang, *J. Solid State Chem.*, **177,** 4394 (2004)

[44]M. Holzinger, J. Steinmetz, D. Samaille, M. Glerup, M. Paillet, P. Bernier, L. Ley, R. Graupner, *Carbon,* **42,** 941 (2004)

[45]A. Felten, C. Bittencourt, P. Montes, G. van Lier, J. Charlier, J, Pireaux, *J. App. Phys.* **98**, 74308 (2005)

[46]R . Blake, Y.K Gun'ko, J.N Coleman, M. Cadek, A. Fonseca, J.B Nagy, W.J Blau *J. Am. Chem. Soc.* **126**, 10226 (2004)

[47]R. Blake, J.N. Coleman, M.T Byrne, J.E McCarthy, T.S Perova, W.J Blau, A. Fonseca, J.B Nagy, Y.K. Gun'ko, *J. Mater.Chem.* **16**, 4206 (2006)

[48]R. Graupner, J. Abraham, D. Wunderlich, A. Vencelova, P. Lauffer, J. Rohrl, M. Hundhausen, L. Ley A. Hirsch, *J. Am. Chem. Soc.* **128**, 6683 (2006)

[49]D. Wunderlich, F. Hauke, A. Hirsch *Chem. Eur. J.* **14**, 1607 (2008)

[50]S. Banerjee, T. Hemraj-Benny, S.S. Wong *Adv. Mater.,* **17,** 17 (2005)

[51]M.S. Dresselhaus, G. Dresselhaus, K. Sugihara, I.L. Spain, H.A. Goldberg, *Graphite fibres and filaments*, Springer (1988)

[52]N.M. Rodriguez, *J Mater Res* **8**,3233 (1993)

[53]D. Chung, *Carbon fibre composites*, Butterworth-Heinemann (1994)

[54]H.L. Cox, , *Br J Appl Phys* **3**, 72 (1952)

[55]J. Bai, *Carbon*, **41,** 1325 (2003)

[56]C.W. Nan, Z. Shi, Y. Lin, *Chem. Phys. Lett.,* **375**, 666 (2003)

[57]M.A.L. Manchado, L. Valentini, J. Biagiotti, J.M. Kenny, *Carbon* **43**, 1499 (2005)

[58]H. Krenchel, *Fibre reinforcement*, Akademisk Forlag, (1964)

[59]P.M. Ajayan, O. Stephan, C. Colliex, D. Trauth, *Science*, **265**,1212 (1994)

[60]H.D. Wagner, O. Lourie, Y. Feldman, R. Tenne, *Appl. Phys. Lett.*, **72** (1998)

[61]O. Lourie, D.M. Cox, H.D. Wagner, *Phys Rev Lett* **81**, 1638 (1998)

[62]L.S. Schadler, S.C. Giannaris, P.M. Ajayan, *Appl Phys Lett* **73**, 3842 (1998)

[63]W.Z. Li, S.S. Qie, L.X. Qian, B.H. Chang, B.H. Zhous, W.Y. Zhou, R.A. Zhao, G. Wang, *Science,* **274**, 1701 (1996)

[64]R. Saito, G. Dresselhaus M.S. Dresselhaus, *Physical Properties of Carbon Nanotubes*, Imperial College Press, (1998)

[65]J.X. Li, Y. Zhang, *Physics E* **28** (2005)

[66]L. Jin, C. Bower, O. Zhou, *Appl Phys Lett* **73**, 1197 (1998)

[67]M.S.P. Shaffer, X.Fan, A.H. Windle, *Carbon,* **36**, 1603 (1998)

[68]M.S.P. Shaffer, A.H. Windle, *Adv. Mater.,* **11**, 937 (1999)

[69]D. Qian, E.C. Dickey, R. Andrews, T. Rantell, *Appl. Phys. Lett.,* **76**, 2868 (2000)

[70]R. Andrews, D. Jacques, D. Qian, T. Rantell, *Acc. Chem. Res.,* **35**, 1008 (2002)

[71]Z. Jin, K. Pramoda, G. Xu, S.H. Goh, *Chem. Phys. Lett.*, **337**, 43 (2001)

[72]E.T. Thostenson, T-W. Chou, *J Phys D: Appl Phys.*, **16**, L77 (2002)

[73]R. Haggenmueller, H.H. Gommans, A.G. Rinzler, J.E. Fischer, K.I. Winey, *Chem. Phys. Lett,* **330,** 219 (2000)

[74]P.M. Ajayan, L.S. Schadler, C. Giannaris and A. Rubio, *Adv Mater* **12**, 750 (2000)

[75]G. Viswanathan, N. Chakrapani, H. Yang, B. Wei, H. Chung, K. Cho, C.Y. Ryu, P.M. Ajayan, *J. Am. Chem. Soc.* **125**, 9258 (2003)

[76]K. Fu, W. Huang, Y. Lin, L.A. Riddle, D.L. Carroll, Y.P. Sun, *Nano Lett.* **1**, 439 (2001)

[77]J.N. Coleman, W.J. Blau, A.B. Dalton, E. Munoz, S. Collins, B.G. Kim, J. Razal, M. Selvidge, G. Vieiro, R.H. Baughman, *Appl Phys Lett* **82**, 1682 (2003)

[78]B. Vigolo, A. Penicaud, C. Coulon, C. Sauder, R. Pailler, C. Journet, P. Bernier, P. Poulin, *Science* **290**, 1331 (2000)

[79]A.B. Dalton, S. Collins, E. Munoz, J.M. Razal, V.H. Ebron, J.P. Ferraris, J.N. Coleman, B.G. Kim, R.H. Baughman, *Nature* **423**, 703 (2003)

[80]M. Shaffer, I.A. Kinloch, *Comps. Sci, and Tech.,* **64,** 2281 (2004)

[81]D.T. Colbert, *Plastic Additives Comp.,* **18** (2003)

[82]B.E. Kilbride, J.N. Coleman, J. Fraysse, P. Fournet, M. Cadek, A. Drury, S. Hutzler, S. Roth, W.J. Blau, *J. Appl. Phys.,* **92,** 4024 (2002)

[83]P.E. Cassidy, *Thermally Stable Polymers,* Dekker, (1980)

[84]www2.dupont.com/Kevlar/en_US/assets/downloads/KEVLAR_Technical_Guide.pdf

[85]DuPont, *Kevlar Technical Guide*, DuPont Advanced Fibre Systems (2000)

[86]Q. Zhang, Y. Liang, S.B. Warner, *J. of Polym. Sci.* **32**, 2207 (1994)

[87]Y. Rao, A.J. Waddon, R.J. Farris, *Polymer*, **13**, 5937 (2000)

[88]K.G. Lee, R. Barton Jr., J.M. Schultz, *J of Polym Sci B: Poly. Phys.*, **33**, 1 (1995)

[89]J.F. Graham, C. McCague, O.L. Warren, P.R. Norton, *Polymer*, **41**, 4761 (2000).

[90]N. Nagashima, S. Matsuzawa, M. Okazaki. *J. Appl. Polym. Sci.* **62**, 1551 (1996)

[91]D.L. Cincera, *Kirk-Othmer Encyclopedia of Chemical Technology, 3d Ed.* John Wiley and Sons, **23**, 848 (1978)

[92]H.N. Friedlander, H.E. Harris, J.G. Pritchard. *J. Polym. Sci. A* **1**, 649 (1966)

[93]F.L Marten, *Encyclopedia of Polymer Science and Engineering*, Wiley Interscience, **17**, 167 (1989)

[94]R.F. Boyer, *Encyclopedia of Polymer Science and Technology*, John Wiley and Sons, **13** (1970)

[95]J.E. Mark, *Physical Properties of Polymers Handbook*, AIP Press, Woodbury (1996)

[96]J. Brandrup, E.H. Immergut, *Polymer Handbook, 3d Ed.* Wiley Interscience, (1989)

[97]D.W.V Krevelen, P.J. Hoftyzer. *Properties of Polymers: Correlations with Chemical Structure*, Elsevier (1972)

[98]J.T. Lutz, *Degradation and Stabilization of PVC*, Elsevier Applied Science Publishers, 264, (1984)

[99]I.I. Rubin, *Handbook of Plastics Materials and Technology,* John Wiley and Sons, 644 (1990)

[100]R.E. Wilfong, *J. Polym. Sci.* **54**, 385 (1961)

[101]H.H. Yu, S-J. Hwang, M-C. Tseng, C.-C. Tseng, *Opt. Commun.* **259**, 187 (2006)

[102]D-H. Kim, M-R. Park, H-J. Lee, G-H. Lee, *Appl. Surf. Sci.* **253**, 4463 (2006)

[103]K. Choi, J. E. Spruiell, J. L. White. *J. Polym. Sci., Polym. Phys. Ed.*, **20**, 27 (1982)

[104]P.H. Lindenmeyer, S. Lustig, *J. Appl. Polym. Sci.* **9**, 227 (1965)

[105]A. Gupta, D. M. Simpson, I. R. Harrison, *J. Appl. Polym. Sci.*, **50**, 2,085 (1993)

[106]L. Mandelkern, , J. Maxfield. *J. Polym. Sci., Polym. Phys. Ed.*, **17**, 1913 (1979)

[107]J.P. Blitz, D.C. McFaddin. *J. Appl. Polym. Sci.* **51**, 13 (1994)

[108]E.M.C. Cernia, A.S. Mancini, *J. Appl. Polym. Sci.* **12**, 789 (1968)

[109]A.F.M. Barton, *CRC Handbook of Polymer-Liquid Interaction Parameters and Solubility Parameters,* CRC Press (1990)

[110]R.L. Boysen, *Kirk-Othmer Encyclopedia of Chemical Technology, 3d Ed.*, Wiley-Interscience, **16** (1981)

[111]D.V. Bibee, *Handbook of Plastics Materials and Technology*, John Wiley and Sons, (1990)

[112]F.C. Stehling, C.S. Speed, L. Westerman, *Macromolecules*, **14**, 698 (1981)

[113]J.H. Hildebrand, R.L. Scott, *The Solubility of Nonelectrolytes, 3rd Ed.*, Reinhold, (1950)

[114]C.M. Hansen, *J. Paint Technology*, 39, **104** (1967)

[115] C. Hansen, *Hansen Solubility Parameters—a User's Handbook*, CRC Press, (1999)

[116]A.F.M. Barton, *CRC Handbook of Solubility Parameters and Other Cohesion Parameters,* CRC Press (1983)

[117]F. Gharagheizi, M. Sattari, M. T. Angaji *Polymer Bulletin.*, **57**, 377 (2006)

[118]F. P. Capote, M.D.L. de Castro, *Ultrasound in analytical chemistry*, Elsevier (2007)

[119]D. Mawhinney, V. Naumenko, A. Kuznetsova, J. Yates, J. Liu, R. Smalley, *Chem. Phys. Lett.* **324**, 213 (2000)

[120]X. Liu, T. Pichler, M. Knupfer, M.S. Golden, J. Fink, H. Kataura and Y. Achiba, *Phys. Rev. B*, **66**, 45411 (2002)

[121]J.S. Lauret, C. Voisin, G. Cassabois, P. Roussignol, C. Delalande, A. Filoramo, L. Capes, E. Valentin, O. Jost, *Physica E*, **21**, 1057 (2004)

[122]S. Giordani, S.D. Bergin, V. Nicolosi, S. Lebedkin, M.M. Kappes, W.J. Blau, J.N. Coleman, *Physica B*, **243**, 2058 (2006)

[123]S.T. Lim, H.J. Choi, M.S. Jhon, *J. Ind. Eng. Chem.* **9**, 1 (2003)

[124]H. Ahmad, K. Tauer, *Progr. Colloid Polym. Sci.* **124**, 107 (2004)

Chapter 2

Kevlar Functionalised Nanotubes For Polymer Reinforcement

2.1 Introduction

Due to the extraordinary mechanical properties and very low densities of carbon nanotubes, they are expected to play an important role in the future of high–tech polymer composites. Nanotubes are able to withstand considerable bending yet return to their original shape.[1,2] This property means they will, in theory, be able to absorb a large amount of energy and it is hoped that the addition of nanotubes to polymers will create stronger composites able to withstand extreme physical conditions. With an exceeding large range of polymeric materials available, and the fact that they are currently used in a wide-array of products, the potential for the application of nano-composite polymers is almost beyond imagination.

As we discussed in the introduction the mechanical properties of nanotubes are extraordinary with both very high strength[3,4] and moduli[5,6,7] reported numerously in the literature. They have already been shown to improve the mechanical properties of polymers when added to them[8] but there is still much research to be done in this area. One of the problems in improving the strengths of carbon nanotube polymer composites lies in the ability to achieve good interfacial stress transfer between the nanotube and polymer matrix.

Theoretically a nanotube side-wall surface is just the same as a graphite sheet, both containing hexagonally arranged sp^2 hybridised carbon atoms. Therefore, at the molecular level, this surface would be expected to be relatively chemically inactive. However in reality they tend to contain defects in the form of 5-,7- and 8-membered rings along with carboxylic acid functionalities.[9] Although we would imagine that defects may reduce the mechanical properties of an individual nanotube it may actually result in an increase in the mechanical properties of a composite material as a whole. This can be explained by the fact that inherent in their chemical structure, pure carbon nanotubes would be expected to be atomically very smooth. As we discussed in the Introduction in **Chapter 1** if we can decrease their smoothness by introducing defects and functionalities it may give them a better 'grip' in the polymer structure.

Another factor for which we have to take account in making nanotube - polymer composites is in finding a way to transfer the stress between the polymer and nanotube, which has much better mechanical characteristics. When added to a polymer, nanotubes

generally might not interact strongly with the individual polymer chains. If we could functionalise the nanotubes so that they would have a stronger interaction with the polymer chains, it may result in better interfacial stress transfer. This would further exploit the mechanical properties of the nanotubes.

Functionalisation of nanotubes is very important for their processing and manipulation[10,11] as currently applications of carbon nanotubes are limited mostly by their insolubility and their low miscibility with most materials. Choosing the functionality is another important step. As it was mentioned above nanotubes generally contain carboxylic acid functionalities on their surface. These are mainly located on the nanotube tips and on side-wall defects. We would expect these functionalities to give some beneficial effect when incorporating the nanotubes in a composite and depending on the desired effect the selection of nanotube functionality is of paramount importance.

2.2 Aims of This Work

The main aim of this part of the work is to prepare and investigate Kevlar functionalised carbon nanotubes (FNTs) as new additives for the reinforcement of various polymer materials. It is expected that the nanotube functionalisation will result in a better grip for nanotubes in the polymer matrix when compared to pristine nanotubes (PNTs).

Kevlar is a well known high-strength polymer, which has been used for a variety of applications including bullet-proof vests, protective clothing and high-performance composites for aircraft and automotive industries.[12,13] Kevlar is comparable to steel in strength, yet has only a fraction of the density. The main aim of our experiment was to combine two ultrastrong materials such as Kevlar and nanotubes in one nanocomposite and investigate this new nano-material as an additive for polymer reinforcement. To achieve this goal we have developed a new nanotube processing procedure, which involves *in situ* purification and Kevlar coating of carbon nanotubes. It was hoped that if we can functionalise the nanotubes with Kevlar, its high strength and stiffness might complement the properties of the matrix polymer and it could act as a "stress-bridge" between the polymer and the nanotube. This will hopefully give an increase in the effect that the nanotubes had on the polymer's strength and modulus.

2.3 Synthesis of Kevlar

Kevlar is an extremely strong and light polymer, which has a very high melting point (550°C) and which is insoluble in all common solvents. A more comprehensive discussion of its structure and properties can be found in **Chapter 1**. It is also a very chemically resistant material. We expected that Kevlar, which contains aromatic groups in the main backbone, would interact with carbon nanotubes *via* π-π interactions wrapping the nanotubes. Also carboxylic groups on the tips of the nanotubes may be linked to Kevlar chains via hydrogen and covalent (e.g. amido-) bonds. That should result in functionalisation of the carbon nanotubes and coating them with Kevlar giving novel nanotube-Kevlar composite materials, which might be potentially used for polymer reinforcement.

The Kevlar was prepared according to published procedure.[14] This was achieved by a polycondensation reaction between terephthaloyl chloride and *p*-phenylenediamine. The synthesised Kevlar was characterised by elemental analysis, TGA and Raman spectroscopy. Raman spectrum (**Figure 2.1: Pure Kevlar**) of Kevlar has shown peaks at 1182 cm^{-1}, 1276 cm^{-1}, 1323 cm^{-1}, 1516 cm^{-1}, 1613 cm^{-1} and 1651 cm^{-1}. This Raman spectrum definitively matched those reported by Prasad and Grubb.[15] Elemental analysis was carried out and returned values of 62 % Carbon, 11.4 % Nitrogen and 4.9 % Hydrogen. The percentage of Oxygen in the sample could not be measured as the sample was burned in an Oxygen atmosphere. The theoretical values for Kevlar are 70.6% Carbon, 11.8% Nitrogen, and % Hydrogen. The discrepancies between theoretical and actual values may be due to residual water in the sample, which would cause the value for Hydrogen to be slightly high and the other values to be slightly low.

The derivative of the TGA curve shows an individual broad peak which reaches its maximum at 550°C (**Appendix**). This peak represents its decomposition temperature and is consistent with similar studies of Kevlar reported in the literature.[16]

2.4 Preparation and Investigation of Kevlar Functionalised Carbon Nanotubes

2.4.1 Functionalisation of thin Multi-walled nanotubes

Nanocyl thin multi walled nanotubes are prepared by chemical vapour deposition and were chosen as they are a commercially readily available source of systematically produced nanotubes. Thin nanotubes were selected so as to give potentially less disruption to the polymer matrix but also their multi-walled structure gives them a better ability to withstand considerable degradation without jeopardising their mechanical integrity. The Nanocyl nanotubes were functionalised and purified by heating Kevlar with Nanocyl thin multi-walled carbon nanotubes) in the mixture of sulfuric (20ml, 95%) and nitric acids (70ml, 65%) under reflux at 100°C for up to 24 hours similar to previously published purification methods.[17] Samples were extracted at time periods of 2, 4, 6, and 12 hours. After 24 hours complete degradation of all materials in the vessel had occurred. The process resulted in purified and Kevlar coated carbon nanotubes. These nano-composites were analysed by transmission electron microscopy (TEM), thermogravimetric analysis (TGA), Raman and Infrared Spectroscopy.

2.4.2 Infrared and Raman spectroscopy studies

In Fourier transform infra-red spectra (FTIR) spectra, pristine nanotubes in general show very few peaks, if any, however FTIR of FNTs show the presence of characteristic Kevlar bands in the range of 400 – 1700 cm^{-1} and 2500 – 3000 cm^{-1} for the samples refluxed over 2, 4 and 6 hours with the 2 hour samples having the most intensive peaks (**Figure 2.1**). The 12 hour sample show little presence of Kevlar bands indicating decomposition of the Kevlar.

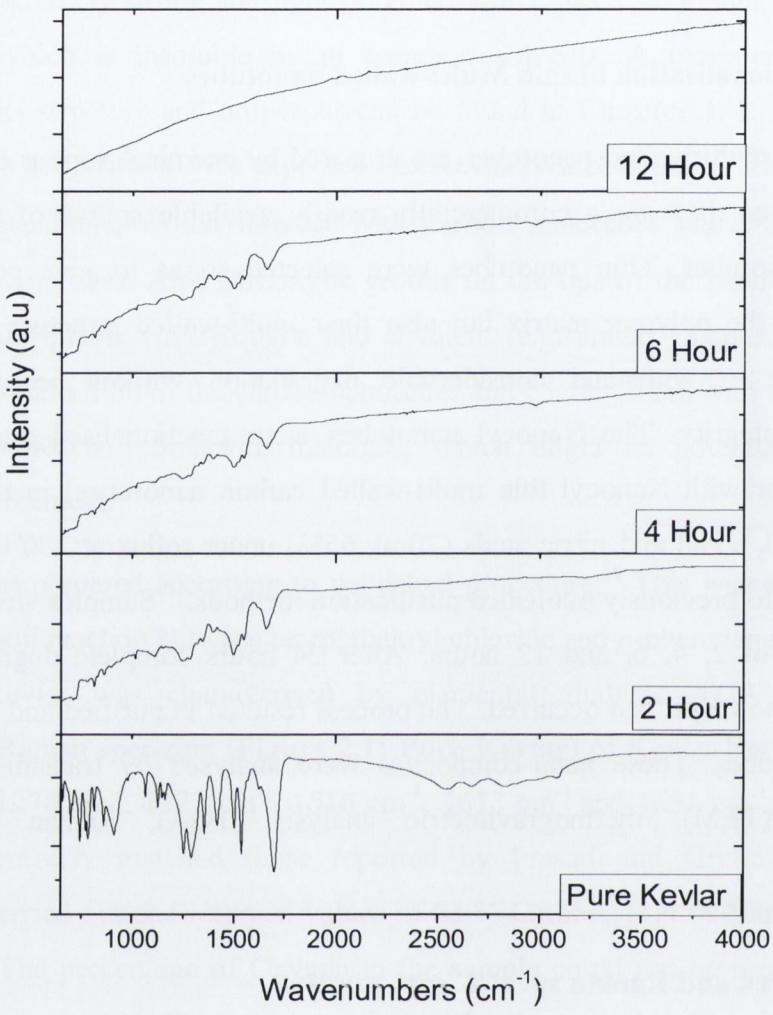

Figure 2.1 Infrared spectra of nanotubes heated for various periods of time (0, 2, 4, 6 and 12 hours) under reflux in a mixture of nitric and sulfuric acid in the presence of Kevlar

Raman spectroscopy can give information[18] about the structure of nanotubes and it can also potentially help to evaluate the degree of nanotube functionalisation.[19,20] When we analyse the PNTs (**Figure 2.2: 0 hours**) we see two peaks at 1335cm^{-1} and 1585 cm^{-1} These correspond to the D and G band respectively. The G band in the spectrum corresponds to that of sp^2 hybridised carbons and is a tangential stretching mode for the carbon-carbon bond. The G band is an intrinsic feature of carbon nanotubes in general, although it is also present in fullerenes and other carbon-based

materials. It can be correlated to the area of graphitisation of the nanotube and from it the degree of graphitisation can be estimated. Large G bands indicate that structurally the nanotube contains a lot of hexagonal carbon rings and conversely a smaller peak indicates less structure indicating a large amount of 5 and 7 membered rings. When the G band decreases it indicates a decrease in structure usually *via* degredation. Conversely, the D band relates to the sp^3 carbon atoms and can be found in any graphitic material. It is the dispersive disorder-induced band, and when it is large it gives an indication of a lot of impurity and other carbon in the sample which is not integrated in the nanotube structure. When we compare the two bands, therefore, we get an indication of how structured and pure the nanotube sample is. The Raman spectra of the FNTs showed the presence of both the nanotubes bands at approximately 1335cm^{-1} and 1585 cm^{-1}, although some shifting is evident depending on the reflux time. We also can see evidence of Kevlar bands (1180, 1276, 1326, 1610 and 1652 cm^{-1}) demonstrating the dual nature of the FNTs. Due to the significant overlap of the D and G bands of the nanotubes with Kevlar peaks it is quite difficult to judge the changes in the intensity of these bands. However, there is a clear difference between the pristine and Kevlar functionalised nanotubes. The spectra taken at 2, 4 and 6 hours of the treatment show the presence of both Kevlar and nanotube peaks. However, when we analyse the spectrum from the sample refluxed for the longest time (12 hours), we find that there remains some highly degraded Kevlar in the sample and we are left with nanotubes that have a different spectrum to the original and previous ones. When the peak areas are compared we can get a ratio between the D and G band. For the pure nanotubes this is approximately 1:1.44 for D:G band. After the longest heating under reflux the ratio changes to 1.55:1. This large increase in the comparative areas indicates that there is a large increase in the amount of disorder in the nanotubes. This is to be explained by the degradation of nanotubes given the highly oxidising acidic environment of the reaction. We cannot infer too much from the other sample as the peaks of the D and G bands, although still present, cannot be discerned accurately from the Kevlar peaks.

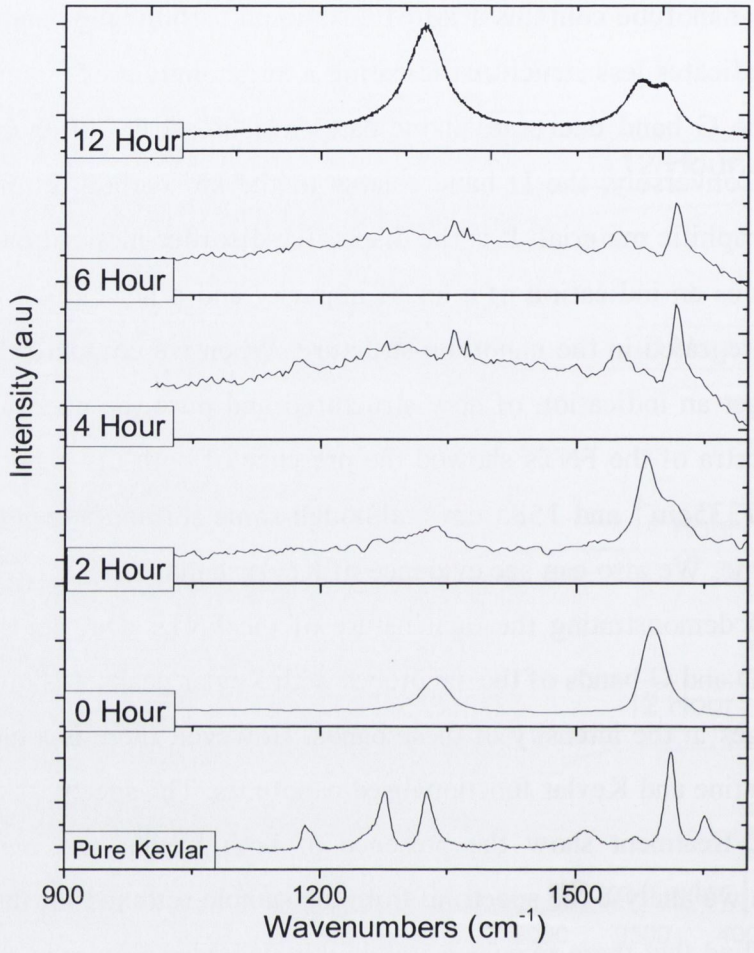

Figure 2.2 Raman spectra of nanotubes heated for various periods of time (0, 2, 4, 6 and 12 hours) under reflux in a mixture of nitric and sulfuric acid in the presence of Kevlar

2.4.3 Transmission electron microscopy analysis

The Transmission Electron Microscopy (TEM) images **(Figure 2.3 A-D)** show that the functionalised nanotubes have considerably larger diameters than pristine ones. This increase in diameter can be attributed to the Kevlar coating. The thickness increased from an average of 12 nm (±2.8 nm) before, to 37 nm (±6.5 nm) after the 2 hour treatment, giving an overall increase of 200%. When we look at the sample after 4 hrs

of the treatment we see a similar increase in nanotube thickness of 34 nm (±5.1 nm). It also appears to show a less uniform or solid coating of the nanotubes than the 2 hour. Ultimately when we look at the sample after 12 hr we can see that both nanotubes and the coating appear to be overwhelmingly degraded. There is to be little structural integrity to the nanotubes and we generally find clumps of material located on the nanotube periphery. If we look at the size of the nanotube, where it appears to be structurally sound, we find that it seems to have reverted mostly back to the original size, indicating that there remains little or no functionality bound to its surface. Overall when we analyse the TEM images we find that we achieve good functionalisation of the nanotubes after a short period of approximately 2 hours. This is followed by a general degradation of the polymer to the point where ultimately it is almost completely oxidised in the harsh acidic and oxidising environment.

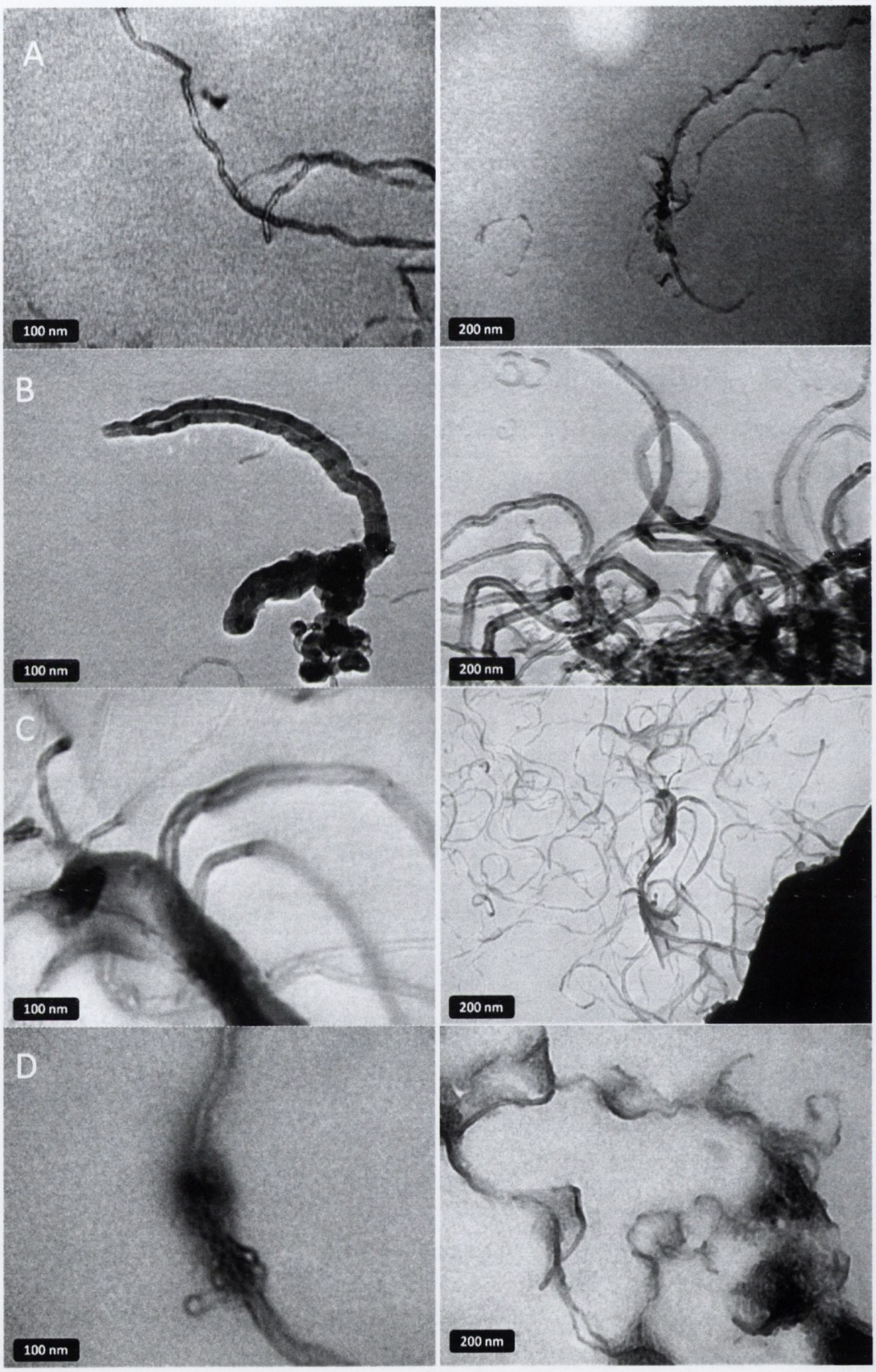

Figure 2.3 TEM images of refluxed nanotubes 0 hr (**A**), 2 hr (**B**), 4 hr (**C**) 12 hr (**D**)

2.4.4 Thermogravimetric analysis

The thermogravimetric analysis (TGA) of the original nanotubes (**Figure 2.4: 0 hours**) shows a broad peak at 605 °C but after the two hour reflux we see a narrowing of the peak and a shift downwards. This indicates the removal of impurities from the nanotubes. The two hour peak also shows the formation of a shoulder which corresponds fairly well with the decomposition of Kevlar at 500 °C. After longer reflux times we can see the formation of a second peak at a much lower temperature of approximately 300 °C. This represents further decomposition of the Kevlar and we can see the peak increase in size as we increase the reflux time. This is to be expected as the highly oxidising environment created by the combination of acids will break down the structure of both the nanotubes and the Kevlar, but initially it creates a much greater opportunity for functionalisation.

Overall the TGA curves showed the nanotube decomposition peak appearing at a lower temperature for each sample, demonstrating degradation of structure. The peak for Kevlar is also shifted downward with the second, further decomposed peak found at an even lower temperature. Eventually after 12 hours we see very small presence of nanotube or Kevlar material in the sample.

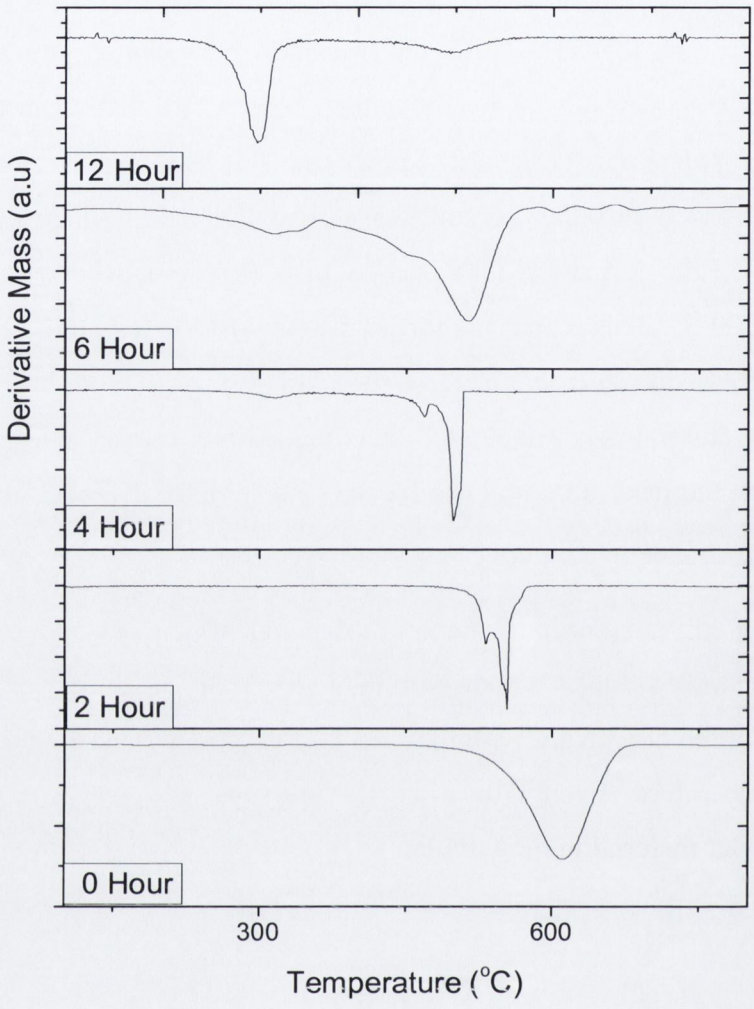

Figure 2.4 TGA curves of nanotubes heated for various periods of time (0, 2, 4, 6 and 12 hours) under reflux in the mixture of acids the presence of Kevlar

2.5 Preparation of Carbon Nanotube Dispersions

One of the major limitations for studies and applications of nanotubes is their insolubility in most common solvents. When nanotubes bundle in a solvent they tend to precipitate on the bottom of the vessel. When nanotubes aggregate and form bundles this often corresponds to a considerable decrease in mechanical properties in comparison to individual nanotubes. One of the ways to debundle the nanotubes is by using ultrasound. The ultra-sonic waves cause areas of compression and rarefaction

when passing through a liquid. In the areas of rarefaction, cavitation bubbles can form due to a decrease in pressure and their implosion can cause high localised temperatures and pressures. When ultrasound is applied to a solvent containing aggregated nanotubes these conditions should cause the nanotubes to be dispersed in the solvent.

We have developed a new technique, which monitors this dispersion and sedimentation over time, and from this we can determine how well a solvent can disperse the nanotubes. The experiment is performed by monitoring the absorbance of a solution, over time, using 4 lasers. We can see a schematic representation of the setup of the apparatus in **Figure 2.5**

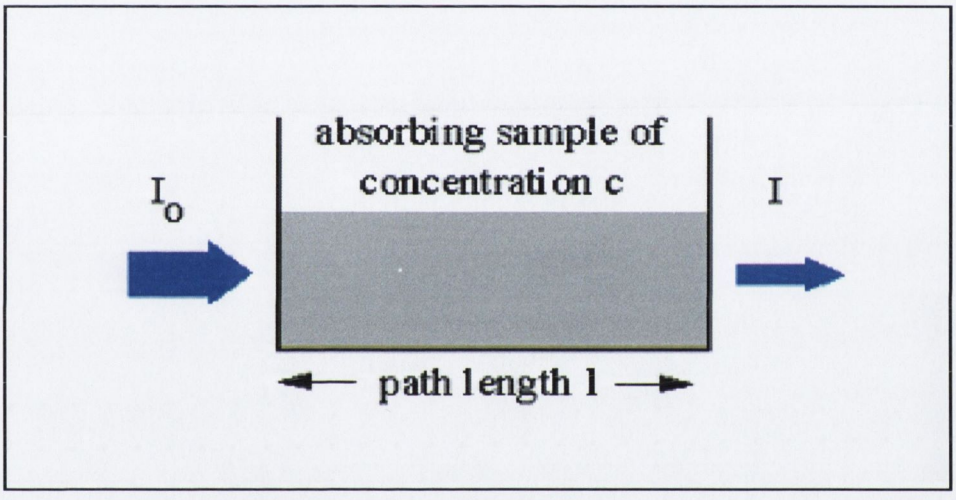

Figure 2.5 Schematic of the sedimentation apparatus

It operates on the principle of the Beer-Lambert Law. The Beer-Lambert law is the linear relationship between absorbance and concentration of an absorbing species and can generally be written as,

$$\mathbf{A = \epsilon.c.l}$$

where, **A** is the absorbance, ϵ is the molar absorptivity with units of L mol^{-1} cm^{-1}, **c** is the concentration of the compound in solution in mol L^{-1}, and **l** is the path length of the sample (the path length of the cuvette in which the sample is contained). Experimental measurements are usually made in terms of transmittance (T), which is defined as,

$$T = I / Io$$

where, I is the light intensity after it passes through the sample and Io is the intensity of the light before it passes through the sample. The relationship between A and T is,

$$A = -\log T = -\log (I / Io)$$

From our measurements of the nanotubes subjected to different times of reflux we can see in **Figure 2.6** that the nanotubes tend to be more stable in the solvent with increased functionality.

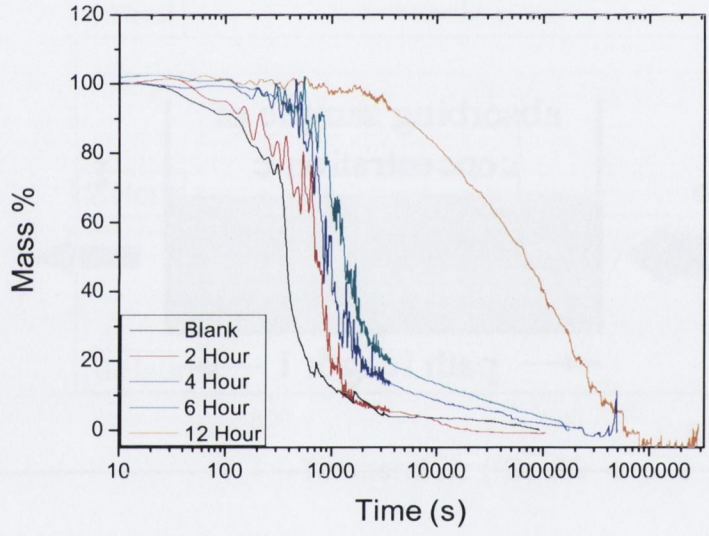

Figure 2.6 Sedimentation curves for functionalised nanotubes; as the level of functionality increases, the stability of the nanotube dispersion increases

2.6 Preparation of Nanotube-Polymer Composite Films

The polymers used for this work are commercially available everyday polymers, polyvinyl chloride (PVC), polystyrene (PS), polyvinyl alcohol (PVA) and polyvinyl acetate (PVAc). These polymers were chosen as they display good solubility in common solvents, including N-methyl-2-pyrollidone (NMP) and have mechanical strengths and moduli that are important for their respective applications. A more comprehensive description of their structures and properties can be found in **Chapter 1**.

All nanotube–polymer composites were prepared by the solution casting technique. This involved dispersing of different concentrations of PNTs or FNTs in a solvent and then dissolving one of the polymers in this dispersion. Variable amounts of pristine and Kevlar-functionalised nanotubes were dispersed in NMP using ultrasonication with a conical sonic horn for 10 minutes to prepare solutions of different concentrations. Then the required polymer was dissolved in this dispersion, again using ultrasonic treatment for 10 minutes. Nanotubes have a strong tendency to aggregate and form bundles which often leads to a considerable decrease in mechanical properties in the resulting composites. However, by using ultrasonication and NMP as a solvent we achieved a very good stable dispersion of nanotubes and dissolved the polymer. The ability of NMP to disperse nanotubes is well reported [21,22] and is discussed in more depth in the introduction. This homogenous mixture was drop-cast on to a glass slide measuring 25 mm x 75 mm and the solvent was allowed to evaporate in a vacuum oven which is operated at a controlled temperature of 60 °C. To ensure complete removal of the solvent the film is left to dry overnight. This resulted in the formation of thin polymer composite films on the slide that can be easily peeled off.

The films produced varied from clear transparent films through to nearly completely opaque, black films as the concentration of nanotubes contained was increased. The films for the different polymers were virtually identical visually for each different polymer and so representative images are shown in **Figure 2.7 A** and **B** respectively. The higher nanotube concentration films tended to have black specs in them, indicating aggregation of the nanotubes within the polymer.

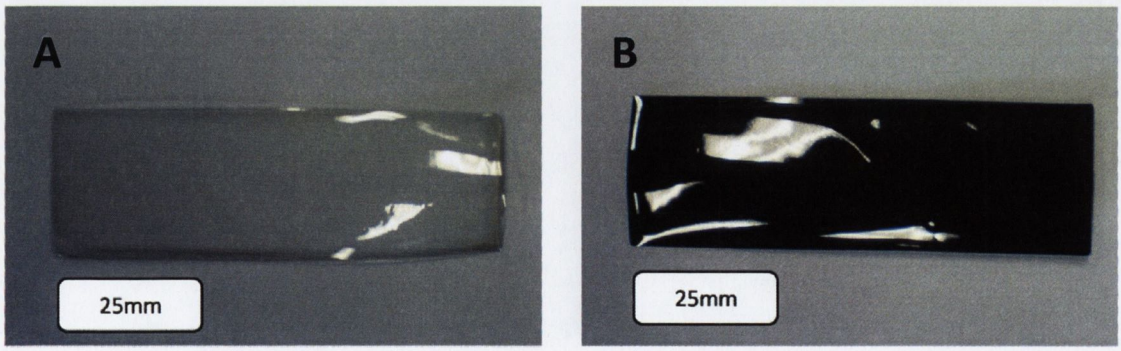

Figure 2.7 Photographs of polymer (PVC) composite films containing 0.0625 mass percentage carbon nanotubes (**A**) and 2 mass percentage carbon nanotubes (**B**)

Following their fabrication and drying, the composite films were lifted from the glass substrate and mechanical tests were performed on them using a Zwick 100 tensile tester. To perform the tests the films were first cut into strips which were then analysed individually. Tensile measurements were carried out to evaluate the relationship between composite morphology and mechanical performance. The data was used to calculate mechanical properties and these are presented in sections **2.7** through **2.10**.

As has been previously reported,[23] SEM can be utilised to analyse the fracture surface of polymer-nanotube composites. In order to investigate composite morphology after fracture, the composite films in this work were fractured by dipping the composite strip into a flask of liquid Nitrogen and then broken. Cross sectional SEM images of the fracture surface of both original PVC and PVC nanotube composites used for mechanical testing are shown in **Figure 2.8 A** and **B** respectively. Representative images are shown again, as microscopically all polymers also are very similar. In the first SEM image we see a relatively flat surface with small lumps of broken polymer protruding. On the second image we can see multiple tubes extending beyond the fracture surface.

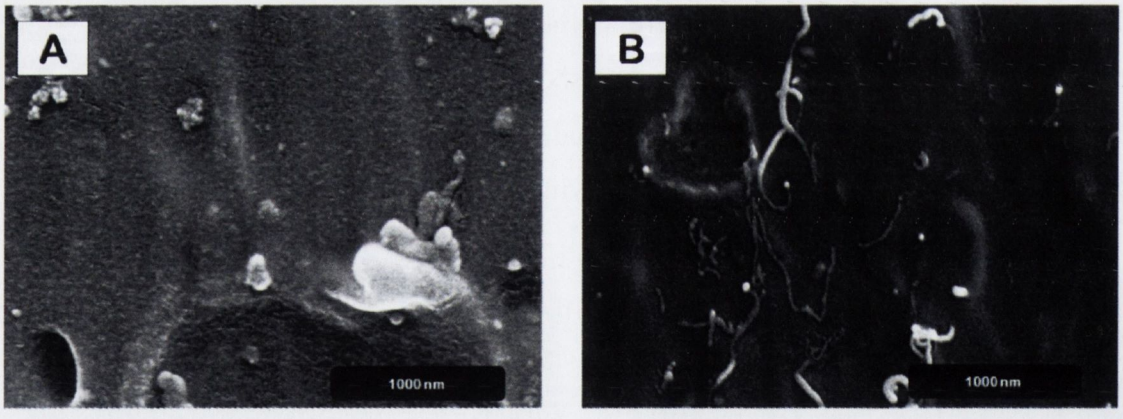

Figure 2.8 Examples of cross-sectional SEM images of the fracture surface of pure PVC (**A**) and PVC-Kevlar functionalised nanotube composite (2.0% NT) (**B**)

As discussed in **Chapter 1** and mentioned above the addition of carbon nanotubes to a polymer can have both positive and negative effects. If we achieve a good interfacial stress transfer of our nanotubes to the corresponding polymer we should see increases in the mechanical properties. Any decreases we find may be due to one of a number of possibilities including, disruption of the polymer structure and aggregation of the nanotubes within the polymer during its formation. Aggregation was in fact evident from SEM analysis in some of the higher concentrations of nanotubes in the polymers in this work and evidence of this can be seen in **Figure 2.9**. This aggregation results in composite films that are inhomogeneous at the nanoscale. The polymer is ultimately filled with aggregates of nanotubes rather than individual nanotubes. These aggregates act as stress concentration centres which act to weaken the film. Nanotubes have a very weak interaction between each other and they can slide under the stress. Therefore, polymer composites containing aggregated nanotubes frequently demonstrate a decrease in their mechanical properties. Ultimately we anticipate all of the factors should play a part and we expect to see a trend of mechanical dependence on the concentration of nanotubes in the polymer matrix. We will also expect to observe a concentration which shows an apparent optimum amount of nanotubes.

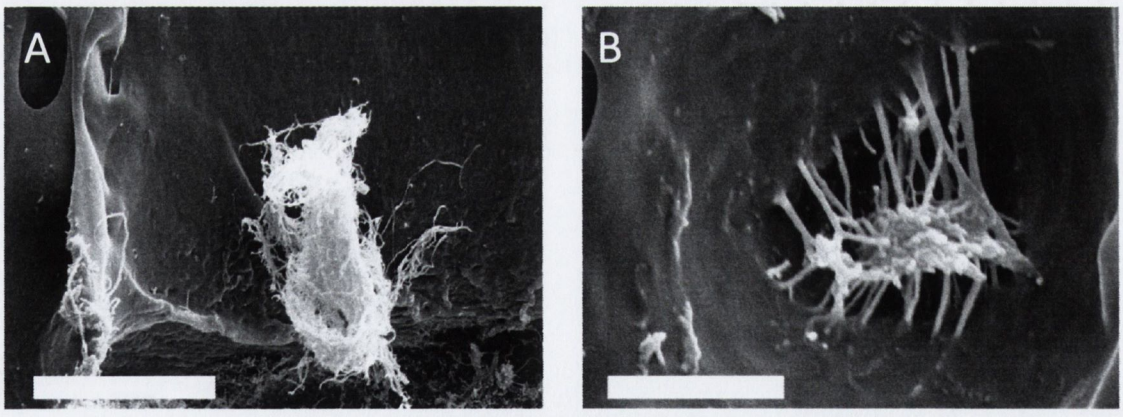

Figure 2.9 Examples of SEM images displaying aggregation in PNT-PS (2 % NT) composite film (scale bar 5 μm) (**A**) and 6 hr refluxed FNT-PS composite film (scale bar 1 μm) (**B**)

2.7 Investigation of Mechanical Properties of Polymer Composites

All nanotube-polymer composites were cut into strips of 2.4 mm in width and 25 mm in length. From the systematic preparation method the thickness was generally found to lie between 30-40 microns for all samples and was measured by a digital micrometer before testing. Mechanical testing was carried out using a Zwick Z100 tensile tester on five separate samples for each polymer. The ultimate tensile strength, Young's modulus, toughness and strain were examined for the pure polymer and each of the polymer composites.

2.7.1 Nanotube - polystyrene composites

The first polymer used was polystyrene. It is a polymer containing aromatic groups, similar to Kevlar, and a more in depth discussion of its properties and applications can be found in **Chapter 1**. Its structure creates the possibility of π-π interactions of the Kevlar functionality with the phenyl component of polystyrene. In this work the mechanical properties of pristine polymer samples were compared with both PNT-PS composites and the 2 hr, 4 hr and 6 hr refluxed FNT-PS composites in sections **2.7.1.1** through **2.7.1.4**.

2.7.1.1 Pristine nanotube - polystyrene composites

The low nanotube concentration PNT-PS composites (**Table 2.1, Figure 2.10**) demonstrated mechanical properties very close to those of the original polymer.

When we look at the tensile strength we find increases at the low concentrations. The best increase is in the 0.125 mass % of nanotubes which demonstrates an increase from 25 MPa for the pure PS to 28 MPa, representing an increase in strength of 12 %. After we reach this maximum we find at the higher concentrations of nanotubes the strength begins to decrease again.

The Young's moduli show a similar trend across the concentration range to the tensile strength. The maximum value found is for that of the 0.0625 % of nanotubes. It increases from 1.8 GPa in the original polymer to 2.1 GPa in the composite which represents a 17 % increase.

The toughness value shows an increase from 2.5 to 3.0 MJ/m^3 in the best case (0.0625 % PNTs). This represents an increase of 20 % on the pure PS. The corresponding strain increase is relatively small (0.2 %).

Overall the best sample appears to be the composite containing 0.0625 % PNTs. It shows a similar tensile strength value and strain to the pure PS but demonstrates the best increase for the Young's modulus (14%) and toughness (20%). In most of the other samples the mechanical properties are either similar or not as good as the pure polymer. The noticeable worsening of all mechanical characteristics can also be observed for the composites at higher mass percentages of PNTs. This can be explained the disruption of polymer structure by increased amount of filler and also by the formation of aggregates within the polymer structure. The reductions are quite dramatic, the strength and modulus are both reduced by almost half (48% and 43% respectively) at the maximum concentration of 2% nanotubes. The toughness decreases by 59% and strain also goes down by 27%. On the whole when we analyse the PNT-PS composites we find considerable increases at low loadings followed by a dramatic reduction in all the mechanical properties as we increase the loading beyond 0.125 % nanotubes. We hope to show that the functionalised nanotubes can both show better increases at the low concentrations and further enhancement as we increase the loading of nanotubes across the concentration range indicating less aggregation and better affinity for the polymer.

Table 2.1 Combined mechanical data for PNT-PS composites

Mass NT (%)	Tensile Strength (MPa)	Error (+/-)	Young's Modulus (GPa)	Error (+/-)	Toughness (MJ/m^3)	Error (+/-)	Strain (%)	Error (+/-)
0	**25**	1.6	**1.8**	0.09	**2.5**	0.60	**1.8**	0.23
0.0625	**25**	3.0	**2.1**	0.33	**3.0**	0.16	**2.0**	0.28
0.125	**28**	1.0	**1.9**	0.13	**2.4**	0.30	**1.7**	0.03
0.25	**21**	0.8	**1.5**	0.16	**2.2**	0.38	**2.1**	0.21
0.5	**19**	2.4	**1.3**	0.23	**1.8**	0.52	**1.9**	0.10
1	**18**	1.3	**1.4**	0.10	**1.5**	0.35	**1.6**	0.25
2	**13**	1.1	**1.0**	0.10	**1.0**	0.21	**1.4**	0.08

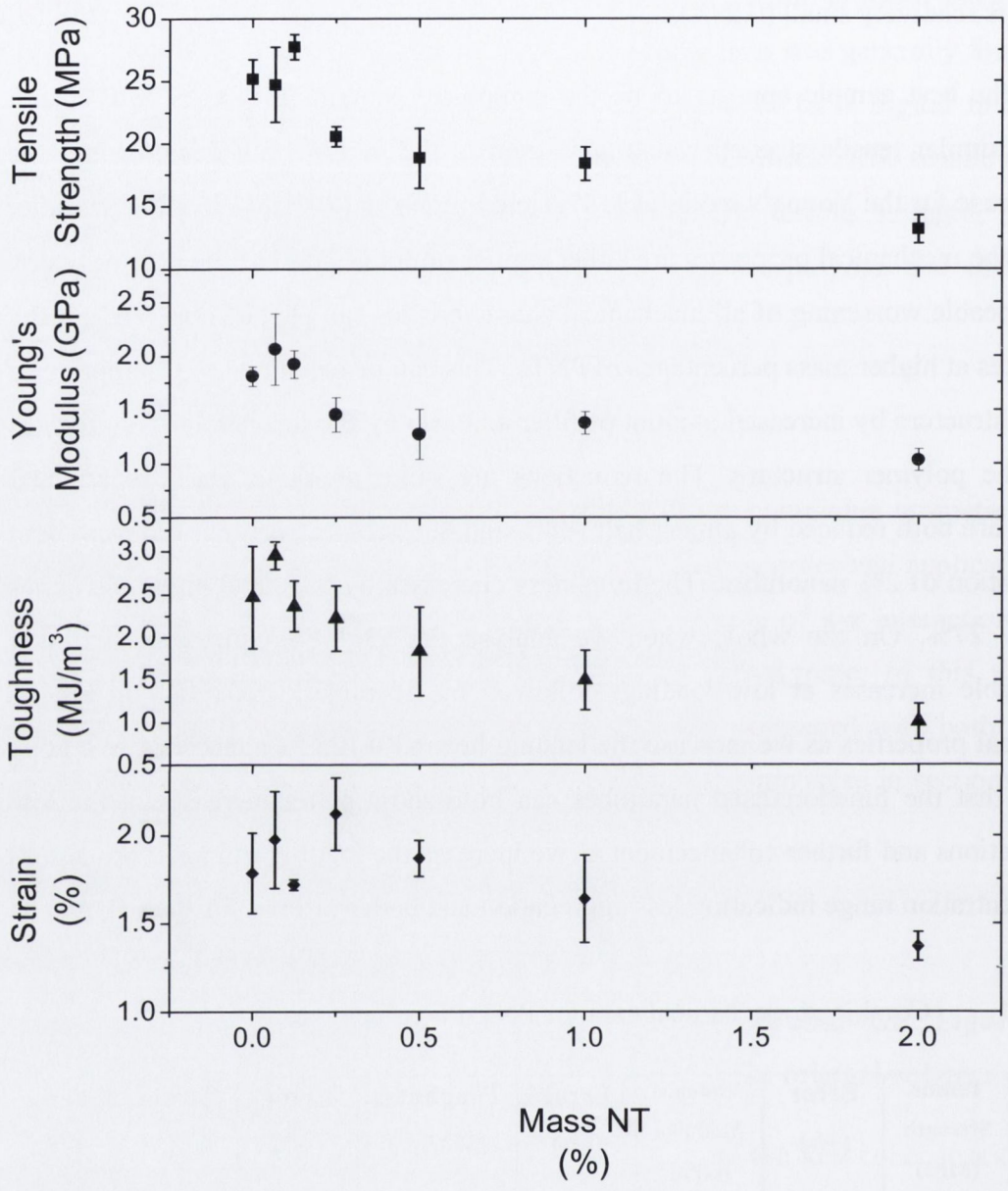

Figure 2.10 Combined mechanical data graph of tensile strength, Young's modulus, toughness and strain for PNT-PS composites against the mass percentage of nanotubes within the polymer film

2.7.1.2 Polystyrene composites containing FNTs refluxed for 2 hours

Mechanical testing of the polystyrene composites containing 2hr refluxed FNTs (**Table 2.2, Figure 2.11**) gave very impressive results in comparison to the pristine nanotubes.

The strength measurements show increases across the whole concentration range and reach a maximum of 30 MPa representing a 20 % increase in strength on the pure PS (25 MPa) at the 0.5% concentration. This is slightly better than the maximum value measured for the pristine nanotubes in PS of 28 MPa (a 12 % increase on the pure polymer), although at a higher loading.

The Young's moduli are also impressive, with a maximum of 2.0 GPa at the 0.5 %, 1 % and 2 % concentration of nanotubes representing an increase of 11 % on the pure PS. It shows that the higher loading of FNTs can also maintain the increases.

Interestingly we see that the toughness also increases without the strain being affected too much, indicating that the sample is capable of withstanding a higher overall load without a corresponding increase in brittleness or ductility. The best value of 3.1 MJ/m^3, at 0.5 % loading, demonstrates a more substantial increase (24 %) on the pure polymer (2.5 MJ/m^3) than the PNT samples (3.0 MJ/m^3). The value for strain in this sample is the same as the strain in the pure PS.

Another interesting effect is that at the higher concentrations the strength and modulus of the polymer composite reaches a maximum and levels off. We would expect that at the higher concentrations the composites would begin to weaken due to aggregation like in the sample with the PNTs. In the PNT samples when the concentration of nanotubes reaches 0.125 % loadings it achieves the best mechanical values. The mechanical properties then decrease substantially in the samples at 0.25% nanotubes and above. In the FNT samples however we can see that the composite retains its high strength and modulus across the concentration range and varies by less than 4 MPa from 0.125% all the way to 2% nanotubes concentration. In general the values that these samples achieve are similar to the PNT samples at low loading but when the mechanical properties of the PNTs sample start to decrease as we move to higher loadings the FNTs can retain their mechanical increase and in some cases achieve further enhancement. This indicates that the nanotubes are better able to grip one another rather than slide over one another as we would expect. Also the increase in the dispersibility of the NTs

in NMP might decrease the amount of aggregation that occurs. Overall the FNTs demonstrate a better ability for mechanical reinforcement and achieve stronger composites albeit at a higher loading of nanotubes in the polymer. We will next analyse FNTs which have been refluxed for a longer periods of time to see if they can demonstrate any further enhancement.

Table 2.2 Combined mechanical data for 2hr refluxed FNT-PS composites

Mass NT (%)	Tensile Strength (MPa)	Error (+/-)	Young's Modulus (GPa)	Error (+/-)	Toughness (MJ/m^3)	Error (+/-)	Strain (%)	Error (+/-)
0	**25**	1.6	**1.8**	0.09	**2.5**	0.60	**1.8**	0.23
0.0675	**27**	1.1	**1.8**	0.11	**2.5**	0.34	**1.9**	0.24
0.125	**27**	2.2	**1.7**	0.28	**2.8**	0.96	**2.1**	0.63
0.25	**26**	1.6	**1.8**	0.08	**2.2**	0.18	**1.6**	0.15
0.5	**30**	1.7	**2.0**	0.10	**3.1**	0.34	**1.8**	0.06
1	**29**	1.4	**2.0**	0.08	**2.5**	0.21	**1.6**	0.12
2	**28**	0.6	**2.0**	0.21	**2.6**	0.17	**1.8**	0.11

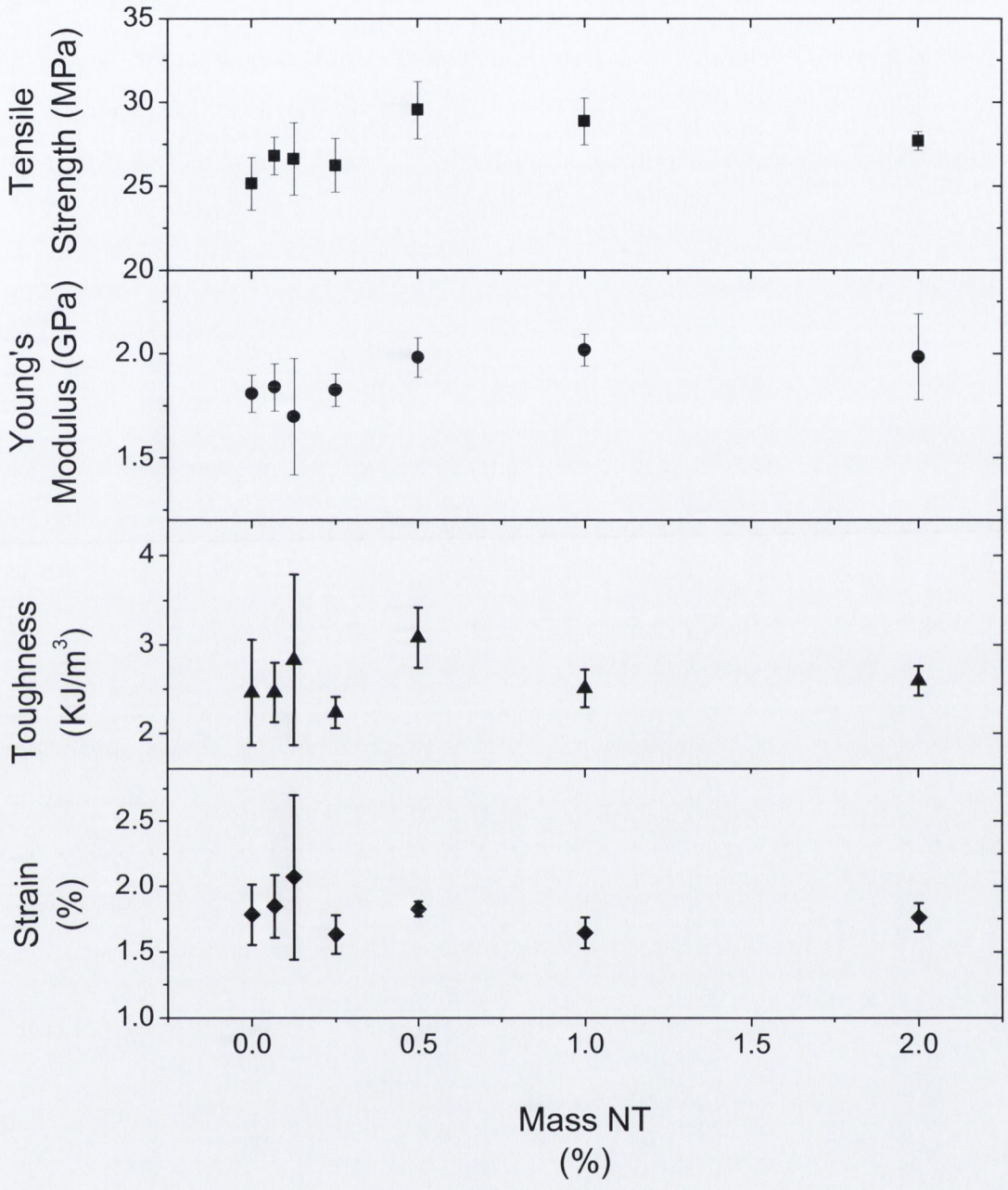

Figure 2.11 Combined graph of tensile strength, Young's modulus, toughness and strain of 2hr refluxed FNT-PS composites against the mass percentage of nanotubes within the polymer film.

2.7.1.3 Polystyrene composites containing FNTs refluxed for 4 hours

When we analyse the 4hr refluxed FNT-PS composites (**Table 2.3, Figure 2.12**) we see that we get similarly impressive results as the 2 hr refluxed FNT-PS composites. The strength measurements show increases again across the whole concentration range and reach a maximum at 30 MPa (0.125 % and 0.5 % loading) again representing an increase of 20% increase in strength on pure PS. This is the same as the maximum value measured for the 2 hour FNTs, although at a lower nanotube loading.

The Young's modulus values show an increase from 1.8 GPa to 2.0 GPa representing an increase on the pure polymer of 11 %, however this value is not as high as the maximum in the PNT-PS composite (2.1 GPa)

The toughness values are also reasonable (maximum of 2.9 MJ/m^3 at 0.0675 %) when compared to the pure PS (2.5 MJ/m^3) and relatively stable over the whole concentration range with the exception of the highest mass % NT sample. The maximum is not as high as the maximum in either the PNT-PS composites (3.0 MJ/m^3, 0.0625 % PNTs) or the 2 hr FNT-PS composites (3.1 MJ/m^3, 0.5 % FNTs).

A particularly noteworthy sample is the 0.125% concentration. It shows substantial increases in strength (20 %), modulus (11 %) and toughness (8 %) with a decrease in strain (-6 %).

Table 2.3 Combined mechanical data 4hr refluxed FNT-PS composites

Mass NT (%)	Tensile Strength (MPa)	Error (+/-)	Young's Modulus (Gpa)	Error (+/-)	Toughness (MJ/m^3)	Error (+/-)	Strain (%)	Error (+/-)
0	**25**	1.6	**1.8**	0.09	**2.5**	0.60	**1.8**	0.23
0.0675	**29**	1.7	**1.7**	0.20	**2.9**	0.07	**2.1**	0.08
0.125	**30**	1.7	**2.0**	0.23	**2.7**	0.29	**1.7**	0.20
0.25	**27**	1.1	**1.7**	0.22	**2.6**	0.37	**2.0**	0.30
0.5	**30**	1.0	**1.9**	0.13	**2.8**	0.14	**1.8**	0.17
1	**29**	1.2	**1.7**	0.22	**2.9**	0.34	**2.0**	0.43
2	**27**	2.1	**1.8**	0.05	**2.3**	0.40	**1.7**	0.17

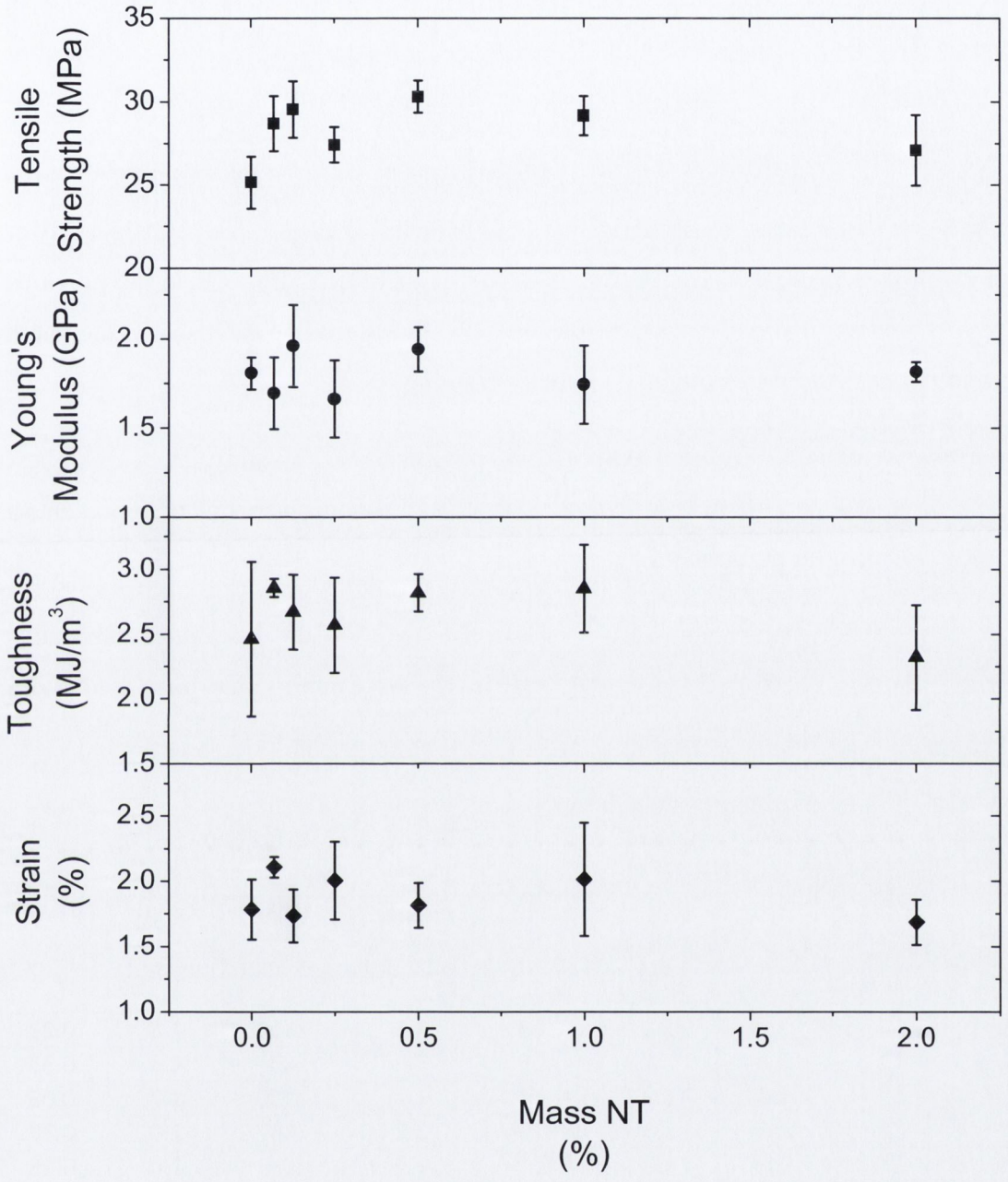

Figure 2.12 Combined graph of tensile strength, Young's modulus, toughness and strain against mass % of 4hr refluxed FNT-PS composites against the mass percentage of nanotubes within the polymer film

2.7.1.4 Polystyrene composites containing FNTs refluxed for 6 hours

When we analyse the FNTs nanotube composites containing Kevlar coated nanotubes refluxed for 6 hours (**Table 2.4, Figure 2.13**) we see that get quite similar results in comparison to the pristine nanotubes, and they are not as large or extensive as the 2 hr or 4 hr FNTs.

The strength measurements show increases again with a maximum at the 0.25 % FNTs concentration of 29 MPa (approximately 12 %) but the values diminish considerably at the higher concentrations of nanotubes. The maximum value is lower than the previous samples. This is probably due to the nanotubes and Kevlar being oxidised in the harsh environment resulting in decomposition and weakening.

The Young's moduli are also lower and diminish considerably at the highest concentration. The maximum value occurs at the 0.125% concentration and represents a negligible increase on the pure PS.

The toughness and strain values are very inconsistent, and the maximum value at a concentration of 0.0625 % FNTs is the same as the maximum value for the PNT-PS composites and is also recorded at the same concentration of NTs.

Table 2.4 Combined mechanical data for 6hr refluxed FNT-PS composites.

Mass NT (%)	Tensile Strength (MPa)	Error (+/-)	Young's Modulus (Gpa)	Error (+/-)	Toughness (MJ/m^3)	Error (+/-)	Strain (%)	Error (+/-)
0	**25**	1.6	**1.8**	0.09	**2.5**	0.60	**1.8**	0.23
0.0625	**28**	0.8	**1.8**	0.15	**3.0**	0.39	**2.1**	0.33
0.125	**28**	1.0	**1.9**	0.14	**2.4**	0.30	**1.7**	0.03
0.25	**29**	1.0	**1.9**	0.20	**2.8**	0.37	**2.0**	0.37
0.5	**28**	2.2	**1.8**	0.12	**2.7**	0.31	**2.0**	0.13
1	**25**	1.9	**1.9**	0.02	**2.1**	0.29	**1.6**	0.08
2	**21**	2.2	**1.5**	0.17	**1.7**	0.32	**1.8**	0.17

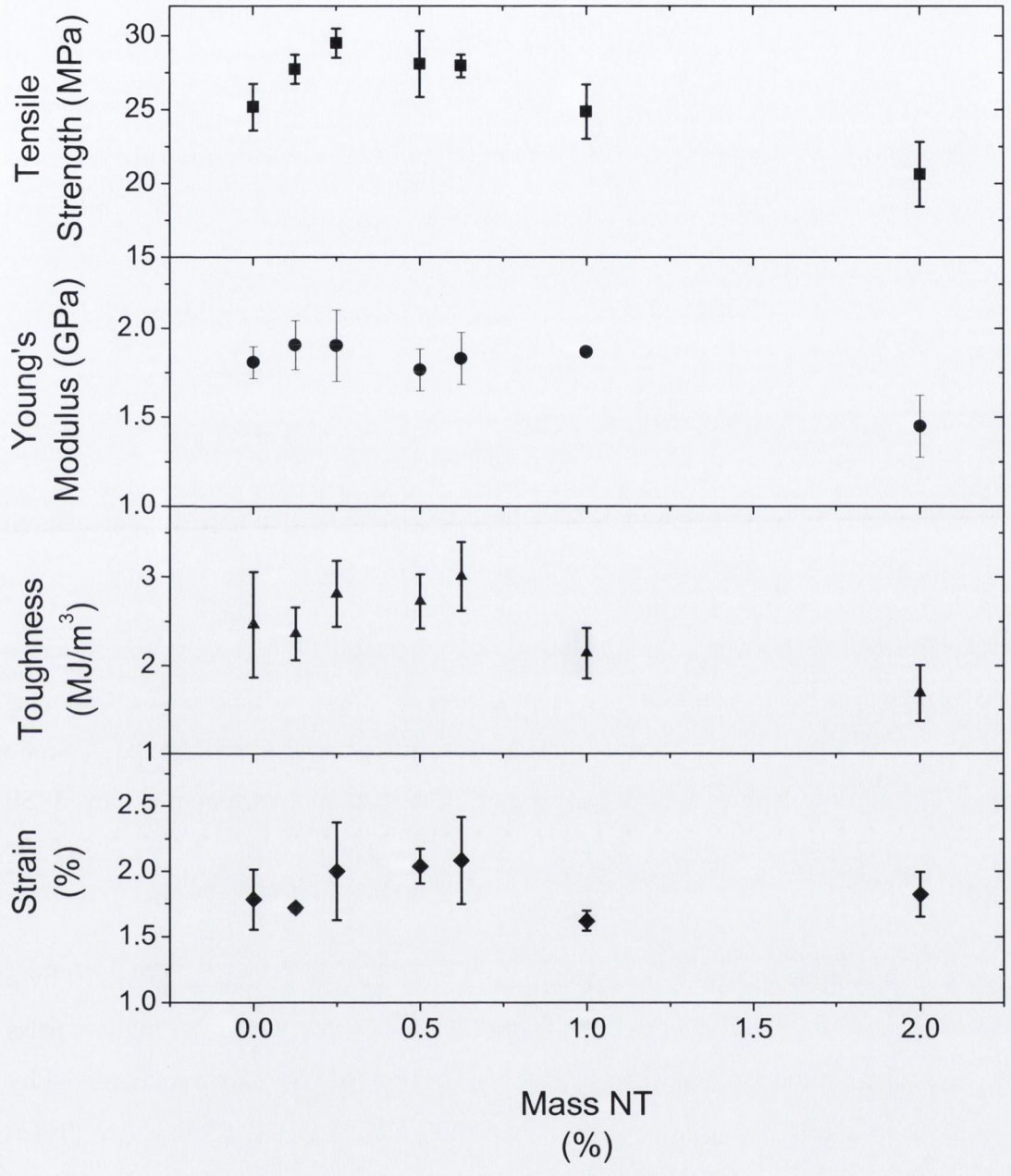

Figure 2.13 Combined graph of tensile strength, Young's modulus, toughness and strain against mass % of 6 hr refluxed FNT-PS composites against the mass percentage of nanotubes within the polymer film

2.7.2 Nanotube-Polyvinyl Chloride Composites

We have shown above that the reflux time has an effect on the ability of the functionalised nanotubes to achieve better mechanical properties. Our new aim was to demonstrate that Kevlar coated nanotubes can be employed as additives to a variety of different polymers. We also want to find if we can achieve more considerable enhancement on a different polymer. The next polymer chosen for analysis was polyvinyl chloride (PVC). A comprehensive review of its properties can also be found in **Chapter 1**. In this work the mechanical properties of pure PVC samples were compared with PNT-PVC composites and the 2 hr, 4 hr and 6 hr refluxed FNT-PVA composites in sections **2.7.2.1** through **2.7.2.4**.

2.7.2.1 Pristine nanotube – polyvinyl chloride composites

We examined the mechanical properties of PNT-PVC composites and compared them to the properties of pure PVC (**Table 2.5, Figure 2.14**).

The addition of PNTs gives an initial increase in strength followed by a reasonably steady decrease at higher nanotube concentrations. As the nanotube concentration is increased, they begin to aggregate causing weakness, similar to the polystyrene samples, and this results in a decrease in strength. The maximum strength achieved (50 MPa at 0.125% conc.) was about a 16% increase in the strength measured for pure PVC (43 MPa).

The Young's modulus section of the graph also shows an initial increase followed by a dramatic decrease for the concentrations from 0.25% upwards. Once the highest mass percentage concentration of nanotubes is reached we find the modulus has decreased by 33 %. The maximum Young's modulus achieved (1.8 GPa at 0.0675 mass % PNTs) was about a 20 % increase on the Young's modulus measured for pure PVC (1.5 GPa).

The toughness and strain begin to decrease immediately after the introduction of nanotubes and throughout the mass percentage range accordingly. This decrease is associated with the increase in brittleness that is often observed when dealing with nanotube-polymer composites and is a well-reported effect in the literature.[24,25] It is not unexpected in a composite sample of this nature. Once we reach the highest

concentration there has been a very dramatic decrease of all the mechanical properties of the composite with respect to the pure polymer.

The PNT results show that initially we achieve some increases in strength and modulus however once we add 0.25 % by mass of nanotubes or more we find that the mechanical properties of the composites are negatively affected. It was anticipated that we can show that the addition of the FNTs will display more considerable increases over the PNTs, with these increases maintained throughout the concentration range, similar to the polystyrene samples.

Table 2.5 Combined mechanical data for PNT-PVC composites

Mass NT (%)	Tensile Strength (MPa)	Error (+/-)	Young's Modulus (GPa)	Error (+/-)	Toughness (MJ/m^3)	Error (+/-)	Strain (%)	Error (+/-)
0	**43**	3.2	**1.5**	0.06	**37.1**	19.23	**116**	59.0
0.0625	**48**	3.0	**1.8**	0.18	**34.7**	11.03	**88**	21.2
0.125	**50**	2.1	**1.7**	0.17	**28.8**	12.68	**76**	32.2
0.25	**36**	2.7	**1.1**	0.16	**6.6**	6.87	**23**	22.8
0.5	**40**	4.1	**1.2**	0.14	**2.5**	1.11	**9**	3.8
1	**33**	3.7	**1.1**	0.14	**1.1**	0.39	**5**	0.8
2	**28**	1.9	**1.0**	0.13	**0.7**	0.24	**4**	0.9

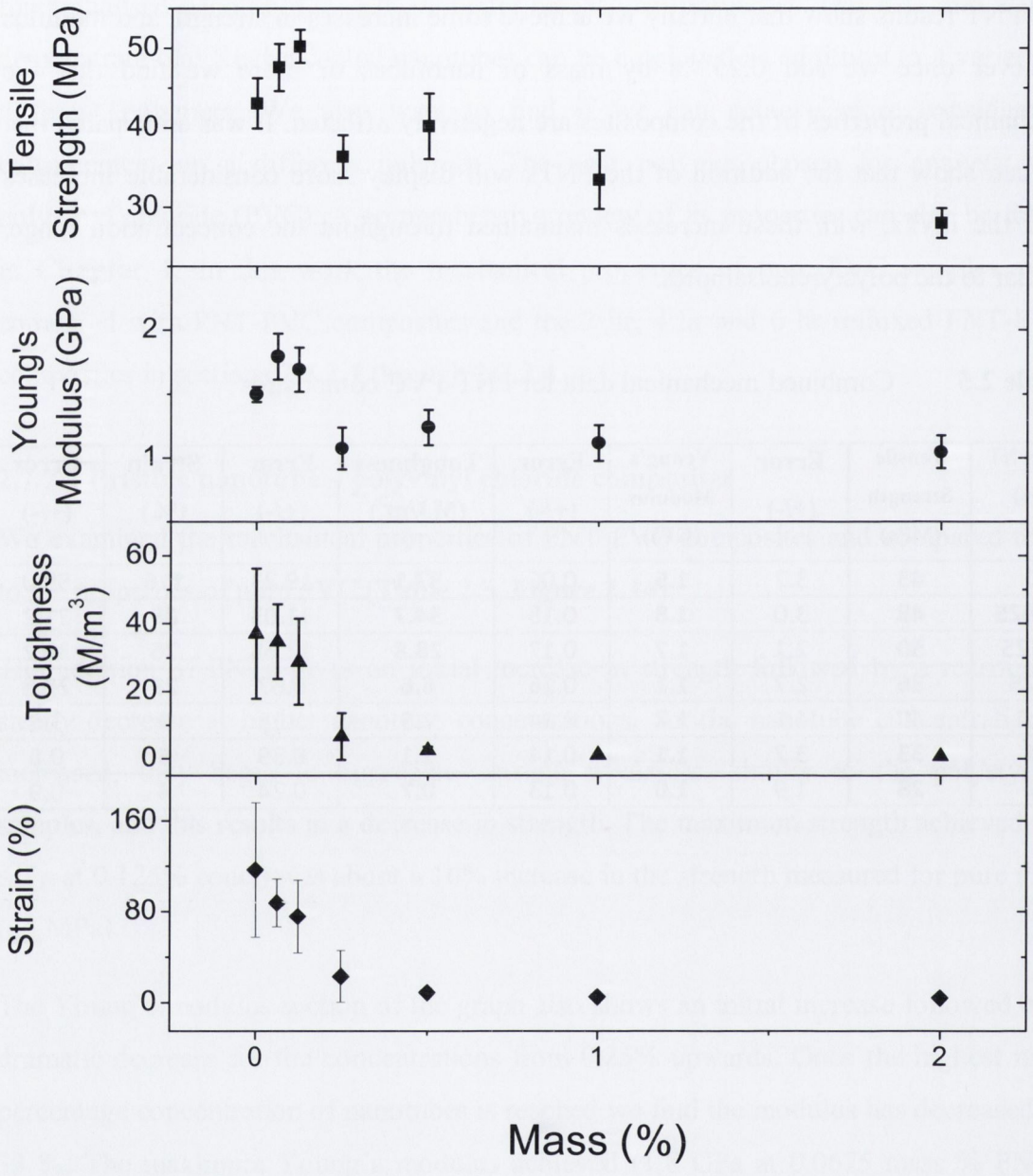

Figure 2.14 Combined graph of tensile strength, Young's modulus, toughness and strain against mass % PNT-PVC composites against the mass percentage of nanotubes within the polymer film

2.7.2.2 PVC composites containing FNTs refluxed for 2 hours

We examined the mechanical properties of PVC and 2hr FNT composites and compared them to the properties of pure PVC (**Table 2.6, Figure 2.15**).

Here we can see an initial increase in strength with the addition of the 2 hr FNTs. The strength continues to increase with increasing nanotube concentration up to the 0.25% nanotube concentration whereupon it begins to level out, but still remaining high. The maximum strength achieved (65 MPa at 1% conc.) was about a 50% increase in the strength measured for pure PVC (43 MPa). Also there was a significant improvement on the maximum strength than that achieved with PNTs (50.2 MPa, 20%). It is evident that the FNTs give a much greater strength increase to the polymer with respect to the PNTs.

The graph shows a considerable increase in Young's modulus also, with most samples measured showing an increase of over 50% on the pure polymer. The maximum Young's modulus achieved (2.5 GPa at 1% conc.) was about a 70% increase in the Young's modulus measured for pure PVC (1.5 GPa) and was also a very significant improvement on the maximum Young's modulus achieved with PNTs (1.8 GPa, 20%).

When we look at the values for toughness and strain we see that they tend to decrease as we increase the nanotube concentration. As noted before, this is expected for a composite sample. Overall the optimum concentration of nanotubes appears to be 1 mass % which gives an increase of over 50 % for both the tensile strength and Young's modulus and the corresponding decrease in toughness is not so considerable when compared to the other samples. Also the toughness is even more impressive when we consider the associated low strain value.

These increases are very substantial and show that the functionalised nanotubes are clearly considerably more effective at transferring stress from the polymer matrix. When we look at the higher mass percentages of nanotubes we find that the increases in mechanical properties occur across the concentration range indicating less aggregation of the nanotubes and a better ability for reinforcement. This is similar to the effect observed on the polystyrene composites; however it is in stark contrast to the PNT-PVC composites. Initially composites fabricated using both types of nanotubes show similar increases at the low concentration ranges. Ultimately the FNT composites showed

further increases after the 0.25 % mass of FNTs and maintained those increases across the concentration range. Conversely the PNT composites showed dramatic decreases at the same mass percentage of PNTs and these decreases were exacerbated as the concentration was increased further.

Table 2.6 Combined mechanical data for 2 hr refluxed FNT-PVC composites

Mass NT (%)	Tensile Strength (MPa)	Error (+/-)	Young's Modulus (GPa)	Error (+/-)	Toughness (MJ/m^3)	Error (+/-)	Strain (%)	Error (+/-)
0	**43**	3.2	**1.5**	0.06	**37.1**	19.23	**117**	59.0
0.0625	**50**	8.7	**1.5**	0.23	**1.6**	0.50	**5**	1.0
0.125	**59**	2.0	**2.2**	0.25	**19.8**	3.42	**42**	4.5
0.25	**62**	2.3	**2.2**	0.20	**11.2**	5.90	**24**	11.9
0.5	**60**	1.9	**2.1**	0.03	**2.1**	0.41	**5**	0.8
1	**65**	4.1	**2.5**	0.33	**17.4**	11.87	**33**	21.1
2	**60**	4.5	**2.1**	0.13	**3.3**	2.88	**7**	5.5

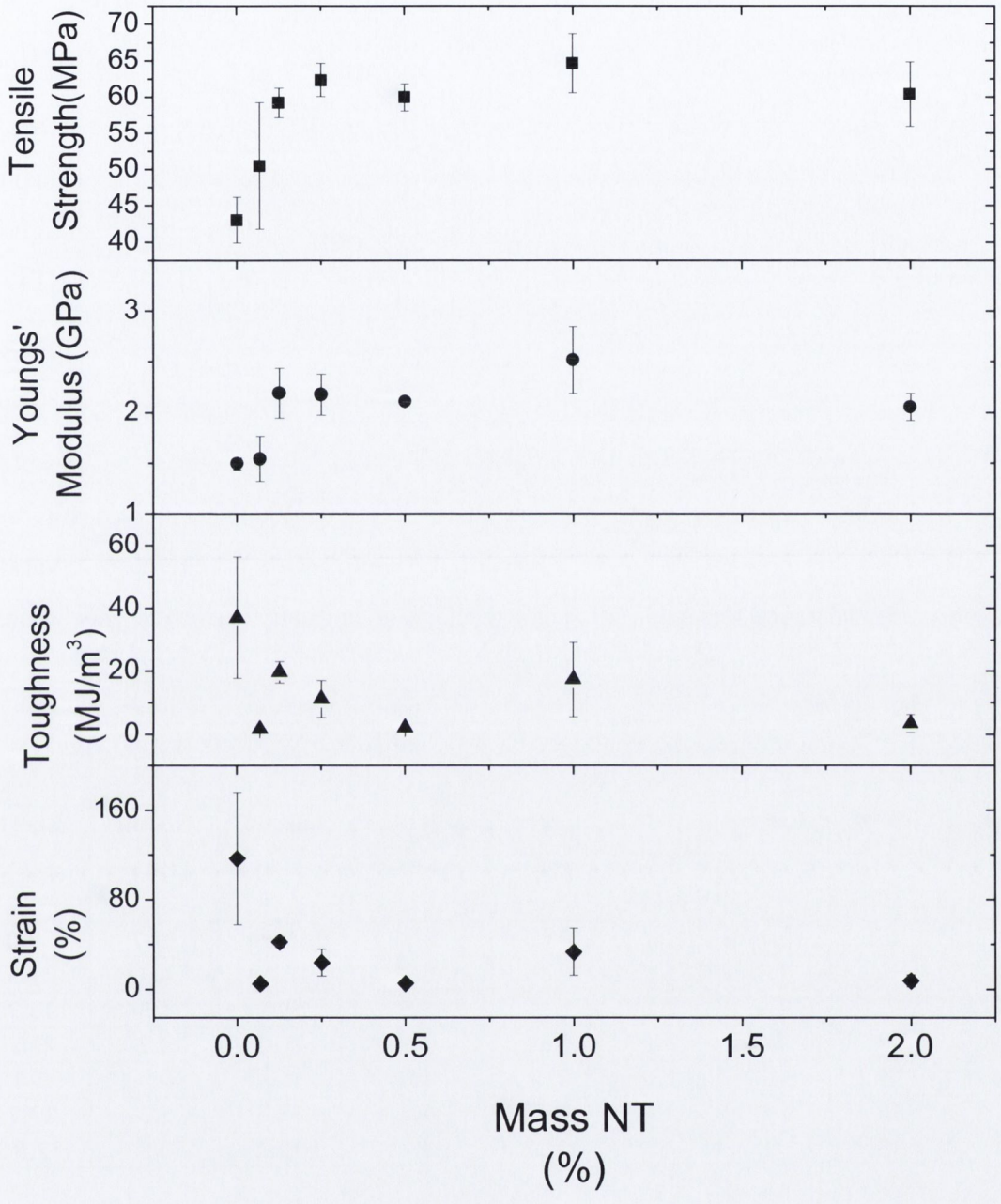

Figure 2.15 Combined graph of tensile strength, Young's modulus, toughness and strain against mass % of 2 hr refluxed FNT-PVC composites against the mass percentage of nanotubes within the polymer film

2.7.2.3 PVC composites containing FNTs refluxed for 4 hours

The FNT-PVC composites containing nanotubes treated for 4 hr were next examined and the mechanical properties were compared them to the properties of pure PVC (**Table 2.7 and Figure 2.16**).

We can see again that we get a large increase in the tensile strength. This reaches a maximum value of 60 MPa representing a 40 % increases on the pure PVC (43 MPa) for the samples with 0.125 and 0.25 % nanotubes, although this maximum is slightly less than the corresponding value for the FNTs refluxed for 2 hr (65 MPa, 1 % FNTs).

The Young's modulus showed increases across the range of concentrations with the maximum value of 2.1 GPa displayed over a large range of concentrations of FNT (0.125 through to 1 % FNTs). The toughness and strain again follow the expected trends of dramatic decreases. The FNT composites also maintain the increases across the concentration range, similar to the 2 hr refluxed samples. As a general observation the 4hr refluxed FNT samples display similar but slightly reduced mechanical properties to the 2 hr refluxed FNT composites.

Table 2.7 Combined mechanical data for 4 hr refluxed FNT-PVC composites

Mass NT (%)	Tensile Strength (MPa)	Error (+/-)	Young's Modulus (GPa)	Error (+/-)	Toughness (MJ/m^3)	Error (+/-)	Strain (%)	Error (+/-)
0	**43**	3.2	**1.5**	0.06	**37.1**	192.3	**11.7**	59.0
0.0675	**59**	1.0	**1.9**	0.14	**18.4**	121.9	**4.7**	37.5
0.125	**60**	2.4	**2.1**	0.15	**5.6**	59.0	**1.3**	13.3
0.25	**60**	2.4	**2.1**	0.10	**2.9**	26.2	**0.7**	5.6
0.5	**55**	5.7	**2.1**	0.07	**1.8**	8.4	**0.5**	2.4
1	**56**	1.6	**2.1**	0.14	**5.8**	63.0	**1.3**	12.7
2	**55**	6.8	**1.9**	0.17	**3.7**	19.2	**0.8**	2.9

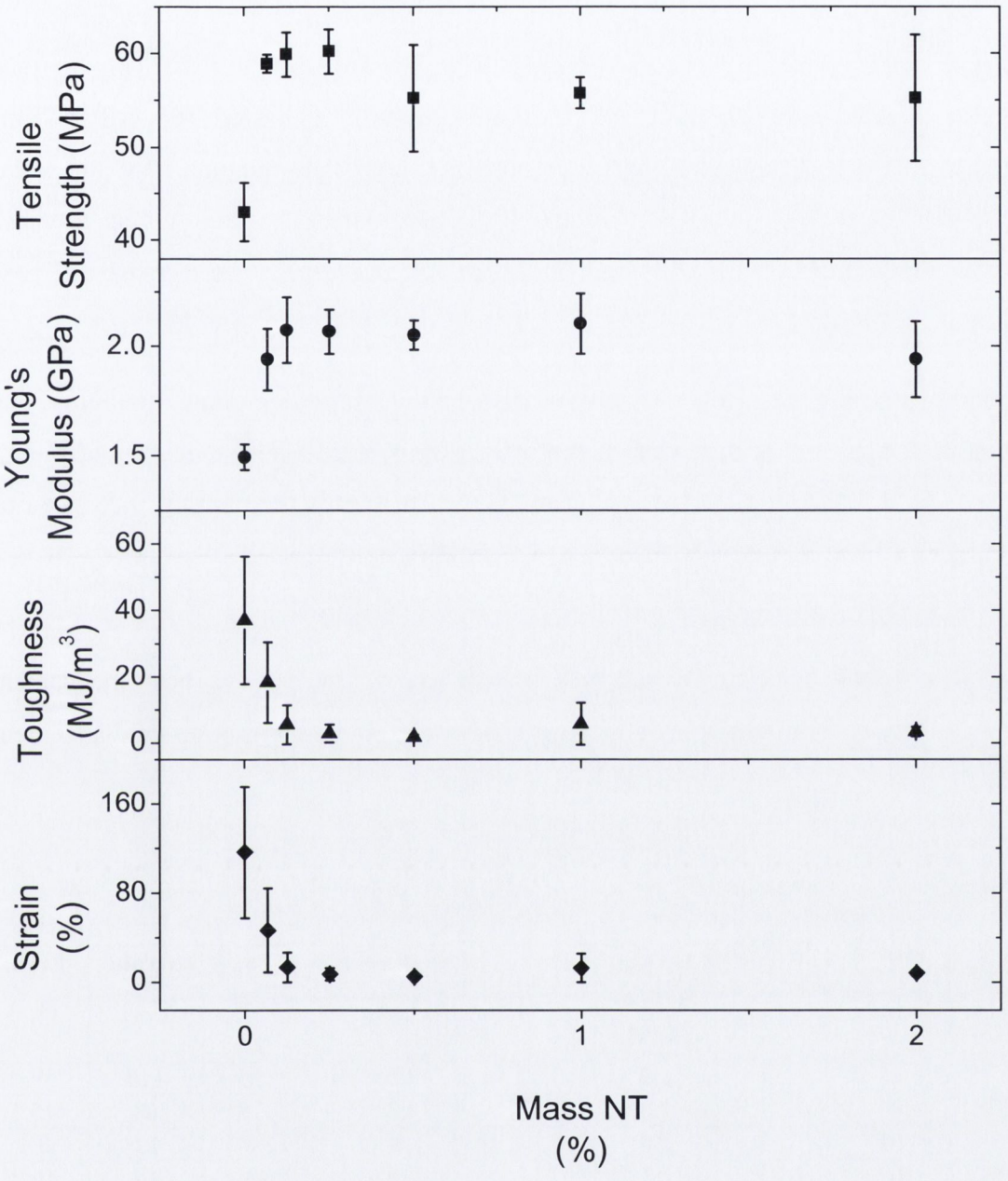

Figure 2.16 Combined graph of tensile strength, Young's modulus, toughness and strain against mass % of 4 hr refluxed FNT-PVC composites against the mass percentage of nanotubes within the polymer film

2.7.2.4 PVC composites containing FNTs refluxed for 6 hours

The mechanical properties of the 6hr refluxed FNT-PVC composites were examined and compared to the properties of pure PVC (**Table 2.8, Figures 2.17**)

Initially, in this graph there is a large increase in strength for the 0.0675% nanotube concentration which is in fact the maximum strength achieved (63 MPa). This represents about a 50% increase in the strength measured from the pure PVC (43 MPa) and is still considerably better than the PNT composites. Following this increase however the tensile strength of the composite starts to decrease as we increase the mass percentage of nanotubes.

The addition of FNTs to PVC also gave a reasonable increase in Young's modulus. The maximum is achieved at a concentration of 0.25 mass % of FNTs and is about a 40% increase on the Young's modulus of pure PVC. The sample containing 0.0675 % of FNTs again shows considerable increase in Young's modulus.

The toughness and strain show dramatic decreases with the exception of the 0.0675 mass % of FNT sample. Overall this sample shows by far the best mechanical properties but it seems the 6 hr refluxed FNT samples show slightly less enhancement in PVC composites than the 2 hr refluxed FNT samples.

Table 2.8 Combined mechanical data for 6 hr refluxed FNT-PVC composites

Mass NT (%)	Tensile Strength (MPa)	Error (+/-)	Young's Modulus (GPa)	Error (+/-)	Toughness (MJ/m^3)	Error (+/-)	Strain (%)	Error (+/-)
0	**43**	3.2	**1.5**	0.02	**37.0**	19.23	**117**	59.0
0.0675	**63**	3.7	**2.0**	0.35	**34.3**	22.18	**68**	45.1
0.125	**61**	2.3	**2.0**	0.18	**4.8**	2.20	**11**	5.1
0.25	**57**	1.1	**2.1**	0.19	**8.0**	7.43	**18**	16.2
0.5	**47**	4.7	**1.9**	0.20	**2.0**	1.98	**6**	4.4
1	**48**	1.9	**1.8**	0.42	**2.4**	1.47	**7**	3.7
2	**43**	6.0	**1.5**	0.41	**1.2**	0.21	**4**	0.6

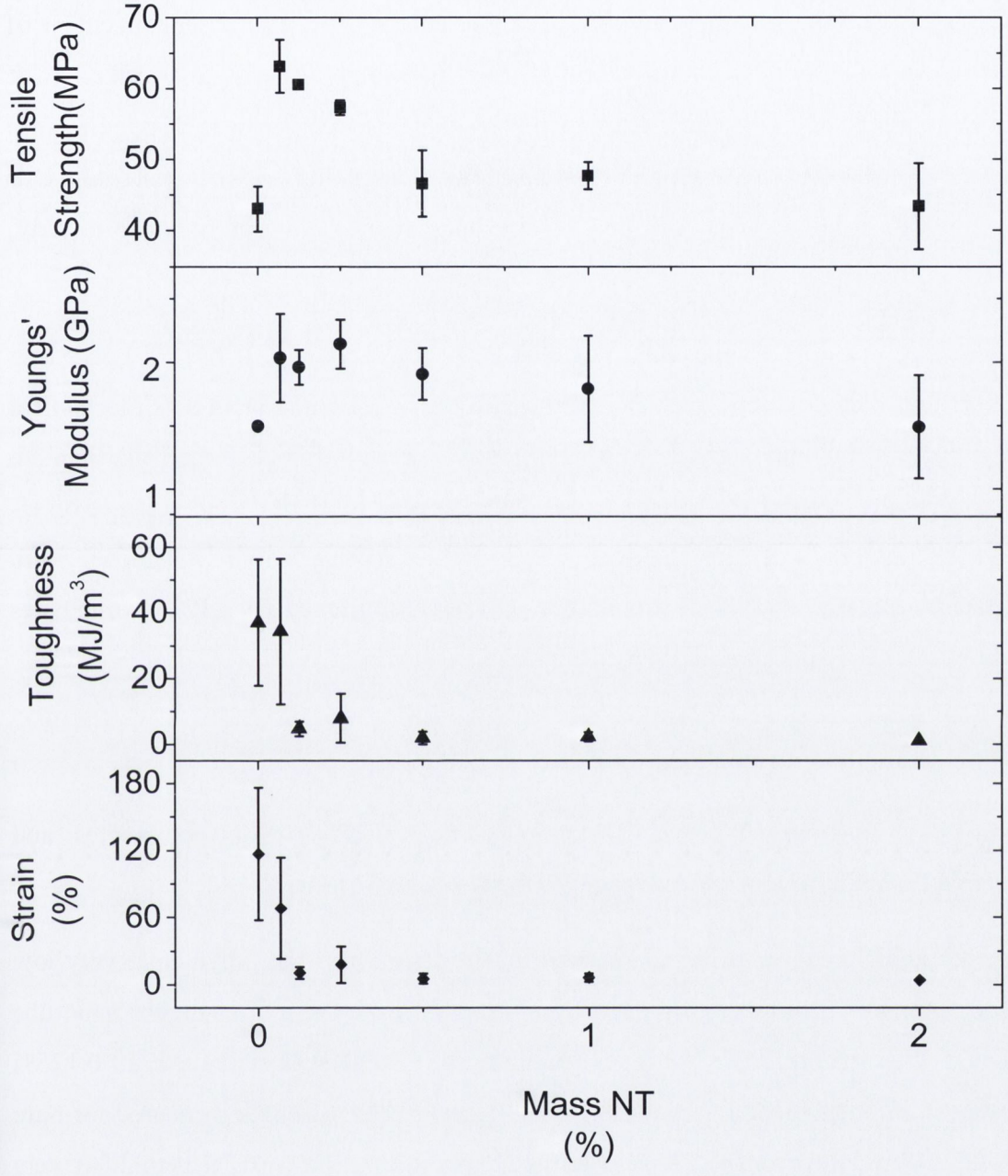

Figure 2.17 Combined graph of tensile strength, Young's modulus, toughness and strain against mass % of 6 hr refluxed FNT-PVC composites against the mass percentage of nanotubes within the polymer film.

2.7.3 Nanotube-PVA composites

The FNTs which were refluxed for 4 hr and 6 hr on the whole, whilst displaying increases on the pure polymer and on the PNTs, do not show further enhancement of either polystyrene or PVC. They are in fact generally slightly less effective at reinforcement when compared to the 2 hr FNTs. For this reason it was decided to stop using the 4hr and 6hr refluxed nanotubes as additives for other polymer materials. Our next aim was to find out if the FNTs were adaptable to another polymer namely, Polyvinyl Alcohol (PVA).

In **Chapter 1** we discuss the importance of PVA commercially. It has an interesting structure and is highly dependent on hydrogen bonding (H-bonding) for its mechanical strength. It was anticipated that the FNTs may have a better affinity to the PVA than the PNTs although structural disruption is also a greater possibility due to its reliance on H-bonds. In this work the mechanical properties of pristine polymer samples were compared with both PNT-PVA composites and the 2 hr refluxed FNT-PVA composites in sections **2.7.3.1** and **2.7.3.2**.

2.7.3.1 Pristine nanotube–PVA composites

Initially we examined the mechanical properties of PVA-PNT composites and compared them to the properties of pure PVA (**Table 2.9, Figure 2.18**).

There is a clear trend in an initial increase in the strength of the polymer at very low concentrations of nanotubes, followed by a sharp drop in strength at higher nanotube loadings. The maximum increase in strength (43 MPa) was achieved at 0.125% nanotube concentration and was about 40 % higher than the strength measured for pure PVA (31 MPa). However the higher nanotube concentration films (0.25 % to 2 %) were very weak and were only 70 – 80 % of the strength measured for pure PVA.

We can then see that the addition of nanotubes causes a decrease in the Young's modulus of the polymer. The decrease is fairly dramatic and ultimately results in a 62% drop at its lowest value (1.1 MPa, 0.25 % PNTs). This could be because of imperfections in the polymer matrix caused by the addition of the nanotubes.

The toughness and strain of the composites demonstrate interesting behaviour. We see an increase in both for the first two concentrations, followed by the expected decrease

from 0.25 to 2 %. The toughness reaches a maximum of 158 MJ/m^3 at 0.125 % PNTs representing a significant increase of 138 % on the pure polymer. The corresponding strain has also increased accordingly.

At the higher loadings (above 0.125 %) we again see considerable decreases in all the mechanical properties, similar to the decrease we see with the PNTs in PS and PVC.

Table 2.9 Combined mechanical data for PNT-PVA composites

Mass NT (%)	Tensile Strength (MPa)	Error (+/-)	Young's Modulus (GPa)	Error (+/-)	Toughness (MJ/m^3)	Error (+/-)	Strain (%)	Error (+/-)
0	**31**	1.4	**2.7**	0.54	**66**	19.2	**260**	73.7
0.0625	**41**	4.1	**1.7**	0.81	**142**	24.4	**426**	60.9
0.125	**43**	4.3	**1.2**	0.59	**158**	12.1	**465**	8.5
0.25	**26**	4.7	**1.1**	0.26	**57**	23.2	**264**	48.7
0.5	**26**	3.6	**1.5**	0.14	**48**	15.1	**223**	60.7
1	**22**	2.2	**1.5**	0.21	**26**	2.9	**152**	4.3
2	**22**	1.0	**1.9**	0.6	**29**	8.2	**169**	45.4

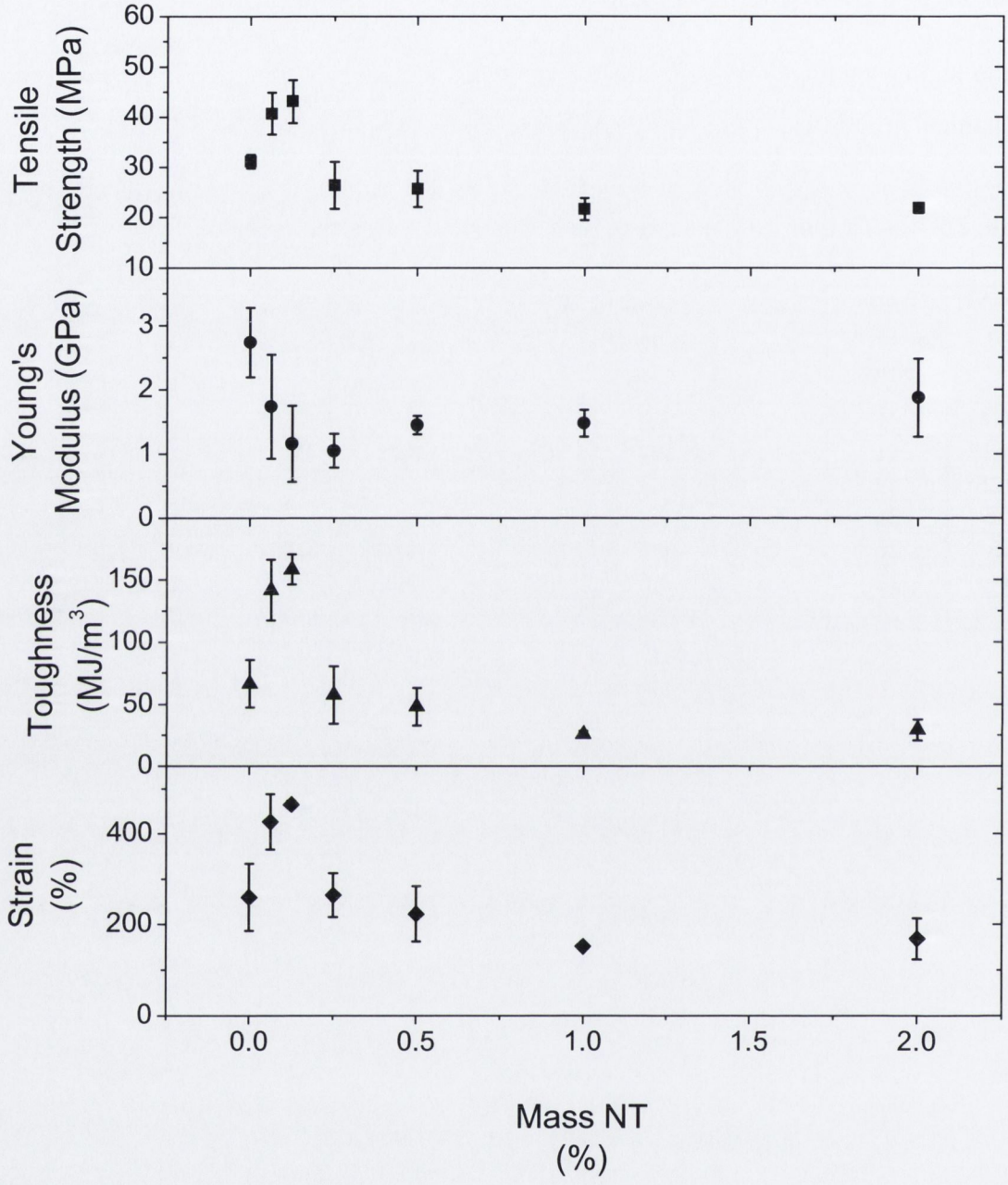

Figure 2.18 Combined graph of tensile strength, Young's modulus, toughness and strain against mass % PNT-PVA composites against the mass percentage of nanotubes within the polymer film

2.7.3.2 PVA composites containing FNTs refluxed for 2 hours

Next the mechanical properties of FNT-PVA composites were examined and compared to the properties of pure PVA (**Table 2.10, Figure 2.19**).

In the graph we can see that the addition of Kevlar coated nanotubes fails to make any considerable increase in the strength of the polymer. Initially the strength of the samples measured is roughly the same as the strength measured for pure PVA, but the strength significantly decreases after the 0.25% nanotube concentration remaining low throughout the mass percentage range.

The Young's modulus data shows much larger increases than was observed in the PNT composites. The data does not seem to follow this trend too closely for every sample; however in the maximum concentration (2 %) we get a Young's modulus value of 6.1 GPa representing a very substantial 122 % increase on the pure PVA (2.7 GPa). Considering that the PNT-PVA samples decreased at all concentrations it makes the increase even more impressive.

The toughness and strain seem to be fairly unaffected by the addition of the FNTs. This is disappointing as the PNT composites demonstrated increases in toughness.

Overall although the addition of FNTs showed increases in the Young's modulus we find the other mechanical properties are worse than in the PNT composites. The more derogatory effect of the FNTs on the composites can be explained by its larger size and therefore greater disruptive capability to the hydrogen bonded structure of the polymer matrix.

Table 2.10 Combined mechanical data for 2 hr refluxed FNT-PVA composites

Mass NT (%)	Tensile Strength (MPa)	Error (+/-)	Young's Modulus (GPa)	Error (+/-)	Toughness (MJ/m^3)	Error (+/-)	Strain (%)	Error (+/-)
0	**31**	1.4	**2.7**	0.54	**66**	19.2	**260**	73.7
0.0625	**32**	4.3	**3.9**	0.57	**66**	25.2	**251**	69.7
0.125	**30**	1.1	**2.2**	0.24	**67**	9.6	**290**	65.2
0.25	**30**	1.7	**4.1**	0.41	**66**	17.2	**267**	56.7
0.5	**24**	4.1	**1.4**	0.14	**40**	8.3	**214**	32.4
1	**26**	2.5	**4.3**	0.74	**40**	16.4	**185**	78.2
2	**28**	1.9	**6.1**	0.27	**69**	17.2	**302**	64.6

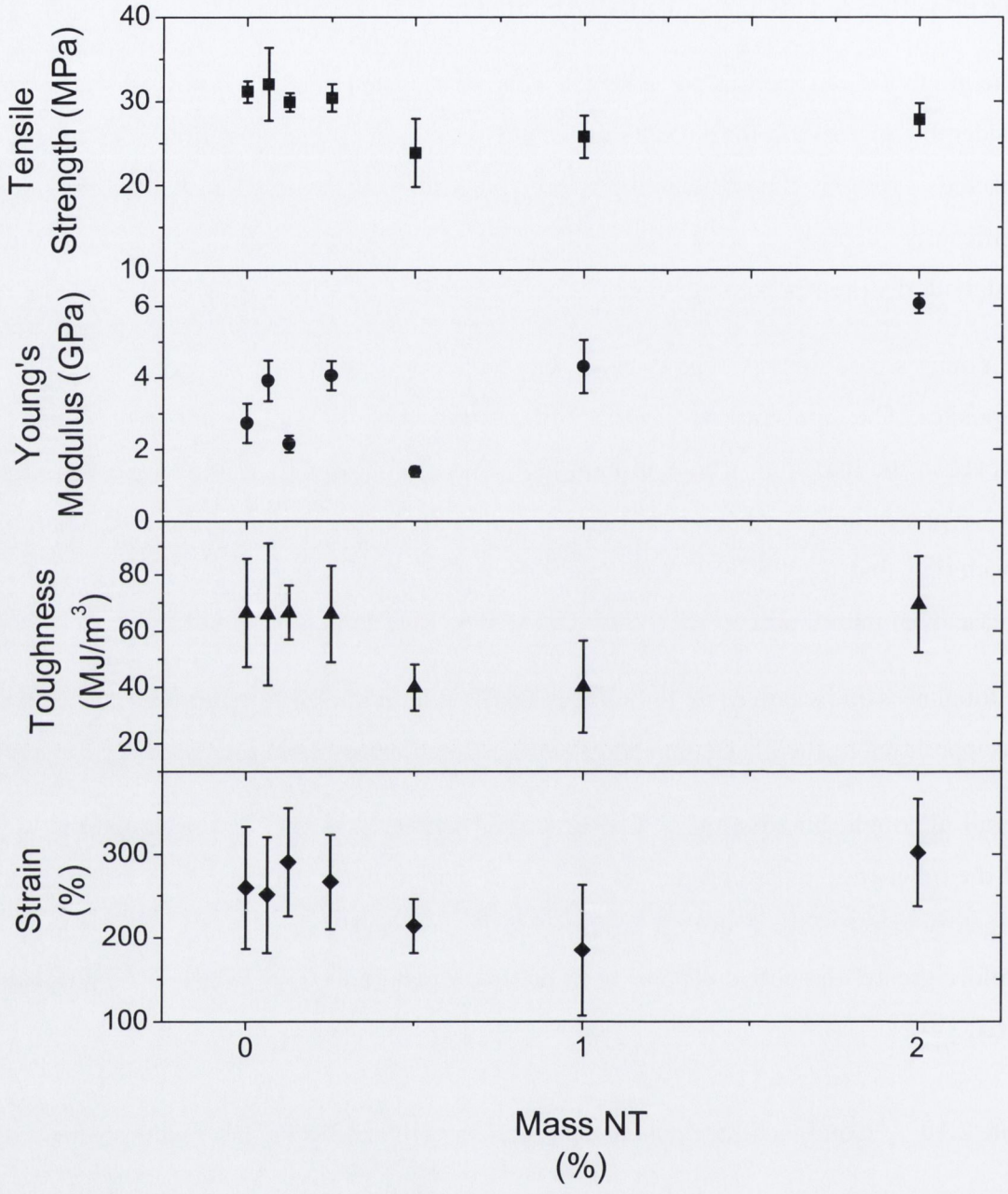

Figure 2.19 Combined graph of tensile strength, Young's modulus, toughness and strain against mass % of 2 hr refluxed FNT-PVA composites against the mass percentage of nanotubes within the polymer film

2.7.4 Nanotube - PVAc composites

As we discussed with the PVA composites we initially expected there would be hydrogen bonding between the Kevlar and PVA molecules in the polymer matrix, thereby increasing the stress transfer between the nanotube and the polymer. It was expected that because of its structure PVA may have facilitated the FNTs better than PNTs and it was hoped that the OH groups in PVA and amido groups in Kevlar might interact via hydrogen bonding. The effect we achieved however was a reduction in the strength, indicating that the polymer matrix may have become disrupted. With this in mind the next polymer selected was polyvinyl acetate (PVAc). Similarly to PVA, PVAc has some polar side groups, but has a larger inter-chain separation and does not undergo hydrogen bonding between the chains in the polymer matrix. We expected that it may therefore be better able to incorporate nanotubes and would thus result in increased mechanical properties. In this work the mechanical properties of pristine polymer samples were compared with both PNT-PVA composites and the 2 hr refluxed FNT-PVA composites in sections **2.7.4.1** and **2.7.4.2**.

2.8.4.1 Pristine Nanotube – PVAc composites

Initially we examined the mechanical properties of PNT–PVAc composites and compared them to the properties of pure PVAc (**Table 2.11, Figure 2.20**).

Here we can see that the addition of nanotubes results in quite significant increase in the strength of the polymer composite in comparison with the pure polymer. This increase can be associated with the increase in concentration of the nanotubes within the polymer matrix. The strength reaches a maximum at a concentration of 0.125% nanotubes and then we observe a decrease in strength. This decrease is most likely due again to the nanotubes forming larger aggregates causing areas of weakness in the sample. However the decrease is not too dramatic and the highest concentration still retains a relatively high strength in comparison to the pure polymer indicating that the bulky nanotubes do not have such a detrimental effect on the polymer structure. This signifies that possibly the PVAc structure is more accommodating than the PVA. The maximum strength achieved (40 MPa at 0.125% conc.) was about a 50% increase in the strength measured for pure PVAc (25 MPa).

We then analysed the Young's modulus to see if the increases are replicated. The addition of PNTs to PVAc gave a large increase in Young's modulus. The maximum modulus measured (2.8 GPa) was achieved at a very low mass percentage of nanotubes (0.0625 %). It was a 182% increase on that of pure PVAc. This increase is not maintained across the mass percentage range however; once the highest concentration is reached we find the modulus is similar to the pure polymer (1.1 GPa).

When we analyse the strain and toughness of the samples we find that they decrease initially and then raise as the nanotube content increases. This is the opposite to what we expect for a polymer with good interfacial stress transfer and may indicate that as the nanotube contents increases we get less stress-strain transfer between the nanotubes and the polymer.

The overall effect of the addition of PNTs to PVAc was a large increase in mechanical properties. At the 1% concentration we achieve a large increase in strength and Young's modulus without a major change in toughness or strain. It indicates that PVAc is the most accepting polymer structure.

Table 2.11 Combined mechanical data for PNT-PVAc composites

Mass NT (%)	Tensile Strength (MPa)	Error (+/-)	Young's Modulus (GPa)	Error (+/-)	Toughness (MJ/m^3)	Error (+/-)	Strain (%)	Error (+/-)
0	**25**	3.6	**1.0**	0.4	**12.1**	8.59	**67**	45.7
0.0625	**37**	5.5	**2.8**	0.4	**1.6**	0.45	**5**	1.3
0.125	**40**	5.5	**2.0**	1.1	**2.9**	1.96	**9**	6.6
0.25	**37**	2.6	**1.7**	0.6	**8.6**	5.29	**31**	15.2
0.5	**35**	2.3	**1.8**	0.5	**12.3**	6.49	**45**	21.8
1	**35**	4.3	**1.1**	0.2	**21.8**	6.57	**81**	13.0

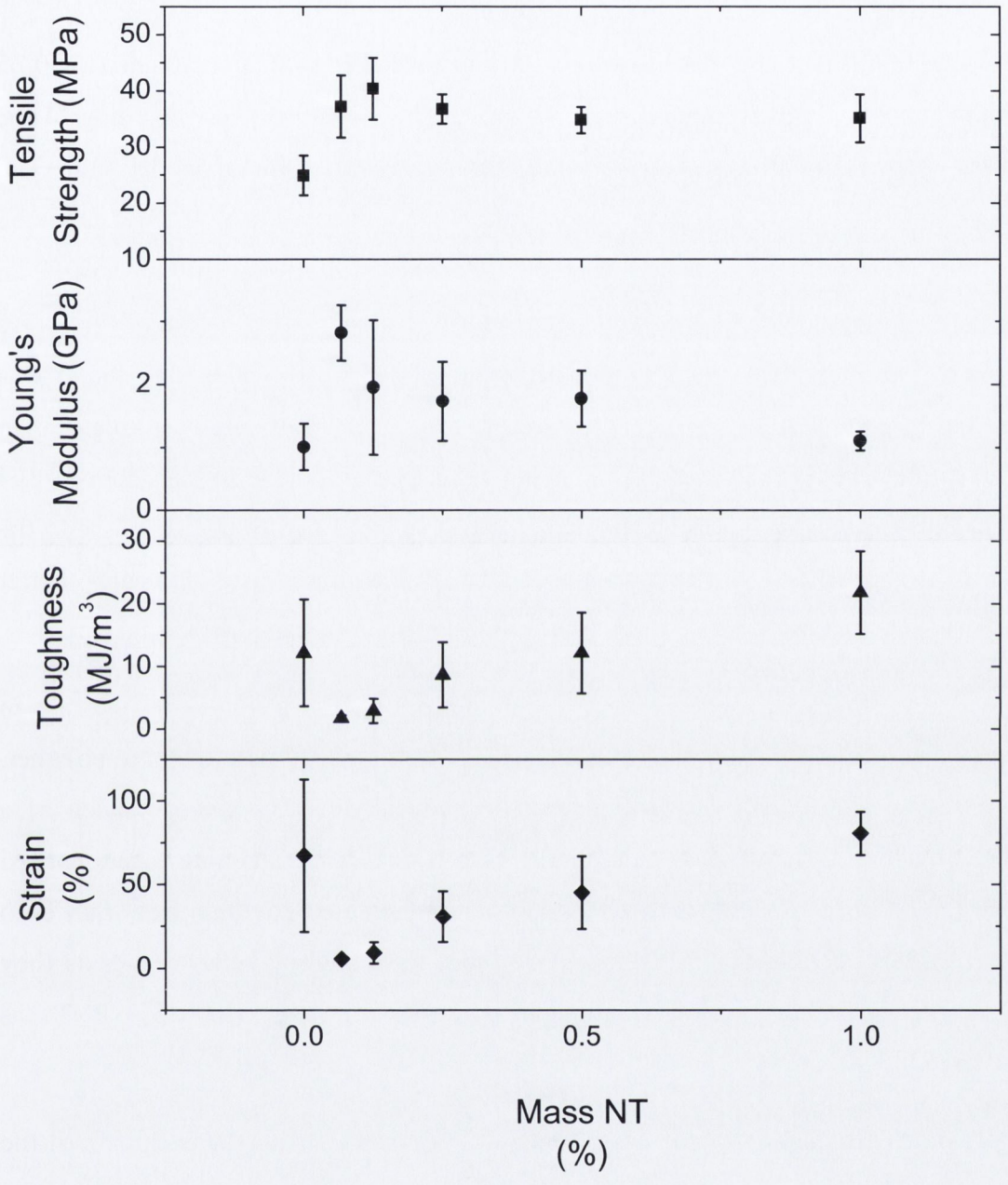

Figure 2.20 Combined graph of tensile strength, Young's modulus, toughness and strain against mass % PNT-PVA composites against the mass percentage of nanotubes within the polymer film

2.7.4.2 PVAc composites containing FNTs refluxed for 2 hours

Next the mechanical properties of the 2 hr refluxed FNT-PVAc composites were examined and compared to the properties of pristine PVAc (**Table 2.12, Figure 2.21**).

According to our measurements there is a very linear increase in strength until the 0.25 % mass concentrations of nanotubes. This is what we would expect according to the rule of mixtures indicating that there are less aggregates forming in the film. The strength increases with nanotube concentration to a maximum at 0.25% nanotube concentration and then starts to decrease. All concentrations measured showed an increase in strength again demonstrating the more accommodating nature of the PVAc structure. The maximum average strength achieved (45.3 MPa at 0.25% conc.) was about an 80% increase on the strength measured for pure PVAc and was greater than the maximum strength achieved with non-functionalised pristine nanotubes above (40.4 MPa). Thus the Kevlar functionalised nanotubes give a greater strength increase to the polymer with respect to the non-functionalised nanotubes. This indicates better interfacial stress transfer between the functionalised nanotubes and the polymer.

The addition of 2 hr refluxed FNTs to PVAc also resulted in a significant increase in Young's modulus. The maximum increase of 173 %, compared with the pure polymer, was observed for the 0.5 % concentration. However, we don't see too much of a difference between the Young's moduli in PVAc composites containing functionalised and pristine nanotubes. They both give a substantial increase but within error they both achieve similar maxima. In fact the pristine tubes gave slightly better results as they achieve their maximum value at a much lower concentration (0.0625% PNTs as opposed to 0.5 % FNTs).

The toughness and strain values decrease for the composites with the exception of the 0.125 % concentration. At the 0.125 % FNT concentration we see an increase in the tensile strength, Youngs modulus and toughness with no corresponding significant increase in strain.

When we look at the mechanical properties overall we find that there is not too much difference between the functionalised nanotube composites and the pristine nanotube composites with only the tensile strength showing a significant increase. Also we find that it is hard to uncover a definable trend for each of the concentrations of nanotubes'

effect on the mechanical properties of the composite as a whole. Where we can see obvious trends in the strength and modulus for the samples it is hard to recognise a trend in the toughness and strain. This is particularly evident in the pristine nanotube composites.

Table 2.12 Combined mechanical data for 2 hr refluxed FNT-PVAc composites

Mass NT (%)	Tensile Strength (MPa)	Error (+/-)	Young's Modulus (GPa)	Error (+/-)	Toughness (MJ/m^3)	Error (+/-)	Strain (%)	Error (+/-)
0	**25**	3.6	**1.0**	0.37	**12.1**	8.59	**67**	45.7
0.0625	**32**	2.9	**1.2**	0.19	**8.7**	4.06	**44**	25.6
0.125	**35**	3.0	**1.9**	0.38	**17.1**	9.21	**69**	35.7
0.25	**45**	7.4	**1.9**	0.43	**5.1**	4.40	**17**	17.5
0.5	**36**	5.9	**2.7**	0.81	**1.6**	0.52	**5**	1.7
1	**32**	3.0	**2.2**	0.47	**6.7**	1.61	**3**	0.3

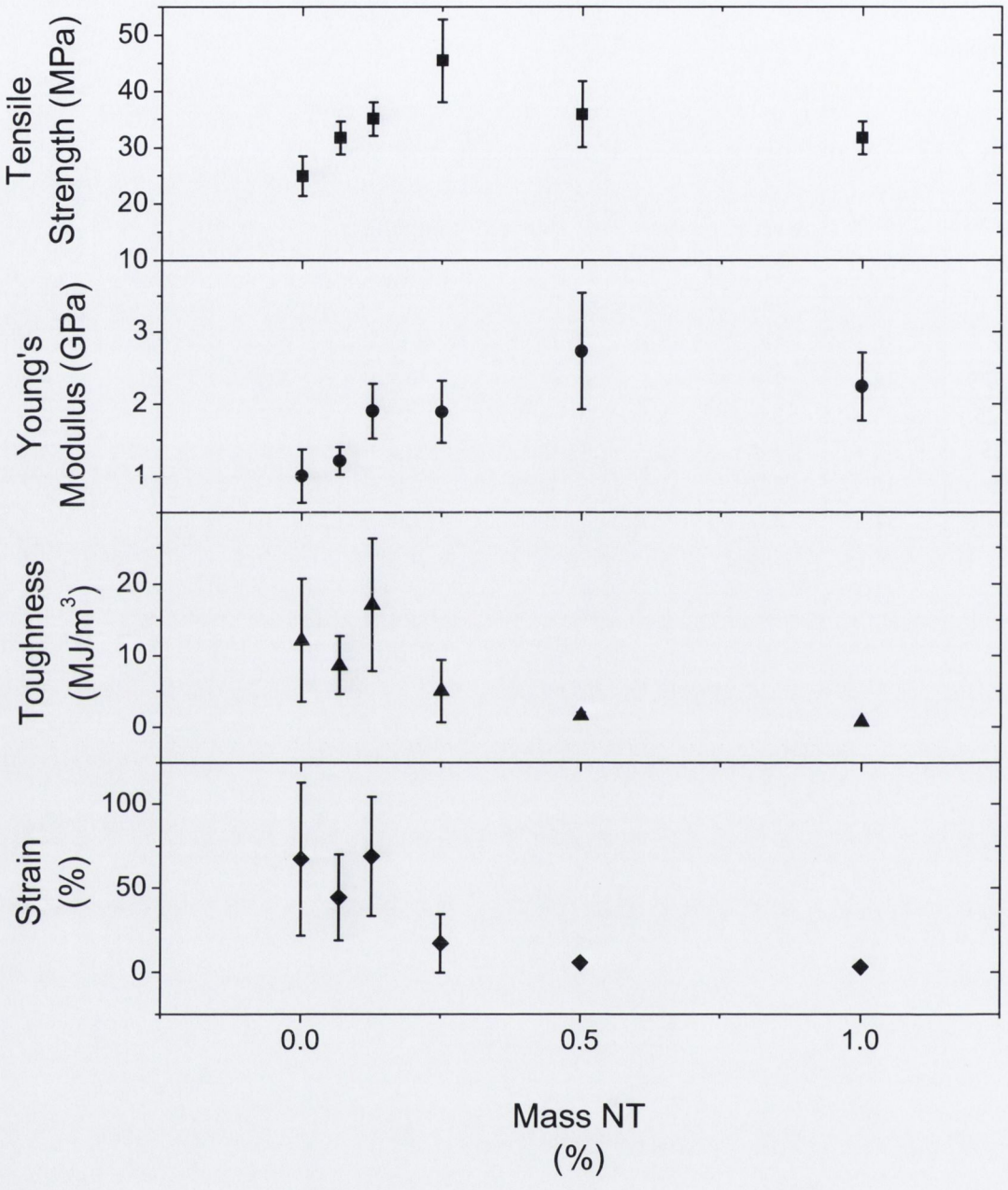

Figure 2.21 Combined graph of tensile strength, Young's modulus, toughness and strain against mass % of 2 hr refluxed FNT-PVAc composites against the mass percentage of nanotubes within the polymer film

2.8 Conclusions

We have developed a new one-step method for purifying carbon nanotubes and functionalising them with a high strength polymer, namely Kevlar. We have found that the length of heating time under reflux can strongly influence the amount of coating we can achieve on the nanotube surface and also the nanotube integrity. Ultimately refluxing for too long results in a complete degradation of both the polymer and the nanotube structure. We have found that the mechanical properties of Kevlar functionalised nanotube - polymer composites strongly depend on the nature of polymer and on the mass percentage of nanotubes. Observing increases in mechanical properties, as a general rule, the mass percentage concentrations of nanotubes which show the most significant increases in all mechanical properties of the PNT were those of the lower mass percentages. Higher mass percentages of PNTs tended to have a derogatory effect on the structure of polymer. This is almost certainly due to the fact that nanotubes tend to aggregate at higher concentrations creating larger bundles. The resulting inhomogeneous composite films at higher mass percentages of PNTs display decreased mechanical properties. In general, the FNT composites showed similar increases to the PNT composites at low mass percentages, with some cases displaying much more substantial increases. As the mass percentage of FNTs in the composites was increased however the FNT composites displayed further enhancement even up to 1 or 2 mass percent of FNTs. This indicates less aggregation and a more homogenous dispersion within the polymer matrix.

Overall as a general rule both PNT composites and FNT composites exhibited improvements in the mechanical properties, with the exception of PVA composites. However, the FNT composites display greater overall enhancement. This greater increase in strength by the functionalised nanotubes can be attributed to reduced aggregation of Kevlar functionalised nanotubes and better interfacial stress transfer between the nanotubes and polymer. We also believe that the presence of very strong Kevlar coating contributes to the improvement of mechanical characteristics.

References

[1]S. Iijima, C. Brabec, A. Maiti, J. Bernholc *J. Chem. Phys.* **104**, 2089 (1996)

[2]M.R. Falvo, G.J. Clary, R.M. Taylor II, V. Chi, F.P. Brooks Jr, S. Washburn, R. Superfine, *Nature*, **389**, 582 (1997)

[3]M. Yu, O. Lourie, M.J. Dyer, T.F. Kelly R.S. Ruoff, *Science*, **287**, 637 (2000)

[4]S. Xie, W. Li, Z. Pan, B. Chang and L. Sun, *J Phys Chem Solids*, **61**, 7 (2000)

[5]K.T. Lau, D. Hui, *Composites Part B*, **33**, 263 (2002)

[6]M.J. Beircuk, M.C. Llaguno, M. Radosavjevic, J.K. Hyun, J.E. Fischer, A.T. Johnson, *Appl.Phys. Lett.*, **80**, 2767 (2002)

[7]C. Wei, D. Srivastava, K. Cho, *Nano. Lett.* **2**, 647 (2002)

[8]R. Saito, M. Fujita, G. Dresselhaus, M.S. Dresselhaus *App. Phys. Lett.* **60**, 2204 (1992)

[9]T.W. Ebbesen, T. Takada, *Carbon,* **33**, 973 (1995)

[10]A. Hirsch, *Angew. Chem. Int. Ed.*, **41**, 1853 (2002)

[11]J.L. Bahr, J.M Tour, *J. Mater. Chem.*, **12**, 1952 (2002)

[12]D. Tanner, J. A. Fitzgerald, B. R. Phillips *Angew. Chem. Int. Ed.* **28**, 649 (1989)

[13]http://www2.dupont.com/Kevlar/en_US/index.html

[14]B. Jingsheng, Y. Anji, Z. Shengqing, Z. Shufan, H. Chang. *J. App. Poly. Sci.*, **26**, 1211 (1981)

[15]K. Prasad, D. T. Grubb *J. App. Poly. Sci.* **41,** 2189 (2003)

[16]K.E. Perepelkin, I.V. Andreeva, E.A. Pakshver I.Y. Morgoeva, *Fibre Chemistry*, **35**, 265 (2003)

[17]J. Liu, A.G. Rinzler, H. Dai, J.H. Hafner, R. Kelley Bradley, P.J. Boul, A. Lu, T. Iverson, K. Shelimov, C.B. Huffman, F. Rodriguez-Macias, Y-S. Shon T. Randall Lee, D.T. Colbert, R.E. Smalley, *Science*, **280**, 1253 (1998)

[18]R. Saito, T. Takeya, T. Kimura, G. Dresselhaus M.S. Dresselhaus, *Phys. Rev. B,* **57**, 4145 (1998)

[19]J. Kurti, G. Kresse, H. Kuzmany, *Phys. Rev. B,* **58**, 8869 (1998)

[20]Y.F. Wang, X. W. Cao, S.F. Hu, Y.Y. Liu, G.X. Lan, *Chem. Phys. Lett.*, **336**, 47 (2001)

[21]S.D. Bergin, V. Nicolosi, P.V. Streich, S. Giordani, Z. Sun, A.H. Windle, P. Ryan, N.P.P. Niraj,. Z.-T. Wang, L. Carpenter, W.J. Blau, J.J. Boland, J.P. Hamilton, J.N. Coleman, *Adv. Mater*, **20**, 1876 *(* 2008)

[22]S. Giordani, S.D. Bergin, V. Nicolosi, S. Lebedkin, M.M. Kappes, W.J. Blau, J.N. Coleman, *J Phys Chem B*, **110**, 15708 (2006)

[23]J.N. Coleman, M. Cadek, R. Blake, V. Nicolosi, K.P. Ryan, C. Belton, A. Fonseca, J.B. Nagy, Y.K. Gun'ko, W.J. Blau, *Adv. Func. Mater.*, **14**, 791 (2004)

[24]J.N. Coleman, U. Khan, Y.K. Gun'ko, *Adv. Mater.* **18**, 689 (2006)

[25]J.N. Coleman, U. Khan, W.J. Blau, Y.K. Gun'ko, *Carbon*, **44**, 1624 (2006)

Chapter 3

Carbon Nanotube-Kevlar Composites

3.1 Introduction

Kevlar is an exceptionally strong material and is manufactured by DuPont in three grades. Even the weakest grade of Kevlar is comparable in strength to steel and only half as dense. Kevlar 129 has the highest tensile modulus of all. It is used for making bulletproof jackets. Our research focuses on the reinforcement of Kevlar 129 using carbon nanotubes. As we discussed in **Chapter 1**, Kevlar displays a very interesting chemical and molecular structure which contributes a great deal to its mechanical strength. We wish to develop a process which will complement these properties without disrupting them to a great extent. By incorporating nanotubes into the structure we wish to achieve good interfacial stress transfer between the pleated layers of the polymer without disrupting the hydrogen bonding matrix or the covalently bonded chemical structure of the Kevlar fibres.

Previous approaches to the preparation of nanotube-polymer composites have been focused mostly on *in situ* polymer synthesis at the presence of nanotubes or by mechanical mixing of the nanotubes with a polymer and processing of composites by solution or melt casting as discussed in **Chapter 1**. Solution casting technique was the basis of our work described in **Chapter 2**. Some of the composites produced by these methods demonstrate increases in mechanical properties. For example a 20% increase of modulus in tension and 24% in compression were observed for 5wt % multiwalled carbon nanotubes (MWNT)/epoxy composites.[1] Using surfactants as the processing aid, Gong *et al*[2] obtained a 30% increase of elastic modulus with the addition of 1wt% nanotubes into the epoxy matrix. For MWNT/PMMA composites, tensile strength increased 7–30%, toughness ~10% and hardness ~43% with the addition of 1–7 wt% acid-treated MWNTs.[3] Our polymer composites demonstrated increases of up to 50 % with pristine nanotube composites.

Recently, it has been reported that nanotubes can be efficiently dispersed in N-methyl-2-pyrrolidone (NMP).[4,5] It is also known that NMP can be used as a solvent for the synthesis, polymerisation and processing of Kevlar.[6] It has also been shown that NMP is capable of swelling Kevlar among other polyaramid fibres.[7] This led us to hypothesise that nanotubes could be incorporated into swelled Kevlar by soaking Kevlar fibers in a dispersion of nanotubes in NMP.

3.2 Aims of This Work

The main aim of our work for this chapter was to prepare new ultra-strong polymer composite materials using carbon nanotube as additives to Kevlar fibres. We hope to explore the technique of polymer swelling and use this to create a novel method of incorporation of nanotubes into a polymer. We will explore the effect of ultrasound on nanotube dispersions and polymer swelling. We expect that the thin nanotubes will penetrate effectively into the polymer matrix and not disrupt the internal structure of a Kevlar fibre. Once we have prepared the polymer composites we aim to analyse them by a variety of techniques. It is hoped we will produce polymer composites with enhanced mechanical properties. To substantiate this we will perform mechanical testing to uncover their mechanical properties. We anticipate that novel reinforced Kevlar composites materials can find a number of potential applications.

3.3 Dispersion of Nanotubes and Sedimentation Studies

The nanotubes selected were curly very thin MWNTs, which were purchased from Nanocyl. They were both relatively inexpensive and posed the least disruptive threat to the polymer matrix. They are similar to the nanotubes used in **Chapter 2** but are generally smaller in diameter. These nanotubes were of a purity of about 95 %. When we look at the TEM images showing the MWNTs (**Figure 3.1**) we can that there is very little graphitic material contained in the sample.

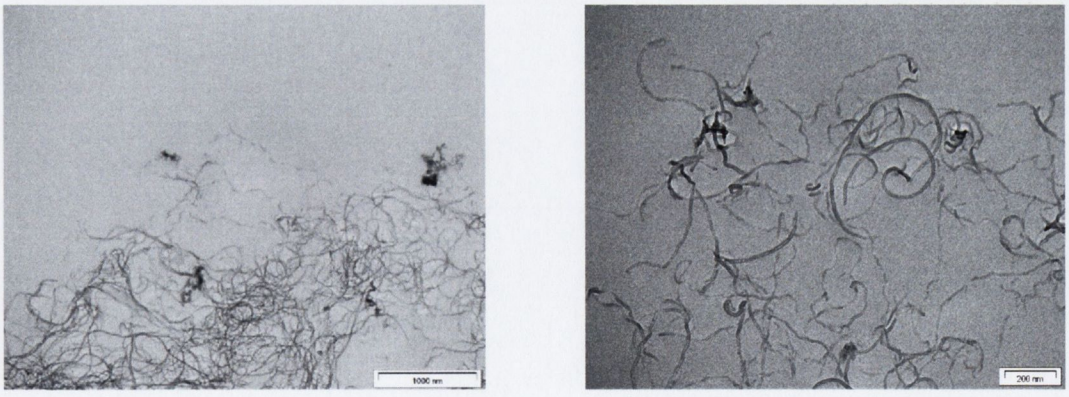

Figure 3.1 TEM images of very thin Nanocyl nanotubes used in this project.

As we discussed in the introduction a very important solvent for the processing and swelling of Kevlar is NMP. This solvent is also remarkably effective at dispersing nanotubes and keeping those dispersions stable. It is important however to consider how effective these solvents are when selecting which to use. Dispersions of nanotubes in both solvents, along with nanotubes in THF for comparison, were made up with a concentration of 0.6 g/l nanotubes. We subjected these dispersions to sedimentation analysis (**Figure 3.2**).

The investigation has shown that both solvents are remarkably stable when compared with the sample in THF (blue curve). The nanotubes in both DMF (red curve) and NMP (black curve) stay dispersed without any precipitation for at least 2 hours. Following these initial results the tests were run for 3 days and it was discovered only about 12% of the nanotubes in the NMP precipitated during this time. The nanotubes in DMF showed a similar sedimentation within 24 hours. However, NMP demonstrates the superior ability both to disperse nanotubes and swell Kevlar. For this reason NMP was chosen as the solvent to prepare stable dispersions of carbon nanotubes.

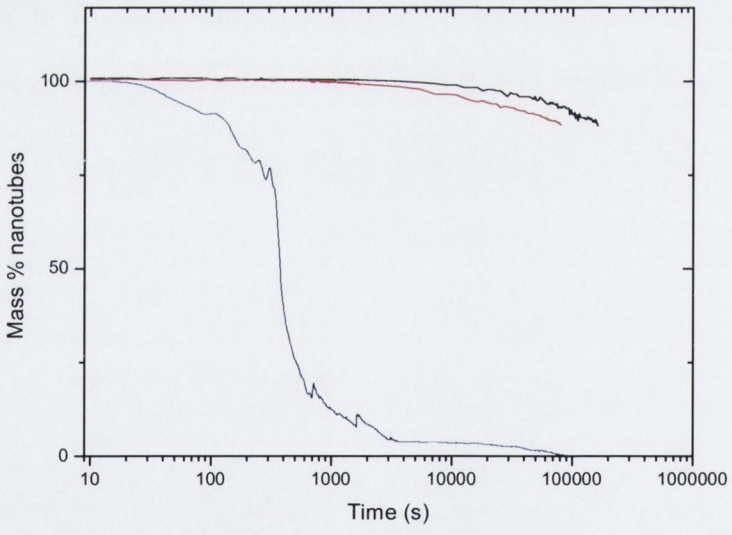

Figure 3.2 Sedimentation curves for nanotubes in NMP (black curve), DMF (red curve) and THF (blue curve)

3.4 Preparation of Kevlar-Nanotube Composite Materials

The process of the preparation of Kevlar-nanotube composites was carried out in three stages. First Kevlar fibres were cut into 1m long strips and weighed. The second step was to create a stable dispesion of nanotubes in NMP, by sonicating under the sonic tip for 10 minutes followed by the sonic bath for two hours. Thirdly the Kevlar fibres were placed in this stable dispersion of nanotubes and further sonication was carried out over different time periods from 5 minutes to 4 hours. The concentrations of nanotubes in NMP were also varied from 0.15 g/l up to 1.8 g/l. Data for both of these preparation conditions are presented here.

When we add the Kevlar fibres to the solution they can be swelled in the NMP. This lets the nanotubes be dispersed within the fibre of the Kevlar by a combination of swelling and diffusion of the nanotubes fibres in NMP. Diffusion can, in general, be characterized by an average displacement from the starting point, x, that varies in time, t, as x is proportional to $(Dt)^{1/2}$, where D is the diffusion coefficient. Similar to Fickian mass transport the transport of nanotubes into the porous swelled polymer by diffusion displays similar temporal behavior with a square root of time dependence. In this case, the intercalated mass uptake as a function of time is given by following equation:

$$\frac{m_{NT}}{m_P} = \left(\frac{m_{NT}}{m_P}\right)_{sat} \sqrt{\left(\frac{16D}{b^2\pi}\right)t}$$

where, $(m_{NT}/m_p)_{sat}$ is the saturated value of the mass uptake, D is the diffusion coefficient and b is the thickness of the fibre.

When the fibres are removed from the NMP they contract again leaving the nanotubes encapsulated within the Kevlar fibre. There are a large amount of nanotubes left on the surface of the Kevlar fibres as can be seen in the Scanning electron microscopy (SEM) images in **Figure 3.3 B** after treatment. We see no nanomaterial on the surface of the pure fibre **Figure 3.3 A**. These nanotubes, which have not been removed by vigorous washing, are expected to be partially incorporated in the Kevlar fibre. When we look at the enlarged images we find the nanotubes protruding out from the exterior surface of the fibre.

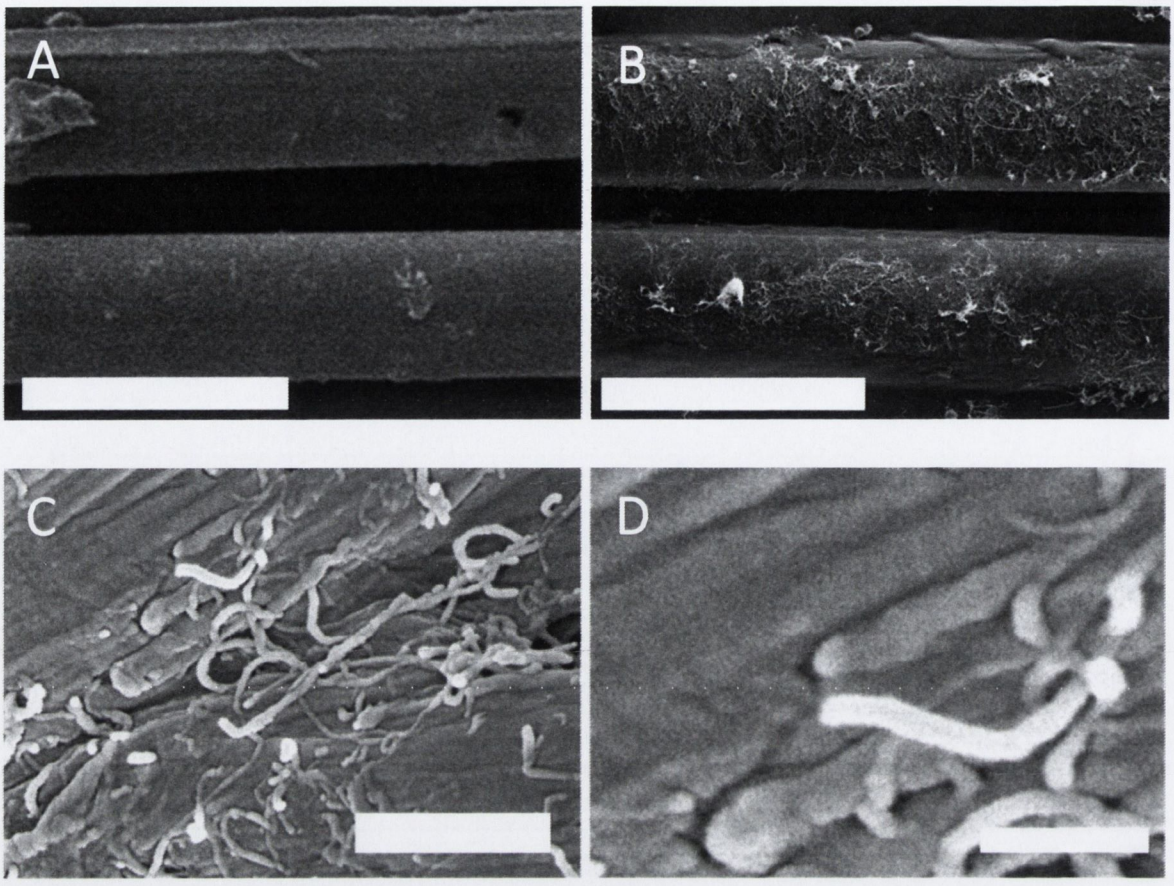

Figure 3.3 SEM images of Kevlar fibres before (**A**) and after (**B-D**) the treatment with nanotube suspension (scale bar is 20 μm for **A** and **B**, 0.5 μm for **C** and 100 nm for **D**)

To verify that the nanotubes are actually within the Kevlar fibres we performed SEM imaging of the cross section of the Kevlar fibres. The following SEM images (**Figure 3.4 A-F**) show the cross section of Kevlar fibres before and after the treatment. In the pure Kevlar sample (**A** and **B**) we see a relatively clean surface with no obvious nanomaterial present. In the images **C** and **D** we see a blade cut Kevlar composite fibre which displays evidence of penetration to the interior of the fibre. We also analysed the fibre which had been fractured in the tensile tester Figure **E** and **F** we can see an abundance of nanotubes protruding from the fracture surface. The previous images of the surface of individual treated Kevlar fibers show a web-like deposit of nanotubes, even after washing. While the breaks don't tend to be particularly clean, the presence of nanotubes in the interior of the fibres can be seen as illustrated in the blow-up on the right hand side image **F**. Taking into account what we observed in the images in

Figures 3.3 we can see that the swelling method achieves nanotube insertion into the interior of the Kevlar fibre as well as surface coating.

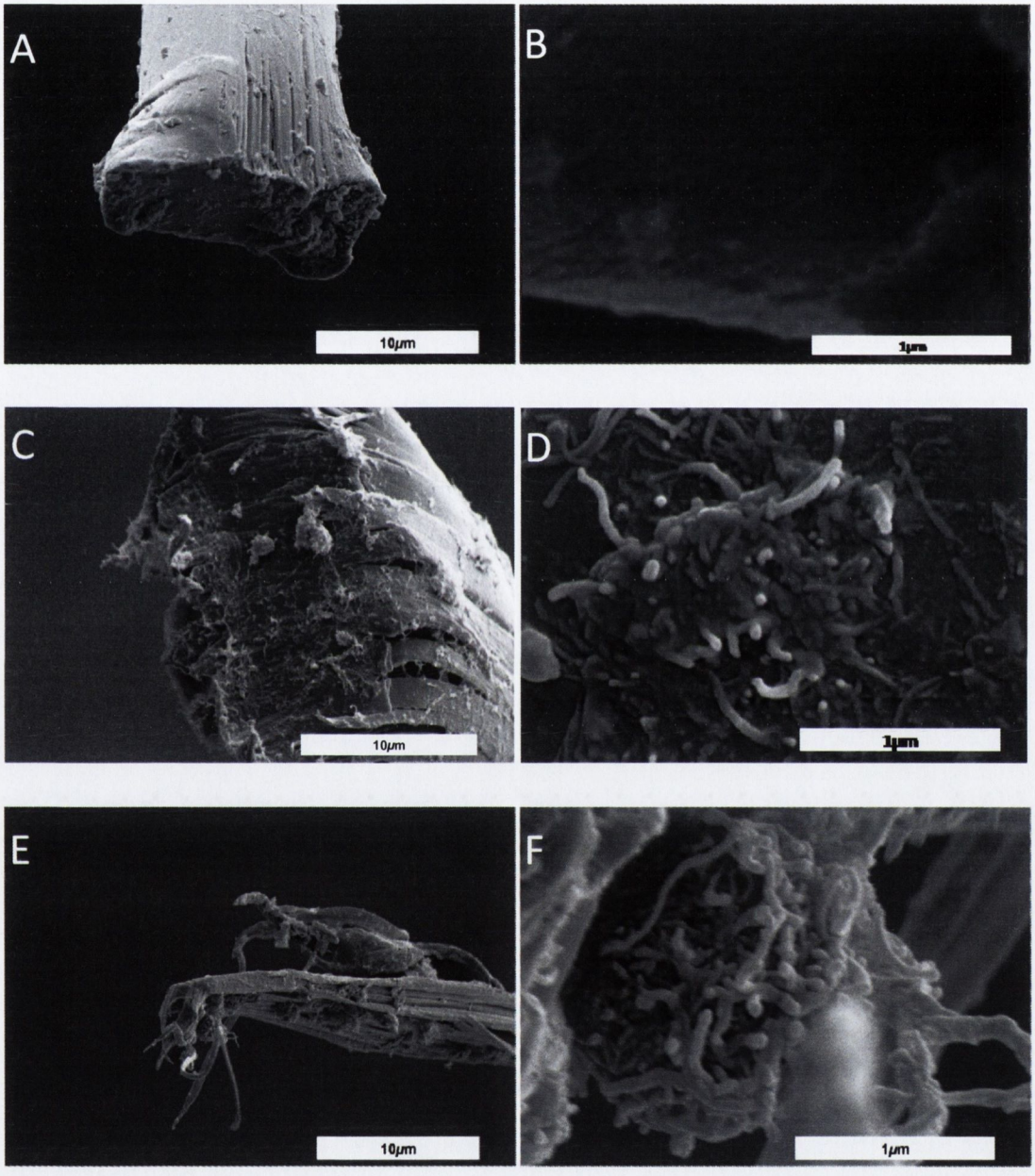

Figure 3.4 SEM images of cross sections for blade cut Kevlar fibres before treatment (**A** and **B**) blade cut composite fibres after treatment (**C** and **D**) and machine fractured composite fibres after treatment (**E** and **F**)

3. 5 Evaluation of Nanotube Mass Uptake

Analysis of the samples showed that swelling of Kevlar yarn in MWNT dispersions under ultrasound in a sonic bath resulted in a measurable mass uptake, which was varied with the sonication time and concentration of nanotubes in solution.

The samples were initially weighed before treatment and then after the following sonication treatment, washing and drying, weighed again. Through control experiments it was found that there was a slight change (1-2%) in the mass of the fibres when they were brought into contact with NMP. We can associate this to the surface finish applied during manufacture by the company who provides the fibre. This coating appears to be at least partially soluble in the NMP and the decrease in mass was associated with the length of time the sample was in contact with the NMP. This had to be taken into account when finding the mass uptake of the Kevlar fibres.

The nanotube mass uptake was found to scale with the square root of soak time **(Table 3.1, Figure 3.5)**, suggesting that the intercalation of nanotubes into Kevlar fibres is diffusion limited. The graph shows the percentage increase in mass due to nanotubes (taking into account the decrease associated with NMP) against the length of time it was sonicated in the NMP. The scale is presented in log form to demonstrate the linear association of the increase with the time. If the increase is according to diffusion process then the slope of the graph on a log scale should be equal to 0.5. The observed slope is 0.47 which indicates a very close match and we can thus determine that the increase is diffusion limited. The mass increase of five different fibres was measured and errors have been evaluated.

Table 3.1 The percentage mass uptake of nanotubes by the composite fibres with the sonication time

Time (s)	**NT Increase (%)**	Error (+/-)	**NMP Decrease (%)**	Error (+/-)	**Total Increase (%)**	Error (+/-)
28800	4.12	0.25	1.98	0.18	**6.10**	0.43
14400	2.91	0.49	1.57	0.26	**4.48**	0.75
3600	1.43	0.13	1.25	0.10	**2.68**	0.22
1800	0.23	0.10	0.87	0.09	**1.10**	0.19

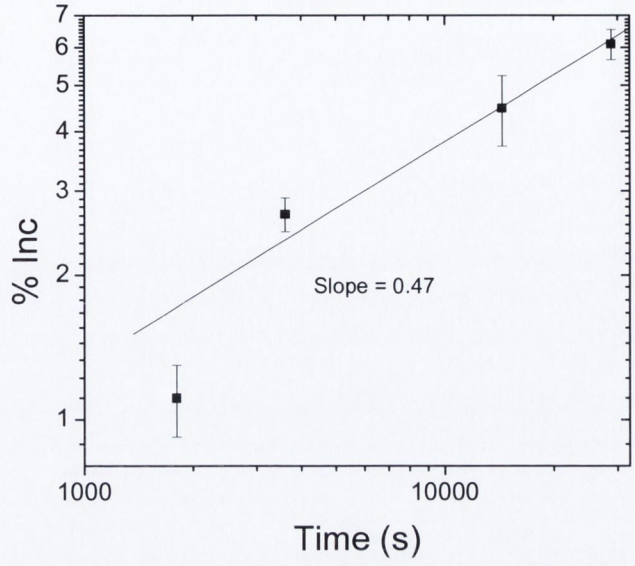

Figure 3.5 The percentage mass increase of nanotubes within the composite fibres according to the time of sonication on a log scale, the linear fit of the data is shown by the line (slope 0.47)

Analysis of the data gives an estimated diffusion coefficient of 5×10^{-16} m2/s.[8] This is significantly lower than the value of 1.3×10^{-12} m^2/s which one can estimate using the Broersma's equations[9] for a MWNT dispersed in the liquid phase. This result is unsurprising as diffusion in the restricted environment of the swelled polymer would be expected to be considerably slower then diffusion in the solvent.

3.6 Investigation of Mechanical Properties of Kevlar Bulk Yarn Composites

Initial mechanical properties of Kevlar bulk yarn samples were measured. Mechanical property testing for the yarn was carried out in the School of Engineering in Trinity College Dublin on an Instron 8501 fatigue machine. In all cases the stress-strain curves were linear, demonstrating brittle failure. Representative stress strain curves can be seen in **Figure 3.2**.

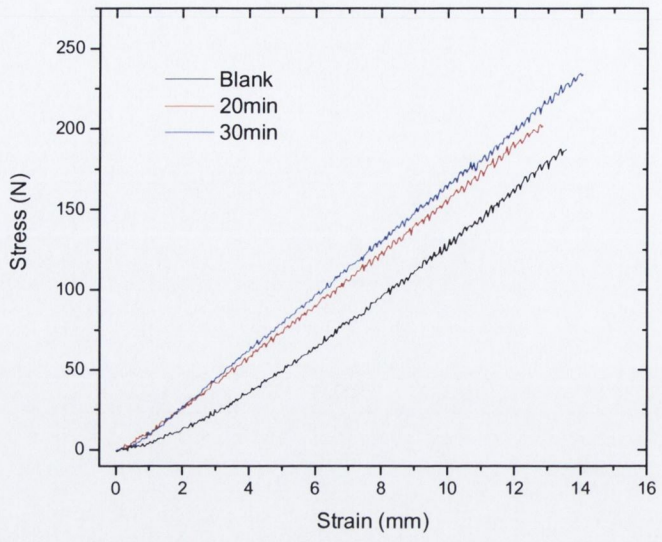

Figure 3.6 Representative stress-strain curves for Kevlar yarn at different sonication times, blank Kevlar (blackcurve), 20 minute sonication (red curve) and 30 minute (blue curve)

From these stress-strain curves we could obtain the four mechanical parameters: Young's modulus, tensile strength, strain at break, and toughness (**Table 3.2, Figure 3.7**)

There is an increase in the tensile strength from the pure Kevlar to a maximum at thirty minutes sonication. It can be seen from this graph the best strength result was found for the sample that was sonicated for thirty minutes and represents an increase in ultimate tensile strength of about 18 %.

The graph for Young's modulus is shown also and we can see that although there are large errors there is a significant change in Young's modulus as we increase the length of swelling time. The Young's modulus reaches a maximum increase of approximately 17% for the sample swelled for thirty minutes.

The toughness values remain quite similar with increasing swelling time, however after 20 minutes it shows a considerable increase and ultimately we achieve a maximum of 25 % after 30 minutes. The strain of the samples remained relatively constant within experimental error for the samples.

When we analyse the data we find that maximum Young's modulus and tensile strength values are achieved at around thirty minutes. Following this with all samples there is a general decrease once the 45 minute time frame is reached indicating we may be overloading the amount of nanotubes within the Kevlar fibre. This can result in aggregation of the nanotubes reducing dispersion of nanotubes in polymer matrix similarly to the effect seen in the samples in **Chapter 2**. Alternatively longer sonication treatment can do some physical damage to Kevlar fibres. All these factors will ultimately decrease the mechanical properties of the fibres.

Table 3.2 Changes in mechanical properties associated with time of swelling treatment

Time of Treatment (m)	Tensile Strength (MPa)	Error (+/-)	Young's Modulus (GPa)	Error (+/-)	Toughness (MJ/m^3)	Error (+/-)	Strain (%)	Error (+/-)
0	**2.2**	0.13	**20.5**	1.09	**20.8**	0.07	**28.4**	0.64
5	**2.3**	0.05	**21.3**	0.54	**21.9**	1.63	**30.5**	0.95
10	**2.3**	0.11	**20.7**	0.83	**22.0**	0.71	**30.3**	2.41
15	**2.3**	0.03	**21.7**	0.20	**21.7**	0.17	**30.6**	0.62
20	**2.5**	0.03	**22.9**	2.74	**23.8**	0.29	**29.5**	8.00
25	**2.4**	0.03	**21.8**	0.45	**24.2**	2.20	**31.5**	0.64
30	**2.6**	0.13	**24.0**	2.80	**26.1**	1.13	**29.8**	6.32
45	**2.4**	0.01	**21.6**	1.60	**22.6**	1.83	**30.0**	2.97

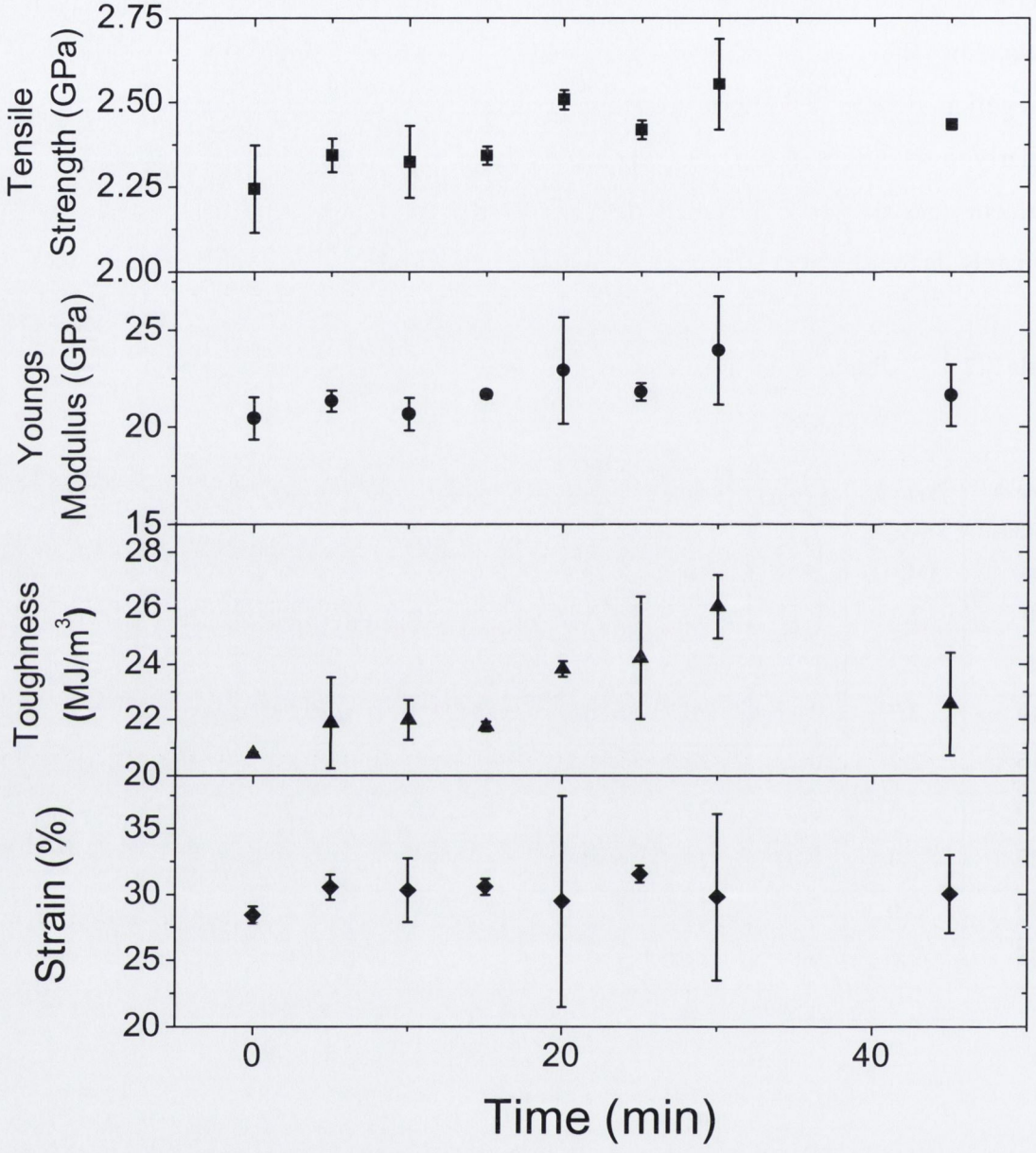

Figure 3.7 Mechanical property graphs for tensile strength, Young's modulus, toughness and strain for Kevlar fibres against the time of swelling treatment

3.7 Investigation of individual Kevlar Micro-fibres

There were considerable measurement difficulties with the bulk yarn samples. This included restricted access to the appropriate machinery and loading difficulties associated with a yarn. These problems had a significant impact on the measured mechanical properties with considerably less Young's modulus values and considerably higher strain values recorded for the sample than would be expected. In general in the literature much of the work on yarn samples is carried out on individual fibres where possible, especially with Kevlar.[10,11,12] Therefore we decided to carry out mechanical testing on individual single micro-fibres of the Kevlar samples prepared at varying concentrations. From the time dependence measurements we found that for a 0.6 g/L concentration of nanotubes in NMP, 30 minutes is sufficient time to give a considerable enhancement to Kevlar fibre. It was decided that further tests would be carried out with varying concentration and constant ultrasonication time at 30 minutes. The concentrations were varied from 0.15 g/l up to 1.8 g/l and then the samples were sonicated for 30 minutes each as this was the optimum time found for the bulk fibre composites.

3.7.1 Mass uptake of Kevlar fibres associated with nanotube concentration

The mass uptake for the samples associated with concentration was measured taking account of the 0.87% decrease for 30 min soaking in NMP in the control sample (**Table 3.3**, **Figure 3.8**). We see that there is an increase in percentage of nanotubes contained in the sample according to the concentration of nanotubes dispersed in the NMP. The mass uptake was found to vary from 0.3% to almost 7% and when we get the slope of the scales almost quadratically with nanotube concentration.

We can see that after swelling for 30 minutes in the 1.5 g/L and 1.8 g/L concentration appear to reach a maximum concentration of nanotubes in the fibre indicating that we have achieved the maximum uptake of nanotubes that the polymer can contain.

Table 3.3 Average mass percentage increase of Kevlar fibres associated with increasing concentration time

Concentration (g/L)	Mass nanotubes (%)	Error (+/-)
1.8	6.8	0.97
1.5	6.7	0.62
1.2	3.7	0.65
0.9	2.1	0.28
0.6	1.1	0.10
0.3	0.4	0.13
0.15	0.4	0.14

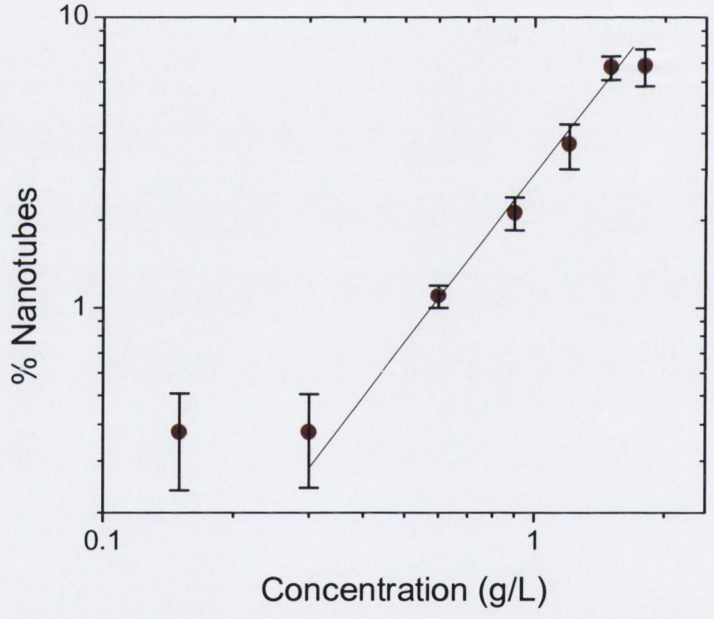

Figure 3.8 Average mass percentage increase of Kevlar fibres associated with increasing concentration shown on a log scale to demonstrate linear quadratic increase (slope of linear fit 1.9)

3.7.2 Thermogravimetric analysis of the composite fibres

We followed the tensile tests with thermo-gravimetric analysis (TGA) (**Figure 3.9**) to see if any change occurs in the compositions of the samples. Firstly we examined a pure Kevlar sample and then compared this to the composite samples with incorporated

nanotubes. Initially when we analyse the curves of temperature against the percentage mass of the samples we find it does not illustrate clearly what occurs throughout the temperature range. However we do see that the samples all seem to decompose at approximately the same temperature with some minor variations that do not correspond necessarily to the composition of the nanotubes and can be associated with the error in the analysis machine.

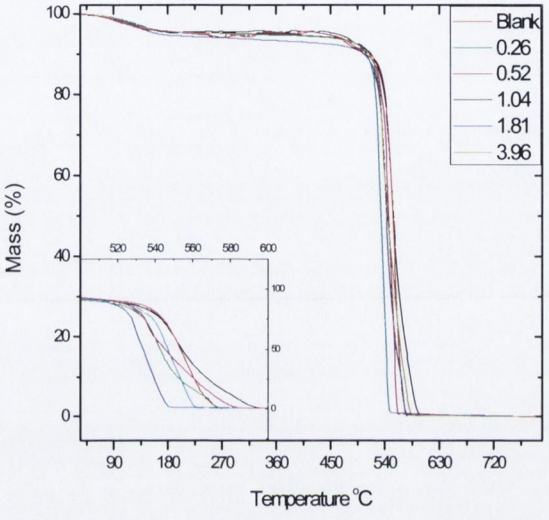

Figure 3.9 TGA curves for Kevlar and Composite Fibres

To gain a better understanding of the effect of the nanotubes on the fibre we can look at the derivatives of the TGA curves (**Figure 3.10**). We can see that pure Kevlar has a decomposition point at approximately 550 °C as is to be expected. When compare this to the TGA curves for the composites, initially we don't see too much of an effect on the curve as we increase the amount of nanotubes. At the higher mass percentage of nanotubes in the composites, however, we can clearly see a broadening of the peak and a second peak at approximately 580°C which corresponds quite well to the temperature at which the nanotubes decompose (610 °C). We also see a significant shifting of the peak (30 °C) in the higher mass percentage samples indicating that the nanotubes are being decomposed more easily. This can be explained as within the polymer matrix, nanotubes are separated from each other and more susceptible to heat penetration. The Kevlar peak also shifts slightly, however in general this is by less than 10 °C across the mass percentage range.

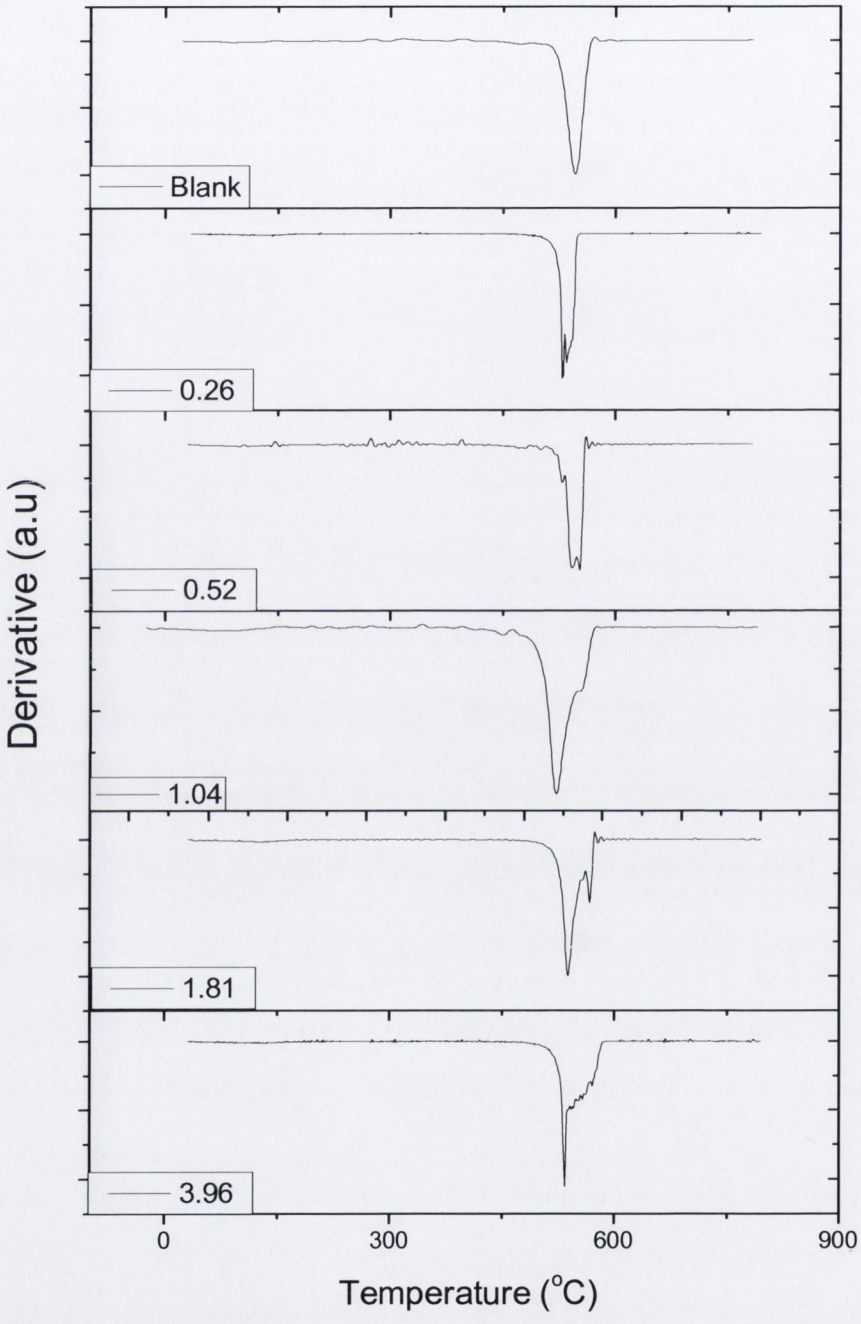

Figure 3.10 Derivative of the TGA curves for Kevlar and composite fibres at different percentage mass uptake of nanotubes

3.7.3 Optical imaging of individual fibres

Initially a number of the fibres were analysed using an optical microscope to determine if there was any change in their size and morphology due to the experiment. We analysed twenty individual fibres and discovered that there was no noticeable change in thickness across this range. The pure Kevlar fibres are extremely uniform along their length and vary little between individual fibre samples. It was found that the fibres remained approximately 10 microns thick (+/- 0.1 μm) as can be seen in the representative samples in **Figure 3.11**. This was the size specified by the manufacturer for the pure Kevlar fibres.

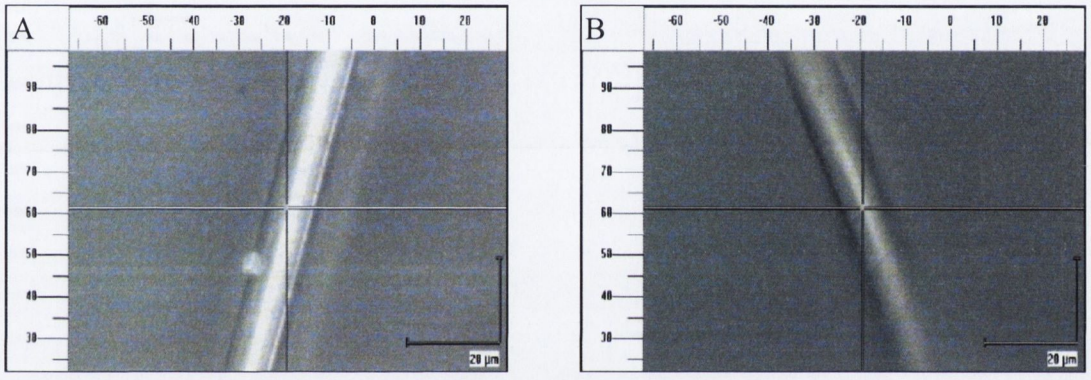

Figure 3.11 Images of representative fibres from optical microscope, pure Kevlar (**A**) and 1.8 % mass of nanotubes composite fibre (**B**)

3.7.4 Mechanical testing of individual fibres at low loading rate

The single fibres were expected to give the most accurate results although due to their small size, manipulation of the samples proved to be extremely difficult. The fibres were mounted in the tensile tester and required adhesion to the surface with glue to attain the most accurate results. The length of the sample was measured using a micrometer and an accurate diameter was measured using microscopy analysis. Mechanical measurements were made on 10 individual fibres isolated from each of the treated yarns. The mechanical measurements were made over two separate strain rates as it has been shown in numerous studies that Kevlar has sensitivity to the rate at which it is placed under tensile stress.[13,14,15] It is important to show that any mechanical enhancement of Kevlar can be maintained over both a high and low loading rate. This is

because Kevlar is very adaptable in its everyday uses. It may need to be strong under a fast rate of strain, like in a bullet proof vest. It may also need to be strong under very low rates of strain like on the sail of a boat. The first strain rate selected for analysis was one of 50 μm/min.

We can see the stress strain curves for the mass percentage which showed the strongest average individual fibre values. This was found to be 1.04 % nanotubes by mass (1.09 % by volume). These are plotted with the pure polymer for comparison at the low strain rate in **Figure 3.12**. When we look at the graph of pure Kevlar against the best recorded composite fibres we find that although there is some overlap the composite samples display clear increases on the pure Kevlar fibre samples, with higher slopes and higher stress achieved form the pure polymer. This demonstrates the capability of this method to develop carbon nanotube-polymer composites with enhanced mechanical properties.

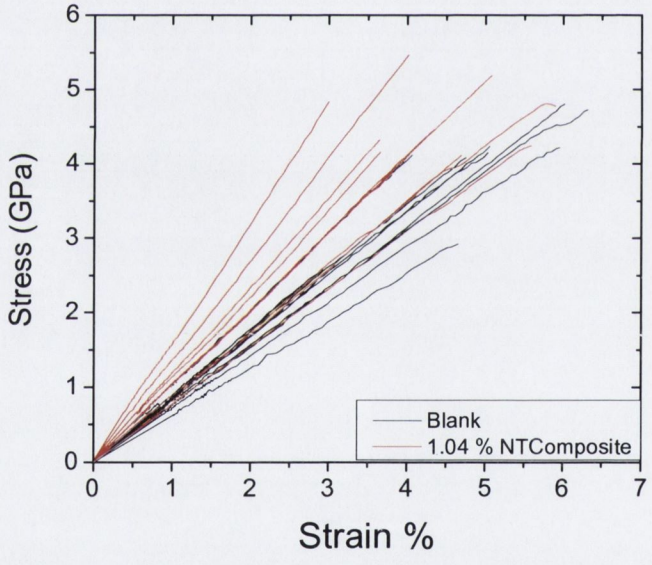

Figure 3.12 Stress-strain curves for individual Kevlar fibres (black) and composite fibres (red)

Experimentally the amount of nanotubes chosen is selected by mass percent (or mass fraction), which were calculated from the mass uptake measurements. However in order to calculate the effective modulus of functionalised nanotubes and the interfacial stress

transfer between the nanotubes and composite volume fraction of nanotubes within the fibre must be calculated. We selected yarns for micro-fibre analysis for which the mass demonstrated close to the theoretical diffusion limited increases. To convert mass fraction to volume fraction, V_f, the amount of nanotubes present in the composite material must be examined,

$$V_f = \frac{N\pi R^2 l_{NT}}{V}$$

Where N is the number of nanotubes in the fibre, R is the average nanotube radius, l_{NT} is the average nanotube length and V is the fibre volume. The average nanotube radius has been calculated from TEM images as R = 12.5 +/- 2.5 nm. The average length of a nanotube is taken as 2 +/- 0.4 μm, again from microscopy analysis. Both nanotubes and Kevlar have a similar density, approximately 1.8 g/mm^3 and 1.44 g/mm^3 respectively so the associated volume fractions are similar but will ultimately give the most accurate approximation of the effective Youngs modulus and tensile strength when compared to theoretical values. In **Table 3.4** we can see the calculated volume fraction against the original mass fraction for the samples measured mechanically.

Table 3.4 Measured mass fraction and corresponding calculated volume fraction values for the composite fibres studied in this work

Mass Fraction	Volume Fraction
0	0
0.0026	0.0021
0.0052	0.0042
0.0104	0.0083
0.0181	0.0166
0.0398	0.0333

When we analyse the tensile strength of the individual composite fibres at low loading rates we find a considerable increase when compared to the pure Kevlar fibres (**Table 3.5**, **Figure 3.13**). We see an immediate increase at the 0.0021 V_f of almost 13 %. This increase is sustained further at the 0.0083 V_f up to 15 % although at the higher volume

fraction of nanotubes we find the value decrease again indicating that we may have inundated the sample with too many nanotubes thereby disrupting the structure and possibly creating aggregates within the fibre. This would have a dramatic negative effect on the mechanical properties of the fibres.

When we analyse the Young's moduli we find increases again and we can see this increase maintained across the range of volume fractions. It reaches a maximum at 0.109 nanotube volume fraction and this represents an increase of approximately 29 % on the original Kevlar fibres. Upon analysis of the toughness values we find that they exhibit an increase to compare with the original fibre, although even at the maximum value it is not too substantial (0.0083 V_f, 5 % increase). We find that the toughness values are maintained even when there is a decrease the strain. This shows that the nanotubes are reinforcing the Kevlar fibres.

Table 3.5 Data for the Mechanical properties of individual Kevlar fibres measured at low loading for tensile strength, Young's modulus, toughness and strain and the corresponding volume fraction of nanotubes within the composite fibre

Volume Fraction	Tensile Strength (GPa)	Error (+/-)	Young's Modulus (GPa)	Error (+/-)	Toughness (MJ/m^3)	Error (+/-)	Strain (%)	Error (+/-)
0	**3.9**	1.09	**84**	19.6	**96**	57.8	**4.7**	1.77
0.0021	**4.4**	0.70	**99**	15.0	**97**	25.4	**4.4**	0.59
0.0042	**3.4**	1.28	**86**	18.7	**80**	55.3	**4.1**	1.64
0.0083	**4.5**	0.69	**108**	24.8	**101**	26.9	**4.6**	0.80
0.0166	**3.9**	0.73	**98**	12.7	**80**	26.1	**4.0**	0.76
0.0333	**3.7**	1.09	**91**	18.7	**88**	49.4	**4.3**	1.51

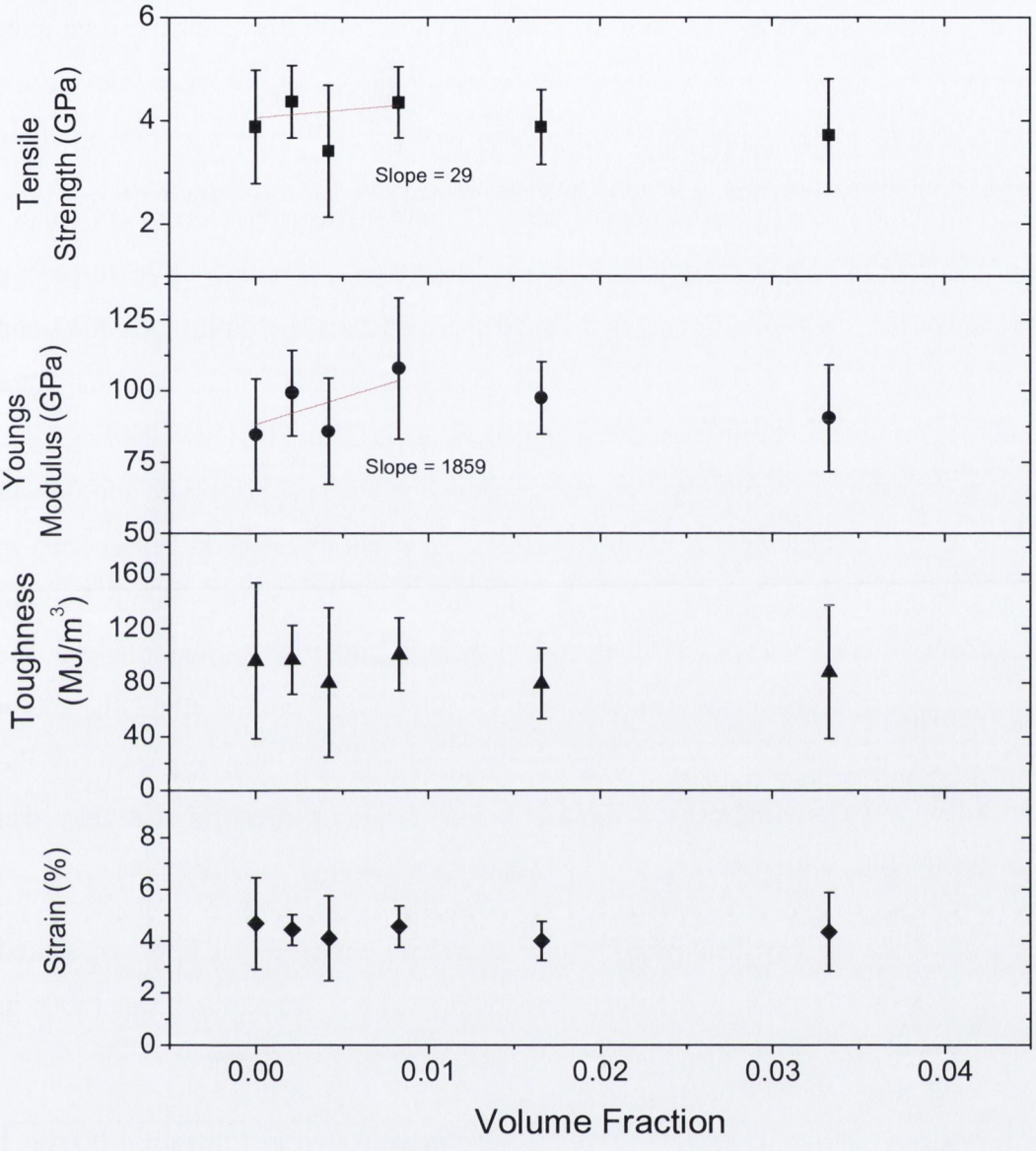

Figure 3.13 Mechanical property graphs of individual composite fibres measured at low strain rate for tensile strength, Young's modulus, toughness and strain against the volume fraction of nanotubes within the composite fibre

3.7.5 Mechanical testing of individual fibres at high loading rate

The next loading rate chosen for analysis was 25 mm/min. The data are shown again as a function of nanotube volume fraction in **Table 3.6** and **Figure 3.14**. For these samples and each mechanical property, we again plot the mean values with standard deviations (closed shapes) but we also plot the maximum observed values (open shapes) to show the theoretical maximum enhancement that could be achieve from this method.

With the high strain rate we again observe increases in the average ultimate tensile strength values from 3.9 GPa for the Kevlar fibre to 4.8 GPa for both the 0.0083 and 0.0166 V_f composite fibres. This represents a substantial increase on the original fibre and displays that the strength increases are generally unaffected by the loading rate. Similarly, the Young's moduli show increases from the original fibre with the 0.0083 and 0.0166 V_f again showing the highest increase. This replicates the increases seen in the composite samples measured at low loading rate, and the same volume fraction samples display those increases over both loading rates. When we analyse the toughness we again see increases on the original fibre. The original fibre displays a lower value for toughness for the high strain rate as has been reported in the literature,[13,14,15] but the composite samples remain tougher indicating that they can reinforce the fibres to a better extent at higher loading rates.

Table 3.6 Data for the Mechanical properties of individual Kevlar fibres measured at low loading and the corresponding volume fraction of nanotubes in the composite fibre

Volume Fraction	Tensile Strength (GPa)	Error (+/-)	Young's Modulus (GPa)	Error (+/-)	Toughness (MJ/m^3)	Error (+/-)	Strain (%)	Error (+/-)
0	**3.9**	0.59	**119**	15.3	**67**	19.2	**3.1**	0.54
0.0021	**4.5**	0.45	**114**	9.9	**91**	21.2	**4.1**	0.64
0.0042	**4.1**	0.19	**119**	27.8	**75**	15.5	**3.6**	0.54
0.0083	**4.8**	0.49	**130**	31.2	**92**	20.1	**3.6**	0.66
0.0166	**4.8**	0.51	**124**	19.4	**99**	30.1	**3.8**	0.87
0.0333	**4.5**	0.43	**117**	20.0	**95**	16.7	**3.7**	0.64

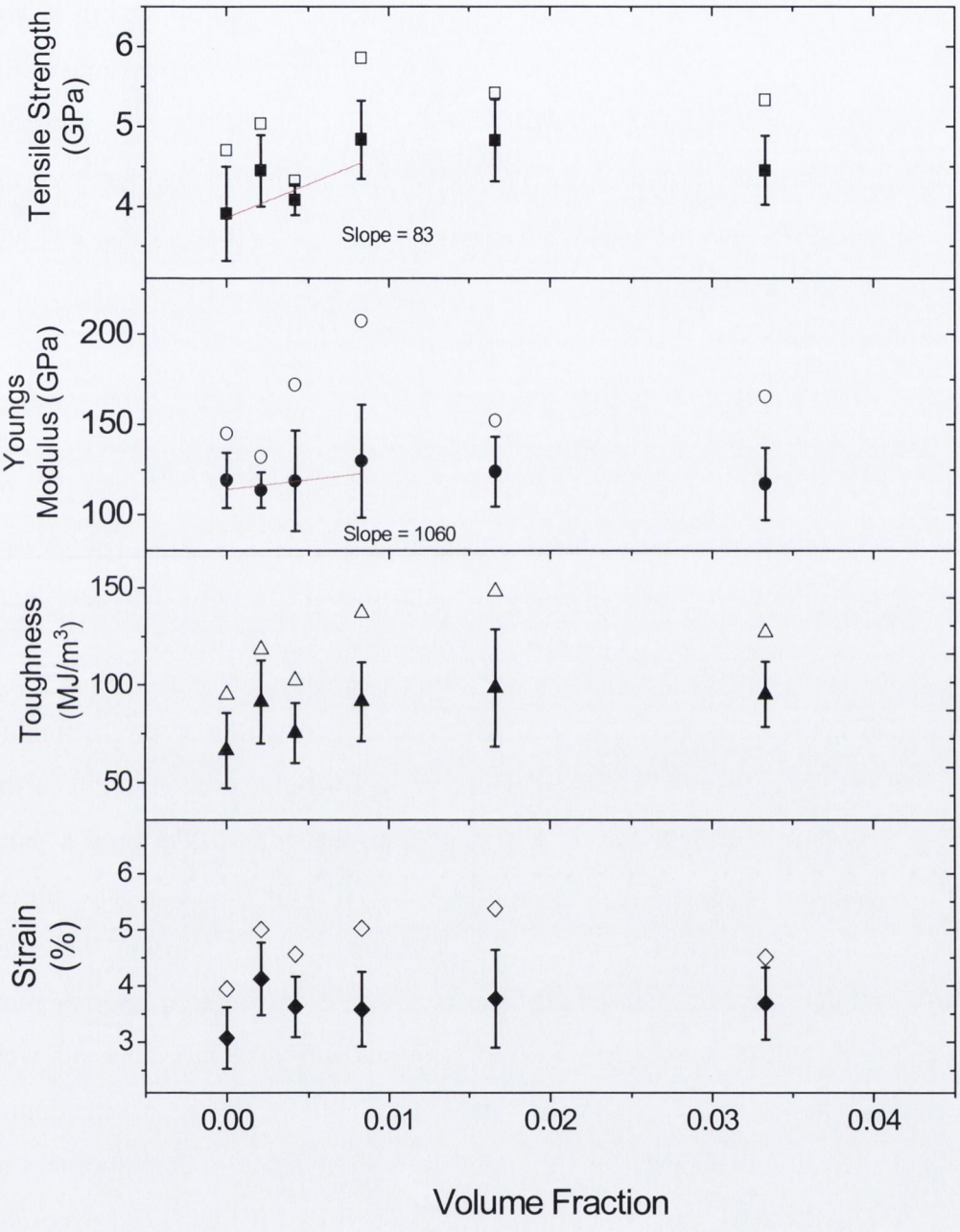

Figure 3.14 Mechanical property graphs of individual Kevlar fibres measured at high strain rate for tensile strength, Young's modulus, toughness and strain against the volume fraction of nanotubes in the composite fibre.

3.7.6 Effective tensile strength and Young's modulus

We can quantitatively represent the reinforcement of both modulus and strength by measuring the rate of increase of strength ($d\sigma/dV_f$) and modulus (dY/dV_f) at low nanotube volume fractions **Table 3.7**.[16] The values were obtained from the slope of the linear fit in **Figure 3.13** and **3.14**. For a homogenous matrix, the theoretical ultimate tensile strength of a composite, σ_T, can be derived under the assumption that the composite has two fracture components. One such component in the bulk polymer and the other is at the polymer/nanotube interface. The tensile strength for such a composite, σ_c, can be expressed as

$$\sigma_c = \left(\frac{l_{nt}\tau}{2r_{nt}} - \sigma_p\right)V_f + \sigma_p$$

where l_{nt} is the nanotube length, r_{nt} is the nanotube radius, v_f is the nanotube volume fraction and σ_p is the ultimate tensile strength of the neat polymer fibre. The interfacial stress transfer, τ, can therefore be calculated from a plot of σ_T against v_f.

This gives us an approximation of the theoretical value, and therefore the maximum possible value of $d\sigma/dV_f$, which should be equal to the overall tensile strength of the nanotubes. When we average the value we acquire from the slope of the lines at both loading rates we get a tensile strength of $d\sigma/dV_f = 56$ GPa for the composite fibres. Different nanotubes will have different strengths as we reported in **Chapter 1** however generally the strengths vary from about 20 GPa for thick MWNT with a large amount of defects to above 100 GPa for very thin MWNTs and SWNT. Our value sits well within this range. The fact that 56 GPa $d\sigma/dV_f$ is very close to the theoretical maximum value indicates that we are achieving a very good stress transfer from the nanotubes to the polymer matrix. That we have values of $d\sigma/dV_f$ of order of the expected nanotube strength highlights the value of using this method to create polymer composites.

Similar trends are also observed when we analyse the values for the Young's modulus. When dealing with the modulus we have to take into account the efficiency factor relating to the orientation of the nanotube within the polymer matrix, η_0,

$$Y_{eff} = \frac{\frac{dY_c}{dV_f} + Y_p}{\eta_0}$$

where, $\frac{dY_c}{dV_f}$ is calculated from the linear fit of the graph of modulus versus V_f for given alkyl chain length. Y_p has been measured as the polymer's modulus. η_0 is generally equal to approximately 0.4 for random planar orientation[17] and should be 1 if the nanotubes are aligned in the polymer matrix. Reports of nanotubes having modulus values in the range of 1 TPa were discussed in the introduction whilst Kevlar has a value of approximately 100 GPa. In our case we get an average value of 1.5 TPa, again very close to the theoretical value. This indicates that in our composite fibres we are achieving aligned nanotubes in the polymer matrix. Although this is unexpected it may be explained by the nanotubes being forced to align by the strict linear orientation of the molecular structure of the Kevlar fibres as we discussed in the introduction. Overall it indicates that we are achieving aligned nanotubes in the Kevlar matrix and also achieving a good interfacial stress transfer between the nanotube and the polymer.

Table 3.7 Values for the experimental and theoretical effective strength and modulus

	$d\sigma/dV_f$	**dY/dV_f**
Low loading	29	1859
High loading	83	1060
Average	56	1460
Theoretical	100 approx	1100 approx

3.8 Conclusions

Thus we have developed a new technique for the fabrication of nanotube- polymer composites. This method is based on the ultrasonic assisted swelling of the Kevlar fibre in a nanotube suspension with the use of an appropriate organic solvent. This represents a novel method for producing polymer composites whereby the composite can be fabricated post-formation to offer a cheap and relatively easy method of composite production. Mass uptake measurements, TGA and SEM analysis of the resulting

composite materials have clearly demonstrated the presence of nanotubes inside a Kevlar matrix. Mechanical measurements of the Kevlar-nanotube composite samples revealed considerable increases in the strength, modulus and toughness of the samples. At the higher loadings we found that the nanotubes within the polymer matrix have a detrimental impact on the mechanical properties indicating that there was some possible aggregation of nanotubes and disruption of the polymer structure. We can also show through theory that we have achieved a very good interfacial stress transfer between the nanotube and the polymer and that the nanotubes are well aligned in the matrix.

We believe that our new approach of incorporating nanomaterials into polymer macromaterials by swelling could be expanded and utilised for other nanosystems and polymer materials. We expect that there will be many possible important applications for this new technique in the future.

References

[1]L.S. Schadler, S.C. Giannaris, P.M. Ajayan. *Appl. Phys. Lett.*, **73**, 3842 (1998)

[2]X. Gong, J. Liu, S. Baskaran, R. D. Voise, J. S. Young *Chem. Mater.* **12**, 1049 (2000)

[3]Z. Jia. Z.Y. Wang, C.L. Xu, J. Liang, B.Q. Wei, D.H Wu S.W. Zhu.. *Mater. Sci. Eng. A*, **271**, 395 (1999)

[4]S. D. Bergin, V. Nicolosi, P. V. Streich, S. Giordani, Z. Sun, A. H. Windle, P. Ryan, N. P. P. Niraj, Z-T. Wang, L. Carpenter, W. J. Blau, J. J. Boland, J. P. Hamilton, J. N. Coleman, *Advanced Materials*, ***20***, 1876 (2008)

[5]S. Giordani, S. D. Bergin, V. Nicolosi, S. Lebedkin, M. M. Kappes, W. J. Blau, J. N. Coleman, *J. Phys. Chem. B*, **110**,15708 (2006)

[6] W.B. Black, J. Preston, *Man-made Fibers. Science and technology, vol. II*, Interscience, 297 (1968)

[7]Kirk-Othmer *The Encyclopedia of Chemical Technology 3rd Ed., vol. III*, Wiley & Sons, New York 213 (1979)

[8]C. J. Frizzell, M. in het Panhuis, D. H. Coutinho, K. J. Balkus, A. I. Minett, W. J. Blau, J. N. Coleman, *Physical Review B*, **72**, 24 (2005)

[9]S. Badaire, P. Poulin, M. Maugey, C. Zakri, *Langmuir*, **20**, 10367 (2004)

[10]B.A. Cheeseman, T.A. Bogetti, *Compos. Struct.*, **61**, 161 (2003)

[11]M. Cheng, W. Chen, *J. Eng. Mat. Tech.* **127**, 197 (2005)

[12]H.H. Yang, *Kevlar Aramid Fiber*, Wiley, (1992)

[13]Y. Wang Y. Xia *Composites Pt. A* **29**, 1411 (1998)

[14]M. Yazici *J. Rein. Plast. and Comp.*, published online (2008)

[15]G.C. Jacob, J.M. Starbuck, J.F. Fellers, S. Simunovic, R.G. Boeman, *J. Appl. Polym. Sci.*, **94**, 296 (2004).

[16]J.N. Coleman, U. Khan, W. J. Blau, Y.K. Gun'ko, *Carbon*, **44**, 9 (2006)

[17]L. Valentini, J. Biagiotti, J.M. Kenny, S. Santucci, *Comps. Sci. and Tech.*, **63**, 1149 (2003)

Chapter 4

Investigation of the Electrical Properties and Optical Transmittance of Polymer-Nanotube Composites

4.1 Introduction

As we have explored in previous chapters, carbon nanotubes can be used to greatly enhance the mechanical properties of polymers. We have shown that if we can achieve a good interfacial stress transfer between the nanotube and the polymer matrix the resulting composite material will have improved strength and modulus with respect to the pure polymer. Carbon nanotubes also have very interesting electrical properties and can be utilised for fabrication of new conductive polymer composites. Over the last few years a lot of research has been focused on the production composites that are both conductive and transparent. Optically transparent materials which can also conduct electricity are required for a wide range of applications from electromagnetic interference shielding to transparent electrodes. In the past these materials have been made, simply by coating glass with metal oxide films, most commonly indium tin oxide (ITO).[1] This has more recently moved towards developing ITO films on the surfaces of polymers with the main area of focus on polyethylene terephthalate due to its excellent optical clarity.[2] However, the standard production techniques are expensive and complicated.[3] In addition the relative scarcity of indium, combined with highly fluctuating prices economically, has recently pushed up the price of ITO. Furthermore, with the rise of organic electronics in recent years it has become apparent that the development of technologies such as e-paper will require flexible, transparent conductors to act as electrodes. Due to its brittle nature,[4] ITO is unsuitable for this area as its conductivity degrades significantly when strained.[5] Thus the development of new transparent conductors with conductivity which is stable against flexing and bending is critical. The added flexibility of polymers gives them a great potential for the development of flexible, transparent, conductive electrodes.

In recent years, one of the main candidates for flexible transparent electrode has been thin films of carbon nanotubes. Due to their high conductivity, single walled nanotubes can be prepared in thin film form with high transparency (~90%) and sheet resistances of a few hundred Ω/□.[6,7] These films are potentially suitable for every application associated with transparent conductors; from antistatic coatings to electrodes.

In the **Chapter 3** we discussed the ability of Kevlar to swell when brought into contact with NMP and DMF. Using nanotube dispersions we developed a new technique to incorporate the nanotubes within the polymer matrix. We have shown that this method

has led to the development of new polymer composites with enhanced mechanical properties. In this chapter we will to try to expand this method to more polymers by varying the type of solvent used. The swelling process has led us to hypothesise that nanomaterials may be incorporated into other polymer without damaging the polymer matrix and resulting in the modification of the composite material. If we can show this to be true it may open a whole new area of possibility to create composites with enhanced electrical and/or mechanical properties. As we discussed in **Chapter 1** a polymers ability to be swelled is greatly enhanced by the cohesion parameter of the solvent it is immersed in. If both solvent and polymer have similar Hildebrand cohesion parameters it indicates good swelling capability for the polymer.

4.2 Aims of This Work

The main aim of this part of the work is to develop our swelling-under-ultrasound approach for the preparation of new conductive carbon nanotube-polymer composite materials from commercially available polymer films. Our specific goal is to fabricate new polymer composites with optimised electrical conductivity and optical transmittance for their potential applications as flexible transparent electrodes. We plan to use a selection of solvents, with particular focus on their solubility parameters, to achieve the best polymer swelling and nanotube infiltration under ultrasound. Another important objective of this project is to investigate new conductive and reinforced polymer composite materials using various instrumental techniques. We expect that our work will result in polymer composites with enhanced electrical and mechanical properties. We believe that our new materials will offer great advantages due the combination of integrated properties such as conductivity, transparency, flexibility and improved mechanical characteristics.

4.3 Preparation and Analysis of Nanotube-Polymer Composite Films

4.3.1 Preparation of composite films by swelling technique

The polymer films selected for study are commonly used commercially available polymers, namely polyethylene (PE), polypropylene (PP) and polyethylene terephthalate (PET). These polymers are discussed in more detail in **Chapter 1** and are

quite resistant to chemical treatment and also very insoluble, but can undergo polymer swelling when the correct conditions of their environment are met..

All polymer-nanotube composite films have been prepared using the following procedure. Nanocyl very thin multi-walled nanotubes were dispersed in 10 ml of either N-methylpyrrolidone (NMP), tetrahydrofuran (THF) or Toluene at the following concentrations, 4mg/ml, 2mg/ml, 1mg/ml, 0.5mg/ml, 0.25mg/ml, 0.2,mg/ml, 0.15mg.ml, 0.125mg/ml, 0.0625mg/ml and 0.03125mg/ml where specified. From analysis of their Hildebrand cohesion parameters we find that these solvents represent good swelling capabilities for each of the polymers in question.

As we saw in **Chapter 2** sedimentation studies showed nanotubes to be very stable in NMP with less than 12 % of the nanotubes sedimenting after a week. However they were not stable in Toluene or THF, with sedimentation occurring within the first few hours, therefore NMP is expected to display the best dispersive capabilities of the solvents whereas, swelling ability is more important for THF and Toluene. The polymer films were cut into strips and placed in various nanotube dispersions in each of the solvents. This mixture was then sonicated using a GEX 750 ultrasonic processor equipped with a conical tip for 5 minutes with a 1 second pulse and power regulated at 20%. Following this it was sonicated for 30 minutes in a Grant XB6 ultrasonic bath. The film was then removed and washed in ethanol under sonication for 30 seconds in the bath. The films were analysed using Scanning Electron Microscopy (SEM) and then electrically tested.

4.3.2 Conductivity measurements of composite films

Conductivity of all films has been measured using a Keithley 2400 sourcemeter. IV curves were measured using a two-probe setup. The potential difference across the sample was varied from 0 V to 100 V with intervals of one volt.

The length, width and thickness of polymer films were measured systematically for each sample. The corresponding current was measured accordingly. From this the bulk conductivity, σ_b, could be calculated according to following equation:

$$\sigma_b = \frac{\frac{dI}{dV} \times l}{w \times t}$$

where $\frac{dI}{dV}$ is the slope of the IV curve, l is the length of the sample, w is the width of the sample and t is the thickness of the sample. Representative curves for a blank polyethylene and 2mg/ml polyethylene sample are shown in **Figure 4.1**

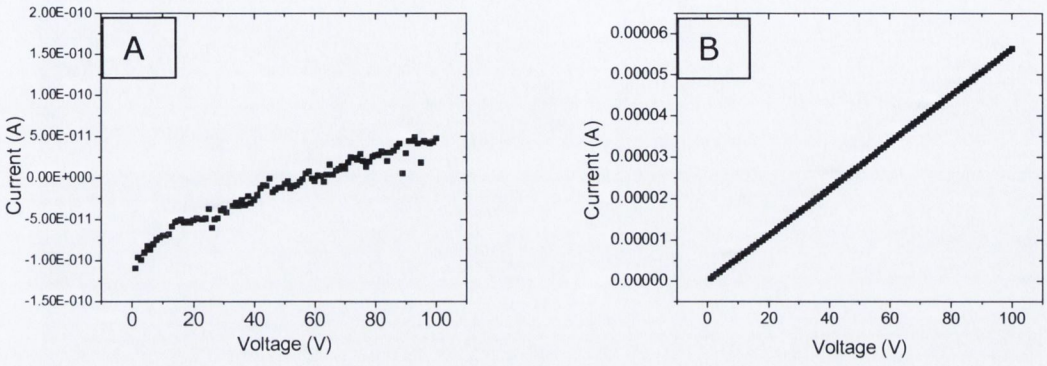

Figure 4.1 Representative IV curves for pure PE (**A**) and nanotube-PE composite (2 mg/ml) (**B**)

4.4 Investigation of Nanotube-Polypropylene Composite Films

Polypropylene films were prepared as specified in section **4.3.1** in various concentrations of nanotubes suspensions in THF, Toluene and NMP. Representative scanning electron microscopy (SEM) images (**Figure 4.2 A-D**) are shown for the highest concentrations of each sample (4 mg/ml). Images are taken at the cross sectional surface edge as this is expected to best demonstrate any penetration. The films all show a similar morphology of the polypropylene cross sectional surface and showed no obvious penetration of nanotubes to the interior of the polymer with any of the solvents.

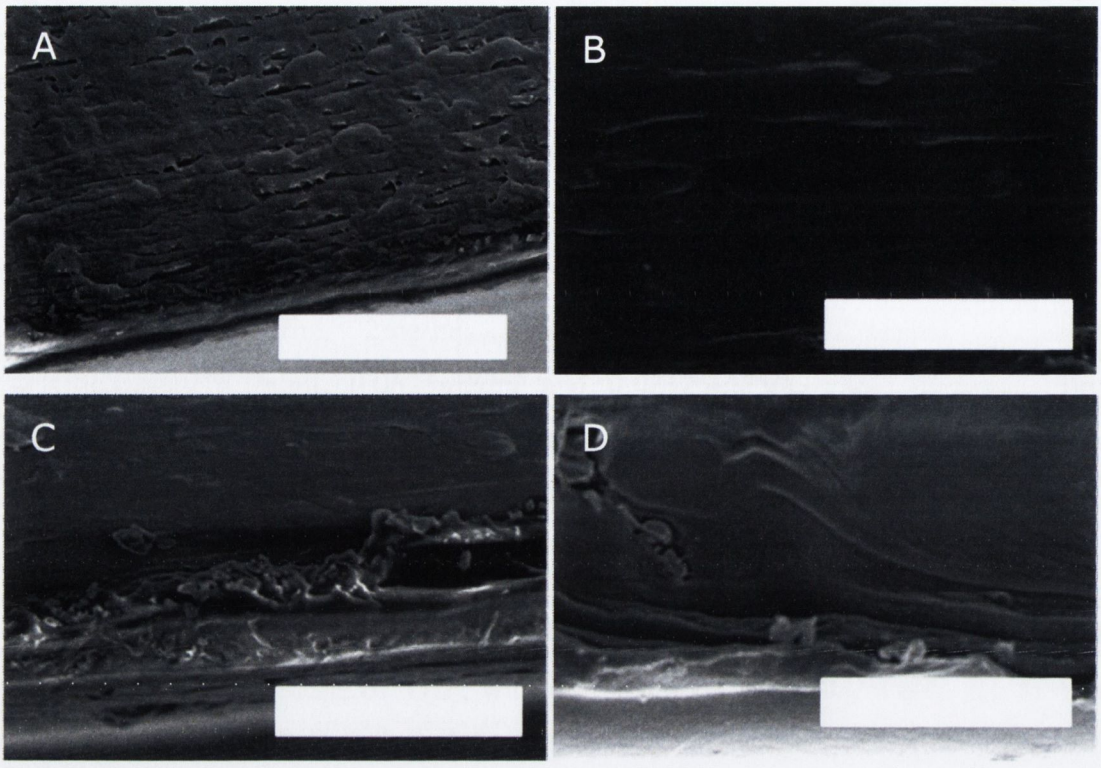

Figure 4.2 (A-D) SEM images of PP showing blank sample (**A**) and the polymer swelled with a dispersion of 4mg/ml NTs in THF (**B**), Toluene (**C**) and NMP (**D**) (scale bar is 10μm)

The conductivity was analysed as specified in section **4.3.2** does show some increases however (**Table 4.1, Figure 4.3**), over an order of magnitude for the film swelled in a 0.125 mg/ml concentration of nanotubes in THF. The increases in Toluene and NMP are not so great but this does indicate that we are seeing some intercalation of the nanotubes into the polymer. We do not expect to find evidence of this penetration through SEM as nanotubes are highly conductive and very little penetration would be required to show an increase in conductivity. Therefore we must assume that we are seeing some minor penetration of nanotubes into the film but overall the technique does not seem to work very efficiently for polypropylene. This is probably because we are not achieving the required amount of swelling of the polymer film in any of the solvents. Referring to section **1.4** we find that, regarding the three solvents used, polypropylene has the least compatible Hildebrand parameter of any of the polymers and this offers an explanation of its lack of swelling ability.

Table 4.1 Electrical conductivity of PP films swelled in THF (red), Toluene (blue) and NMP (green) with very thin MWNT

Conc. (g/L)	Conductivity in THF σ_b (S/m)	Error (+/-)	Conductivity in Toluene σ_b (S/m)	Error (+/-)	Conductivity in NMP σ_b (S/m)	Error (+/-)
4	**4.00×10^{-6}**	5.94×10^{-7}	**5.10×10^{-7}**	9.96×10^{-8}	**4.67×10^{-7}**	7.03×10^{-8}
2	**2.56×10^{-6}**	3.33×10^{-7}	**1.85×10^{-6}**	2.04×10^{-7}	**7.34×10^{-7}**	1.61×10^{-7}
1	**2.71×10^{-6}**	9.87×10^{-7}	**3.05×10^{-7}**	7.81×10^{-8}	**6.63×10^{-7}**	5.65×10^{-8}
0.5	**2.52×10^{-6}**	1.42×10^{-7}	**2.94×10^{-7}**	8.39×10^{-8}	**2.02×10^{-6}**	1.27×10^{-7}
0.25	**2.97×10^{-6}**	3.92×10^{-8}	**3.25×10^{-7}**	2.11×10^{-7}	**1.88×10^{-6}**	4.36×10^{-8}
0.125	**7.05×10^{-6}**	8.28×10^{-7}	**7.13×10^{-7}**	1.50×10^{-7}	**1.03×10^{-6}**	2.15×10^{-7}
0.0625	**1.02×10^{-6}**	2.11×10^{-7}	**1.49×10^{-6}**	1.37×10^{-7}	**1.24×10^{-6}**	1.26×10^{-7}
0.03125	**4.67×10^{-6}**	6.85×10^{-7}	**4.66×10^{-7}**	1.17×10^{-7}	**1.92×10^{-6}**	3.28×10^{-7}
0	**2.18×10^{-7}**	1.48×10^{-8}	**2.18×10^{-7}**	1.48×10^{-8}	**2.18×10^{-7}**	1.48×10^{-8}

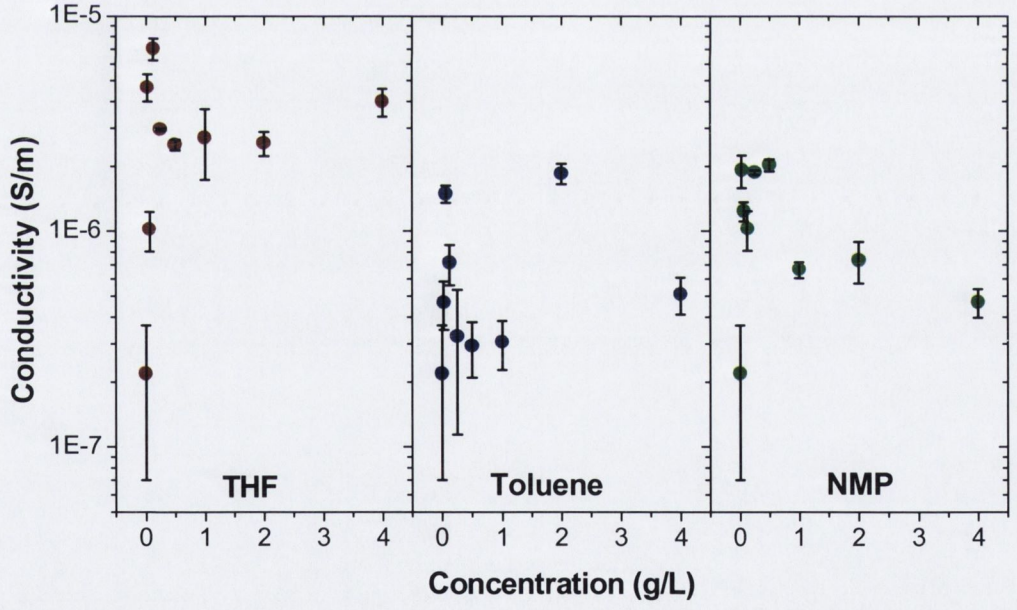

Figure 4.3 Electrical conductivity results for PP films swelled in THF (red), Toluene (blue) and NMP (green) against the concentration of MWNTs in the solvent.

4.5 Investigation of Nanotube-Polyethylene Terephthalate Composite Films

Polyethylene terephthalate represents one of the most promising polymers in the transparent electrodes industry due to its high transmittance. Further discussion of this polymer can be found in **Chapter 1**. Polyethylene terephthalate films were prepared in various concentrations of nanotubes dispersions in THF, Toluene and NMP as specified in section **4.3.1**. Initial SEM analysis of the cross sections of the samples showed no obvious penetration of nanotubes to the interior of the polymer with NMP (**Figure 4.4, D**). However the polymer films swelled in Toluene (**Figure 4.4, C**) and THF (**Figure 4.4, B**) demonstrated penetration of nanotubes of 300 nm and 6 μm respectively. However the penetration of the sample swelled in THF does not seem to be homogenous throughout the polymer with other areas of the same cross sectional surface showing little or no penetration. Representative images are shown for the highest concentrations of each sample (4 mg/ml).

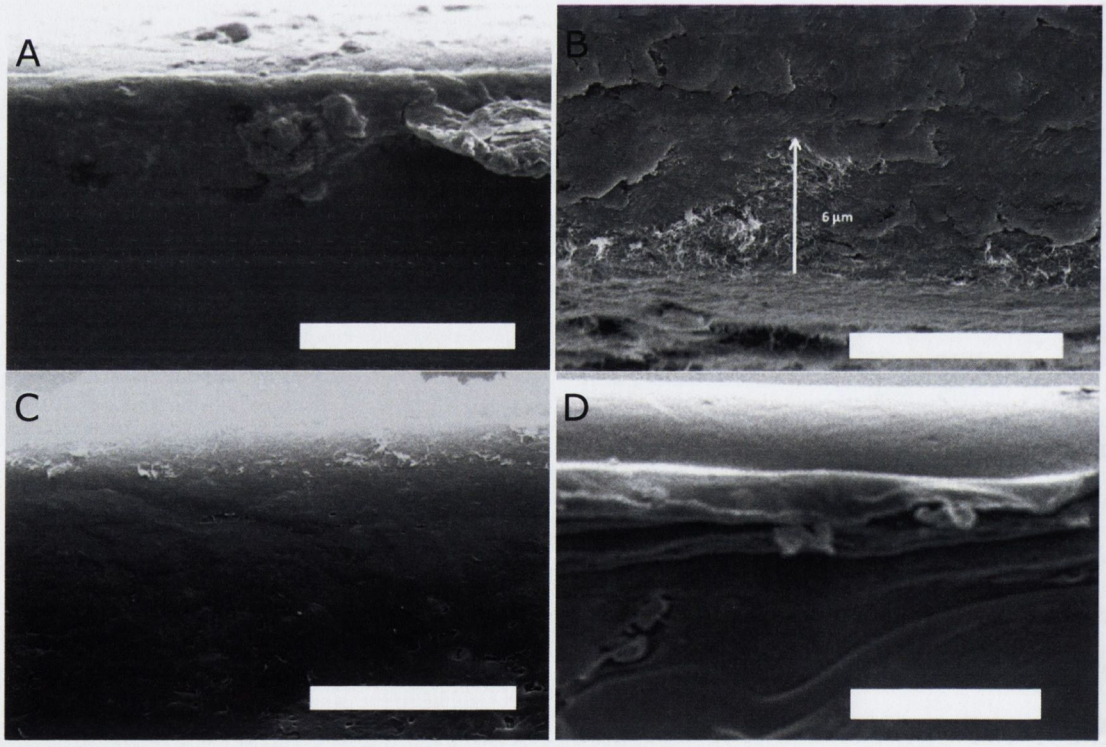

Figure 4.4 (A-D) SEM images of PET showing blank sample (**A**) and the polymer swelled with a dispersion of 4mg/ml NTs in THF (**B**), Toluene (**C**) and NMP (**D**) (scale bar is 10μm)

The conductivity was analysed as specified in section **4.3.2**. When we look at **Table 4.2** we see that the conductivity increases for composites prepared in NMP again are not substantial, but we do however observe very significant rise in conductivity for the composite sample obtained from both THF and Toluene. This is unsurprising given the considerable penetration observed in the SEM images however the magnitude of the enhancement is very considerable. We can see the conductivity trend when we look at the graphs (**Figure 4.5**). The samples swelled in both THF and toluene; demonstrate enhancement as the concentration of nanotubes is increased. As we raise the concentration of the nanotubes we make a greater amount of nanotubes available for penetration. The maximum individual sample obtained was for THF at a concentration of 2 mg/ml and was measured at 0.0179 Siemens per metre and represents an increase of over 5 orders of magnitude on the pure polymer.

Table 4.2 Electrical conductivity of PET films swelled in THF (red), Toluene (blue) and NMP (green) with very thin MWNT

Conc. (g/L)	Conductivity in THF σ_b (S/m)	Error (+/-)	Conductivity in Toluene σ_b (S/m)	Error (+/-)	Conductivity in NMP σ_b (S/m)	Error (+/-)
4	**1.79×10^{-2}**	1.97×10^{-4}	**9.88×10^{-4}**	2.19×10^{-4}	**1.45×10^{-7}**	5.75×10^{-8}
2	**5.23×10^{-3}**	8.70×10^{-5}	**7.11×10^{-5}**	4.36×10^{-6}	**1.00×10^{-7}**	2.25×10^{-8}
1	**2.09×10^{-3}**	4.93×10^{-5}	**1.19×10^{-4}**	2.59×10^{-5}	**1.79×10^{-7}**	2.49×10^{-8}
0.5	**5.83×10^{-6}**	9.14×10^{-7}	**6.90×10^{-6}**	2.01×10^{-6}	**1.13×10^{-7}**	1.58×10^{-8}
0	**6.33×10^{-8}**	1.86×10^{-8}	**6.33×10^{-8}**	1.86×10^{-8}	**6.33×10^{-8}**	1.86×10^{-8}

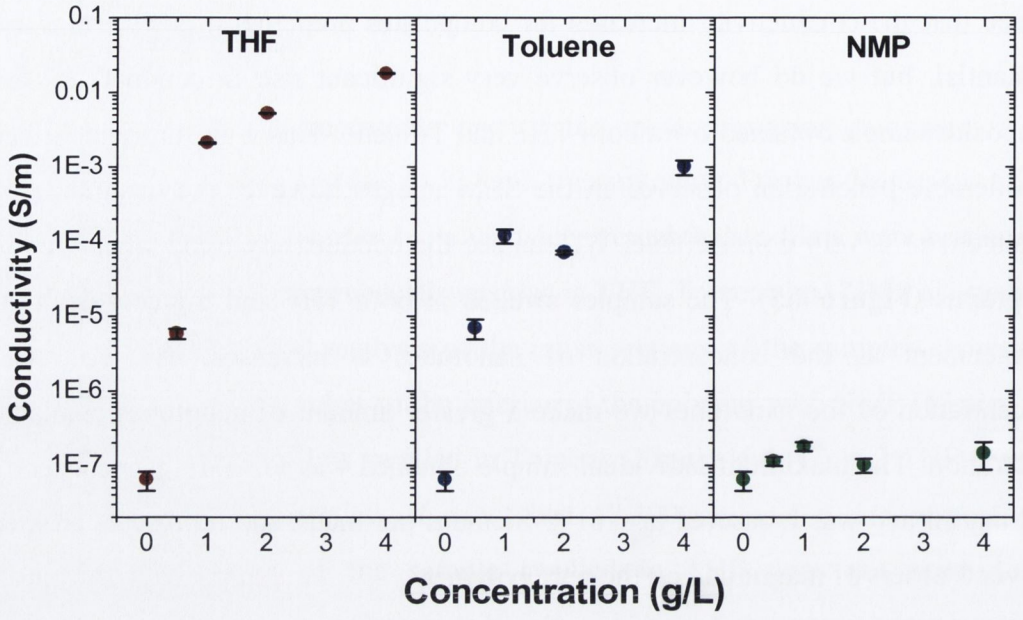

Figure 4.5 Electrical conductivity results for PE films swelled in THF (red), Toluene (blue) and NMP (green) against the concentration of MWNTs in the solvent

4.6 Investigation of Nanotube-Polyethylene Composite Films

Polyethylene represents a very interesting polymer with respect to its potential use in transparent flexible electrodes. As was discussed in **Chapter 1**, it is generally more flexible and has good transparency and optical properties, similar to polyethylene terephthalate.

4.6.1 Investigation of polyethylene film swelling in NMP, toluene and THF

Polyethylene films were prepared as specified in section **4.3.1** in various concentrations of nanotube suspensions in THF, Toluene and NMP. Initial SEM analysis of the cross sections of the samples showed little or no penetration of nanotubes to the interior of the polymer NMP, however cross sectional and surface analysis of films in THF and Toluene showed good nanotube penetration into the cross sectional edge. Representative images (**Figure 4.6**) are shown for the highest concentrations of each sample (4 mg/ml).

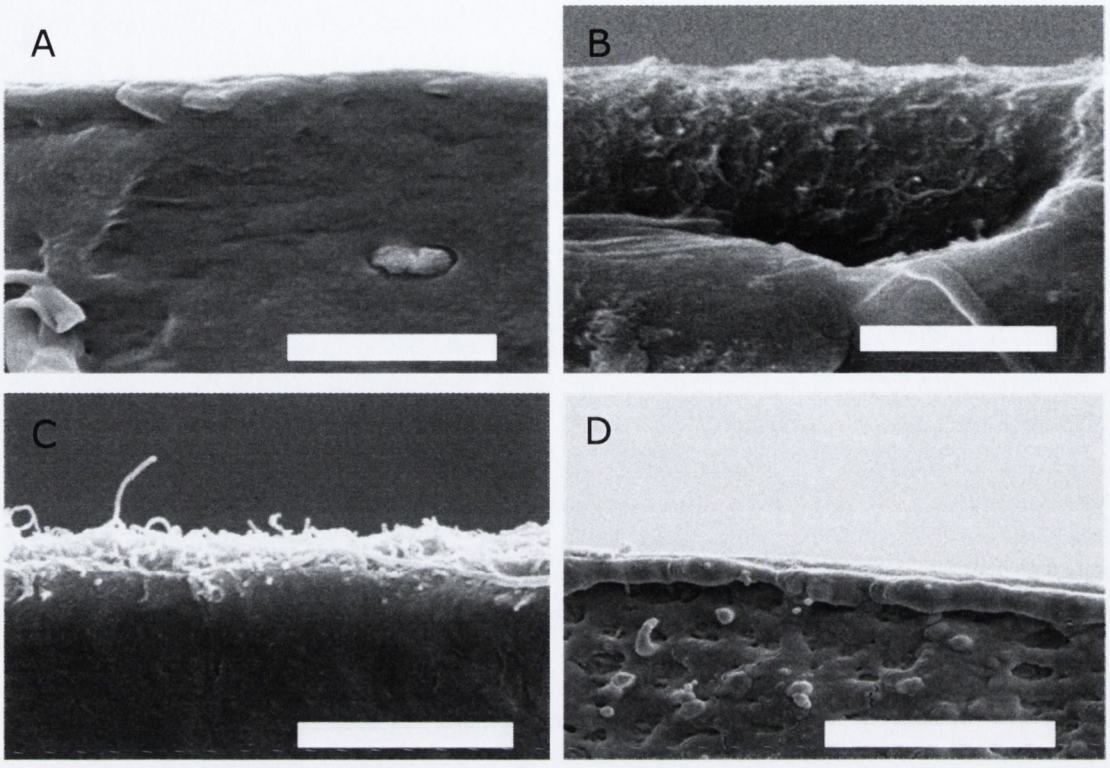

Figure 4.6 (A-D) SEM images of PE showing blank sample (**A**) and the polymer swelled with a dispersion of 4mg/ml NTs in THF (**B**), Toluene (**C**) and NMP (**D**) (scale bar is 1 micron)

The conductivity was analysed as specified in section **4.3.2**. We can see in **Table 4.3**, and **Figure 4.7** how the increases for composites prepared in NMP are again not substantial. We do however observe very large conductivity increases for the composite sample prepared in THF and Toluene. The maximum individual sample obtained was for THF at a concentration of 2 mg/ml and was 0.4 Siemens per metre and the average sample at a concentration of 4 g/L demonstrates a conductivity of 0.36 S/m representing an increase of over six orders of magnitude on the original polymer. This demonstrates a very substantial increase and displays the potential of this method for producing transparent conductive plastic composites.

Table 4.3 Electrical conductivity of PE films swelled in THF (red), Toluene (blue) and NMP (green) with very thin MWNT

Conc. (g/L)	Conductivity in THF σ_b (S/m)	Error (+/-)	Conductivity in Toluene σ_b (S/m)	Error (+/-)	Conductivity in NMP σ_b (S/m)	Error (+/-)
4	**0.36**	0.05	**5.4×10^{-2}**	5.74×10^{-3}	**1.05×10^{-5}**	6.92×10^{-6}
2	**0.29**	0.11	**5.4×10^{-2}**	4.89×10^{-4}	**7.70×10^{-6}**	4.57×10^{-6}
1	**0.32**	0.06	**0.17**	1.15×10^{-3}	**2.57×10^{-6}**	4.78×10^{-8}
0.5	**0.05**	2.3×10^{-4}	**5.98×10^{-2}**	5.72×10^{-4}	**8.49×10^{-6}**	8.09×10^{-6}
0.25	**0.10**	1.0×10^{-3}	**2.65×10^{-2}**	5.18×10^{-4}	**1.39×10^{-6}**	7.37×10^{-7}
0.125	**7.3×10^{-7}**	3.68×10^{-8}	**9.92×10^{-3}**	9.69×10^{-4}	**1.69×10^{-6}**	1.25×10^{-7}
0.0625	**3.00×10^{-7}**	7.25×10^{-8}	**8.6×10^{-4}**	3.90×10^{-5}	**3.12×10^{-6}**	1.58×10^{-6}
0.03125	**4.66×10^{-7}**	9.44×10^{-8}	**3.76×10^{-7}**	9.8×10^{-8}	**3.62×10^{-6}**	2.62×10^{-6}
0	**2.97×10^{-7}**	4.41×10^{-8}	**2.97×10^{-7}**	4.41×10^{-8}	**2.97×10^{-7}**	4.41×10^{-8}

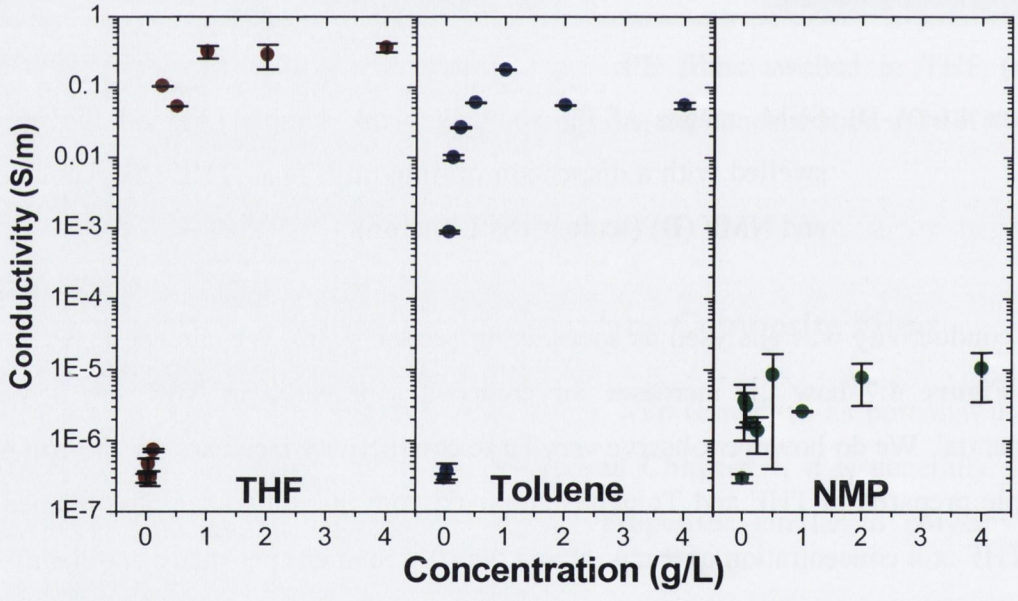

Figure 4.7 Electrical conductivity results for PE films swelled in THF (red), Toluene (blue) and NMP (green) against the concentration of MWNTs in the solvent

As the PE film swelled in nanotube dispersions in THF showed the best conductivities and most homogeneous penetration it was decided to analyse these composites in detail to explore their overall composition. Of particular interest was the SEM image which showed the depth of nanotube penetration into the polymer. We analysed the surface

morphology of the prepared polymer composites of which there are selected images in **Figure 4.8 (A-C)** and more comprehensive images in the **Appendix.** Also we analysed the cross-section edge of the films to determine the depth penetration of the nanotubes. A more comprehensive SEM analysis was undertaken to measure the approximate thickness of the surface nanotube layer but we can see representative images of the composite films in **Figure 4.8 (D-F)** again with more comprehensive images in the **Appendix**.

From these images it is clear that the nanotubes do not just form a surface coating but occupy a thin top layer of the polyethylene film. From the surface images (Figure 4.8 A-C) we can see how the nanotube concentration on the surface increases by the raising of the nanotube concentration in solution. When we look at the cross sectional images we can also see that the penetration of the nanotubes appears to be restricted to only a few hundred nanometres into the composite film. Although there may be deeper penetration that is undetectable on the SEM, it would have a negligible influence on the electrical conductivity when compared to the nanotube composite layer on the surface due to the sheer amount of nanotubes in this surface layer. We can again see that the concentration of the nanotubes in the surface layer increases as the concentration of nanotubes in the solvent is raised.

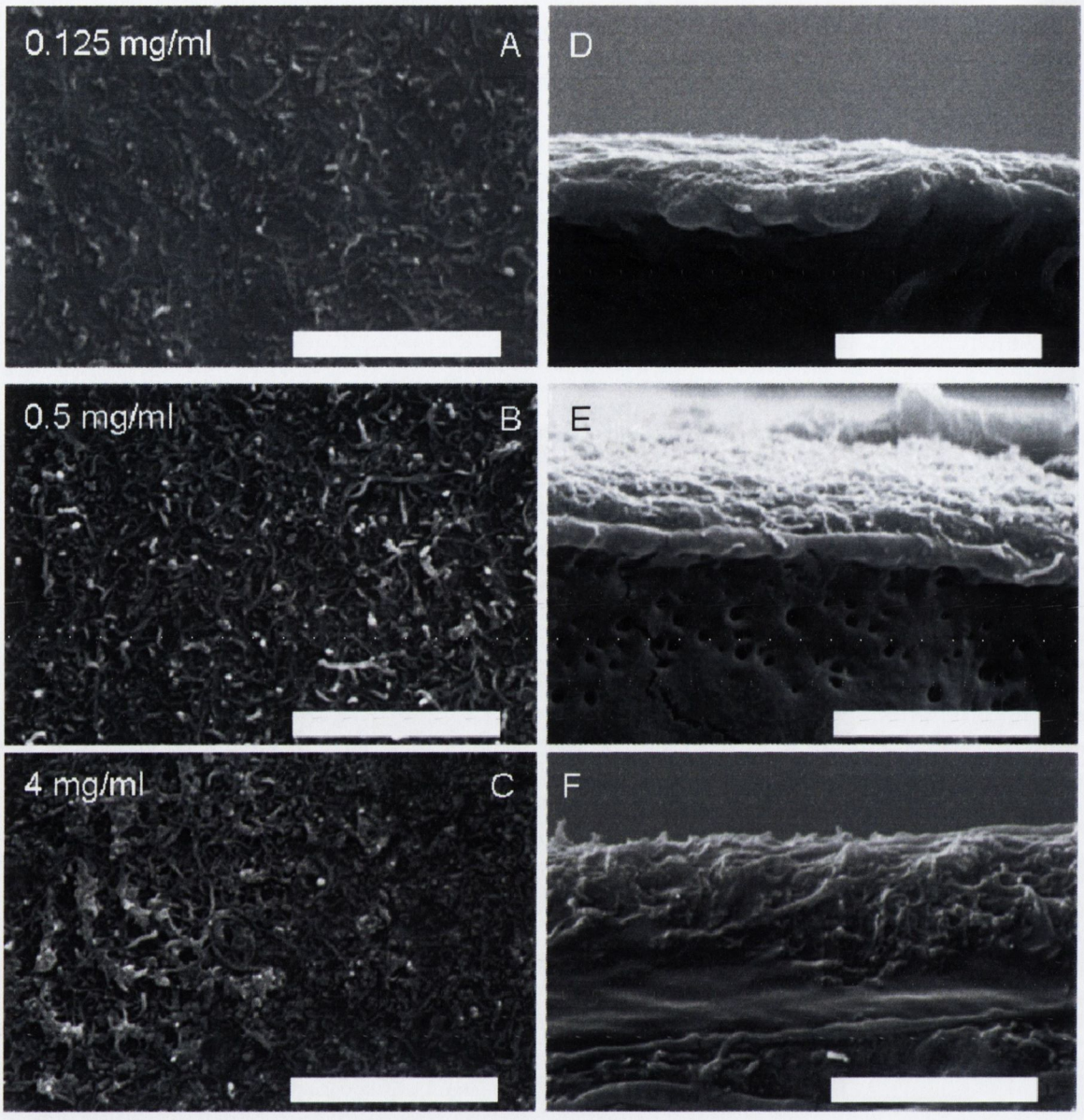

Figure 4.8 (A-F) Selected SEM images of surface **(A-C)** and cross-section/surface edge **(D-F)** of films prepared for a range of dispersion concentrations: 0.125mg/ml, 0.5 mg/ml and 4.0 mg/ml. In all cases the scale bar is 1 micron.

For each composite film, the nanotube penetration depth, *t*, was estimated for 4 images with 10 different positions on each. This data is presented in the **Table 4.4** and **Figure 4.9** as a function of nanotube dispersion concentration. We can see that generally each individual nanotube layer is approximately 250 nm thick for most composites. This indicates that the depth of penetration of the nanotubes does not depend on the concentration of the nanotube dispersions. We would expect the swelling to be

independent of nanotube concentration and dependent only on the solvent swelling capabilities and swelling time.

Table 4.4 Average composite layer thickness compared to the nanotube concentration in THF

Nanotube Conc. in THF (g/L)	Average Layer Thickness (µm)	Error (+/-)
0.03125	**0.25**	0.040
0.0625	**0.24**	0.059
0.125	**0.17**	0.043
0.15	**0.25**	0.084
0.2	**0.22**	0.050
0.25	**0.30**	0.078
0.5	**0.26**	0.056
1	**0.26**	0.070
2	**0.29**	0.057
4	**0.73**	0.167

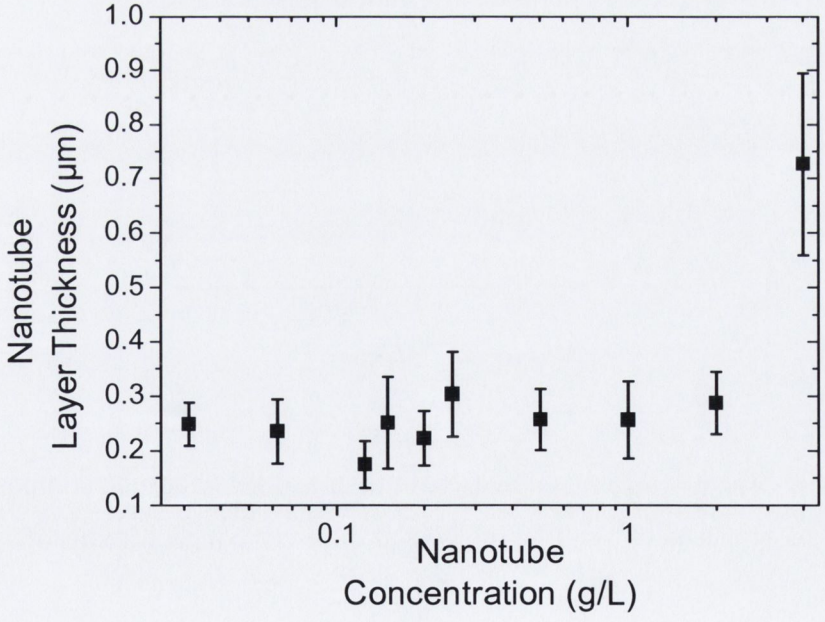

Figure 4.9 Composite layer thicknesses in PE as measured by SEM versus nanotube concentration in THF

4.6.2 Transmittance measurements of nanotube-polymer composite films

Transmittance was measured using a home-built sample holder by a Cary Varian 50 scan UV-visible Spectrophotometer. Transmittance is the fraction of incident light of known wavelength that passes through a given sample. It is given as a percentage calculated by $T = I / I_0$ where I_0 is the intensity of the incident light and I is the intensity of the light coming out of the sample. The transmittance of all composite films swelled in the different nanotube concentrations dispersed in THF was measured.

As expected there was a decrease in transmittance of polymer composite films as the concentration of nanotubes added increased. This replicates what we observed in the SEM images in **Figure 4.8**. Selected curves for the transmission through all samples are shown in **Figure 4.10**. We can see a general decrease in the transmission of light as we increase the nanotube concentration.

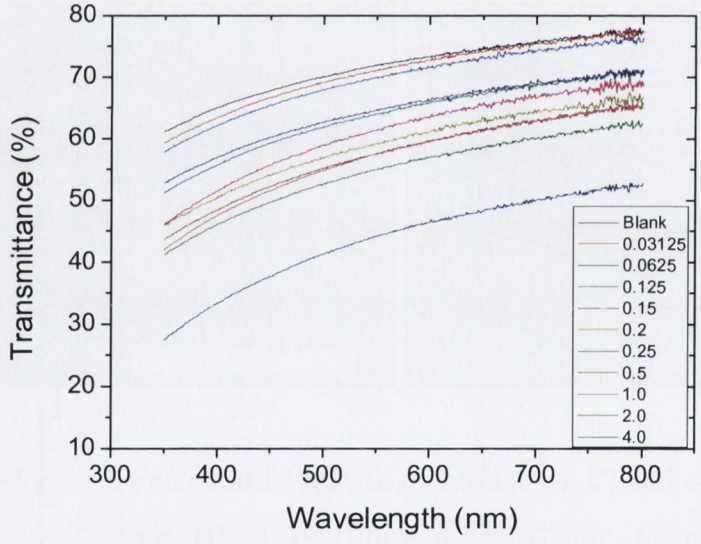

Figure 4.10 Selected curves for absolute transmittance of PE nanotube composite films prepared by swelling in THF at different concentrations of nanotubes (0.03125 through 4 mg/ml nanotubes).

To get a comprehensive analysis the transmission was measured at a wavelength of 550 nm for five separate areas for each sample and compared to the original polyethylene (**Figure 4.11**). As expected, the transmittance again decreases as we increase the dispersion concentration. We can see that overall most of the samples have relative

transmittance of approximately 80% or above. This is a considerably high transmittance, which is also accompanied by high increase in the film conductivity.

Table 4.5 Average transmittance relative to the original polymer of the PE samples swelled in various concentrations of nanotubes in THF

Concentration	Relative Transmittance (% at λ = 550 nm)	Error
0.03125	98.7	0.60
0.0625	92.7	1.51
0.125	89.6	1.52
0.15	90.9	3.25
0.2	90.2	0.79
0.25	89.1	0.99
0.5	81.1	1.69
1	79.6	0.25
2	77.2	1.81
4	60.7	1.27

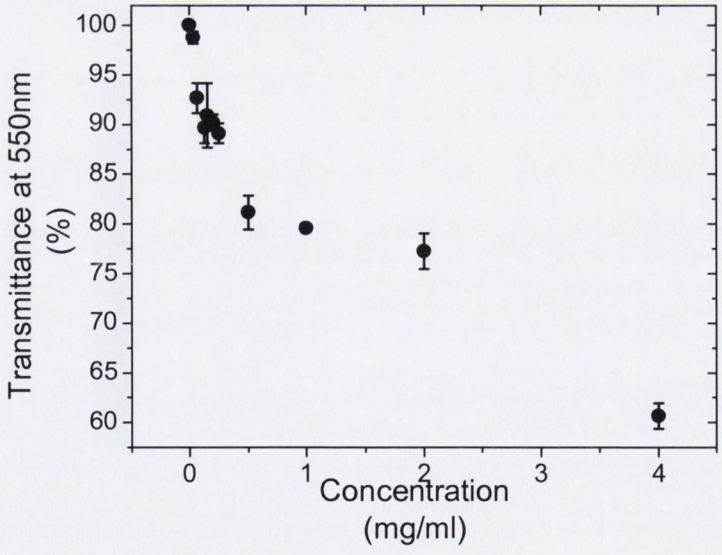

Figure 4.11 Relative transmission values of polyethylene composite films immersed in varying concentrations of nanotube dispersions in THF at λ=550nm

Ultimately we can see that as we increase the concentration of the nanotubes within the film we are decreasing the amount of light that can pass through it i.e the dark nanotubes will absorb more and more light when there are more of them in the film.

Knowing this we can use the data obtained from the transmission measurements, coupled with the measured film thickness, to calculate the optical absorption co-efficient associated with these nanotube films, α. The transmittance, T, is described by the Lambert-Beer law:

$$T = 10^{-\alpha(2t)}$$

The factor of 2 comes from the fact that there is a nanotube layer on each side of the film as confirmed by the SEM analysis. We later use this expression to calculate α as shown in **Figure 4.13**. We can also use this data to estimate the volume fraction of nanotubes in the surface layer, V_f, by modelling the surface layer as a solid solution of nanotubes in the polymer matrix. Under these circumstances, the absorption coefficent of the surface layer can be approximated as,

$$\alpha = \varepsilon C_{Layer}$$

Where, ε is the extinction coefficient of the nanotubes and C_{layer} is the average concentration (in g/L) of the nanotubes within the nanotube layer. We can relate C_{Layer} to V_f using,

$$C_{Layer} = \rho_{NT} V_f ,$$

where ρ_{NT} is the nanotube density (~1800 kg/m^3).[8] This means that the volume fraction of nanotubes in the surface layer is given by,

$$V_f = \alpha / \varepsilon \rho_{NT}$$

Given that we have measured α, and know ρ_{NT} from the literature, we need only ε to calculate V_f. We find ε by assuming it to be invariant for solid solutions and liquid phase dispersions of MWNTs in solvents (albeit at a much lower concentration).

Therefore the transmittance of dispersions of thin MWNTs in THF was measured as a function of concentration (**Table 4.5**, **Figure 4.12**). From the corresponding absorbance we could calculate ε at approximately 1220 ml mg^{-1}m^{-1}, a value of the same order as that of SWNTs in solvents (3000-3500 ml mg^{-1}m^{-1}).[9,10]

Table 4.6 Transmission and corresponding absorbance measurements through nanotube dispersions at selected concentrations in dispersion in THF

Concentration	Transmittance (% at λ = 550 nm)	Absorbance
0	100	1
0.03125	53.41	1.87
0.0625	21.72	4.60
0.125	2.38	41.95

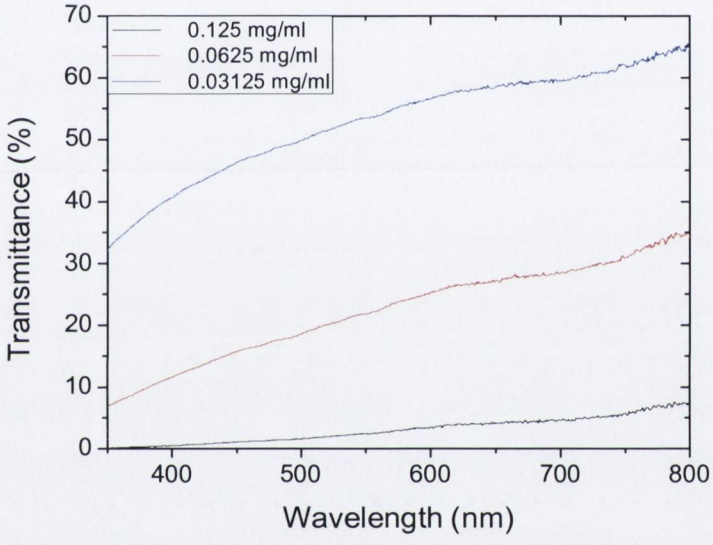

Figure 4.12 Selected transmission curves for nanotube dispersions in THF with respect to the pure solvent

Consequently we can use this to calculate the volume fraction of nanotubes in the surface layer from the absorption coefficient as mentioned above. The absorption coefficient of the polymer composite layer and the corresponding volume fractions are shown in **Table 4.7**, **Figure 4.13**. This shows that while the thickness of the surfaces remains constant, the volume fraction of nanotubes increases with increasing dispersion concentration, saturating at approximately 8 % by volume. As we used a value for thickness for the nanotube layer this figure represents the nanotube concentration in the composite layer only. It is clear from this figure that α increases with increasing dispersion concentration (C_{Disp}) before saturating at $\alpha \approx 1.5 \times 10^5\ m^{-1}$ for $C_{Disp} > 1$mg/ml.

This increase can only be associated with increasing nanotube concentration in the composite layer. This is to be expected for as we increase the concentration of nanotubes in the dispersion we are providing more nanotubes to enter the film. The saturation point at approximately 8% of nanotubes by volume is quite considerable, but when we extend this to the total volume of the polymer film, V_T, which is 46 μm thick we find the volume fraction of nanotubes for the whole film is only approximately 0.106%.

As we analyse each of the samples we see that generally the total volume fraction is fairly low and increases as we get to the higher dispersion concentrations. This is to be expected as we found that penetration of the nanotubes was generally restricted to the areas close to the surface. This explains the relatively high values we found for the transmission.

Table 4.7 Absorption coefficients at corresponding volume fractions

Dispersion Conc. (g/L)	**Absorption Coefficient, α**	**Error (+/-)**	**Layer Volume Fraction, V_f(%)**	**Error (+/-)**	**Polymer Volume Fraction V_T, (%)**	**Error (+/-)**
0.03125	**0.56 x 10^5**	0.89 x 10^4	**2.51**	0.40	**0.028**	0.004
0.0625	**0.89 x 10^5**	2.25 x 10^4	**4.04**	1.02	**0.041**	0.011
0.125	**1.20 x 10^5**	3.00 x 10^4	**5.46**	1.36	**0.040**	0.010
0.15	**0.95 x 10^5**	3.19 x 10^4	**4.31**	1.45	**0.045**	0.016
0.2	**0.95 x 10^5**	2.13 x 10^4	**4.31**	0.96	**0.042**	0.009
0.25	**0.74 x 10^5**	1.89 x 10^4	**3.33**	0.86	**0.044**	0.011
0.5	**1.66 x 10^5**	3.60 x 10^4	**7.52**	1.63	**0.086**	0.018
1	**1.83 x 10^5**	5.04 x 10^4	**8.29**	2.28	**0.095**	0.026
2	**1.85 x 10^5**	3.68 x 10^4	**8.40**	1.66	**0.106**	0.021
4	**1.46 x 10^5**	3.36 x 10^4	**6.59**	1.52	**0.210**	0.024

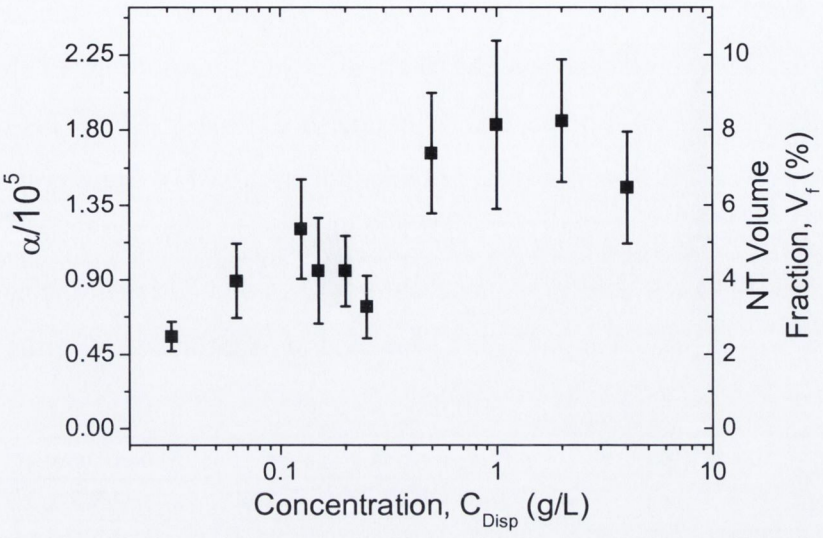

Figure 4.13 Film absorption coefficient (α) of PE film swelled in nanotube dispersion in THF, versus dispersion concentration, enabling us to work out the Volume fraction of nanotubes in the composite layer (right axis)

4.6.3 Measurement of sheet resistance and conductivity of composite layer

The sheet resistance, R_s, is a commonly used measurement of resistance for films that have a uniform thickness. It is a measurement of the resistivity and is therefore independent of the thickness. It can be easily found from the I-V curves of the individual polymer films measured by the two probe method.

$$R_s = \frac{\frac{dV}{dI} \times l}{w}$$

The sheet resistance as a function of dispersion concentration is shown in **Figure 4.14 (Top).** We see that it initially falls sharply with increasing dispersion concentration, saturating at less than 10^5 Ω/□ for a dispersion concentration of 1 mg/ml. The sheet resistance can be translated into an accurate conductivity, σ, using:

$$\sigma = \frac{1}{R_s t}$$

Where, t, is the thickness of the nanotube layer measured by SEM for each film individually as was shown in **Figure 4.19** above. The resultant conductivity is shown in

Figure 4.14: Bottom, illustrating the very rapid increase in conductivity as the dispersion concentration is increased toward 0.5 mg/ml. At higher dispersion concentrations, the conductivity reaches values as high as 66 S/m (**Table 4.8**). The measured value for the pure polyethylene sample is 5.2×10^{-7} S/m. This represents an increase of over 8 orders of magnitude on the conductivity of the pure polymer.

Table 4.8 Calculated sheet resistance and layer conductivities of the nanotube composite layer of PE films swelled in nanotube dispersions in THF

Concentration (g/L)	Sheet Resistance (Ω/□)	Conductivity (S/m)
0	8.3×10^{10}	5.2×10^{-7}
0.03125	5.4×10^{10}	7.5×10^{-5}
0.0625	8.7×10^{10}	4.9×10^{-5}
0.125	3.1×10^{10}	1.8×10^{-4}
0.15	3.6×10^{7}	0.11
0.2	4.1×10^{6}	1.09
0.25	2.1×10^{5}	15.9
0.5	4.1×10^{5}	9.6
1	8.9×10^{4}	44.1
2	5.2×10^{4}	66.4
4	7.1×10^{4}	19.3

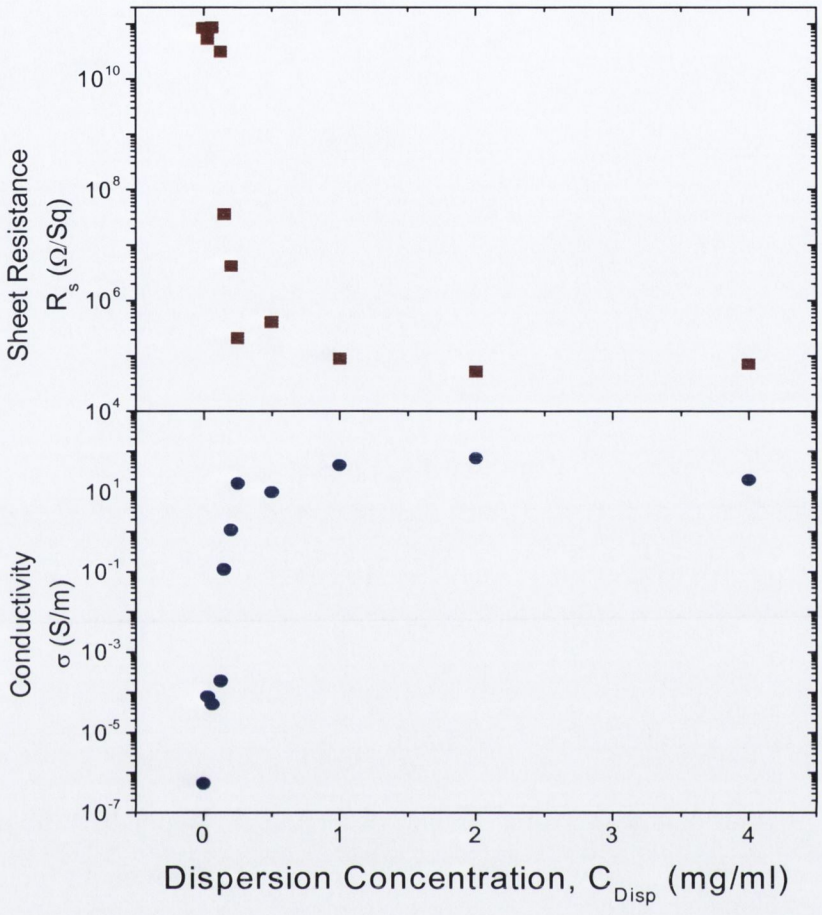

Figure 4.14 Graph of the dispersion concentration of nanotubes against the Sheet Resistance (red squares) and the layer Conductivity (blue circles) of the composite films swelled in nanotube dispersions in THF

From the data above we can plot the conductivity against the transmittance which shows us the relative transmittance values of the highest conductivity films (**Figure 4.15**). We find that we can still achieve high transmittance at relatively high conductivity (16 S/m, 90% and 66 S/m, 77 %).

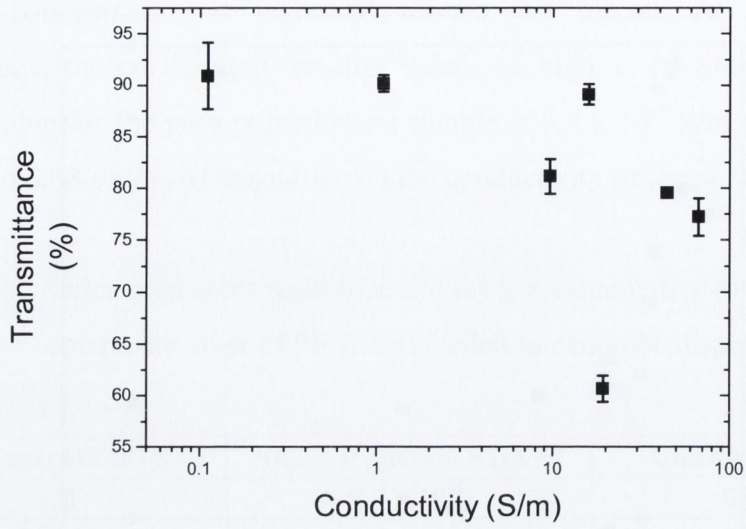

Figure 4.15 Graph of conductivity against transmittance of the polyethylene composite films swelled in nanotube dispersions in THF

4.6.4 Determination of percolation threshold

The conductivity of our composite films as a whole is largely dependent the ability of our highly conductive nanotubes to form a conductive network throughout the layer. As the polyethylene is highly insulating, the only way to get a current to pass from one end of the composite to the other is for it to pass through the conducting nanotubes provided they come into contact with one another. The volume fraction at which the nanotubes form an interconnecting network will instigate a dramatic change in the overall conductivity of the composite. It should occur over a relatively small volume fraction range, which is evident in our prepared composites. For a composite composed of conducting particles in an insulating matrix, the conductivity is predicted to scale with volume fraction as,

$$\sigma = \sigma_0 (V_f - V_{f0})^s$$

Where, V_{f0} is the percolation threshold; the critical volume fraction for the onset of current flow. σ_0 is a constant which depends on the conductivity of the filler particles and s is the percolation exponent, which is expected to depend on the dimensionality of the composite with calculated values of $s \approx 1.33$ and $s \approx 2.0$ in two and three dimensions respectively.[11,12]

For randomly arrayed rod-like fillers, the percolation threshold scales with the aspect ratio[13] as,

$$V_{f0} = \frac{0.6 d_{NT}}{l_{NT}}$$

where, d_{NT} and l_{NT} are the mean nanotube diameter and length respectively. The value is generally quite low for fillers like carbon nanotubes[11]

For most nanotube-based composites, σ_0 has been low due to the presence of a barrier to electron tunnelling between adjacent nanotubes.[14] in the insulating polymer. However, in the absence of such barriers, σ_0 can approach[15] conductivity values found for nanotube only films, ie 10^4-10^5 S/m.[16]

The conductivity data as function of volume fraction was fitted using the percolation equation as shown in **Figure 4.16**. A very good fit is obtained, confirming that the infiltrated tubes form a percolative network. From the fit we can extract values for the percolation threshold of 4 vol% which is higher than expected for carbon nanotubes[11] and suggests a low aspect ratio of 15 which would be much lower than expected for the nanotubes used. This may be due to the partial in-plane alignment of the tubes in the surface layer which increases the percolation thresholds for rod-like fillers.[17,18] The measured value of percolation exponent of s=1.8 is between the universal 3-dimensional value of s_{3D}=2.0 and the 2-dimensional value s_{2D}=1.33.[19]

Most importantly, however, we measure σ_0=1.2×10^4 S/m, which is a relatively very high value, higher than found for most composites. In the absence of polymer tunnelling barriers, σ_0 is expected to be of the same order as the conductivity of a nanotube only film. This has been measured to be ~500 S/m for a film of MWNTs similar to those used here.[20] This shows that by our swelling method we can achieve good connectivity between adjacent nanotubes in the polymer composite.

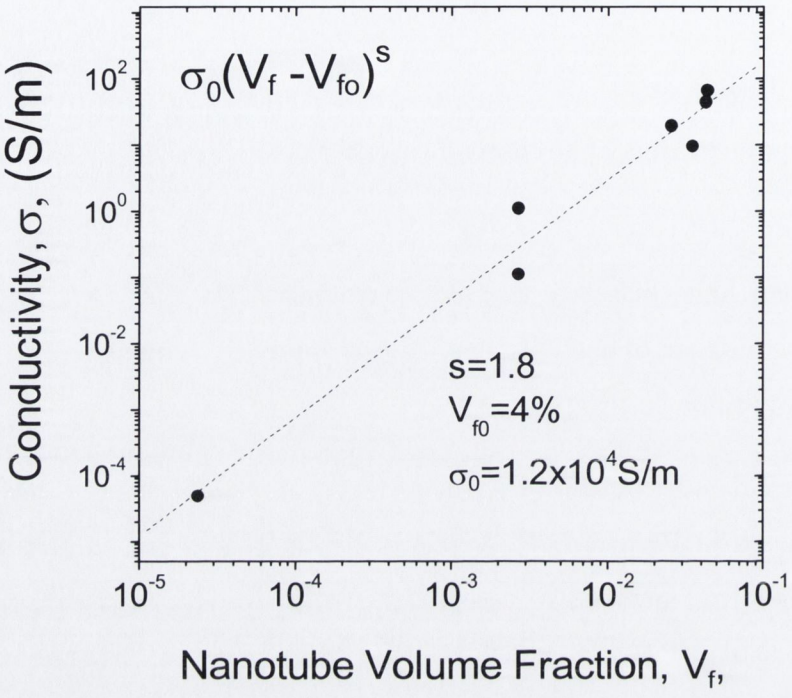

Figure 4.16 Nanotube volume fraction against conductivity for evaluation of percolation threshold

4.7 Acid treatment of PE Composite Films

It has been shown that acid treatment can increase the conductivity of nanotubes and composite films.[21,22] This is associated with a number of effects, removal of catalyst, purification of nanotubes and destruction of defective sites on the nanotube surface. It is generally time dependent and too much time will have a negative effect on the conductivity. The highest conductivity film was immersed in different types and concentrations of acid. Polyethylene films swelled in 2 mg/ml concentration of nanotubes in THF were subjected to three separate acidic treatments a 4:1 Sulfuric : Nitric acid mix, 35 % HCl treatment and 37% HCl treatment. Polymer composite films were immersed in the separate acidic environments for periods ranging from 1 minute to 1 hour. When the 1 hour acid treatment of the film is analysed under SEM **(Figure**

4.17) we find partial degradation of the nanotubes on the surface of the film. This is most likely due to the oxidising effect of the acids on the nanotubes.

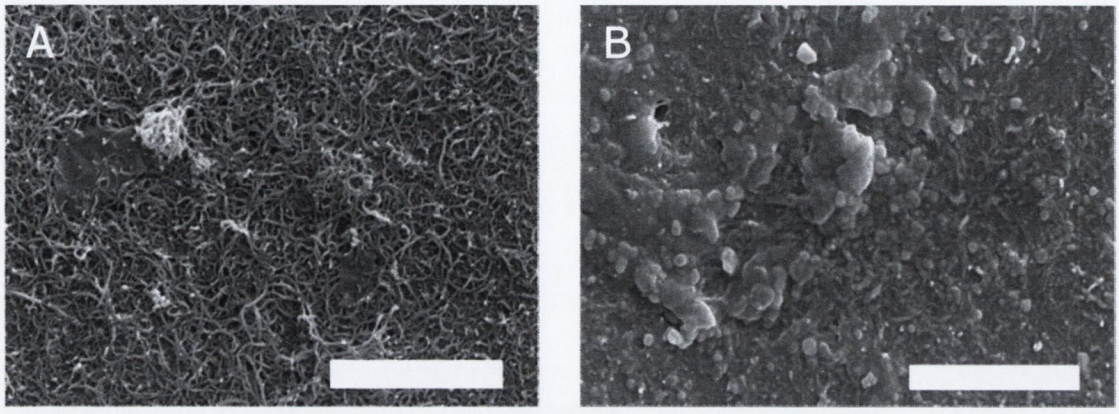

Figure 4.17 SEM images showing surface morphology of PE film swelled in 2 mg/ml concentration of nanotubes in THF before (**A**) and after (**B**) treatment in Nitric : Sulphuric acid mix (scale bar is 2 μm)

Initially there was no noticeable effect on conductivity observed from the immersion in a 4:1 Sulfuric : Nitric acid mixture, however conductivity decreased dramatically by over an order of magnitude after an hour immersion, which can be attributed to the oxidising effect of the acid treatment (**Table 4.9**, **Figure 4.19**). The films immersed in hydrochloric acid both showed a considerable increase in conductivity and the SEM analysis indicated little or no degradation from the acidic environment. It is not surprising that there is no oxidising effect associated with the hydrochloric acid as it is not an oxidising agent, however the associated decrease with respect to time of the conductivity may be explained by the dissolution of the iron catalyst from the nanotube.

Table 4.9 Time dependence of conductivity of PE composite film first swelled in a 2 mg/ml dispersion of very thin MWNTs in THF and then immersed in various concentrations of acid

	Conductivity(S/m)		
Time (min)	**Nitric/Sulphuric**	**HCl (35%)**	**HCl (37%)**
0	66.42	63.51	61.20
1	57.26	130.18	71.17
2	70.14	125.43	72.27
5	64.99	102.90	173.74
10	43.59	99.15	157.28
20	12.68	109.67	150.73
30	6.63	86.72	28.55
60	1.68	81.74	2.22

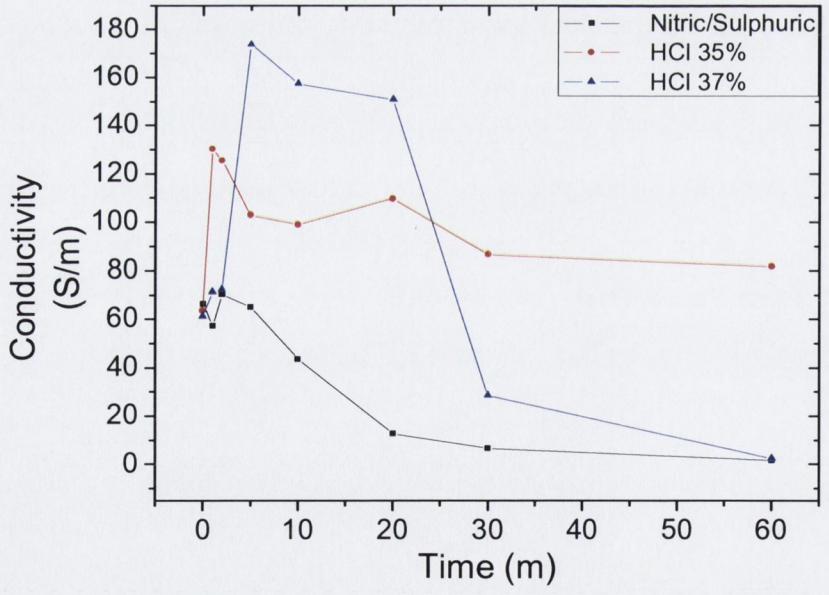

Figure 4.18 Time dependence of conductivity of PE composite film first swelled in a 2 mg/ml dispersion of very thin MWNTs in THF and then immersed in various concentrations of acid

4.8 Metal Treatment of Composite Films

A second approach to increase the maximum conductivity was attempted by treatment with the highly conducting metals gold and silver. To functionalise with gold the sample was immersed in a 0.03M gold solution of $HAuCl_4.3H_2O$ which is a source of Au^{3+}. For silver deposition a second sample was immersed in 0.03M $AgNO_3$ which produces Ag^+. Due to the high reduction potential of the nanotubes it was expected that metal reduction would occur on the surface of the nanotube. It was anticipated that this addition of a highly conducting metal to the nanotube would result in an overall increase of conductivity to the composite layer of the polymer film. Although silver may show relatively small increases, gold shows a considerable increase within the first ten minutes (**Table 4.10**, **Figure 4.19**). This would be expected if the gold was deposited between individual nanotubes to create a less resistant network, however there is also the potential to form electron traps when gold is deposited on the surface of the tube. This may decrease the overall conductivity and is most likely responsible for the decrease observed from 10 minutes onwards.

Table 4.10 Time dependence of conductivity of PE composite film first swelled in a 2 mg/ml dispersion of very thin MWNTs in THF and then immersed in gold or silver solution

	Conductivity (S/m)	
Time (min)	**Gold**	**Silver**
0	62.92	65.90
1	83.95	70.94
2	81.07	70.91
5	103.83	69.80
10	84.49	66.10
20	47.38	64.42
30	49.64	42.77
60	35.03	34.00

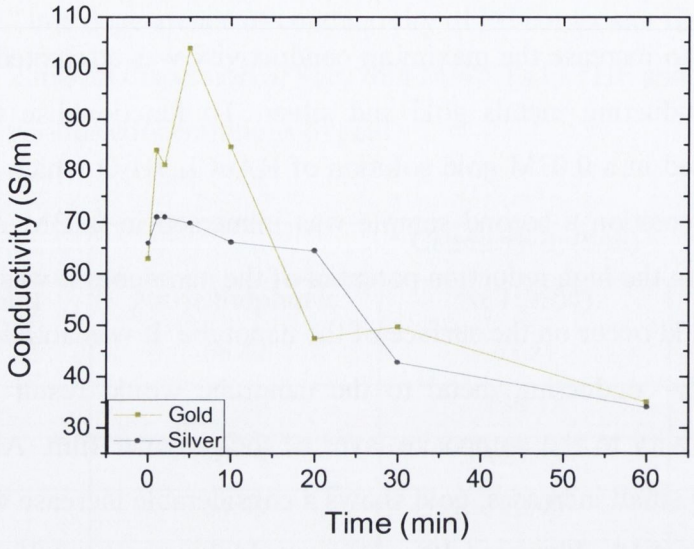

Figure 4.19 Time dependence of conductivity of PE composite film first swelled in a 2 mg/ml dispersion of very thin MWNTs in THF and then immersed in gold or silver solution

After we had found the best sample for conductivity was represented by the nanocyl multi-walled nanotubes in polyethylene swelled in THF it was decided to try and expand the research to different nanotubes which may represent a better possibility for conducting composites. It was decided to use Single-walled nanotubes (SWNTs), although they are generally more expensive and less available.

4.9 SWNT-Polyethylene Composites

4.9.1 Investigation of conductivity of SWNT-PE composite films

Selected types of SWNTs are more conductive than MWNTs it was hoped that if we could create a similar composite using these nanotubes it would result in a composite with even greater conductivity. The SWNTs chosen were Hipco nanotubes as they demonstrate one of the highest conductivities. The composite was prepared using by the same method as the highest conductivity MWNT composite film. The pure polyethylene film was immersed in a dispersion of Hipco SWNTs at various concentrations in THF. Due to the high cost and low availability of these nanotubes, samples were prepared up to a maximum concentration of 1 mg/ml. We observed an

increase up to a maximum of 0.14 Siemens per metre (**Table 4.11**, **Figure 4.20**). The highest conductivity sample (1mg/ml) was also immersed in a similar gold solution in section **4.6** for 5 minutes to try and deposit gold on the surface of the nanotubes and thereby increase its conductivity. This is represented by the hollow circle in **Figure 4.21** and represents an increase up to 0.35 Siemens per metre which is a 150 % increased on the measured sample. We find that the SWNT do show very large increases in the conductivity in the bulk polymer and they are of the same order as the MWNT samples. If we could increase the concentration further we might find even larger enhancement.

Table 4.11 Electrical conductivity results for PE films swelled in THF with various concentrations of dispersion of Hipco SWNTs

Concentration (g/L)	**Conductivity (S/m)**	**Error (+/-)**
0	**2.97×10^{-7}**	4.41×10^{-8}
0.03125	**1.02×10^{-6}**	1.87×10^{-7}
0.0625	**0.010**	4.04×10^{-4}
0.125	**0.0054**	1.11×10^{-4}
0.25	**0.015**	0.00109
0.5	**0.027**	8.94×10^{-4}
1	**0.142**	0.00416

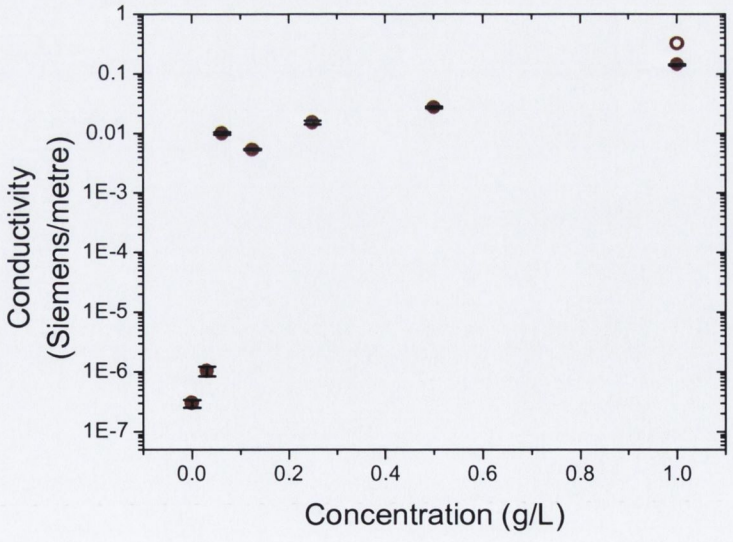

Figure 4.20 Electrical conductivity results for PE films swelled in THF with various concentrations of dispersion of Hipco SWNTs

4.9.2 Transmittance measurements of SWNT-PE composite films

Again we measured the transmittance of the samples. Visually the SWNTs were not as homogenously distributed as the MWNTs and the transmittance across the sample varied considerably at high concentrations. Both the conductivity and transmittance were relatively very high, with the value at 1 g/L dispersion concentration measuring a conductivity of 0.142 Siemens per metre and a transparency of around 90 % (**Table 4.12**, **Figure 4.21**). The MWNT films demonstrated transmittance at similar conductivities of approximately 80 %. This indicates that we require a lower amount of SWNTs to achieve similar conductivities. This demonstrates the better potential for creating even greater transparency conductive films with the SWNTs. These films warrant further conductivity analysis according to their layer thickness, however this could not be undertaken as the single walled nanotubes were too thin (< 5 nm) to be resolved under SEM and therefore the nanotube layer thickness could not be measured accurately.

Table 4.12 Transmittance values of PE–Hipco SWNT composite films

Concentration (mg/ml)	Transmittance at (% at λ = 550 nm)	Error (+/-)
0	**100**	0
0.03125	**99.6**	0.75
0.0625	**96.3**	1.10
0.125	**92.8**	0.69
0.25	**94.9**	3.80
0.5	**92.0**	2.95
1	**90.4**	4.83

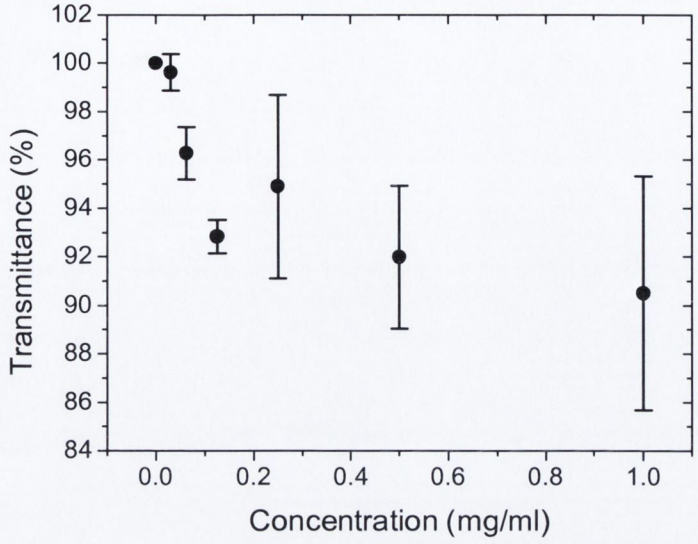

Figure 4.21 Graph of transmittance values for PE - Hipco SWNT composite films

4.10 Conclusions

We have found that our method for preparing polymer composites by our swelling technique can produce polymers with greatly enhanced electrical conductivity. The polypropylene does not show much of an increase in conductivity and this is evident when we look at the SEM images and see very little penetration of nanotubes within the polymer. With polyethylene, however, we achieved an eight orders of magnitude increase in its electrical conductivity when we prepared a composite by swelling in THF. We found that we achieve a very consistent and relatively uniform depth penetration of the nanotubes. We also achieved good conductivity results in nanotube-PET composite. It was evident from the SEM analysis and transmittance measurements that we have very good penetration of the nanotubes into this polymer. In fact the penetration was deepest in PET but resulted in a much less homogenous distribution of the nanotubes. We found that the conductivity is not necessarily dependent on the depth of penetration but more on the amount of nanotubes in the top layer and their proximity to each other creating a good percolation threshold. Polyethylene demonstrated a measureable layer of nanotube composite enabling us to calculate the electrical surface conductivity of the composite layer. We have also found that transmittance of the polymer composites still remains high when nanotubes are incorporated, which would

be important for any potential applications. We have achieved high conductivities while retaining a good transparency in the composites.

Further experiments illustrate the effectiveness of the treatment and show it can be expanded to other nanotubes, namely Hipco single-walled nanotubes. Eventually when the electrical potential of nanotubes are fully realized we have shown a method for preparing good electrically conducting composites in which the polymer and the type of nanotube may be adjusted depending on the composite required. Finally we have also shown that post-production treatment of the polymer composite can yield even higher conductivities when we treat the films with acid or coat them with gold or silver metals.

References

[1]H.H. Yu, S-J. Hwang, M-C. Tseng C-C. Tseng, *Opt. Commun.*, **259**, 187 (2006)

[2]D-H. Kim, M-R. Park, H-J. Lee G-H. Lee, *Appl. Surf. Sci.*, **253**, 409 (2006)

[3]S. Watcharotone, D.A. Dikin, S. Stankovich, R. Piner, I. Jung, G.H.B. Dommett, G. Evmenenko, S.E. Wu, S.F. Chen, C.P. Liu, S.T. Nguyen, R.S. Ruoff, *Nano Lett.*, *7*, 1888 (2007)

[4]Z. Chen, B. Cotterell, W. Wang, *Eng. Fract. Mech.*, **69**, 597 (2002)

[5]S.K. Park, J.I. Han, D.G. Moon, W.K. Kim, *Japanese J. of App. Phys. Pt 1*, **42**, 623 (2003)

[6]C.M. Aguirre, S. Auvray, S. Pigeon, R. Izquierdo, P. Desjardins, R. Martel, *App. Phys. Lett.*, 88 (2006)

[7]H.Z. Geng, K.K. Kim, K.P. So, Y.S. Lee, Y. Chang, Y.H. Lee, *J.A.C.S.*, **129**, 7758 (2007)

[8]M.S.P. Shaffer, A.H. Windle, *Adv. Mat.*, **11**, 937 (1999)

[9]S. Giordani, S.D. Bergin, V. Nicolosi, S. Lebedkin, M.M. Kappes, W.J. Blau, J.N. Coleman, *J. Phys. Chem. B*, ***110***, 15708 (2006)

[10]B.J. Landi, H.J. Ruf, J.J. Worman, R.P. Raffaelle, *J. Phys. Chem. B*, **108**, 17089 (2004)

[11]W. Bauhofer, J.Z. Kovacs, *Composites Science and Technology, In Press, Corrected Proof* (2008)

[12] Stauffer, D.; Aharony, A. *Introduction to percolation theory*; Taylor and Francis: London, (1992)

[13]E.J. Garboczi, K.A. Snyder, J.F. Douglas, M.F. Thorpe, *Physical Review E* **52**, 819 (1995)

[14]B.E. Kilbride, J.N. Coleman, J. Fraysse, P. Fournet, M. Cadek, A. Drury, S. Hutzler, S. Roth, W.J. Blau, *J. App. Phys.* **2002**, *92* 4024.

[15]F.M. Blighe, Y. Hernandez, W.J. Blau, J.N. Coleman, *Adv. Mat.*, **19**, 4443 (2007)

[16]Z.C. Wu, Z.H. Chen, X. Du, J.M. Logan, J. Sippel, M. Nikolou, K. Kamaras, J.R. Reynolds, D.B. Tanner, A.F. Hebard, A.G. Rinzler, *Science*, **305**, 1273 (2004)

[17]Du, F. M.; Fischer, J. E.; Winey, K. I. *Physical Review B*, 72 (2005)

[18]A. Behnam, J. Guo, A. Ural, *J. App. Phys*, **102**, 7 (2007)

[19]D. Stauffer, A. Aharony, *Introduction to percolation theory*; Taylor and Francis (1992)

[20]Y. R. Hernandez, A. Gryson, F.M. Blighe, M. Cadek, V. Nicolosi, W.J. Blau, Y. K. Gun'ko, J.N. Coleman, *Scripta Materialia*, **58**, 69 (2008)

[21]P.G. Jang, K.S. Suh, M. Park, J.K. Kim, W.N. Kim, H.G. Yoon, *J. App. Poly. Sci.* **106**, 110 (2007)

[22]K-I. Nakayama, Y. Asakura, M. Yokoyama, *Molec. Cryst. Liq. Cryst.* **424**, 217 (2004)

Chapter 5

Investigation of Mechanical Properties of Nanotube-Polymer Composites

5.1 Introduction

As we discussed in the previous chapter our method for preparing polymer composites by our swelling technique can produce polymers with greatly enhanced electrical conductivity. This was most evident with polyethylene (PE) when we prepared a composite by swelling in THF. We also achieved good conductivity results for polyethylene terephthalate (PET). It was evident from the SEM analysis and transmittance measurements that this was because we achieved good penetration of the nanotubes into the polymer. Generally this was restricted to some extent to the areas close to the surface layers. As we saw with the Kevlar in **Chapter 3** we could also increase the mechanical properties of a polymer if we get penetration of nanotubes into the polymer matrix. This may be important for the polymers that we analysed in the previous chapter. We decided to study the mechanical properties of our prepared PE and PET composites to see if we could achieve mechanical enhancement compared with the pure polymer. This would mean that overall we can influence considerably, the electrical and mechanical properties of pre-formed polymers by the swelling technique. The polypropylene studied in the previous chapter displayed very little penetration of nanotubes and very low conductivity increases; therefore it was not used in our further studies.

Mechanically PE and PET are considerably different. Their mechanical characteristics are discussed in **Chapter 1** and we can see that PET is a much stronger material than PE; however PE has a significantly better toughness. Overall, like most polymers, both require reasonably good mechanical properties in their everyday usage.

Polymer swelling can also be greatly influenced by treatment with supercritical fluid as it was previously reported.[1,2] This could represent a potentially exciting new area of research which we can explore and if we can expand our swelling technique further by using supercritical fluid instead of organic solvent and ulstrasound, it may present a new path to developing polymer composites by a swelling technique. Some research has also shown the intercalation of large molecules into polymer using a similar swelling technique.[3] The density of supercritical CO_2, and therefore its solvent strength, can be adjusted quite easily by changing the temperature or pressure. This enables the degree of swelling of a polymer to be controlled and ultimately we can achieve

penetration of small particles, namely nanotubes, between the fluid phase and the swollen polymer.

5.2 Aims of This Work

The main aim of this part of our work is to demonstrate an enhancement of the mechanical properties of our prepared polymer-nanotube composite films. We intend to show that our method of producing polymer composites with enhanced mechanical properties can be extended beyond just Kevlar fibres and into a wider range of different polymeric materials and that these materials can be enhanced both electrically and mechanically using this technique. We also aim to further explore our swelling technique and test if we can use super-critical CO_2 (SC-CO_2) for the preparation of polymer-carbon nanotube composites.

5.3 Mechanical Studies of PET Composites

As was discussed in the introduction, PET has a relatively high tensile strength when compared to most of the other polymers researched in this work and many of its wide range of applications many are dependent on its mechanical strength, including its importance in pressurised containers. A simple effective way of increasing its mechanical properties by post-processing would be important due to the large amount of products currently in existence. It could help increase the shelf-life of already formed materials or lead to the development of stronger products during processing. In **Chapter 4** we discussed the preparation of PET-carbon nanotube composites, which demonstrated good penetration of nanotubes into the polymer matrix. In fact the deepest penetration we have found so far was in PET swelled in THF and measured at least 6 μm into the polymer. Overall, however, the distribution of nanotubes was not homogeneous and there were areas of the polymer which showed little or no penetration at all. In the following pages we explore the changes in mechanical properties associated with the composites we prepared by our swelling technique using three different solvents, NMP, Toluene and THF. These solvents have different Hildebrand parameters and are of different polarities and therefore offer some variation in swelling ability, which important in our studies.

5.3.1 Nanotube-PET composites prepared in NMP

MWNT-PET composites have been prepared as described in section **4.3.1** by swelling PET films in carbon nanotube suspension in NMP. The polymer film was cut into five strips of approximate dimensions 2.4mm x 25mm x 120μm and its mechanical properties were measured using the Zwick 100 tensile tester. These properties were compared to pristine polymer which underwent the same treatment and are presented in **Table 5.1** and **Figure 5.1**

The mechanical properties of MWNT-PET composites showed no significant changes depending on the concentration of nanotubes in the solvent. The tensile strength, Young's modulus, toughness and strain for all concentrations remained relatively consistent within the error. This was expected as the SEM analysis (**Figure 4.4 D**) showed very little penetration of the nanotubes into the sample.

Table 5.1 Combined mechanical data for PET films Swelled in NMP with Nanocyl very thin MWNT

Conc. NT (g/L)	Tensile Strength (MPa)	Error (+/-)	Young's Modulus (GPa)	Error (+/-)	Toughness (MJ/m^3)	Error (+/-)	Strain (%)	Error (+/-)
0	**226**	8.3	**2.31**	0.40	**41.7**	5.9	**28.5**	2.8
0.3125	**198**	22.4	**2.14**	0.34	**28.5**	9.4	**23.3**	5.0
0.0625	**190**	34.5	**2.18**	0.38	**27.4**	12.9	**22.6**	6.9
0.125	**214**	16.5	**2.25**	0.39	**35.4**	8.8	**26.9**	4.1
0.25	**231**	14.0	**1.76**	0.66	**43.1**	5.7	**30.0**	2.6
0.5	**210**	27.1	**1.83**	0.33	**36.1**	14.1	**26.9**	6.7
1	**227**	15.5	**2.21**	0.42	**41.6**	10.9	**28.9**	5.3
2	**215**	22.4	**1.98**	0.12	**36.9**	12.9	**27.0**	5.7
4	**217**	21.6	**1.98**	0.44	**39.9**	10.5	**28.7**	4.8

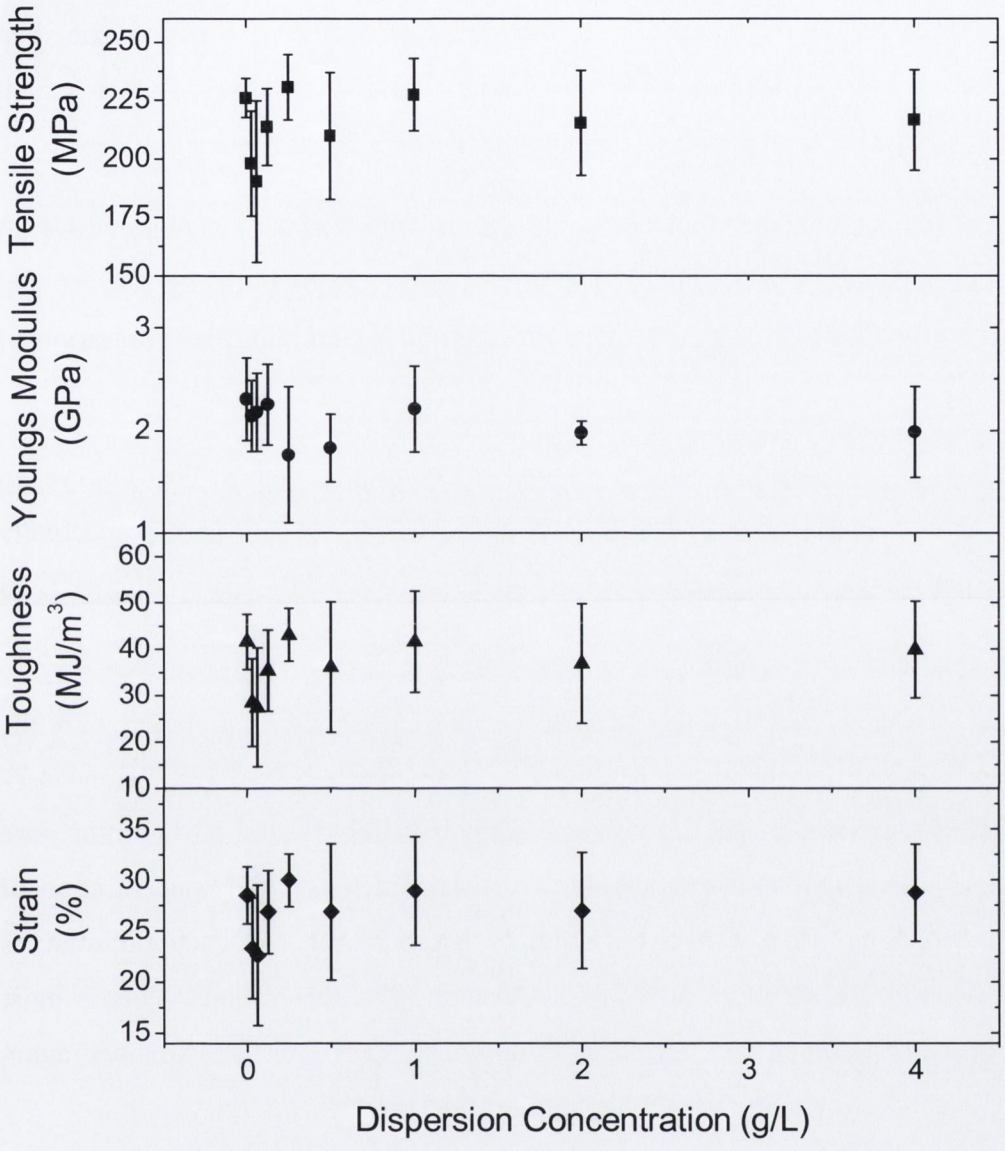

Figure 5.1 Combined graph of tensile strength, Young's modulus, toughness and strain against concentration of very thin MWNT dispersions in NMP for swelled PET films

5.3.2 Nanotube-PET composites prepared in toluene

PET samples prepared by swelling in MWNT suspension in Toluene were analysed for mechanical properties in the same way as the samples swelled in NMP described in section **5.3.1** above. These properties were compared to the pure polymer which underwent the same treatment and are presented in **Table 5.2** and **Figure 5.2**

We did see some penetration of nanotubes into this polymer under SEM (**Figure 4.4 C**) which is not too surprising given the solubility parameters of both the solvent and polymer. They demonstrate a good affinity to each other explaining the infiltration of the nanotubes.

When we look at the tensile strength we see some improvements. We observe an increase at higher concentrations of 1 g/L and 2 g/L to 240 and 239 MPa respectively which represents approximately about 6% of an increase over the pure polymer (226 MPa).

The Young's modulus also shows increases at the lower concentrations with the 0.03125 and 0.0625 g/L concentrations showing large increases to 2.57 GPa and 2.77 GPa respectively. These represent increases of approximately 11 and 20 % on the pure polymer (2.31 GPa). This is a considerable enhancement but as the concentration of nanotubes is increased further we see the Young's modulus decrease again and in fact is reduced below that for the pure polymer at the highest concentrations. This is most likely due to overloading of the polymer with nanotubes and could be explained again by some aggregation of nanotubes and disruption of the polymer matrix.

When we analyse the toughness we see that there are initial decreases associated with the concentration, however, at the higher concentrations we see some increases on the pure polymer (41.7 MJ/m^3). At a dispersion concentration of 1 g/L we see a value for toughness of 49.9 MJ/m^3 representing a 20% increase. This is also the concentration which showed the highest value for the tensile strength. The corresponding strain values show increases at the higher concentrations also but overall there is not a dramatic change in the strain.

Overall, considering the mechanical properties we find that PET swelled in the nanotube dispersion in toluene can demonstrate enhancement of its mechanical properties due to penetration of the nanotubes within the polymer matrix. This

replicates the increases we saw in the electrical conductivity of the samples in **Chapter 4**. The sample swelled in the 1 g/L concentration of nanotubes demonstrated the highest increases in both tensile strength and toughness. We have therefore found that we can enhance both the electrical conductivity and mechanical properties of PET by swelling in nanotube dispersions in toluene.

Table 5.2 Combined mechanical data for PET films swelled very thin MWNT dispersion in toluene.

Conc. NT (g/L)	Tensile Strength (MPa)	Error (+/-)	Young's Modulus (GPa)	Error (+/-)	Toughness (MJ/m^3)	Error (+/-)	Strain (%)	Error (+/-)
0	**226**	8.3	**2.31**	0.40	**41.7**	6.0	**28.5**	2.8
0.03125	**213**	15.3	**2.57**	0.38	**31.6**	7.3	**24.1**	3.5
0.0625	**199**	22.2	**2.77**	0.15	**28.6**	9.4	**22.9**	4.5
0.125	**227**	17.2	**2.26**	0.44	**40.8**	11.0	**29.0**	5.9
0.25	**228**	18.7	**2.36**	0.41	**41.9**	11.8	**29.0**	5.9
0.5	**222**	16.9	**2.36**	0.30	**40.3**	10.4	**28.8**	4.4
1	**240**	8.4	**2.12**	0.38	**49.9**	11.0	**32.8**	5.3
2	**239**	9.5	**1.99**	0.50	**47.0**	6.0	**31.7**	2.8
4	**227**	22.2	**2.07**	0.20	**40.9**	12.9	**28.6**	5.8

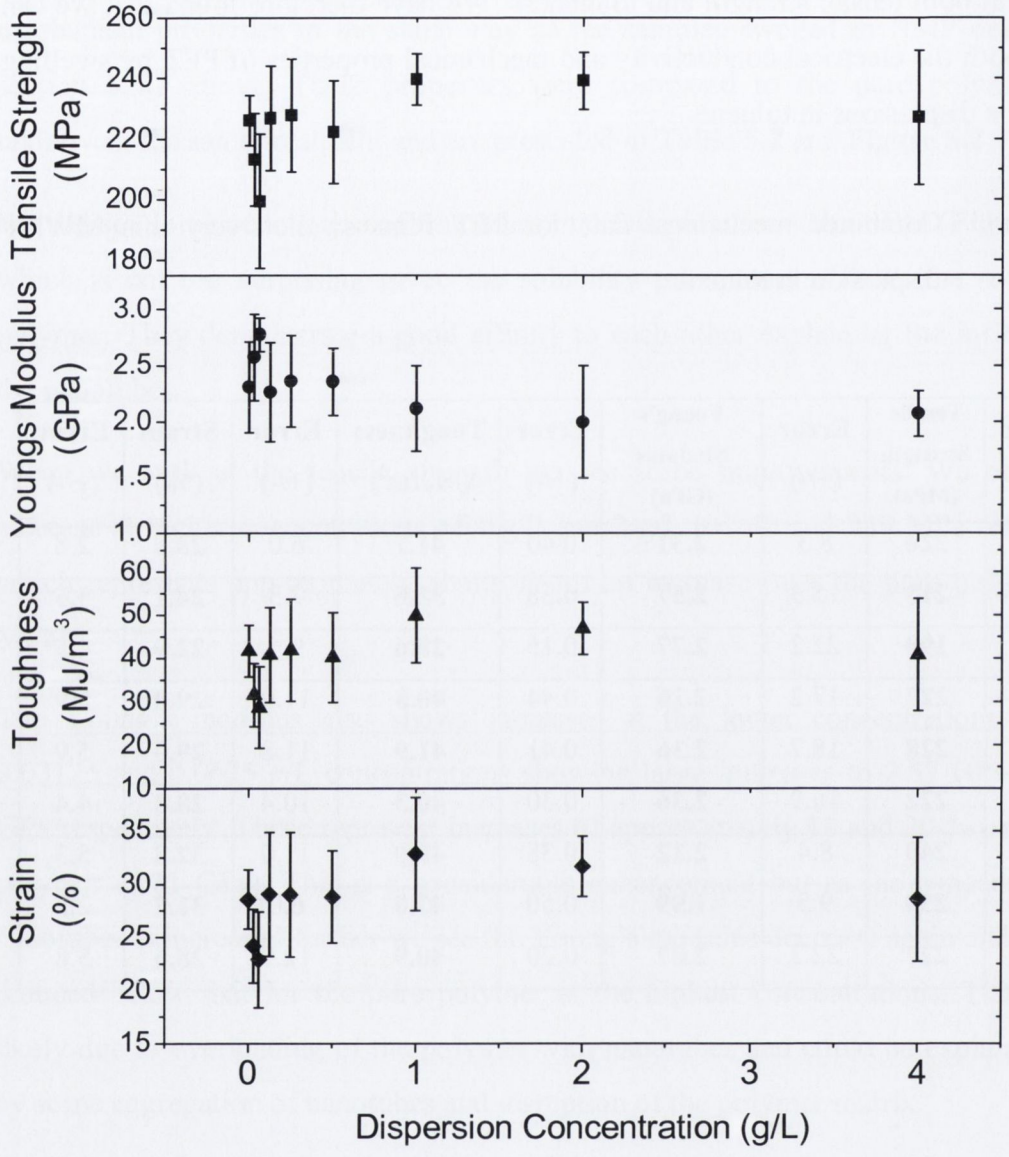

Figure 5.2 Combined graph of tensile strength, Young's modulus, toughness and strain against concentration of very thin MWNT dispersions in toluene for swelled PET films.

5.3.3 Nanotube-PET composites prepared in THF

The PET samples fabricated by swelling in nanotube suspension in THF were also analysed for mechanical properties by the same method as the samples in **5.3.1** above. These properties were compared to pure polymer which underwent the same solvent treatment and are presented in **Table 5.3** and **Figure 5.3**.

From the SEM analysis in **Chapter 4** we found that the samples swelled in THF gave the deepest penetration of nanotubes, of any of the samples; up to 6 μm. This may be due to the closest matching Hansen parameters of THF and PET. In taking into account all the solvents and polymers, PET and THF show the best affinity for the polar, δ_p (6.2 and 5.7 respectively), and total, δ_T (20.0 and 19.4), cohesive energy parameters, with good affinities for the dispersion, δ_d (18.0 and 16.8), and hydrogen bonding, δ_h (6.2 and 8.0), parameters also, thus offering the best swelling capability. We would expect that this should result in a comparatively good enhancement in the mechanical properties of the polymer.

When we analyse the tensile strength we see an increase at the 0.0625 g/L concentration to 243 MPa from the pure polymer (226 MPa) representing an increase of approximately 8 %. There is a general increase at almost all concentrations which is not too surprising as we saw some nanotube penetration at even very low concentrations when we analysed the samples using SEM.

The Young's moduli of the composites demonstrate increases on the pure polymer (2.31 GPa) at most of the concentrations. The best increases were observed for the samples immersed in the higher concentrations of nanotubes with the 1, 2 and 4 g/L showing increases of around 9 % (2.50, 2.49, 2.51 GPa respectively) indicating some nanotube penetration. The PET film swelled in 4 g/L nanotube suspension demonstrated the maximum increase observed.

When we analyse the toughness we see that it achieves a considerable increase again at the 0.0625 g/L concentration. The maximum value for the sample of 58.6 MJ/m^3 represents an increase of over 40% on the pure polymer (41.7 MJ/m^3). We do however observe the toughness decrease at the higher concentrations of nanotubes. This decrease is replicated in the tensile strength measurements where we saw a decrease from the maximum value at the higher concentrations.

Overall with the PET films swelled in the THF we find that we can achieve considerable enhancement of the polymer utilizing the swelling method at low concentrations. The best individual film appears to be the sample swelled in a nanotube concentration of 0.0625 g/L of nanotubes. It demonstrates increases in all the mechanical properties with the highest values strength and toughness for any of the composites. The higher concentration dispersions do not show considerable increase on the pure polymer, with the exception of the Young's modulus. We saw the best increases in the electrical properties of the samples swelled in THF and it is unsurprising that we find the best enhancement of the mechanical properties for these samples as well.

Table 5.3 Combined mechanical data for PET films swelled in THF with Nanocyl very thin MWNT

Conc. NT (g/L)	Tensile Strength (MPa)	Error (+/-)	Young's Modulus (GPa)	Error (+/-)	Toughness (MJ/m^3)	Error (+/-)	Strain (%)	Error (+/-)
0	**226**	8.3	**2.31**	0.40	**41.7**	6.0	**28.5**	2.8
0.3125	**223**	27.0	**2.41**	0.37	**45.8**	24.0	**31.1**	10.7
0.0625	**243**	13.4	**2.40**	0.67	**58.6**	11.0	**36.9**	4.4
0.125	**236**	23.9	**2.17**	0.46	**48.4**	21.5	**31.4**	9.0
0.25	**230**	19.2	**2.05**	0.37	**49.1**	17.5	**33.0**	8.6
0.5	**223**	18.7	**2.34**	0.36	**49.7**	17.1	**34.0**	7.5
1	**224**	19.6	**2.50**	0.50	**43.8**	10.7	**30.4**	4.5
2	**235**	10.5	**2.49**	0.16	**44.2**	6.9	**30.0**	2.7
4	**223**	16.5	**2.51**	0.32	**41.3**	9.9	**29.2**	4.4

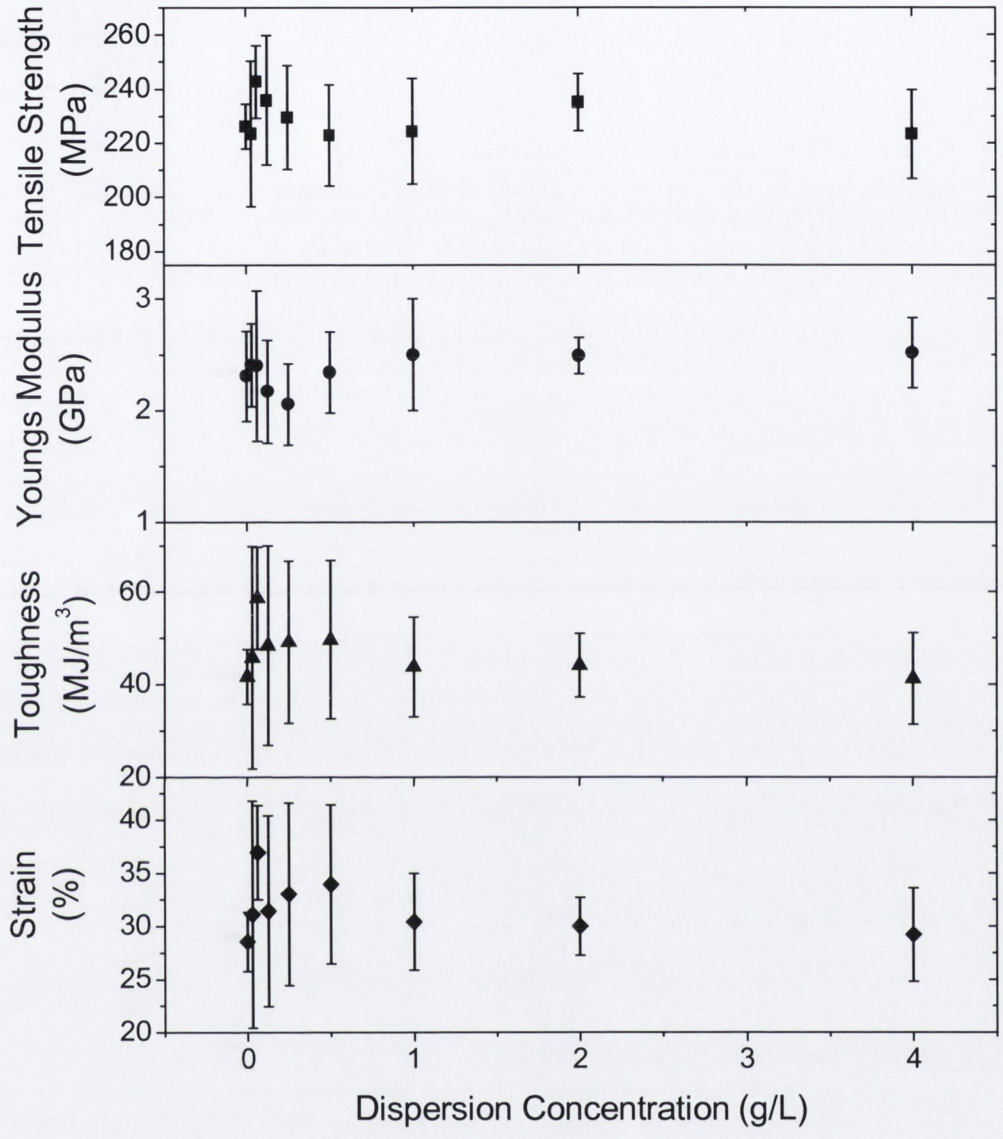

Figure 5.3 Combined graph of tensile strength, Young's modulus, toughness and strain against concentration of very thin MWNT dispersions in THF for swelled PET films

5.4 Mechanical studies of nanotube-polyethylene composites

As we discussed in the introduction, polyethylene has a considerably high toughness but a relatively low tensile strength. It is a very important and widely used polymer and therefore enhanced mechanical properties, tensile strength in particular, would be important for many of its applications.

5.4.1 Nanotube-PE composites prepared in NMP

PE samples prepared by swelling PE films in MWNT suspension in NMP were analysed for mechanical properties in the same way as the PET described in section **5.3.1** above. The polymer film was prepared properties were compared to pure polymer which underwent the same treatment and are presented in **Table 5.4** and **Figure 5.4**.

When we analyse the tensile strength we see no improvements over the pure polymer, this is not surprising as the films displayed no considerable penetration into the polymer matrix in NMP when analysed by SEM (**Figure 4.6 D**). Overall the mechanical characteristics of the samples do not display any substantial increases and stay the same within experimental error. This can be explained by the fact that PE undergoes only a very limited swelling in NMP. As a result too few nanotubes penetrate inside polymer to have any impact on its mechanical properties.

Table 5.4 Mechanical data table for NMP swelled PE films with various concentrations of very thin MWNT

Conc. NT (g/L)	Tensile Strength (MPa)	Error (+/-)	Young's Modulus (GPa)	Error (+/-)	Toughness (MJ/m^3)	Error (+/-)	Strain (%)	Error (+/-)
0	**25**	1.7	**1.9**	0.26	**105**	13.6	**572**	58
0.03125	**26**	2.9	**2.4**	0.23	**106**	22.3	**666**	76
0.0625	**25**	1.6	**2.2**	0.19	**108**	12.5	**635**	51
0.125	**22**	2.7	**2.3**	0.46	**80**	22.9	**422**	114
0.25	**24**	3.0	**2.4**	0.12	**100**	23.3	**529**	95
0.5	**21**	3.5	**1.9**	0.21	**104**	44.9	**605**	215
1	**24**	5.2	**2.5**	0.77	**100**	44.2	**485**	156
2	**26**	2.8	**2.3**	0.69	**105**	40.2	**476**	175
4	**20**	6.8	**1.9**	0.58	**85**	73.3	**463**	325

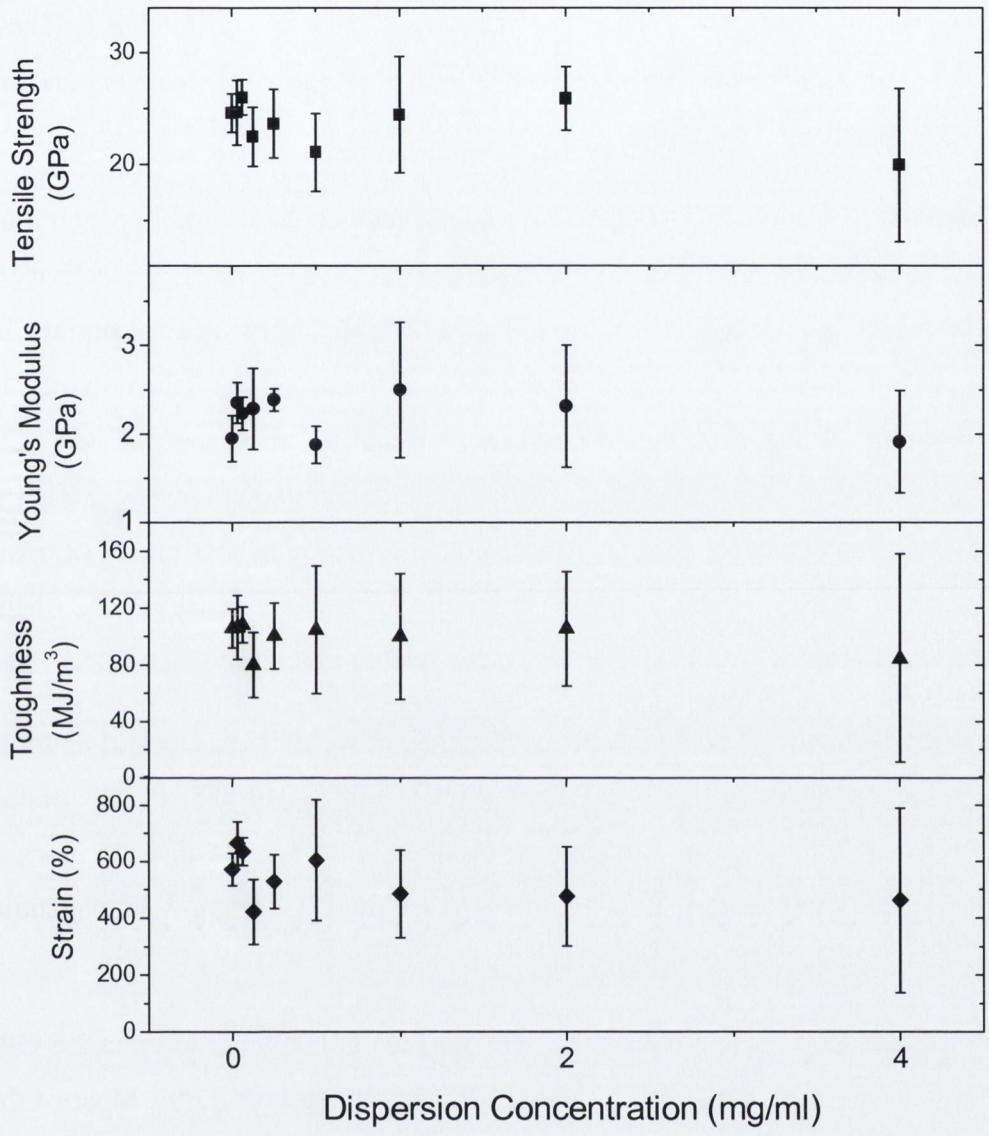

Figure 5.4 Combined graph of tensile strength, Young's modulus, toughness and strain against concentration of very thin MWNT dispersions in NMP for swelled PE films

5.4.2 Nanotube-PE composites prepared in toluene

The PE samples swelled in Toluene were analysed for mechanical properties in the same way as the PET samples swelled in NMP described in section **5.3.1**. These properties were compared to pure polymer which underwent the same treatment and are presented in **Table 5.5** and **Figure 5.5**

The SEM analysis of the PE films swelled in toluene showed considerable penetration of nanotubes into the polymer matrix. When we analysed the electrical conductivity it demonstrated very high conductivities also. This is not too surprising considering the very similar Hildebrand and Hansen parameters for both the solvent and the polymer. In taking into account all the solvents and polymers, PE and toluene show the best very good affinity for total, δ_T (18.2 and 18.1), cohesive energy parameters, with exactly the same affinities for the dispersion, δ_d (18.0 and 18.0), and hydrogen bonding, δ_h (2.0 and 2.0), parameters, offering excellent swelling capability. We would expect some of the best enhancement in mechanical properties for any solvent polymer interaction.

It is unsurprising then when we look at the tensile strength we find increases of up to 20 % on the original polymer (25 MPa). This is represented by the 0.5 g/L dispersion concentration which achieves a tensile strength of 30 MPa. In fact we find increases at all concentrations of nanotubes showing that we are achieving good homogenous composites.

The Youngs moduli show increases from 1.9 GPa for the pure polymer to up to 2.5 GPa at the 1 g/L dispersion concentration. This represents an increase of 32 %. Most of the dispersion concentrations demonstrate an increase on the pure polymer for the Young's modulus values.

The values for toughness display increases also. The sample swelled in the 4 g/L sample demonstrates the best enhancement on the pure polymer (105 MJ/m^3). It achieves a toughness of 139 MJ/m^3 representing an increase of 32 %. We see that we also get a corresponding increase in strain.

Overall with the samples swelled in toluene we find that we achieve reasonable increases in the mechanical properties across the dispersion concentration range. These samples showed relatively homogenous penetration of nanotubes and good electrical

enhancement as discussed in **Chapter 4**. This is consistent with the improvement we find when we analyse the mechanical properties.

Table 5.5 Mechanical data table for toluene swelled PE films with various concentrations of very thin MWNT

Conc. NT (g/L)	Tensile Strength (MPa)	Error (+/-)	Young's Modulus (Gpa)	Error (+/-)	Toughness (MJ/m^3)	Error (+/-)	Strain (%)	Error (+/-)
0	**25**	1.7	**1.9**	0.26	**105**	13.6	**572**	58
0.03125	**27**	3.0	**2.4**	0.48	**132**	20.2	**663**	73
0.0625	**26**	3.2	**2.2**	0.25	**116**	22.8	**571**	74
0.125	**28**	2.5	**2.3**	0.36	**125**	13.6	**597**	45
0.25	**29**	2.8	**2.4**	0.21	**138**	19.2	**660**	51
0.5	**30**	3.2	**1.9**	0.26	**135**	24.6	**608**	85
1	**29**	2.2	**2.5**	0.21	**135**	14.0	**616**	35
2	**27**	2.2	**2.3**	0.24	**130**	12.4	**672**	38
4	**29**	2.1	**1.9**	0.25	**139**	16.3	**650**	56

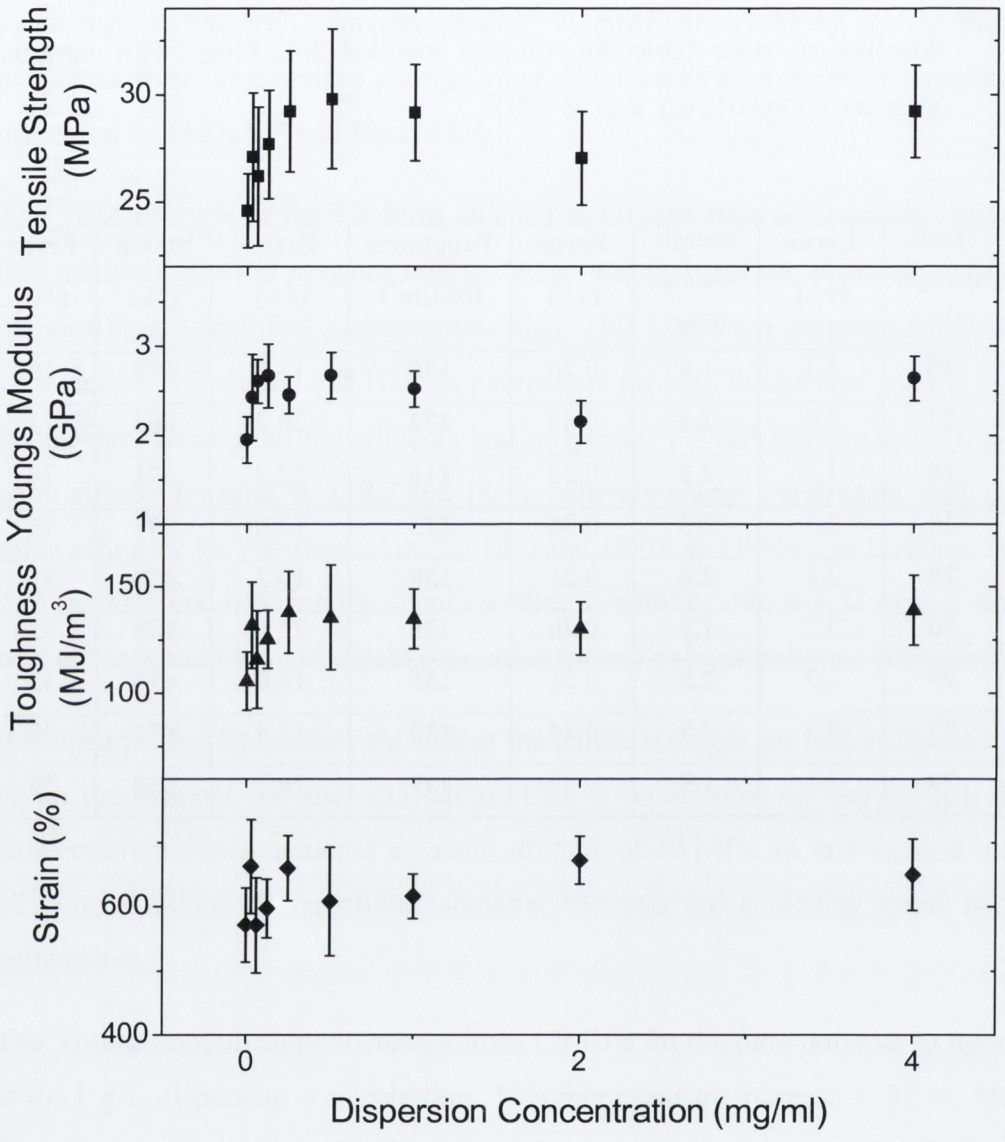

Figure 5.5 Combined graph of tensile strength, Young's modulus, toughness and strain against concentration of very thin MWNT dispersions in toluene for swelled PE films

5.4.3 Nanotube-PE composites prepared in THF

The PE samples were immersed and swelled in various nanotube concentrations in THF. They were then analysed for mechanical properties in the same way as the samples swelled in NMP described in section **5.4.3**. These properties were compared to pure polymer which underwent the same treatment and are presented in **Table 5.6** and **Figure 5.6**.

This composite demonstrated the best electrical conductivity and most homogenous penetration of nanotubes among all the composites tested. The SEM analysis (**Figure 4.8**) showed relatively homogenous penetration of up to 1 μm into the polymer matrix.

When we look at the tensile strength we see increases of up to 32 % on the original polymer (25 MPa) for the sample swelled in 1 g/L dispersion of nanotubes in THF (33 MPa).

Again with the Young's modulus values we find increases in most of the composites. The Youngs modulus shows larger increases up to a maximum at the 1 g/L concentration (3.1 GPa), which is also where we found the concentration of nanotubes in the polymer layer reached a maximum in **Chapter 4**. This represents an increase of over 60 % on the pure polymer (1.9 GPa).

When we look at the toughness we again see increases. These are most substantial at the highest concentrations of nanotubes with the sample at 0.5 g/L concentration in particular showing an increase of about 45 % on the pure polymer. The corresponding strain did not increase substantially for this sample but overall we did see it generally increase on the pure polymer.

As we discussed in the previous chapter the largest amount of nanotubes were evident in the higher concentrations and the transmittance measurements gave us a good approximation of the amount of nanotubes in the sample overall. At its highest we saw that in the polymer composite layer we were seeing a maximum of up to about 8 % volume of nanotubes (1 and 2 g/L samples). This represents a value of about 0.01 % by volume of nanotubes in the polymer overall when we take into account the thickness of the polymer. Assuming that most of these nanotubes are in the surface layer we are therefore seeing a very considerable enhancement of the polymer. We can see an increase in many of the samples in the concentration range although once the highest

concentration is reached the strength and modulus reverts back to similar values as the pure PE. This concentration by far showed the deepest penetration and amount of nanotubes (up to 0.2 % by mass) within the polymer matrix and it is most likely having a negative effect due to aggregation and disruption of the polymer structure.

As we discussed in **Chapter 1**, the full potential of polymer enhancement by the creation of nanotube-polymer composites is yet to be realised. The results presented in this chapter, and the results for polyethylene swelled in nanotube dispersions in THF in particular, indicate that if the swelling method can be optimised, with particular attention paid to enhancing the mechanical properties, it may offer a new route to creating polymer composites with enhanced mechanical properties.

Table 5.6 Mechanical data table for THF swelled PE films with various concentrations of very thin MWNT

Conc. NT (g/L)	Tensile Strength (MPa)	Error (+/-)	Young's Modulus (GPa)	Error (+/-)	Toughness (MJ/m^3)	Error (+/-)	Strain (%)	Error (+/-)
0	**25**	1.7	**1.9**	0.26	**105**	13.6	**572**	58
0.03125	**27**	2.1	**2.7**	0.08	**115**	16.5	**566**	57
0.0625	**25**	1.9	**2.4**	0.30	**111**	14.4	**599**	61
0.125	**30**	1.9	**2.9**	0.22	**143**	17.2	**622**	48
0.25	**30**	2.7	**2.4**	0.29	**143**	20.5	**660**	65
0.5	**33**	2.2	**3.0**	0.25	**152**	22.7	**633**	82
1	**29**	2.4	**3.1**	0.47	**134**	17.4	**729**	50
2	**31**	2.5	**2.5**	0.25	**140**	15.3	**662**	51
4	**24**	1.0	**1.8**	0.23	**123**	31.7	**810**	143

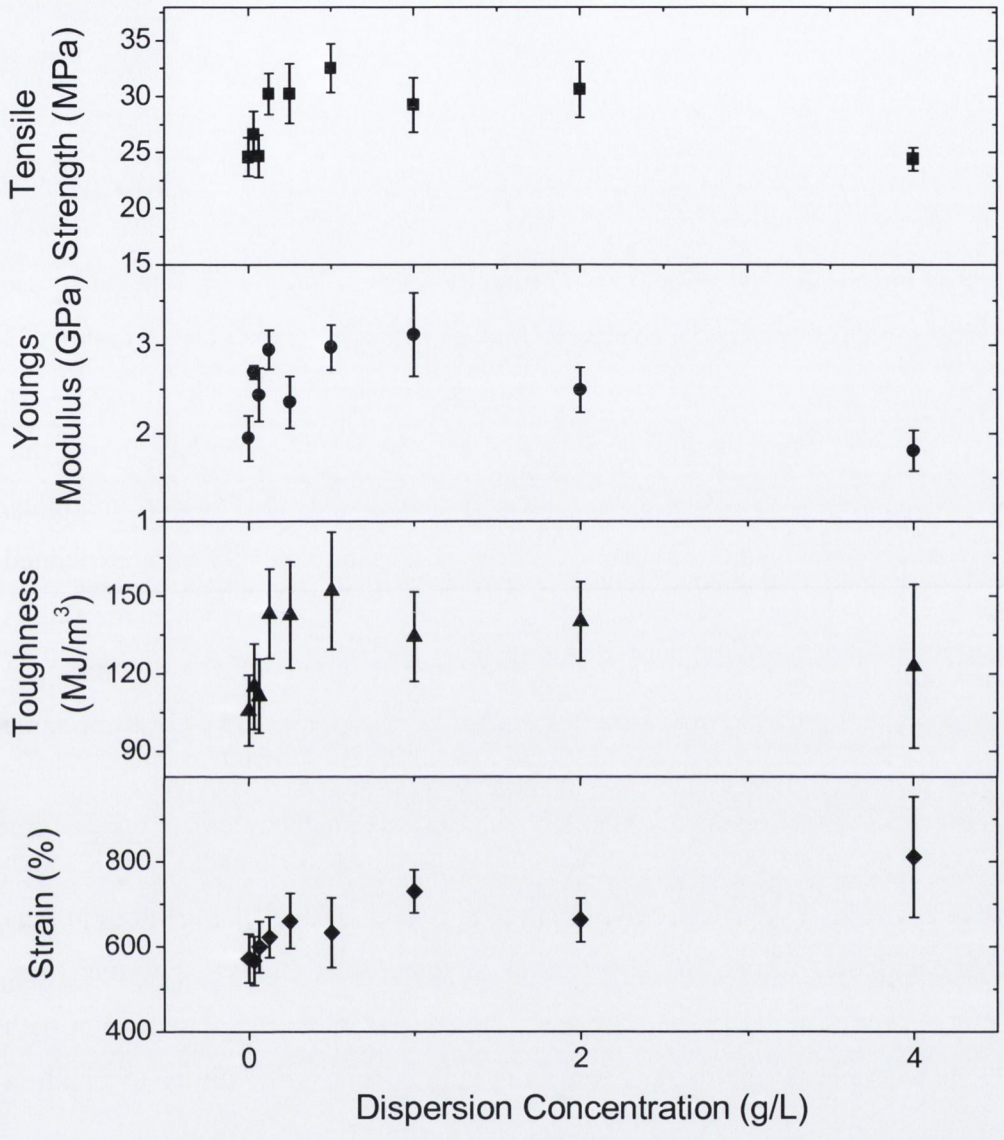

Figure 5.6 Combined graph of tensile strength, Young's modulus, toughness and strain against concentration of very thin MWNT dispersions in THF for swelled PE films

5.5 Nanotube-Polyethylene Composites Prepared in Supercritical CO_2

5.5.1 Preparation of SC-CO_2 swelled nanotube-PE composite films

Supercritical fluids have a variety of interesting properties including having characteristics of both liquid and gas. This gives them an ability to penetrate solid materials like a gas, but also to act like a liquid by maintaining a solution.[4,5] It is this property which can enable them to act as a carrier for molecules and particles enabling them to penetrate inside a polymer matrix. Carbon dioxide is a very desirable gas to use for supercritical analyses due to the relatively low temperature (31°C) and pressure (73 atm) needed to achieve superfluidity. As was discussed in section **5.1** it has been shown in the past to swell polymers including polyethylene. Recent research has shown that just swelling polyethylene in SC-CO_2 can have an impact on the Youngs modulus, toughness and strain, decreasing the former and increasing the latter.[6] This is explained by the plasticisation of a polymer due to its absorption of CO_2. Evidence for this is generally found in an increased melting temperature of the polymer.[6] For this reason it was decided to prepare pure polymer samples treated with supercritical CO_2 at the same temperature and pressure for comparison to nanotube samples.

The experiments were carried out in National University of Ireland, Cork, with nanotubes dispersed in NMP at a concentration of 1 g/L. A high concentration was chosen to give the best chance of penetration of nanotubes into the polymer. The temperature was kept constant by immersion of the apparatus in a regulated water bath at 50 °C. NMP was chosen as the solvent due to its considerable ability to create a stable dispersion of nanotubes as was discussed in **Chapter 3**.

5.5.2 SEM analysis of SC-CO_2 swelled nanotube-PE composite films

SEM analysis demonstrated considerable penetration of the nanotubes deep into the polymer matrix and we observed nanotubes in many areas. An example of the penetration can be seen in **Figure 5.7**. The nanotube penetration does not appear to be homogeneous throughout the polymer sample with sections of the polymer clearly showing no nanotubes protruding, whilst other areas of the same image show many nanotubes protruding from the cross sectional surface. We can see this clearly in **Figure 5.7 B**.

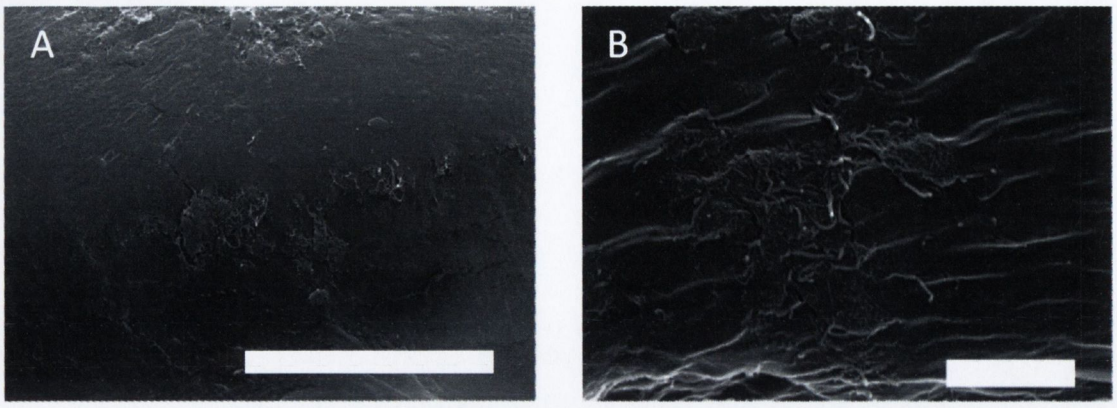

Figure 5.7 SEM image of polyethylene composite cross section after treatment with nanotubes in supercritical CO_2 at a pressure of 34.5 MPa (Scale bars **A**: 10 μm **B**: 1 μm)

5.5.3 DSC studies of SC-CO_2 swelled nanotube-PE composites

As we discussed in section **5.4.1** SC-CO_2 treatment tends to increase the melting temperature, T_m, of a polymer. When we measured the highest concentration samples from section **5.2** and **5.3** we found no considerable change in the T_m. This is most likely due to the fact that the swelling mostly affects the surfaces of the polymer. When we use supercritical CO_2 however we find that swelling is much more absolute and when we look at the DSC of the samples swelled at the highest pressure we find that it show a large shifting of the peak of the T_m in the polymer samples after treatment in CO_2. This indicates that the supercritical fluid has a considerable effect and increases the plasticisation of the polymer. It seems to affect both the pure and nanotube samples evenly indicating the difference between the nanotube sample and the swelled pure sample is minor and that the supercritical CO_2 has a much larger influence on the polymer than the nanotubes do.

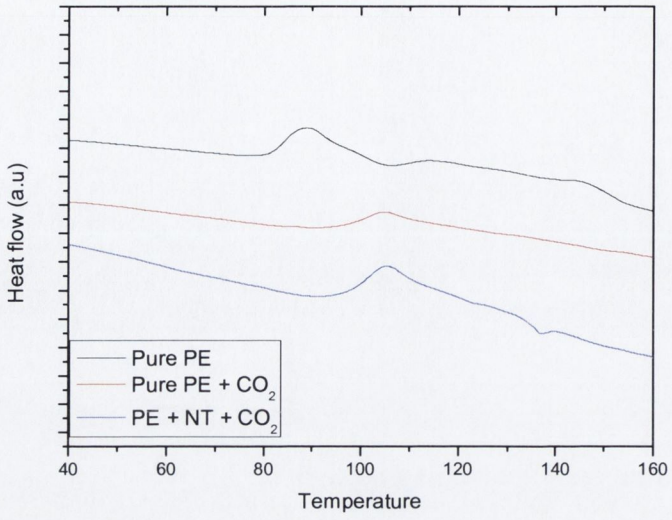

Figure 5.8 DSC curves for Polyethylene films demonstrating the variation in the melting temperature for pure polyethylene (black line), polyethylene swelled in SC CO_2 (red line) and swelled in SC CO_2 in the presence of nanotubes (blue line)

5.5.4 Mechanical properties of SC-CO_2 swelled nanotube-PE composites

The representative stress strain curves for the treatment of PE at 34.5 MPa are shown in **Figure 5.9**. We see a considerable difference in strain for the sample swelled in the absence of nanotubes. When we look at the stress-strain curves we also find that after reaching the yield point the blank samples swelled in supercritical CO_2 show a change in the overall stress-strain curve with a decrease in stress after the yield point. When we look at the nanotube sample it seems relatively unaffected by the treatment indicating that they must be better able to reinforce the polymer therefore not affecting the toughness in the same way.

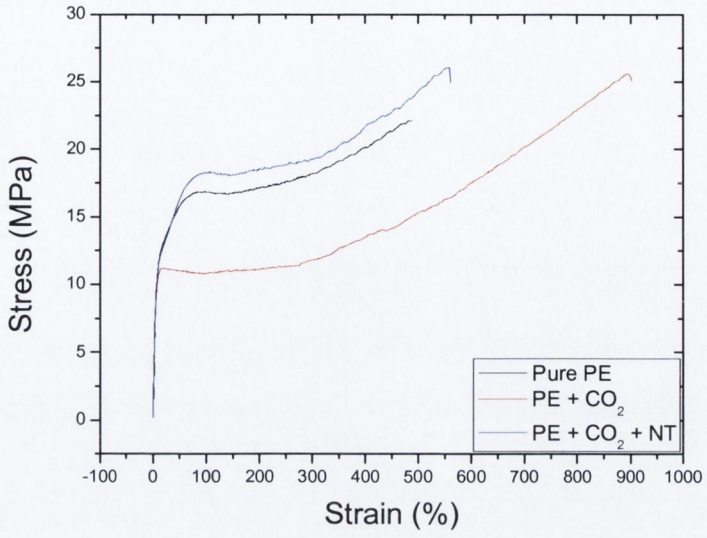

Figure 5.9 Representative stress-strain curves for pure polyethylene (black line), polyethylene swelled in SC CO_2 (red line) and swelled in SC CO_2 in the presence of nanotubes (blue line)

When we analyse the results in **Table 5.7** and **Figure 5.8** we see the effect of the supercritical CO_2 on pure polyethylene and how the variation in pressure affects the mechanical properties of the polymer. The tensile strength is generally unaffected but we do see slight decreases in the Youngs modulus and increases in the toughness and strain due to the treatment. The polymer is absorbing the CO_2 thereby inducing plasticisation and we find that the ductility of the sample is increased. This increased ductility gives a corresponding increase in the toughness. This is an expected effect of the polymer as we discussed in section **5.4.2**.

We can then compare the effects of the nanotubes on the mechanical properties of the polymer. We find again that there is a negligible difference in tensile strength of the sample when the large error bars are taken into account. The Young's moduli however increase with the nanotube samples whereas the control samples showed minor decreases. The value at the highest pressure (48.2 MPa) represents an increase of almost a third (32.5%) on the original polymer, and when compared to the control sample it is even greater. A decrease in Young's modulus is normally expected in a sample treated

with supercritical fluid, but the increase displayed here can be associated to the nanotube in the polymer matrix.

Although all samples show an increase in the toughness on the original polymer this may be due to the treatment with SC-CO_2.This is confirmed when we compare the toughness of the control sample against the nanotube samples and we find that generally there is a negligible difference between them.

When we look at the strain we can see increases with respect to the samples treated with supercritical CO_2. The samples swelled with the nanotubes show some decreases with respect to the strain when compared to the samples without nanotubes.

Table 5.7 Mechanical data table for PE films swelled in CO_2 with Nanocyl very thin MWNT

Conc. NT (g/L)	Pressure (MPa)	Tensile Strength (MPa)	Error (+/-)	Young's Modulus (GPa)	Error (+/-)	Toughness (MJ/m^3)	Error (+/-)	Strain (%)	Error (+/-)
0	**0**	**25**	1.7	**1.9**	0.26	**105**	13.6	**572**	58
0	**34.5**	**25**	5.1	**1.8**	0.21	**123**	31.5	**919**	128
0	**48.2**	**24**	4.3	**1.6**	0.37	**133**	29.3	**794**	117
1	**34.5**	**26**	3.9	**2.4**	0.16	**124**	23.3	**796**	88
1	**48.2**	**25**	2.7	**2.5**	0.37	**133**	29.3	**507**	112

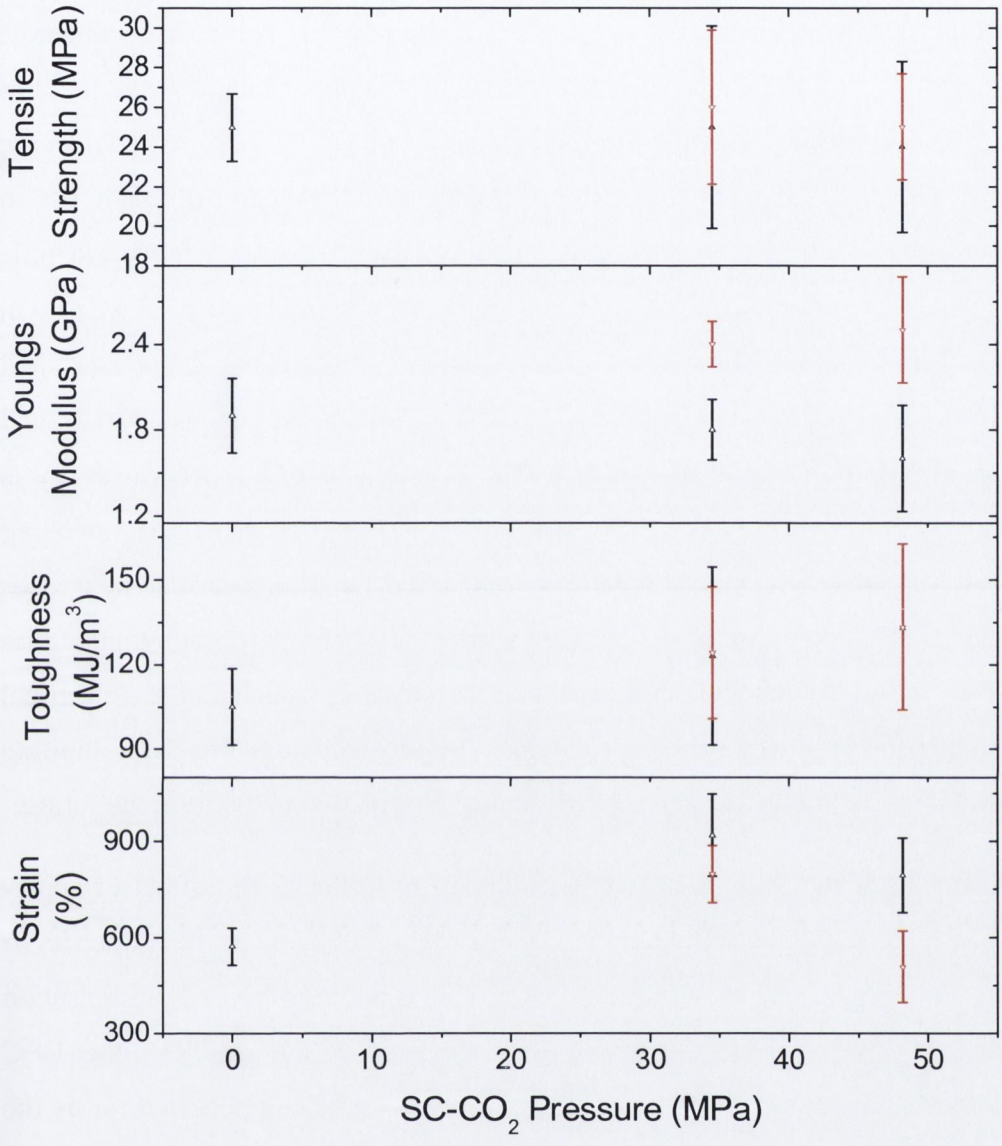

Figure 5.10 Combined graph of tensile strength, Young's modulus, toughness and strain of PE composites (prepared by swelling technique with a 1 g/L very thin MWNT in NMP and SC-CO_2) against the pressure of supercritical carbon dioxide

5.6 Conclusions

In this work we have found that the samples in which we found greatly increased electrical properties due to nanotube penetration of the polymer can also demonstrate some enhancement of their mechanical properties. The samples which showed the best penetration of nanotubes in **Chapter 4** also show better mechanical properties than the pure polymer. We found that for the samples swelled in a dispersion of nanotubes in NMP although the solvent shows a good dipersion of nanotubes we achieve too little swelling to have a considerable effect on the polymer. This is similar to what we saw in the electrical measurements. The dispersive capability of toluene is not as good as NMP but the swelling capability is greater and we find much better penetration and enhancement. Ultimately with THF we find that although its dispersive capability is worse again we find very good penetration. Overall this indicates that swelling capability of the solvent is much more important. We have shown that by proper solvent selection the swelling method presents a novel way of incorporating nanotubes into a polymer. This ultimately demonstrates that it is possible to enhance the electrical and mechanical properties of a variety of polymers by this technique thereby exhibiting its adaptability and capability for the development of polymer composites in the future.

We have also further expanded our swelling method by utilising the effect of super-critical carbon dioxide. This usually tends to negatively affect some of the properties of the polymer, namely Young's modulus and strain. This is due to increased plasticisation in the polymer and we observed this effect when we analysed the samples under DSC analysis. However, we shown that these negative effects can be compensated for by the introduction of dispersed carbon nanotubes into the environment. The nanotubes can be incorporated into the polymer to a greater extent than the solvent-swelling technique and the resulting composite is reinforced further. It shows better mechanical properties than the both the original polymer and the polymer which was treated under the same pressure and solvent conditions in SC-CO_2. We believe that this technique has a good potential for the fabrication of new reinforced polymer-nanotube composites.

References

[1]A.R. Berens, *Transport of Plasticizing Penetrants in Glassy Polymers*, ACS Symposium Series, American Chemical Society, **423**, 92 (1990)

[2]J. von Schnitzler, R. Eggers, *J. Supercrit. Fluids* **16**, 81 (1999)

[3]A. R. Berens, G. S. Huvard, R. W. Korsmeyer, F. W. Kunig, *J. Appl. Polym. Sci.*, **46,** 231 (1992)

[4]M. A. McHugh, V. J. Krukonis, *Supercritical Fluids Extraction: Principle and Practice*, 2nd Ed, Butterworth-Heinemann (1994)

[5]C. A. Eckert, B. L. Knutson, P. G. Debenedetti, *Nature*, **383**, 313 (1996)

[6]Y-T. Shieh, J-H. Su, G. Manivannan, P. H. C. Lee, S. P. Sawan, W. D. Spall, *J. Appl. Polym. Sc.* **59**, 695 (1996)

Chapter 6

Experimental Methods

6.1 General Procedures

All chemicals where were purchased from Sigma-Aldrich Company unless it is specifically mentioned. Very thin and thin Curly multiwall nanotubes were purchased from Nanocyl (www.nanocyl.be). Straight arc-discharge multi-walled nanotubes were provided by the Blau group, School of Physics, Trinity College Dublin. Kevlar yarn was kindly provided by du Pont. Low density polyethylene and isotactic polypropylene film were purchased from BPI Packaging Limited. Polyethylene terephthalate film was kindly provided by Dow Corning. The ultra-sonic tip used was Model CV33 with ¼ inch tip. The ultra sonic processors used were model GEX 750 or a Bandelin Sonoplus HD2200. The ultra-sonic bath used was a Grant XB6 at 50 Hz. The transmission electron microscopy (TEM) images were taken on both a Hitachi H-7000 electron microscope and a Joel 100cx electron microscope where specified. The samples were prepared by deposition and drying of a drop of the sample dispersed in ethanol onto a formvar coated 400 mesh copper grid. The scanning electron microscopy (SEM) images of the samples were obtained using a Hitachi S-4300 scanning electron microscope, which was operated from 5.0 kV to 20 kV depending on the sample used and coating required. Non-conductive samples were coated with either pure gold or gold-palladium alloy to a coating thickness of 10-15nm. Room temperature Raman spectra were measured with a Reinshaw 1000 micro-Raman system. The excitation wavelength was 633 nm from an AR^+ ion laser (Laser Physics Reliant 150 Select Multi-Line) with a typical laser power of approximately 20 mW in order to avoid excessive heating. The 100x magnifying objective of the Leica microscope was capable of focusing the beam into a spot of approximately 1 μm diameter. The thermal gravimetric analysis (TGA) was carried out on a Perkin Elmer Pyris 1 TGA machine. Samples were burned in a flowing air environment at 20 ml/min. They were burned over a temperature range from 30°C to 900°C at a rate of 10°C/min. Thermal properties and polymer morphology were studied by differential scanning calorimetry (DSC) using a Perkin Elmer Diamond DSC power compensation instrument. Scanning rate was 30 °C/min. Sedimentation studies were carried out with an assembled sedimentation apparatus consisting fundamentally of four LED's situated opposite to 4 light detectors. In the space between, a 1cm cuvette was placed containing the sample for analysis. The light detector registers the intensity of the light transmitted through the sample over a selected time range at intervals of every ten seconds. Samples were prepared firstly by ultrasonication using the Model

GEX 750 as referred to above. Samples were then sonicated for 5 minutes at 20% intensity. Immediately following this they were placed in the sedimentation apparatus for analysis. Transmission values were measured using a Cary Varian 50. Electrical measurements were carried out using a Keithley 2400 sourcemeter. IV curves were measured using a two-probe setup. The potential difference across the sample was varied from 0 V to 100 V with intervals of one volt. Mechanical measurements were carried out using different machines depending on the sample being tested. The preparation procedure, machine and software used for each particular sample type will be referred to in the text where appropriate. Experiments in supercritical carbon dioxide were carried out at National University of Ireland, Cork under supervision of Dr John O 'Callaghan. Fluorescent microscope images were taken using a Nikon Eclipse T300 in the SNIAM by Alex Rakovich (School of Physics, TCD).

6.2 Experimental methods for Chapter 2:

Kevlar Functionalised Nanotubes For Polymer Reinforcement

6.2.1 Synthesis of Kevlar

The synthesis of Kevlar was carried out according to the published procedure.[1] 1,4-phenylenediamine (1.04g, 0.0096 mol) was dissolved in a mixture of hexamethylphosphoramide (16ml) and dimethylacetamide (8ml) under a nitrogen atmosphere. This mixture was then cooled to 0 °C and terephthaloyl chloride (1.95g, 0.0096 mol) was added under stirring. The mixture turned into a thick paste and was left over night at room temperature. Buchner filtration was carried out using a polychlorotrifluoroethylene filter with a pore size of 0.45 microns over a sintered glass frit. The polymer was then washed with (2x10ml) water and then (2x10 ml) of acetone. The product was a yellow coloured powder and gave a yield of 1.58g (70 %).

IR, Raman and Decomposition point definitively match those reported in the literature[1,2,3]

FTIR (KBr, cm^{-1}): 3327(NH), 1646(s, C=O) 1299(s, C-N), 867(aromatic) 1516(s, C=C,ar)

Raman: 1182, 1277, 1323, 1507, 1571, 1613, 1650 cm^{-1}

Elemental Anal. Calc. $C_6H_6N_2O_2$: C, 70.6; H, 4.2; N, 11.8. Found: C, 62; H, 4.9; N, 11.4

TGA: Decomposition point of Kevlar, one peak at 550°C

6.2.2 Preparation of Kevlar coated nanotubes

Thin nanocyl nanotubes were functionalised with Kevlar according to the following manner. Nanocyl nanotubes (0.2g) were added with Kevlar (0.6g) in a mixture of nitric acid (70ml) and sulphuric acid (20ml) and sonicated in the sonic bath for 30 minutes to enable good separation and dispersion of the nanotubes. The vessel was then refluxed for 12 hours at 100°C. Samples were extracted from the reaction vessel after 1, 2, 4, 6 and ultimately 12 hours of reaction. Each extraction was allowed to cool to room temperature and any excess acid was decanted. The remaining solution was then slowly neutralised by the addition of $NaHCO_3$ in water. After the neutralisation process, the solution was allowed to settle overnight before the excess water was decanted off. This was followed by three further additions of water and decantations. The Kevlar functionalised nanotubes (FNTs) were filtered by Buchner filtration using a teflon filter with a pore size of 0.45 μm and then washed first with water (2x10ml) and then with acetone (2x10ml).

Pure Nanotubes:

FTIR: 1323, 1576, 1603 cm^{-1}

Raman: 1335, 1590 cm^{-1}

TGA: 1 peak 605 °C

2 hour FNTs:

FTIR: 740, 783, 910, 1124, 1245, 1290, 1354, 1418, 1534, 1696, 2534, 2556, 2665, 2832, 3083 cm^{-1}

Raman: 1265, 1335, 1372, 1502, 1532 1582, 1613 cm^{-1}

TGA: 2 peaks 532, 556 °C

4 hour FNTs:

Raman: 1180, 1263, 1277, 1303, 1356, 1372, 1502, 1549, 1579, 1617, 1645 cm^{-1}

FTIR: 709, 722, 779, 813, 896, 1016, 1111, 1244, 1499, 1548, 1656, 2164, 3218 cm^{-1}

TGA: 3 peaks 314, 458 (shoulder), 515 °C

6 hour FNTs:

Raman: 1179, 1257, 1277, 1303, 1355, 1372, 1500, 1550, 1577, 1616, 1644 cm^{-1}

FTIR: 779, 812, 1242, 1499, 1659, 2980 cm^{-1}

TGA: 3 peaks 314, 468, 500 °C

12 hour FNTs:

FTIR: 1985, 2052, 2345 cm^{-1}

Raman: 1323, 1576, 1603 cm^{-1}

TGA: 2 Peaks: 314, 500 °C

6.2.3 Sedimentation studies

Nanotubes (1 mg) were dispersed in 10 ml of solvent, and sonicated under the sonic tip for 5 minutes. From this solution a 1 cm^3 cuvette was filled immediately after sonication. The cuvette was sealed with a cap and the cap was further sealed with para-film™ taking care not to obscure where the light emitters would transmit through. This was then immediately placed in the sedimentation machine until the sedimentation occurred. The light emitted every 10 second for the first hour and then this was changed to once every 30 sec for the remaining time.

6.2.4 Preparation of polystyrene films

Pure polystyrene pellets (300 mg, M_w 230,000) were dissolved in NMP (10ml) under ultrasound using the ultrasonic tip for 10 minutes. 3.8ml was of the solution was extracted and drop cast onto a glass rectangular slide with the dimension's 2.5 cm x 7.5 cm. The film was left for 48 hours in a vacuum oven at 60°C to evaporate off the solvent completely. Then the polymer film was removed from the surface of the glass slide.

Different nanotube concentrations of polystyrene composite films were prepared by first dispersing nanotubes of different concentrations in NMP to which the polymer was then added. Nanotubes (12 mg) were dispersed in NMP (20ml) using the ultrasonic tip for 10 minutes. 10mls of this mixture was extracted to create the first solution and the remaining 10ml was diluted with a further 10ml of NMP, halving its concentration.

This process was repeated four further times to create six solutions of different concentrations in total. 300 mg of polystyrene was slowly added to each mixture and dissolved by sonicating for a further 10 mins. This created mixtures where the percentage of nanotubes to polymer was 2%, 1%, 0.5%, 0.25%, 0.125%, 0.0625%. 3.8ml of these dispersion solutions was extracted and drop cast onto the glass slide

The procedure was repeated to create the functionalised polystyrene nanotube composite films where the functionalised nanotubes were heated under reflux for the 2, 4 and 6 hour.

6.2.5 Preparation of polyvinyl chloride films

Pure PVC pellets (300 mg, M_w 233,000) were added to NMP (20 ml) and polymer-nanotube composite films were prepared analogously to the procedure used in **6.2.4**.
All PVC films were stored under the same conditions.

6.2.6 Preparation of polyvinyl alcohol films

Pure PVA pellets (300 mg, M_w 72,000) were added to NMP (20ml) and composite films were prepared analogously to the procedure used in **6.2.4** with the exception that films were prepared with the 2 hr refluxed FNTs only.

All PVA films were stored under the same conditions at 4°C immediately following preparation to minimise moisture absorption affects.

6.2.7 Preparation of polyvinyl acetate films

Pure PVAc pellets (300 mg, M_w 140,000) were added to NMP (20ml) and polymer composite films were prepared analogously to the procedure used in **6.2.4** with the exception that films were prepared with the 2 hr refluxed FNTs only.

6.2.8 Mechanical testing of prepared polymer films

Tensile testing was carried out on all films described in preparations **6.2.4** to **6.2.7** using a Zwick Z100 tensile tester in the Biomechanical Engineering Department of the National University of Ireland Galway University Testing. The machine was equipped with a load cell of 100 N, jaw spacing of 15 mm and operated with a strain rate of 15

mm/min. The polymer was cut into strips on a cutting tool, which cut five strips of equal width of 2.4 mm at a time. The thickness of each strip was measured before the strip was placed into the Zwick machine for mechanical testing. The measurements for width and thickness were inputted into the machine. The machine then stretched the sample under tension until the sample broke. The process was repeated approximately five times for each film so average mechanical properties could be measured.

6.3 Experimental methods for Chapter 3

Carbon Nanotube-Kevlar Composites

6.3.1 Sedimentation studies of nanotubes

Sedimentation studies of carbon nanotube dispersions in THF, DMF and NMP were carried out analogously to those studied in **6.2.3**.

6.3.2 Preparation of Kevlar-nanotube composite fibres with varying time

Thin nanocyl MWNTs (60 mg) were added to NMP (100 ml). This mixture was treated using the ultrasonic tip for a period of 10 minutes to create a dispersion of the nanotubes. The dispersion was then placed in the sonic bath for a further 2 hours. Kevlar 129 yarn was cut into strips 1m long and each end was tied. The fibre was then weighed and its length was measured accurately before being put into a round bottom flask containing the nanotube dispersion. The mixture was sonicated for periods ranging from 5 minutes to 4 hours. Kevlar fibres were removed from the solution and washed by sonication in ethanol (100 ml) for 30 seconds. This was repeated in a second bath of ethanol. They were then washed again in ethanol without sonication to remove any residual NMP. They were then straightened and allowed to dry in a vacuum oven at 50 ^{o}C for one week to remove any residual ethanol. Following this the Kevlar fibres were weighed again and a net weight change was calculated.

6.3.3 Preparation of Kevlar–nanotube composite fibres with varying concentration

Thin nanocyl MWNTs (360 mg) were added to NMP (100 ml). This mixture was placed under sonic tip for a period of 10 minutes to create a dispersion of the nanotubes. The dispersion was place in the sonic bath for a further 2 hours. The dispersion was

diluted with a further 100 ml of NMP and 100 ml of the combined dispersion was extracted to create the first concentration of nanotubes (1.8 mg/ml). The remaining 100ml was diluted again and this procedure was repeated to create nanotube dispersions of 1.5 mg/ml, 1.2 mg/ml, 0.9 mg/ml, 0.6 mg/ml, 0.3 mg/ml and 0.15 mg/ml. Kevlar 129 was cut into strips 1m long and each end was tied. The fibre was then weighed and its length was measured accurately before being placed into a round bottom flask containing one the nanotube dispersions. The mixture was sonicated in the sonic bath for a period of 30 minutes. This was repeated for each separate concentration. To obtain an average mass uptake, the experiment was repeated for 5 seperate bulk fibres.

Kevlar fibres were removed from the solution and washed as described in **6.2.1**. They were again straightened and allowed to dry in a vacuum oven at 50°C for one week to remove any residual ethanol. The Kevlar fibres were weighed again and a net weight change was calculated.

6.3.4 Mechanical testing of bulk Kevlar yarn

Mechanical testing of the bulk Kevlar yarn was carried out in the School of Engineering in Trinity College Dublin on an Instron 8501, 50 KN/Servo-hydrolic fatigue testing machine. Software was Instron Series IX tensile testing. Grips used were Instron wire testing grips. Jaw spacing was set at 60 mm and the speed was 25mm/min. The fibre was cut into sections of 1 metre in length. The sample was stretched under tension until broken. The process was repeated three times for each sample enabling to calculate average values of mechanical parameters.

6.3.5 Mechanical testing of individual Kevlar fibres at low loading rate

Mechanical testing of single Kevlar fibre samples at low loading rate was carried out in Materials Ireland laboratory, Trinity College Dublin. Individual samples were loaded into a Diamond DMTA machine from Perkin Elmer with jaw spacing set at 5mm and strain rate of 50μm/min. Software used was Muse Measurement, Version 3.4 U (Build 666) © SII Nanotechnology Inc. 1989-2003. Sample was stretched under tension until broken. The process was repeated 10 times for each sample enabling average mechanical properties to be measured.

6.3.6 Mechanical testing of individual Kevlar fibres at high loading rate

Mechanical testing of single Kevlar fibre samples at high loading rate was carried out in School of Physics, Trinity College Dublin. Individual samples were loaded into a Zwick 100 with Jaw spacing at 15 mm and strain rate of 25 mm/min. Software used was Zwick testXpert (II). Sample was stretched under tension until broken. The process was repeated 10 times for each sample enabling average mechanical parameters to be calculated.

6.4 Experimental methods for Chapter 4:

Investigation of the Electrical Properties and Optical Transmittance of Polymer-Nanotube Composites

6.4.1 Preparation of nanocyl MWNT nanotube dispersions

Samples of nanocyl very thin MWNTs were added to THF (10ml), Toluene (10ml) or NMP (10ml) where specified, according to the concentrations of the solutions of 4mg/ml, 2mg/ml, 1mg/ml, 0.5mg/ml, 0.25mg/ml, 0.125mg/ml, 0.0625mg/ml and 0.03125mg/ml of nanotubes. Sample was placed under ultrasound using the ultrasonic tip for 10 minutes. Sample was then sonicated using the ultrasonic bath for 2 hours.

6.4.2 Preparation of MWNT-polypropylene composite films

Nanotube-polypropylene composite films were prepared using our developed technique of swelling polymer film under ultrasound in carbon nanotube suspension. Polypropylene strips of uniform size were cut and placed in nanotube suspensions in THF, Toluene and NMP as prepared in procedure **6.4.1**. Contol experiments were run on films immersed in the pure solvents. This was sonicated for 5 minutes with a 1 second pulse (1s delay between pulses) and power regulated at 20% (of 750W) using the ultrasonic tip. Immediately following this, the sample tube was transferred into a sonic bath where it remained under ultrasound for 30 minutes. After treatment, each nanotube-polyethylene film was washed with ethanol in a sonic bath for 30 seconds. The nanotube-polyethylene composite films were then dried under vacuum at 40°C for 48 hours to ensure all traces of solvent had evaporated. Samples were then cut into strips of known width, length and thickness.

6.4.3 Preparation of MWNT-polyethylene terephthalate films

Nanotube-polyethylene composite films were prepared analogously to the preparation method for polypropylene films described in procedure **6.4.2**. Nanotube dispersion concentrations in solvents used were 4mg/ml, 2mg/ml, 1mg/ml and 0.5mg/ml in THF, Toluene and NMP as prepared in procedure **6.4.1**

6.4.4 Preparation of MWNT-polyethylene films

MWNT-polyethylene composite films were prepared analogously to the preparation method for polypropylene films described in procedure **6.4.2**. Nanotube dispersion concentrations in solvents used were 4mg/ml, 2mg/ml, 1mg/ml, 0.5mg/ml, 0.25mg/ml, 0.125mg/ml, 0.0625mg/ml and 0.03125mg/ml in THF, Toluene and NMP as prepared in procedure **6.4.1**

6.4.5 Polyethylene composite film treatment using sulphuric/nitric acid

Polyethylene film prepared in the 2mg/ml concentration of THF as described in procedure **6.4.4** were immersed in a 4:1 Nitric (67%, 80ml) : Sulphuric (95%, 20ml) acid mixture for time periods of 1, 2, 5, 10, 20, 30 and 60 minutes.
After each immersion, sample was removed, washed in water and dried in the fan oven at 30 ^{o}C for 1 hour. Conductivity measurements were made initially and following each successive treatment.

6.4.6 Polyethylene composite film treatment using hydrochloric acid

Polyethylene film prepared in the 2mg/ml concentration of THF as described in procedure **6.4.4** was immersed in a Hydrochloric acid (35%, 100 ml) for time periods of 1, 2, 5, 10, 20, 30 and 60 minutes. A separate film was also immersed in Hydrochloric acid (37%) for the same time periods.
After each immersion sample was treated by the same post formation treatment as described in **6.4.5**. Conductivity measurements were made initially and following each successive treatment.

6.4.7 Polyethylene composite film treatment using gold solution

An aqueous gold solution was made from HAuCl4.3H2O, (0.03 M) which provides a source of Au^{3+} ions. The highest conductivity polyethylene film prepared in the 2 mg/ml concentration as described in procedure **6.4.4** was immersed in the solution for period of 1, 2, 5, 10, 20, 30 and 60 minutes. After each immersion sample was treated by the same post formation treatment as described in **6.4.5**. Conductivity measurements were made initially and following each successive treatment.

6.4.8 Polyethylene film treatment using silver solution

An aqueous silver nitrate solution was made from $AgNO_3$ (0.03 M) which provides a source of Ag^+ ions. The highest conductivity polyethylene film prepared in the 2 mg/ml concentration as described in procedure **6.4.4** was immersed in the solution for period of 1, 2, 5, 10, 20, 30 and 60 minutes. After each immersion sample was treated by the same post formation treatment as described in **6.4.5**. Conductivity measurements were made initially and following each successive treatment.

6.4.9 Preparation of Hipco SWNT nanotube dispersions

Samples of Hipco SWNTs were added to THF (10ml) according to the concentrations of the solutions of 1mg/ml, 0.5mg/ml, 0.25mg/ml, 0.125mg/ml, 0.0625mg/ml and 0.03125mg/ml of nanotubes. Sample was placed under ultrasound using the ultrasonic tip for 10 minutes. Sample was then sonicated using the ultrasonic bath for 2 hours.

6.4.10 Preparation of Hipco SWNT-polyethylene composite films

Hipco SWNT-polyethylene composite films were prepared analogously to the preparation method for polypropylene films described in procedure **6.4.2** with the exception that the nanotube dispersions used are those which were described in procedure **6.4.9**.

6.5 Experimental methods for Chapter 5

Investigation of Mechanical Properties of Nanotube-Polymer Composites

6.5.1 Preparation of polyethylene films with supercritical CO_2

Samples were placed into a 50-ml stainless steel cell heated to 50 °C and pressurized with CO_2 to the desired pressure using a 260 ml Isco syringe pump (Lincoln, NE). The pressures used were varied from 34.5 to 48.2 MPa. The system was left to stand for 4 hrs before sample immersion. Carbon nanotubes (2 mg) were dispersed in NMP (20 ml) in the ultrasonic bath for 1 hour. This dispersion was placed in the stainless steel cell. Polyethylene film was suspended at the opposite end of the cell. Cell was sealed and pressure was applied. Cell was immersed in a thermally regulated water bath at 50 °C under pressure for 4 hours. Following this cell was inverted to allow film interaction with solvent dispersion. Cell was immersed in the bath for a further 2 hours. Sample was removed and washed twice with ethanol in the ultrasonic bath for 20 seconds.

6.5.2 Mechanical testing of PE and PET films

Tensile testing was carried out on all films described in preparations **6.4.3**, **6.4.4** and **6.5.1** using a Zwick Z100 tensile tester in the School of Physics in Trinity College Dublin. The machine was equipped with a load cell of 100N, jaw spacing of 15mm and operated with a strain rate of 15 mm/min. The polymer was cut into strips on a cutting tool, which cut five strips of equal width of 2.4mm at a time. The thickness of each strip was measured before the strip was placed into the Zwick machine for mechanical testing. The measurements for width and thickness were inputted into the machine. The machine then stretched the sample under tension until the sample broke.

The process was repeated approximately five times for each film so average values of mechanical parameters could be calculated.

6.6 Experimental methods for Chapter 7:

Conclusions and Future Outlook

6.6.1 Investigation of the interaction between carbon nanotubes and NMP

Carbon nanotubes (10 mg) were dispersed in NMP (10ml). Sample was sonicated for 4 hours in sonic bath. Solvent was removed by evaporation for 1 week in vacuum oven.
TGA: Decomposition Peak 320, 655 °C

6.6.2 Preliminary investigation of interaction between C_{60} and NMP

C_{60} (10 mg, 1 mg) was added to NMP (10ml). Sample was sonicated in the sonic bath for 10 minutes. During this time the solvent visually changed from clear with a black sediment to dark brown throughout with no sediment. Yield: 1.37 mg.

TGA: 2 peaks 340, 569 °C
C^{13}NMR: 178.1, 139.9, 59.6, 57.3, 29.1, 27.6, 23.4, 17.7
MS EI (m/z): 200, 201, 213, 219, 301, 345, 361, 487, 556, 578, 721
Elemental Anal Calc C_{60}: C, 100; Found C, 60.25; H, 4.51; N, 3.11.

6.6.3 Preparation of polyethylene quantum dot composite

Cadmium telluride quantum dots (1 x 10^{-2} mol, 10 mg) were dispersed in tetrahydrofuran (10 ml) using ultrasonication with the sonic tip. Polyethlene film was suspended in the dispersion and sonicated using the sonic bath for 30 minutes. The film was then removed and washed with ethanol in a sonic bath for 30 seconds. The nanotube-polyethylene composite films were then dried under vacuum at 40 °C for 48 hours to ensure all traces of solvent had evaporated.

6.6.4 Preparation of polyethylene terephthalate quantum dot composite

Cadmium telluride quantum dots (1 x 10^{-2} mol, 10 mg) were dispersed in tetrahydrofuran using ultrasonication with the sonic tip. Polyethlene Terephthalate film was and underwent the same treatment as Polyethylene film in, washing and drying as in **6.6.3**.

6.6.5 Preparation of supercritical CO_2 swelled Kevlar fibre

Samples were prepared analogously to the procedure described in **6.5.1** with the exception that Kevlar fibre was used in the place of polyethylene film. Two separate fibres were placed in the cell for 2 hours and 24 hours respectively.

6.6.6 Mechanical testing of supercritical CO_2 swelled Kevlar

Mechanical testing of individual SC-CO_2 swelled Kevlar fibres was carried out analogously to the fibres tested in **6.3.5**.

References

[1]B. Jingsheng, Y. Anji, Z.S. Quing, Z. Shufan, H. Chang, *J. Appl. Polym. Sci.*, **26**, 1211 (1981)

[2]K. E. Perepelkin, I. V. Andreeva, E. A. Pakshver, I. Yu. Morgoeva *Fibre Chemistry* **35**, 265 (2003)

[3]Prasad, D. T. Grubb *J. App. Poly. Sci.* **41**, 2189 (2003)

Chapter 7

Conclusions and Future Outlook

7.1 Conclusions

The area of research into carbon nanotubes is a very dynamic field. New discoveries in nanotube physics and chemistry are by now very common and have helped nanotechnology become a common term not just in science but in the general world. Carbon nanotube research itself has shifted away from purely their investigation and manipulation to more applicable areas in the hope that their theoretically amazing potential can be utilized in the everyday world. In this work we have developed new approaches to the development of materials, which should contribute to the further growth of the area of carbon nanotube composites.

For the first time we have developed new Kevlar coated nanotubes which were analysed by a variety of methods including SEM and Raman spectroscopy, which showed dramatic changes in the physical and chemical properties of the nanotubes. Sedimentation analysis also showed that the nanotubes were better stabilised with increasing functionalisation. The length of reflux time defined the appearance of the nanotubes with the two hour reflux achieving an average increase in thickness of approximately 200%. This was replicated in the 4 hour sample but ultimately over the longest time period of 12 hours the Kevlar and nanotubes were decomposed resulting in reduced size and considerable destruction of their structure. We have demonstrated that we could achieve functionalisation with a well-known and extensively studied high strength polymer with intent to specifically target composite mechanical enhancement. This inevitably led to the creation of polymer composites to compare and contrast their mechanical properties, not just with the pure polymer but also with pristine nanotube composites also. Initially we analysed different time refluxed polymers to see if the reflux time had any effect on the nanotubes performance. It was evident from the polystyrene and polyvinyl chloride measurements that the different reflux times had little or no effect on the functionalised nanotubes performance. We did however see quite a dramatic effect from the functionalised nanotubes over their pristine counterparts with enhancements of 50% on strength against just 20% respectively in the PVC composites. Similar but not so dramatic improvements were found in the polystyrene composites where the functionalised nanotube composites again outperformed their pristine counterparts. We again found that the time of reflux did not have show any increased improvement so it was decided to focus on the functionalised

nanotubes which showed the best enhancement and try and expand it to other polymers to see if the enhancement would be universally adaptable or more polymer specific. Therefore we expanded our study to include polyvinyl alcohol and polyvinyl acetate and found that both the functionalised nanotubes and the pristine nanotubes had a negative impact on the mechanical properties of the polyvinyl alcohol, indicating considerable disruption of its matrix. PVA has a well renowned dependence on hydrogen bonding to maintain its molecular stability and strength and this was no doubt disrupted by the nanotubes. Our analysis of PVAc however, again showed increases for the composite prepared with pristine nanotubes and these were again enhanced further with the functionalised nanotubes exhibiting their adaptability.

A second approach for the development of carbon nanotube-polymer composites involved the integration of dispersed carbon nanotubes into a solvent-swollen polymer. Kevlar has long been considered one of the most significant advancements in the field of high strength polymers. It was discovered more than 40 years ago but to this day is still considered the yardstick to which other high strength polymers are compared. Considerable obstacles had to be overcome to prepare Kevlar nanotube composites. These included the insolubility of Kevlar, the inability to separate nanotubes and the limited investigation that had previously been associated with the topic in the literature. This restricted composite formation by more traditional methods. Although Kevlar is quite insoluble much research had been done into its swelling capabilities in certain solvents. Sedimentation investigations also showed that nanotubes were particularly dispersible in NMP, a solvent which was capable of swelling Kevlar. It was anticipated that if we could combine the nanotubes and Kevlar in an NMP environment we could achieve nanotube penetration into the polymer *via* polymer swelling and nanotube dispersion. This was achieved through ultrasonication and dispersion of nanotubes in NMP followed by immersion of the Kevlar with further sonication to achieve adequate swelling. Upon SEM analysis of the finished product we found that we had indeed accomplished this feat. Further analysis by TGA and mass uptake confirmed that the nanotube uptake of the Kevlar was concentration dependent.

Mechanical measurements of the composite samples revealed considerable increases in the strength and toughness of the samples. From these measurements and theoretical calculations we could ascertain that we had achieved a good interfacial stress transfer between the nanotube and the polymer. At the higher loadings however, we found that

the nanotubes had a detrimental impact on the mechanical properties of the fibres indicating that there was some possible aggregation of nanotubes and disruption of the polymer structure. We have also demonstrated that our new method of fabricating nanotube-Kevlar composites could be expanded for the fabrication of other polymer composites.

For this reason it was decided to try and expand the technique to other polymers with more significance to their electrical conductivity applications, including the development of transparent conductive electrodes. The polymers used were polypropylene, polyethylene and polyethylene terephthalate.

Each of the polymers were treated with varying concentrations of nanotubes in three different solvents; NMP, chosen for its ability to disperse nanotubes, toulene and THF chosen for their good theoretical swelling abilities. Analysis of polypropylene found little evidence of penetration of the nanotubes into the polymer matrix with any of the solvents, indicating a lack of solvent swelling ability. Corresponding conductivity measurements were predictably low with increases in the region of only 1 order of magnitude and the polymer remained highly insulating. The NMP swelled polyethylene terepthalate sample also remained highly insulating and following analysis of the THF and Toluene swelled samples this indicated that swelling capability was much more important than nanotube dispersive capability of the solvent. Polyethylene terephthalate penetration appeared much more extensive with the THF and Toluene samples with infiltration of the nanotubes into the polymer to a depth of over six microns. The infiltration wasn't homogeneous however. The conductivity was substantially enhanced when compared to the pristine polymer and showed an increase of almost 5 orders of magnitude. The polyethylene samples showed even more substantial increases in conductivity and the sample swelled in THF in particular demonstrated consistent and relatively uniform penetration into the polymer. We have also carried out systematic, quantitative analysis of the samples swelled in each of the different concentrations of nanotubes dispersed in THF.

Scanning electron microscopy showed that the penetration depth was independent of concentration of the nanotubes in the THF. Transmission measurements, however, showed that the concentration of nanotubes in the composite layer was dependent on the concentration of nanotubes in the solvent. Using the transmission of nanotubes in

the solvent as a control we were able to work out the approximate mass fraction of nanotubes in the polymer as a whole. It was revealed from these measurements that we could achieve high conductivity (66 S/m) whilst retaining high transparency (79 %). Chemical modification of the composite by both acid treatment and by metal treatment of the nanotubes *in situ* resulted in some enhancement of the conductivity without a corresponding reduction in transparency. Hipco SWNT incorporation was also achieved with THF and polyethylene as the SWNTs were shown to have better conductivity. This resulted in similar conductivities to the MWNTs however comprehensive analysis could not be carried out due to the smaller size of the SWNTs.

We showed that mechanical properties of these polymers can be enhanced as well, with the strength of polyethylene swelled in THF increasing by up to 45% and Young's modulus of the samples increasing by over 60 %. This shows that our swelling method can be adapted to a variety of different polymers resulting in a considerable increase in conductivity and mechanical enhancement of the polymer in question. We have demonstrated that it can be tailored for different polymers and different types of nanotubes.

We finally presented a variation in the swelling technique utilising the effect of supercritical carbon dioxide to swell the polymer in the presence of nanotubes. We achieved good penetration of nanotubes and enhanced mechanical properties of the composite. This demonstrates that our swelling technique can also utilise supercritical fluids to fabricate new nanotube-polymer composites.

We believe that the swelling-under-ultrasound technique developed in this project has several competitive advantages. So far all existing approaches to the fabrication of nanotube-polymer composites involve complicated, expensive, time- demanding processing techniques such as solution casting, melting, moulding, extrusion, and in situ polymerisation. In addition all these technologies need large amounts of expensive carbon nanotubes to be used. In all of these techniques nanotubes must either be incorporated into a polymer solution, molten polymer or mixed with the initial monomer before the formation of the final product (e.g. yarn, ribbon, film, etc.). Our technology is different because it enables the incorporation of nanotubes into already formed polymer products by swelling in carbon nanotube suspension. Therefore, only a very small percentage (~1%) of nanotubes is needed to produce reinforced polymer

composites with potentially high electrical and thermal surface conductivity. Also the bulk of the nanotubes are incorporated only in a very thin (several hundreds of nm) polymer layer. As result our polymer composite materials are expected to be cheaper (require minimal amount of carbon nanotubes), light, mechanically strong (having an increased tensile strength and Young modulus), robust, easy to process, have high electrical conductivity and easy to integrate. We think that this approach can also be extended for other nanomaterials (various nanoparticles, nanowires etc.) This should open new opportunities in the fabrication of novel polymer composite materials with multitude applications.

7.2 Future Outlook

Many aspects of this project have a clear potential for further development. Future studies on functionalised nanotube composites could involve a variation on many of the parameters used in this work, changing the types of nanotubes used or their polymer functionality. The technique could be expanded to include many more polymers, which in turn may have a greater interaction with the nanotubes creating much stronger materials.

For the polymer swelling technique the potential is immeasurable, again we can develop stronger materials by our method which can be employed on a preformed polymer. We can also control the amount of nanomaterial the final composite can contain. If more research can be done into the subject we can explore the most adequate solvent for swelling of a specific polymer. This work has also shown that we can increase the conductivity of a polymer by almost nine orders of magnitude; further research into the subject may yet yield even higher conductivities. We are currently three orders of magnitude away from the most conductive materials known, gold and silver. Further exploration of the type of nanotube used, or even other nanomaterials like gold or silver nanorods may help us bridge this gap.

We have also performed some preliminary studies, which showed some interesting results and potential for further research. Some of these aspects are discussed below.

7.2.1 Interaction of nanotubes and NMP

When analysing the TGA of a nanotube sample after having been in contact with NMP we discovered a slight shift in the decomposition temperature and the formation of a second derivative peak. No change was observed in nanotubes immersed in any other solvent. This led us to speculate that the NMP might be chemically affecting the nanotubes in some way.

The nanotubes were immersed in NMP and sonicated for 4 hours. They were then filtered, using a Teflon filter, and dried. A TGA curve was obtained and compared to a curve of pure nanotubes (**Figure 7.1**). It was expected that if no effect occurred it should give the same decomposition temperature for the nanotubes. When we look at the TGA curve of the nanotubes that have been interacted with NMP we see it has changed quite dramatically. We see a decrease in mass at an earlier point but overall it takes longer to decrease to the minimum.

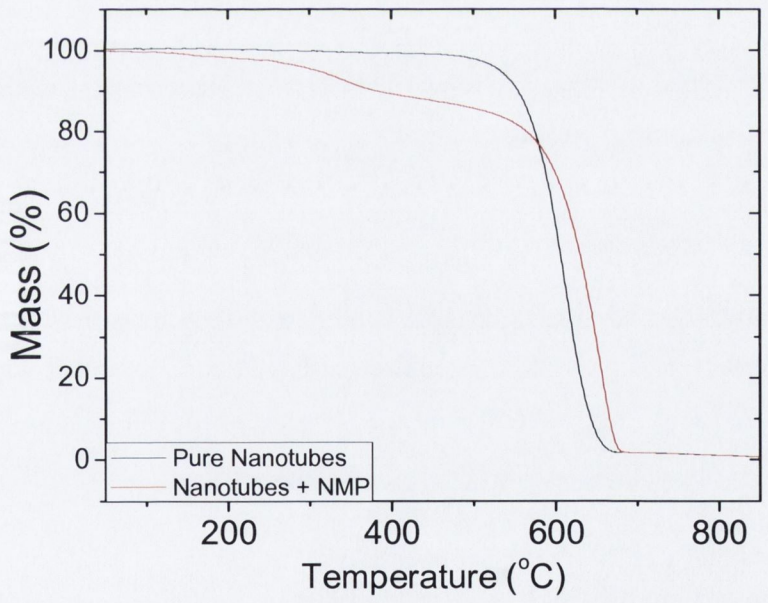

Figure 7.1 TGA curves for pure nanotubes (black line) and nanotubes after sonication in NMP (red line)

We then analysed the derivative of the curves and we find that we can see that the pure nanotubes decompose at approximately 605°C. When we looked at the nanotubes after

dispersion in NMP we noticed that the peak has in fact shifted upwards to 655°C. There is also a small peak at 320°C, indicating that we have a secondary product in the sample. (**Figure 7.2**)

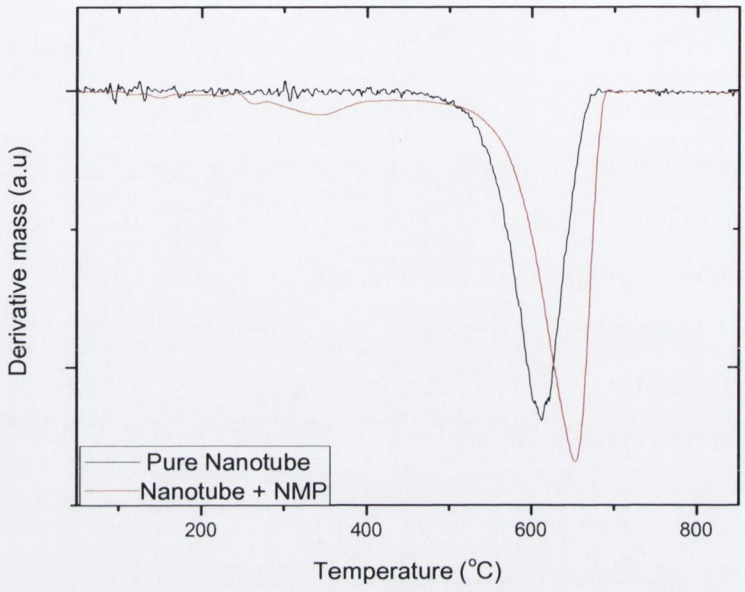

Figure 7.2 Derivative of the TGA curves for pure nanotubes (black line) and nanotubes after sonication in NMP (red line)

It was decided to run preliminary investigations on whether NMP may have an effect on nanotubes. Ultimately, due to their very low solubility and as there was no noticeable difference in any other testing on the nanotubes that have been in contact with NMP. In our future work we would like to continue our studies on the interactions of carbon nanotubes with NMP as well as with other similar type solvents.

7.2.2 Interaction of C_{60} and NMP

It was also decided to investigate whether NMP would have any interaction with C_{60}. C_{60} is a similar structure to nanotubes in that it has an sp^2 hybridised structure and it was felt that having a similar surface morphology and chemistry to nanotubes, it would be a good representation of any possible reactions which may occur between NMP and nanotubes.

Two separate experiments were run. In the first a 0.1g/L dispersion of C_{60} in NMP was made up and placed under sonication for 10 minutes in the sonic bath. In the second we used a concentration of 1 g/L. C_{60} is generally not very soluble but it does dissolve somewhat in solvents like toluene, benzene and other analogous aromatics. These solutions are generally clear and pink/purple in colour. When we mixed C_{60} with NMP however we found that both solutions turned dark brown and opaque. Visually we see the C_{60} change from a black powder to a dark brown film on the surface of the evaporating dish (**Figure 7.3**). We ran control experiments of C_{60} dispersed in ethanol, toluene and DMF which gave no change in appearance.

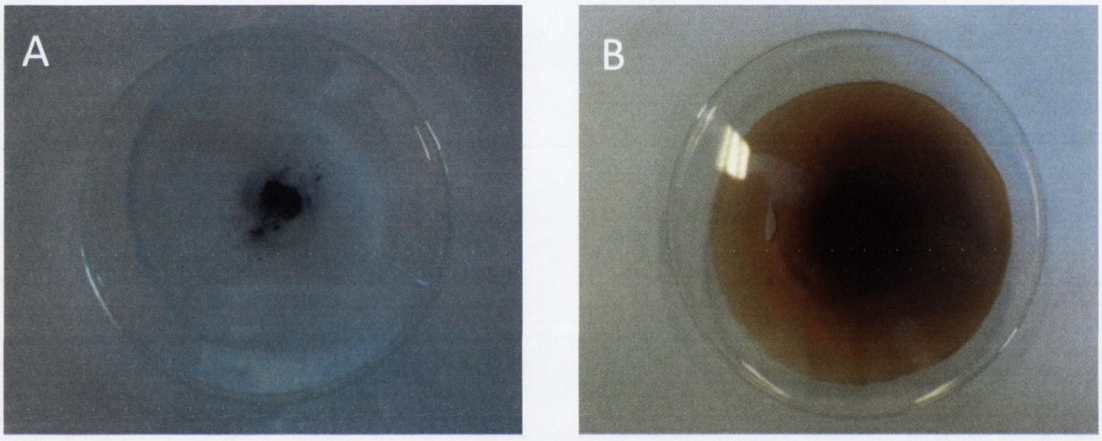

Figure 7.3 Visual changes in colour and physical appearance of C_{60} represented by pure C_{60} powder (**A**) and C_{60} after treatment in NMP (**B**) on a glass evaporating dish

Following this it was found that the low concentration sample of C_{60} in NMP was soluble in a variety of solvents however the sample from the high concentration was insoluble in all solvents tried including polar solvents like water and non-polar solvents like hexane. This was very interesting but led to an inability to examine the high concentration by conventional methods. Therefore it was decided to focus on the low concentration water-soluble product.

When compare the product to pure C_{60} using elemental analysis (**Table 7.1**) we find that the content of carbon in the product has decreased considerably with the content of nitrogen and hydrogen increasing. This method is unable to obtain the mass of oxygen

however it indicates there is probably a considerable amount contained in the sample as there are no other elements available for reaction. There is a 35% increase in mass of the sample from the treatment.

Table 7.1 Elemental analysis data for pure C_{60} and C_{60} product after treatment with NMP

	Mass of Carbon (%)	Mass of Hydrogen (%)	Mass of Nitrogen (%)	Mass of Other Elements(%)	Total (%)
Pure C_{60}	99.73	0.21	0	0.06	100
Product	60.25	4.51	3.11	32.13	100

When we analyse the samples using TGA (**Figure 7.4**) we find that there has been a significant shifting of the peaks and the formation of a second peak in the product. This is similar to the TGA of the nanotubes where a second peak also forms.

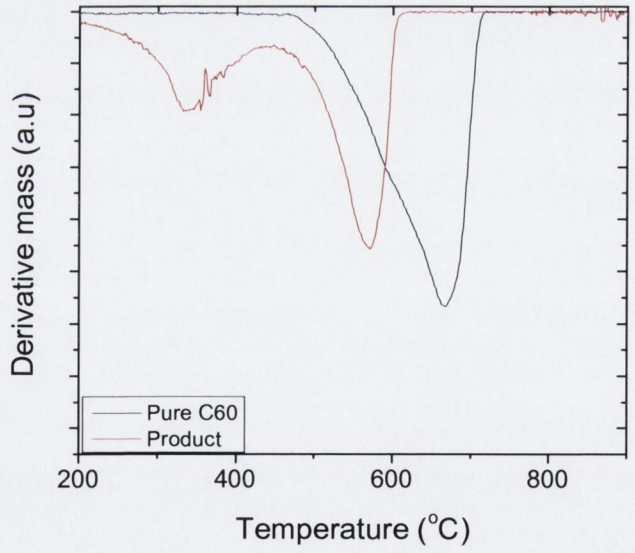

Figure 7.4 TGA curves for pure C60 (black line) and C60 after treatment with NMP (red line)

Raman spectroscopy shows the characteristic peaks from the C_{60} molecule have disappeared and the spectrum remains flat for the product, indicating a loss of structure in the C_{60} molecule (**Figure 7.5**).

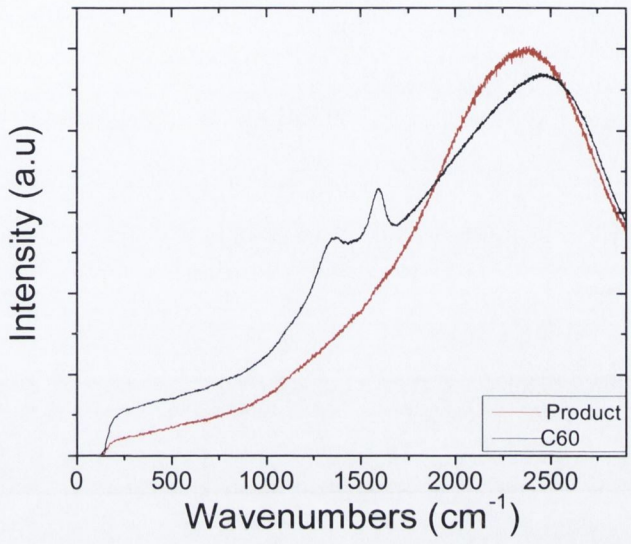

Figure 7.5 Raman Spectroscopy of pure C_{60} (black line) and the product (red line)

NMR and mass spectroscopy studies showed considerable differences in the product. Whereas C_{60} examined by ^{13}CNMR shows just one peak as all carbons are in the same chemical environment, the product shows an array of peaks, only four of which show up in the pure NMP and one corresponding to C_{60}. This dramatic change in the NMR indicates considerable destruction of the structure of the fullerene molecule, and this is confirmed when we look at the mass spectroscopy which also has a large amount of peaks.

In the future we plan to investigate all these processes in details in order to understand and explain the nature of the structure and properties of new fullerene adducts.

7.2.3 Polyethylene film swelling with quantum dots

It was decided to explore the possibility of expanding the swelling technique to see if it could be used to incorporate other nanomaterials. Cystein capped Cadmium Telluride quantum dots (CdTe QDs) were chosen for their similar size offering good penetration potential and optical fluorescence capabilities enabling uncomplicated study. Polyethylene film was placed in a dispersion of CdTe QDs in THF and sonicated for 5 minutes under the sonic tip and half an hour in the sonic bath. This is the same

treatment that we utilized in the preparation of PE films with nanotube solutions. The QDs size was in the range 5-6 nm and it was expected that they could be incorporated into the polymer film in a similar manner to the nanotubes. When we look at the cross section (**Figure 7.6, A**) we can see penetration of the QDs into the polymer matrix, however we see penetration only to a shallow depth into the polymer. This is similar to what we were seeing in the SEM from the nanotubes samples where penetration occurred only to a depth of about 250 μm. When we look at the surfaces of the polymer (**Figure 7.6, B** and **C**) we find that they display quite similar surfaces with the quantum dots showing some aggregation and a lack of homogeneity.

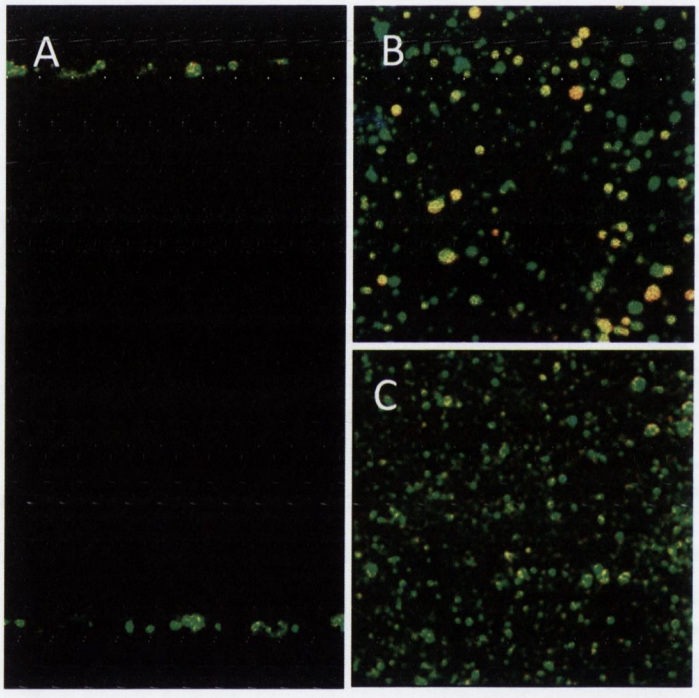

Figure 7.6 Fluorescence imaging of the cross sectional (**A**), top (**B**) and bottom (**C**) surfaces of polyethylene film after swelling treatment with Quantum dots dispersed in THF

7.2.4 Polyethylene terephthalate film swelling with quantum dots

Polyethylene terephthalate film was then suspended in another dispersion of Cadmium Telluride quantum dots in THF and sonicated for 5 minutes under the sonic tip and half an hour in the sonic bath. When we look at the cross section (**Figure 7.7 A**) we see

penetration to a considerable depth into the polymer. This is a much deeper penetration than we saw for the polyethylene but is more expected as we saw deeper penetration from the PET samples swelled in nanotube dispersions. Also we can see that one side of the polymer displays a much better ability to allow penetration than the other. This may however be due to any one of a number of factors. Firstly the polymer surfaces may not have the same nanostructure, secondly the sonic bath may not display the same homogeneity throughout. Overall though it helps explain the visual differences we found in the nanotube composite samples. When we look at the surfaces of the polymer (**Figure 7.7 B** and **C**) we find that they display considerably surfaces with the quantum dots again showing some aggregation and a lack of homogeneity.

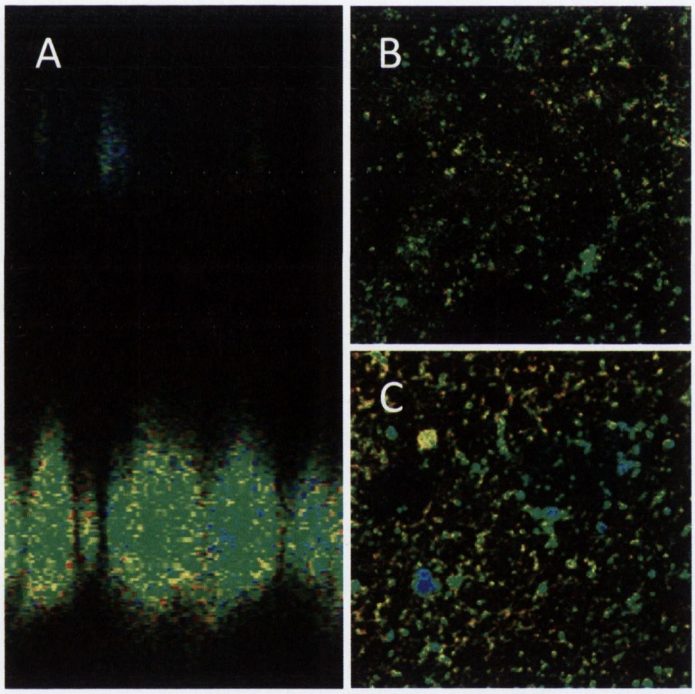

Figure 7.7 Fluorescence imaging of the cross sectional (**A**), top (**B**) and bottom (**C**) surfaces of polyethylene terephthalate film after swelling treatment with Quantum dots dispersed in THF.

7.2.5 Kevlar fibre swelling with supercritical CO_2

Following the composite preparation using polyethylene swelled in SC CO_2 it was decided to explore the possibility of swelling Kevlar in the same environment Kevlar fibre was placed in the stainless steel cell with a 1 g/L nanotube dispersion in NMP. The cell was placed in a water bath at 50°C and the pressure was increased to 48.2 MPa for two hours. Following this the cell was inverted to let the solvent interact with the polymer. The sample was left in this environment for 1 hour. The procedure was repeated with a second sample treated for 24 hours.

SEM analysis was carried out for both samples. The resulting images contained unexpected features and can be seen in **Figure 7.8**. The sample treated for one hour (**Figure 7.8 A** and **B**) displayed interesting crystalline features throughout many of the fibre samples. When we zoom in we can see the quite remarkable crystallites protruding from within the fibre in all directions. After 24 hour treatment we see that the fibre now contains globules protruding from within the matrix (**Figure 7.8 C** and **D**). As we discussed for the polyethylene we found that the SC CO_2 treatment could increase crystallisation within the polymer matrix. A similar effect could occur in Kevlar and we could be seeing the formation of Kevlar crystallites As we mentioned in Chapter 5 this may result in an increase in the T_m of Kevlar although it cannot be confirmed by DSC studies as the T_m is well above the range of study for the machine.

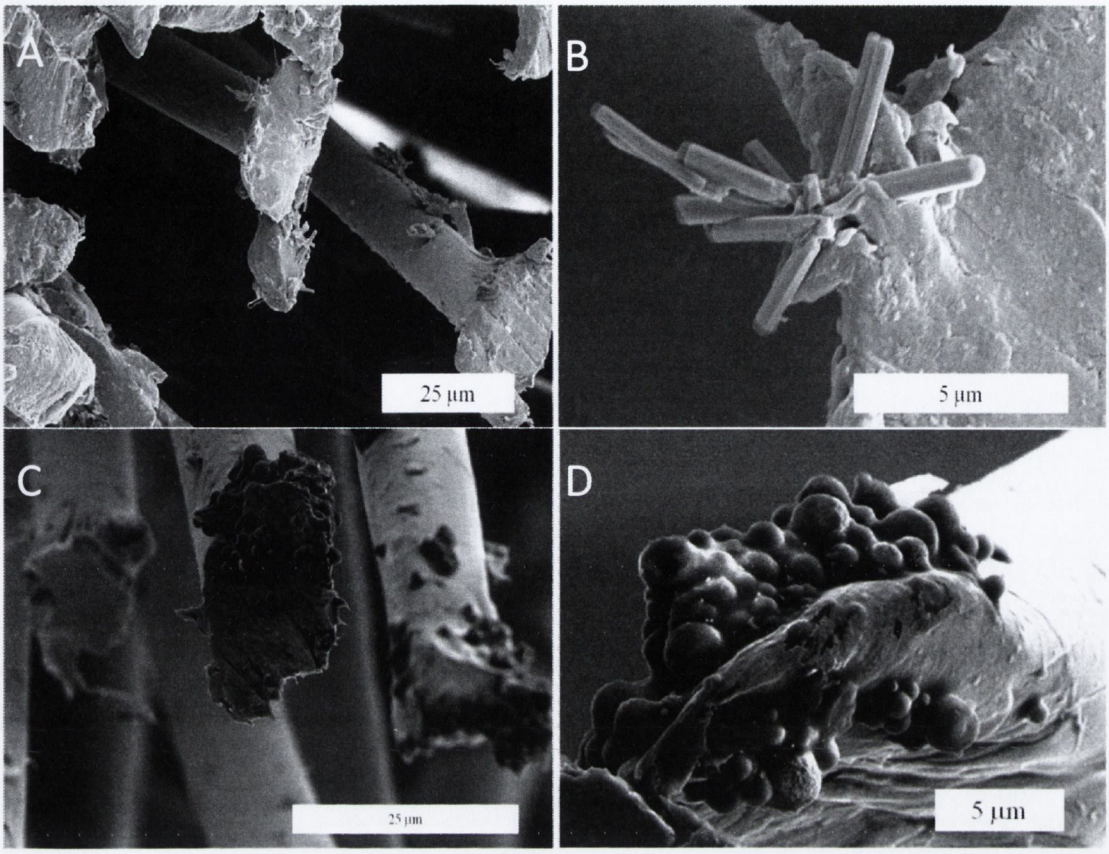

Figure 7.8 SEM images of Kevlar fibre swelled in SC CO_2 for a period of 1 hour (**A** and **B**) displaying crystallites protruding from the interior of the fibre and 24 hours displaying globules on the surface of the fibre (**C** and **D**)

We have also done some preliminary studies of the mechanical properties of the fibres and representative curves can be seen in **Figure 7.9** showing a considerable difference in the fibre sample treated for 1 hour. Ultimately we are observing a time dependant effect on Kevlar due to the treatment and further studies would enable us to further explore the effect of SC CO_2 treatment.

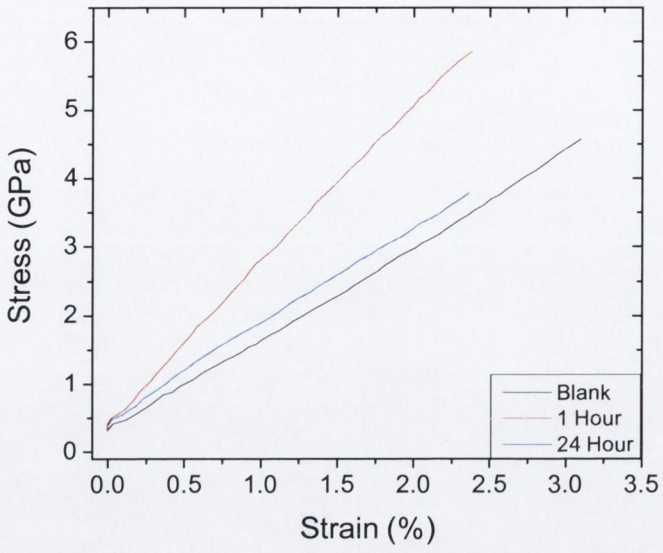

Figure 7.9 Representative mechanical stress-strain curves for the blank Kevlar fibre (black line), fibre treated for 1 hour (red line) and fibre treated for 24 hours (blue line)

Thus our preliminary studies have demonstrated that there is the possibility of interaction between carbon nanotubes and NMP. This will need to be fully explored in the future to discover if other solvents have an effect on carbon nanotubes or C_{60} and ultimately whether the dispersibility and stability of carbon nanotubes depends not just on the physical properties of a solvent but its chemical properties as well.

We have shown that our solvent swelling technique can be used for the preparation of new polymer-quantum dot composites with interesting photonic properties. In the future we would like to expand our approach for the preparation of conductive, magnetic and fluorescent polymer composites with a broad range of potential applications. This will be achieved by swelling of selected polymer fibres and thin films in metal (e.g Ag and Au), magnetic (Fe_3O_4) and fluorescent (various quantum dots, e.g CdS, CdSe, CdTe) nanoparticles suspensions and investigation of properties of these new composites. Since a wide range of inorganic particles and nanotubes can be incorporated into different types of polymers, these new composites could be suitable for a wide range of applications. For example, conductive polymer-carbon nanotubes and polymer-metal nanoparticles might be used in different electrical devices as flexible conductive electrodes, thermal sensors, low power circuit protectors and over current

regulators. Magnetic particles-polymer composites can be used for electromagnetic interference (EMI) shielding of medical equipment in hospitals and consumer electronics. Fluorescent nanoparticle- polymer composites might find an application in smart interactive textiles, sensors and as components for optical communications.

Finally we have shown an effect of supercritical fluid in the presence of nanotubes dispersed in a solvent can change the physical morphology of Kevlar. In the future it will be important to establish the effect of the selection of a different solvent, the time dependence of treatment and also further exploring the full physical and mechanical characteristics of fibres treated in this way.

Appendix

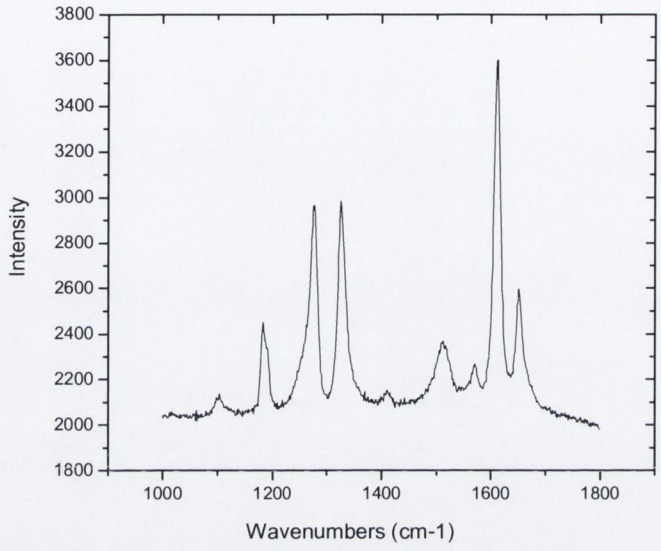

Raman spectrum of Kevlar

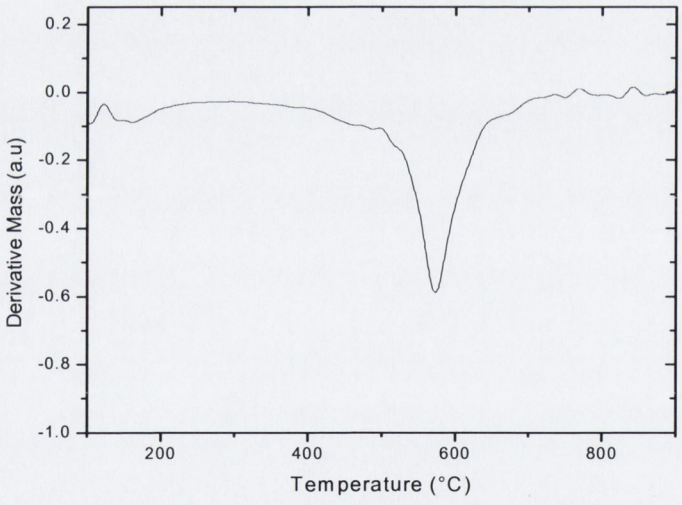

Derivative of the thermogravimetric analysis curve of Kevlar

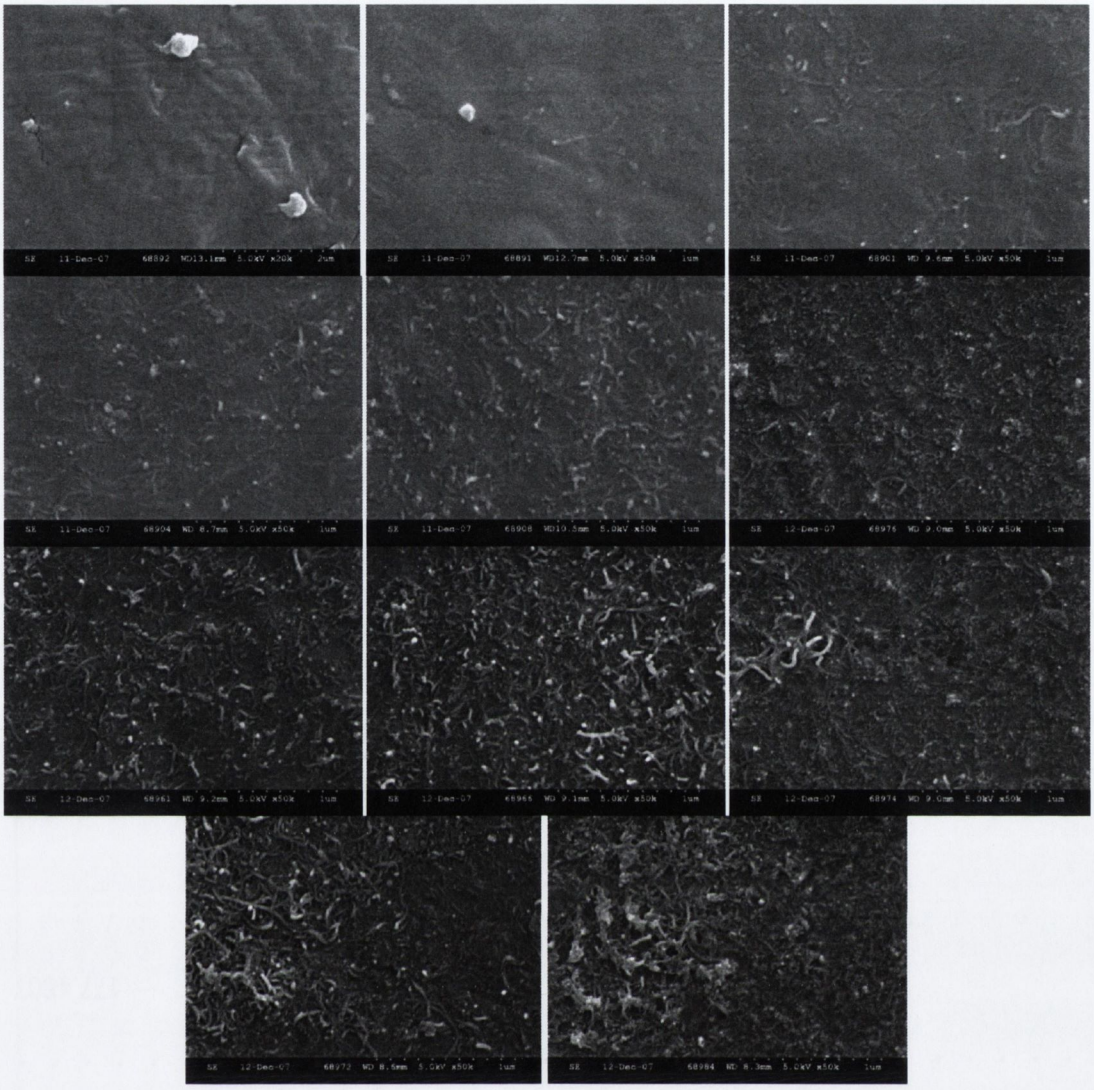

SEM images of composite film surface for increasing concentration of nanotube dispersions in THF

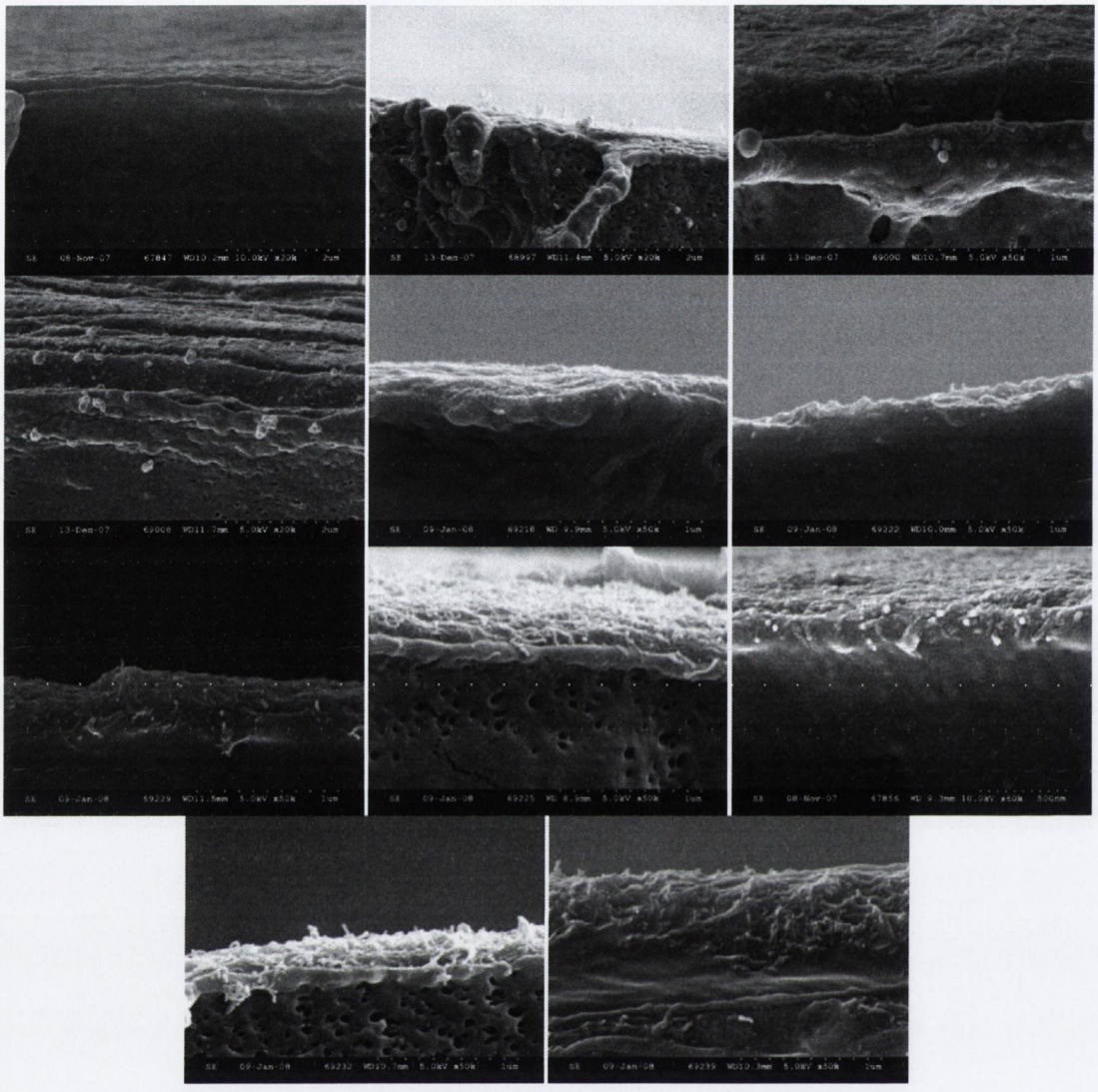

SEM images of composite cross sectional surface for increasing concentration of nanotube dispersions in THF

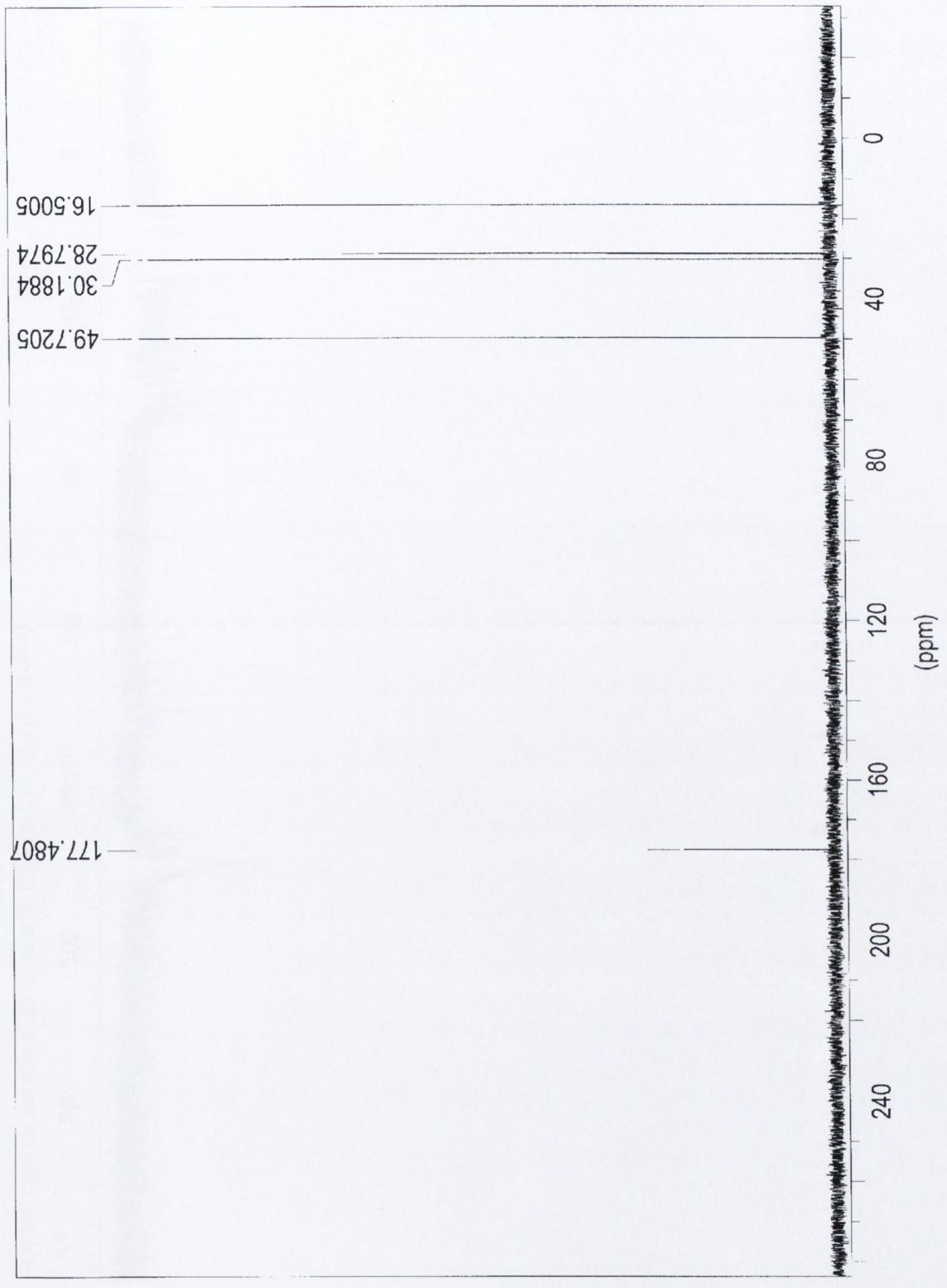

C^{13}NMR of pure C_{60} in D_2O

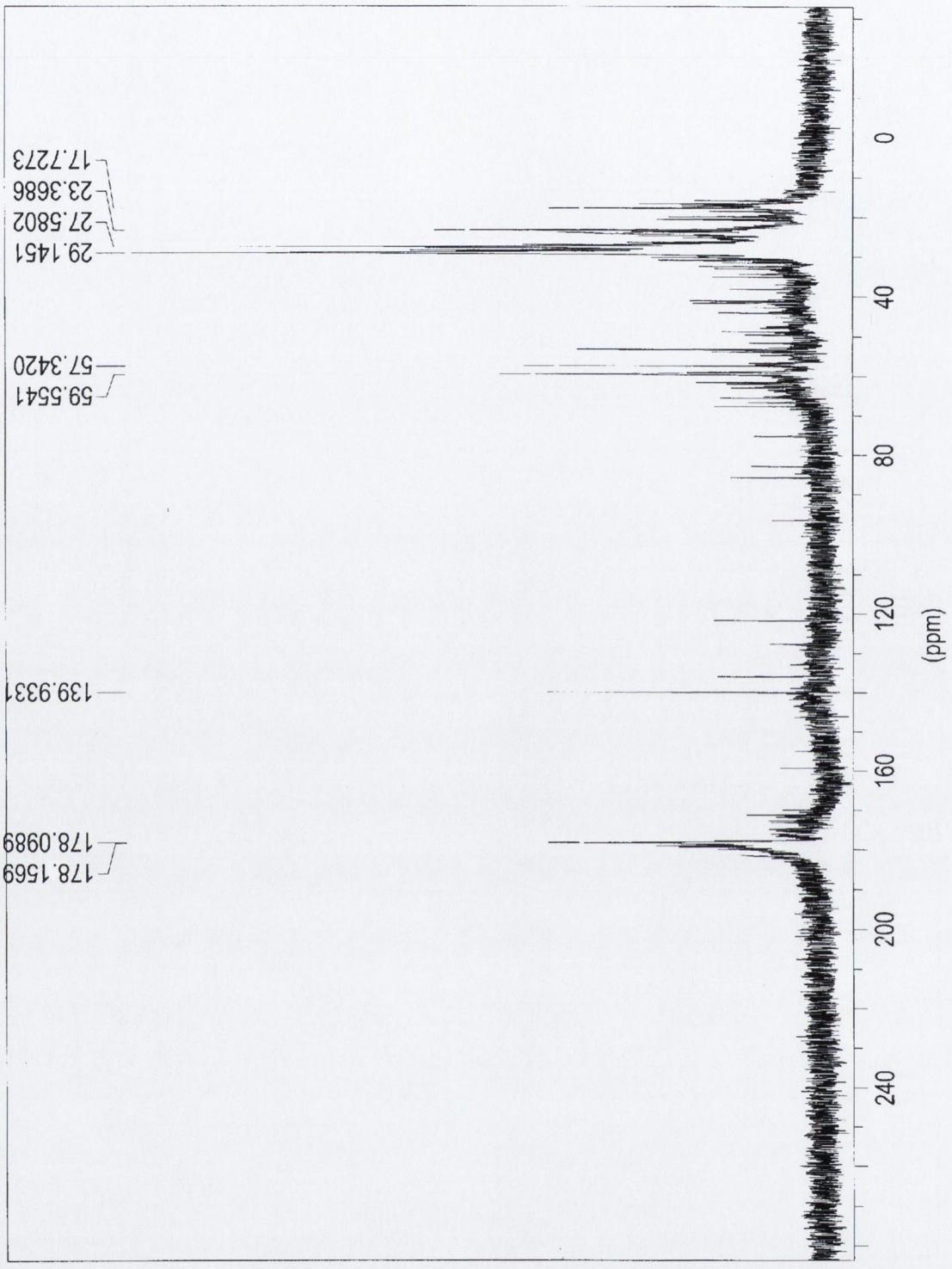

C^{13}NMR of C_{60} + NMP product in D_2O

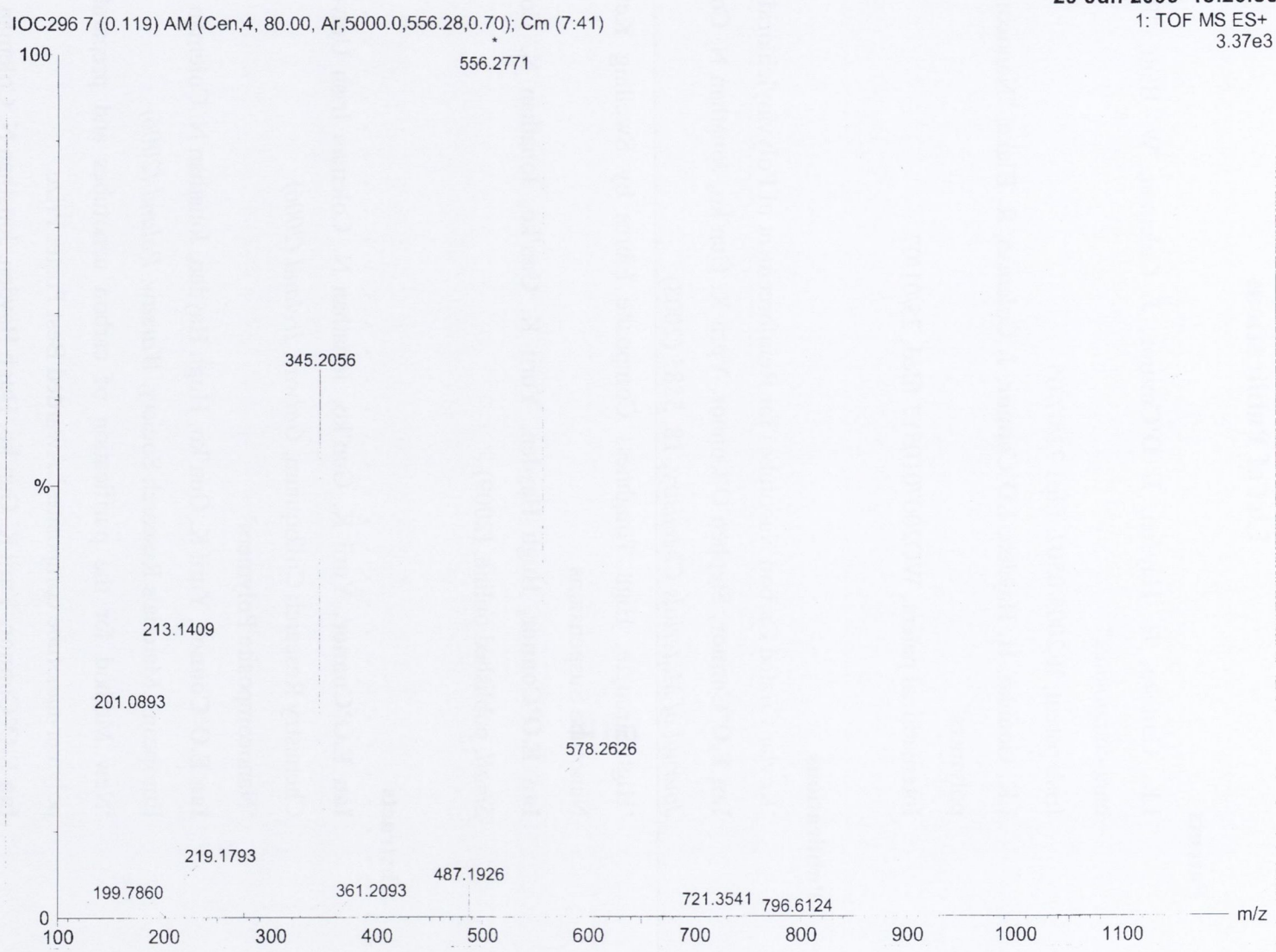

Mass Spectrum of C_{60} + NMP product

List of Publications

Patents

I.K. Gounko, H. Hayden, **I. O'Connor**, J. Coleman, W. Blau, "Polymer nanocomposites"

Irish patent, IE2005/0502, filed 22/07/05.

I.K. Gounko, H. Hayden, **I.O'Connor**, J. Coleman, R. Blake, "Nanocomposite polymers"

International patent, WO2007010517 filed, 25/01/07.

Publications

'Kevlar Coated Carbon Nanotubes for Reinforcement of Polyvinylchloride'

Ian E.O'Connor, Stephen O'Connor, Yurii K. Gun'ko, Jonathan N. Coleman, *Journal of Materials Chemistry*, **18**, 5585 (2008)

'High-Strength, High Toughness Composite Fibres by Swelling Kevlar in Nanotube Suspensions'

Ian E.O'Connor, Hugh Hayden, Yurii K. Gun'ko, Jonathan N. Coleman, *Small*, published online, (2009)

Abstracts

Ian E.O'Connor, Yurii K. Gun'ko, Jonathan N. Coleman Irish Universities Chemistry Research Colloquium, *Galway, Ireland (2006)*

'Nanocomposite Polymers'

Ian E.O'Connor, Yurii K. Gun'ko, Hugh Hayden, Jonathan N. Coleman European - Materials Research Society, *Warsaw, Poland (2006)*

'New Method for the purification of carbon nanotubes and preparation of polymer-nanotube composites' Awarded Best Poster Prize

Ian E.O'Connor, Yurii K. Gun'ko, Hugh Hayden, Jonathan N. Coleman Chemon Tubes, *Arcachon, France* (2006)

'Preparation of polymer-nanotube composites'